2.3 Condensed molecules

2.3.0 Introduction and general remarks

Molecular solids exhibit a unique characteristic:

– *The electronic structure of the isolated molecule in the gas phase is to a large extent preserved upon formation of the molecular solid.*

This, of course, is caused by the generally weak intermolecular van der Waals interaction between the molecular moieties in the crystal. Therefore, X-ray structure determination on molecular crystals is usually believed to provide us with the "gas phase structure" of the molecule. The above stated persistence is in contrast to the case for metals and many solid compounds with strong electron-sharing bonding, where the constituents often do not maintain their atomic or molecular identity. In photoelectron spectra the persistence of the electronic structure of the gas phase moiety is documented by a one-to-one correspondence between the spectrum of the solid and the vapor. However, certain changes between solid phase and gas phase spectra have been observed. The main differences are:

– *A shift of the ion states in the solid towards lower binding energies*

– *A broadening of the photoemission peaks in the solid.*

Theories have been developed [78D2, 80D] that allow one to understand this shift via polarization of the surrounding molecules by the created hole localized on one moiety. The polarization of the surrounding molecules stabilizes the final ion state, and thus leads to a decrease in binding energy (polarization energy). It is quite evident that holes remain localized in the solid state. The local or extended nature of electronic states in molecular solids is determined by a competition between fluctuation in the local site energies of these states (which tend to localize them) and the hopping probability for inter-site excitation transfer (which tend to delocalize them). These site fluctuation ingredients determine the larger line widths in the photoemission spectra of molecular solids, and also the temperature dependence of the line widths, which has been observed experimentally [80S1]. In thinking about excitations in molecular solids it may cause conceptual difficulties to consider these excitations in terms of the traditional energy band theory of solids. Rather, such excitations should be regarded as localized entities which move through the solid via hopping. The localized nature of the hole states reflects itself in the population of hole states that involve the excitation of more than one electron i.e. so called shake up states. Shake up satellites [86C] are caused by excitations among the valence excitations in the presence of a hole, and are thus due to 2-hole-particle (2hp) states. Their intensity is governed by the projection of the created 2hp-ion state onto the frozen hole state, which can be thought to be created through a sudden removal of an electron, fast enough that the remaining electrons cannot adjust to the change of the potential. The shake up lines show the same polarization shifts as the regular hole states as expected if the valence electron distribution does not change upon condensation into a van der Waals solid.

UV photoelectron spectra have been reported for a wide variety of molecular compounds exceeding the present data collection by far. The criterion for inclusion of a species in the present data base was the existence of rather complete sets of information covering a wide range of experimental results using electron spectroscopic techniques and related theoretical calculations. For those readers interested in specific aspects of the physics of special molecular solids for which electron spectroscopy was used as a peripheral method several detailed review papers are recommended [79G, 78D1, 85S, 80S2, 83K3, 87K, 87I, 87F1]. All of these papers stress various aspects of the fact that molecular solids offer important prospects in material science, covering polymers, organic superconductor, Langmuir-Blodgett films for application as molecular membranes, and new types of electronic devices, as well as applications in non-linear optics, and lithography.

The presented data collection provides a data base for selected relatively simple molecules which have been studied in the gas phase and in the solid phase. We have selected mostly small and medium sized molecules with up to ten atoms, and only added benzene, annulated hydrocarbons, oligo-phenyls, and saturated hydrocarbons. Table A lists the types of spectroscopic information we present for 21 species of different size, varying from diatomics (e.g. N_2, CO, O_2) to polyatomics (e.g. anthracene: $C_{14}H_{10}$), and two molecular series. For each molecule the available information is indicated in Table A. We combine structural and spectroscopic information on the free gaseous molecule, and compare this with structural and spectroscopic information on the molecular solid.

Table A. Type of spectroscopic information for selected molecules in the gas phase and in the solid phase given in this chapter.

No.	Species	Gas			Molecular solid												
		1	2	3	4	5	6	7	8	9	10	11	12	13	14	15	16
1	N_2	×	×	×	×	×	×	×		×	×	×	×			×	×
2	CO	×	×	×	×	×	×	×		×	×	×					×
3	O_2	×	×	×	×	×	×			×	×	×					×
4	NO	×	×	×	×	×	×		×	×	×	×					×
5	I_2	×	×	×	×	×	×	×	×		×						
6	H_2O	×	×	×	×	×	×	×	×	×	×				×		×
7	CO_2	×	×	×	×	×	×	×		×	×	×	×			×	
8	NH_3	×	×	×	×	×	×			×	×				×		
9	C_2H_2	×	×	×	×	×	×			×	×	×	×				
10	C_2H_4	×	×	×	×	×	×	×		×	×	×	×			×	
11	CH_4	×	×	×		×	×			×	×	×					
12	CF_4	×	×	×	×	×	×			×	×	×	×				
13	CCl_4	×	×	×		×	×			×	×	×	×				
14	SF_6	×	×	×	×	×	×			×	×	×	×			×	
15	S_8	×	×	×	×	×	×	×	×	×						×	
16	C_6H_6	×	×	×	×	×	×	×	×	×	×			×	×		
17	NC_5H_5	×	×	×	×	×	×	×	×	×	×	×					
18	$C_{10}H_8$	×	×	×	×	×	×	×	×	×						×	
19	$C_{14}H_{10}$	×	×	×	×	×	×	×	×	×		×				×	
20	$C_{18}H_{12}$	×	×	×	×	×	×	×	×	×	×	×				×	
21	Glycine	×	×	×	×	×	×	×	×	×							
22	*p*-Phenyls		×	×	×	×	×	×	×			×				×	
23	C_nH_{2n+2}	(×)	×	(×)	(×)	(×)	×	×	×	×	×	×					

1: Point group of the isolated molecule.
2: Bond lengths and bond angles.
3: Electronic configuration in the ground state of the isolated molecule.
4: Space group of the molecular solid.
5: Structure of the solid.
6: Outer valence electron spectrum of the molecular solid in comparison with the gas phase spectrum.
7: Inner valence electron spectrum of the molecular solid in comparison with the gas phase spectrum.
8: Core electron spectrum of the molecular solid in comparison with the gas phase spectrum.
9: Theoretical assignment of the observed ion states.
10: Polarization energies of some ion states.
11: Ion state cross-sections as a function of photon energies.
12: Table of resonance structures in the cross-sections.
13: Auger spectrum of the molecular solid.
14. Penning ionization electron spectrum of the molecular solid in comparison with the gas phase spectrum.
15: Electronic excitation spectrum in the valence electron region.
16: Electronic excitation spectrum in the core region.

For some small di- and triatomics rather full sets of data are available. Examples are N_2, CO, O_2, CO_2. For some condensed molecular solids data even on the cross-sections of inner valence satellites exist. On the other hand, reports of angle resolved valence electron spectra with respect to band mapping (E vs. k) have been very scarce so far [79G, 86S]. However, for some of the species physisorbates on metal surfaces (see for example [87K]) have been studied using angle resolved techniques. These data are not included in the present review because the observed intermolecular arrangement may be dictated by the structure of the substrate. Thus the data may not represent the properties of the condensed molecular solid.

There are other small molecules, e.g. NO, I_2, H_2O, and glycine, listed which show rather strong intermolecular interactions in the solid state, either in the neutral ground state of the system, i.e. NO, or in the ionized state, i.e. I_2.

Large amounts of data have been collected by several research groups on various organic molecules [85K1]. The quantity of interest is the polarization energy which has been discussed on the basis of extended sets of different organic molecules in a land mark paper by Inokuchi and collaborators [81S2]. We concentrate here on some series of compounds, namely saturated hydrocarbons, C_nH_{2n+2} (with n varying from 1 to 36), annulated benzoid hydrocarbons with the number of rings increasing from 1 to 4, and oligo-phenyl compounds varying the number of rings from 1 to 4.

In order to be able to use the present collection, we explain in the following, using the CO (molecule No. 2) as an example, the type of information and the ordering of the data: The first three columns are dedicated to properties of the free gaseous molecule covering the point group ($C_{\infty v}$ for CO), bond lengths (1.13 Å for CO) and angles (if possible) and the electronic configuration in the ground state ($^1\Sigma^+$). The remaining 13 columns are concerned with properties of the molecular solid. Columns 4 and 5 mark the space group and the structures of the molecular solid. As indicated within the data collection, CO exhibits two solid phases. They differ in the intermolecular arrangement of the CO molecules. Since these arrangements are isomorphic with solid N_2 we refer to the drawings shown for the latter solid. The temperature ranges in which the various solid phases exist are given (if known). The size of the unit cell is indicated by *a*, *b*, and *c*. Columns 6, 7, and 8 cover the photoelectron spectra of the outer valence region (in comparison with gas phase spectra), the inner valence electron region, and the core region. The spectrum of the solid (taken with synchrotron radiation at $\hbar\omega = 40$ eV) exhibits the characteristic differences with respect to the gas phase spectrum (taken with HeII radiation $\hbar\omega = 40.8$ eV) mentioned above: Firstly, the binding energies of the ion states in the solid shift to lower binding energies by about 1.2 eV. Secondly, the line widths increase in the solid so that the vibrational fine structure observed in the gas phase is lost. The presentation of the inner valence region has been separated from the outer valence region, because it is well known that in the inner valence region strong many-particle effects are effective leading to the appearence of satellite structure which sometimes do not allow a straightforward interpretation and assignment even for the gas phase spectra. We show spectra taken at different photon energies of the gas ($\hbar\omega = 1487$ eV and 50.3 eV) in comparison with the solid phase ($\hbar\omega = 60$ eV). In addition we present a computer simulation of the inner valence region on the basis of results of ab-initio calculations which are summarized as a table. Core-electron spectra of solid CO have not been published. The following column (9) indicates that the asssignment of the observed features on the basis of theoretical calculations for the isolated molecule is reported. Column 10 indicates whether the differences in binding energies between the ion states in the gas phase and in the solid phase, i.e. the polarization energies of the various ion states, are tabulated. The energies tabulated are vertical binding energies and are given with respect to the vacuum level. Column 11 refers to the photon energy dependences of the cross-sections of the various ion states in the solid. The set of figures connected with cross-sections begins, if possible, with a series of electron distribution curves taken at different photon energies. Here, kinetic electron energy of binding energy is plotted versus photon energy. The range of photon energies for CO covers 14 eV···140 eV. The cross-sections of the various ion states as a function of photon energies have been plotted and compared with those in the gas phase. Column 12 marks whether any resonance feature appearing in the cross-sections plotted can be assigned. The last four columns cover the Auger (AES) spectrum (column 13), the Penning ionization electron spectrum (PIES, column 14), and the electronic excitation spectra (valence: column 15; core: column 16) if available. While the Auger spectra as well as the PIE-spectrum of solid CO have not been published the core electron excitation spectrum has been recorded using EELS.

Acknowledgements

In the process of collecting and assembling the presented information a number of coworkers have been extremely helpful. I am particularly grateful to Mrs. H. Böhm, Mrs. H. Koslowski, Dr. A. Lawitzki, Mrs. C. Risse, Mr. H. Rayess, Mr. I. Hemmerich and Dr. B. Tasche.

Dr. B. Bartos, Dr. H. Hamann and Mr. Th. Mull are acknowledged for reading and correcting the manuscript.

2.3.1 Nitrogen (N_2)

Isolated molecule

1. Point group: $D_{\infty h}$
2: Bond length: 1.055 Å
3: Ground state electron configuration:

$$^1\Sigma_g^+: \underset{N(1s)}{(1\sigma_g)^2(1\sigma_u)^2} \mid \underset{N(2s),\ N(2p)}{(2\sigma_g)^2(2\sigma_u)^2(1\pi_u)^4(3\sigma_g)^2} \mid \underset{\text{empty}}{(1\pi_g)^0(3\sigma_u)^0}$$

Molecular solid

a) Cubic N_2 $T<35$ K [73L1, 65W]
4: Space group: T_h^6 (Pa3) (evidence for $P2_13$ structure acc, to [88L])
5: Structure of the solid:

unit cell: $a=5.644$ Å (at 4.2 K) [65W]; 5.684 Å ($T=34$ K) [88L]

Atomic positions:
$+(u, u, u; u+1/2, 1/2-u, \bar{u}; \bar{u}, u+1/2, 1/2-u; 1/2-u, \bar{u}, u+1/2)$
$u \approx 0.054$

See also Fig. 1.

b) Hexagonal N_2 35 K $<T<$ melting [71L1, 65W]
4: Space group: $P6_3/mmc$ [88L]
5: Structure of the solid:

unit cell: $a=4.037$ Å, $c=6.592$ Å ($T=36$ K) [88L]

Atomic positions:
hcp with center positions at 0, 0, 0; 1/3, 2/3, 1/2.
Atoms are not in fixed positions but rotate around the center positions.

6. Outer valence photoelectron spectrum of the molecular solid [82L1] in comparison with the gas phase [70T]: Fig. 2.
7: Inner valence photoelectron spectrum of the molecular solid [83E] in comparison with the gas phase [74G1, 80K]: Figs. 3, 4.
8: Core photoelectron spectrum of the molecular solid in comparison with the gas phase: not reported.
9: Theoretical assignment of the observed ion states: Table 1.

A computer simulation of the spectra on the basis of the results in Table 1 is shown in Fig. 4.

10: Polarization energies of some ion states: Table 2.
11: Ion state cross-sections as a function of photon energies of solid N_2 in comparison with gaseous N_2: Figs. 5···11.
12: Table of resonance structures in the cross-sections: Table 3.
13: Auger spectrum of the molecular solid in comparison with the gas phase: not reported.
14: Penning ionization electron spectrum of the molecular solid in comparison with the gas phase: not reported.
15: Electronic excitation spectrum in the valence electron region: Fig. 12.
16: Electronic excitation spectrum in the core electron region: Fig. 13.

Table 1. N_2. Vertical binding energies E_b and intensity coefficients $(x_p^{(n)})^2$ obtained from 2ph-TDA calculations for gaseous N_2. States with $(x_p^{(n)})^2 < 0.01$ are omitted except for the first satellites in each symmetry [83S1]. ε_p: Hartree-Fock orbital energy. All energies relative to E_{vac}. 2ph-TDA: 2particle-hole-Tamm-Dancoff-approximation [a] [70T], [b] [74A2], [c] [80K]. [d] These orbitals are not occupied in the Hartree-Fock ground state. Non-vanishing intensity coefficients $(x_p^{(n)})^2$ for the satellite states n arise from ground-state correlation.

Orbital	HF $-\varepsilon_p$	2ph-TDA		Ext. 2ph-TDA		Experiment E_b [eV]	Leading configurations
		E_b [eV]	$(x_p^{(n)})^2$	E_b [eV]	$(x_p^{(n)})^2$		
$1\pi_u$	16.80	16.38	0.91	16.85	0.92	17.0[a]	$1\pi_u^{-1}$
		28.63	<0.01	28.63	<0.01		$2\sigma_u^{-1}3\sigma_g^{-1}1\pi_g$
		35.53	<0.01	35.57	<0.01		$2\sigma_u^{-1}3\sigma_g^{-1}1\pi_g$
$3\sigma_g$	17.28	14.21	0.88	15.70	0.91	15.6[a]	$3\sigma_g^{-1}$
$2\sigma_u$	21.17	17.22	0.81	18.96	0.82	18.8[a]	$2\sigma_u^{-1}$
		24.98	0.04	25.13	0.07	25.2[b]	$3\sigma_g^{-1}1\pi_u^{-1}1\pi_g$
		35.9	0.04	35.34	0.02		$3\sigma_g^{-1}1\pi_u^{-1}1\pi_g$
$2\sigma_g$	40.27						
		28.87	0.14	29.20	0.10	29.4[c]	$2\sigma_u^{-1}1\pi_u^{-1}1\pi_g$
		36.41	0.49	37.43	0.30		$2\sigma_u^{-1}1\pi_u^{-1}1\pi_g$
		37.53	0.01	37.56	0.10		$3\sigma_g^{-2}4\sigma_g$
		39.18	0.01	38.97	0.14		$3\sigma_g^{-1}1\pi_u^{-1}2\pi_u$
		39.25	0.04	39.25	0.04		$3\sigma_g^{-1}2\sigma_u^{-1}3\sigma_u$
		40.02	0.09	39.94	0.15		$2\sigma_u^{-2}4\sigma_g$
		40.76	0.09	40.62	0.06		$1\pi_u^{-2}5\sigma_g$
							$2\sigma_g^{-1}$
$1\pi_g$ [d]	−3.66						
		24.36	<0.01	24.38	<0.01		$1\pi_u^{-2}1\pi_g$
		24.56	<0.01	24.56	<0.01		$3\sigma_g^{-2}1\pi_g$
$1\delta_u$ [d]	−58.55						
		25.47	<0.01	25.48	<0.01		$3\sigma_g^{-1}1\pi_u^{-1}1\pi_g$
		26.26	<0.01	26.26	<0.01		$3\sigma_g^{-1}1\pi_u^{-1}1\pi_g$
$1\delta_g$ [d]	−43.78						
		29.33	<0.01	29.33	<0.01		$2\sigma_u^{-1}1\pi_u^{-1}1\pi_g$
		31.55	<0.01	31.56	<0.01		$2\sigma_u^{-1}1\pi_u^{-1}1\pi_g$

Table 2. N_2. Vertical binding energies for solid and gaseous N_2, and polarization energies E_{pol}; E_b w.r. to E_{vac}. For (A–D) see Fig. 6.

State	Vertical binding energies [eV]						E_{pol} [eV]
	Solid					Gas	
	[82L1]	[75H1]	[78N]	[79S]	[83E]	[70T]	
$^2\Sigma_g^+$ $(3\sigma_g)$	15.1	14.0*)	15.3	14.8	15.0	15.6	0.5···0.6
$^2\Pi_u$ $(1\pi_u)$	16.6	15.2*)	16.7	16.3	16.5	16.98	0.4···0.5
$^2\Sigma_u^+$ $(2\sigma_u)$	18.3	17.5*)	18.5	18.1	18.2	18.78	0.4···0.5
$^2\Sigma_u^+$ (A)	25.0				25.0	25.2	≈0.2
$^2\Sigma_g^+$ (B)	28.0				28.5	29.4	≈0.9···1.5
$^2\Sigma_g^+$ (C)					32.0	32.5	≈0.5
$^2\Sigma_g^+$ (D)					37.0	38.0	≈1.0

*) Adiabatic binding energies.

Table 3. Energy positions of resonance structures in absorption and photoemission cross-sections [83F1].

Orbital	Solid [83F1, 83E]		Gas [77P1, 80K]		Assignment
	$\hbar\omega$ eV	E_k eV	$\hbar\omega$ eV	E_k eV	
$3\sigma_g$	18.5	3.4	–	–	–
	28.0	12.9	28.1	12.5	$3\sigma_g \rightarrow 3\sigma_u$
$1\pi_u$	–	–	14.2	−2.8	$1\pi_u \rightarrow 1\pi_g$
	19.5	2.9	(20.0)	(3.0)	$1\pi_u \rightarrow 3\sigma_u$
$2\sigma_u$	–	–	12.8	−4.6	$2\sigma_u \rightarrow 1\pi_g$
	21.3	3.0	–	–	–
$2\sigma_g$	53.0	15.5	≈50	≈12.0	$2\sigma_g \rightarrow 3\sigma_u$

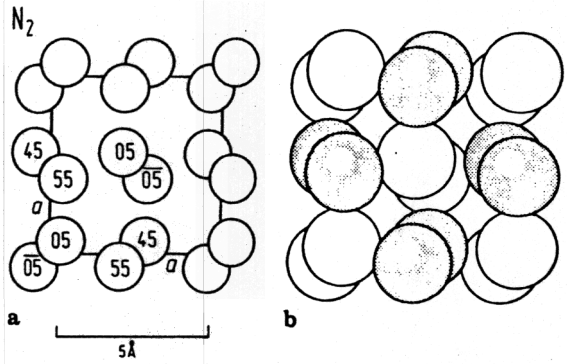

Fig. 1. N_2. a) A projection down a cubic axis of the low-temperature form of solid N_2. Fractional coordinates of the atoms are indicated (×100). b) A packing drawing of the close-packed cubic structure of solid N_2 viewed along a cubic axis [65W].

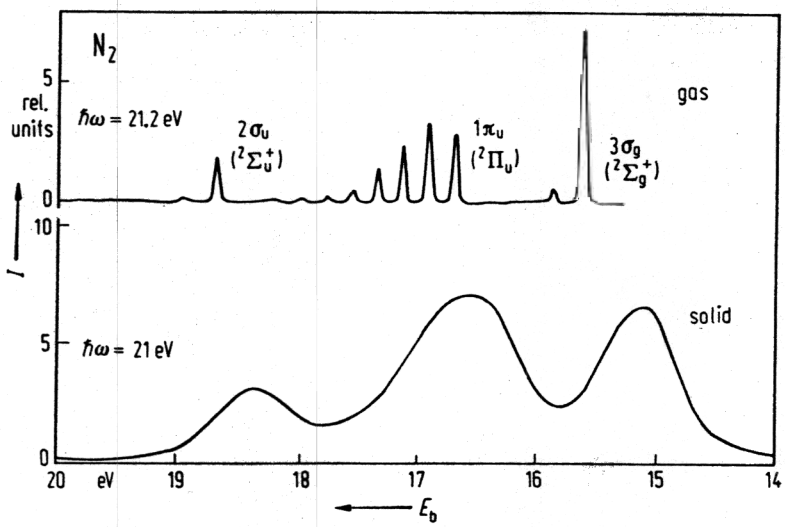

Fig. 2. N_2. Photoelectron spectra of gaseous [70T] and solid [82L1] N_2 in the outer valence region (system at T=20 K). E_b w.r. to E_{vac}.

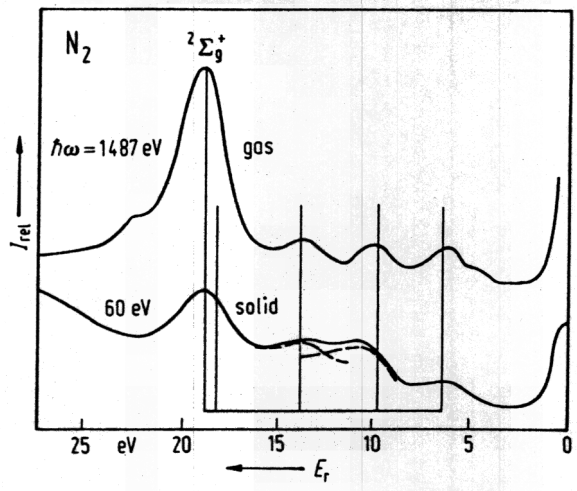

Fig. 3. N_2. Photoelectron spectra of gaseous [74G1] and solid [83E] N_2 in the inner valence region. Spectroscopic final states are indicated. E_r: energy relative to $2\sigma_u$.

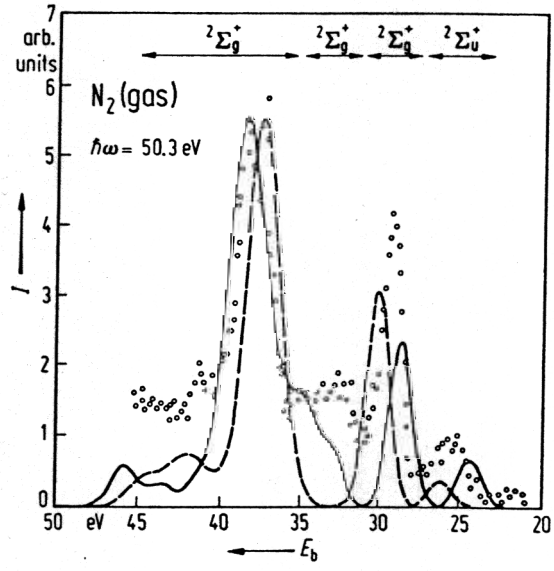

Fig. 4. N_2. Inner valence-shell photoelectron spectrum of gaseous N_2 for $\hbar\omega = 50.3$ eV incident photons; circles: experimental values obtained employing a synchrotron light source and an ≈ 0.2 eV electron monochromator band pass [80K]. (——) POLCI and (----) SECI calculations [81L1] obtained employing the energies and spectroscopic factors reported in [77S1], and static-exchange orbital transition moments determined from the Stieltjes-Tchebycheff development. SECI: single-excitation CI calculation, POLCI: polarization CI calculation.

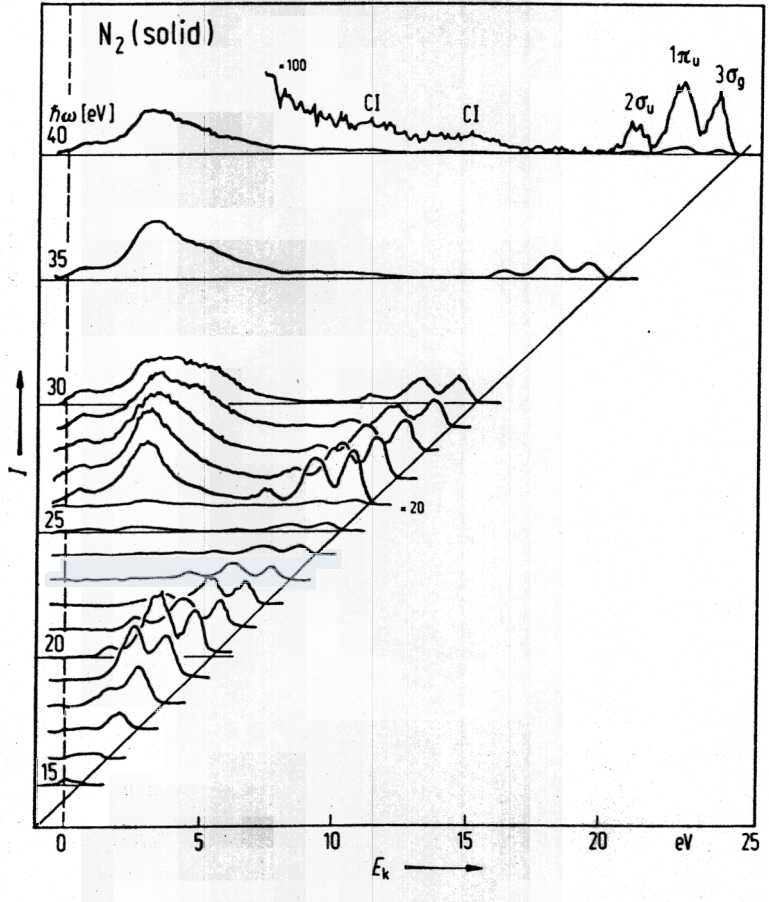

◀ Fig. 5. N_2. Electron distribution curves of solid N_2 as a function of photon energy ($\hbar\omega$: 15 eV···40 eV) [82L1, 83F1]. CI: configuration interaction (structures).

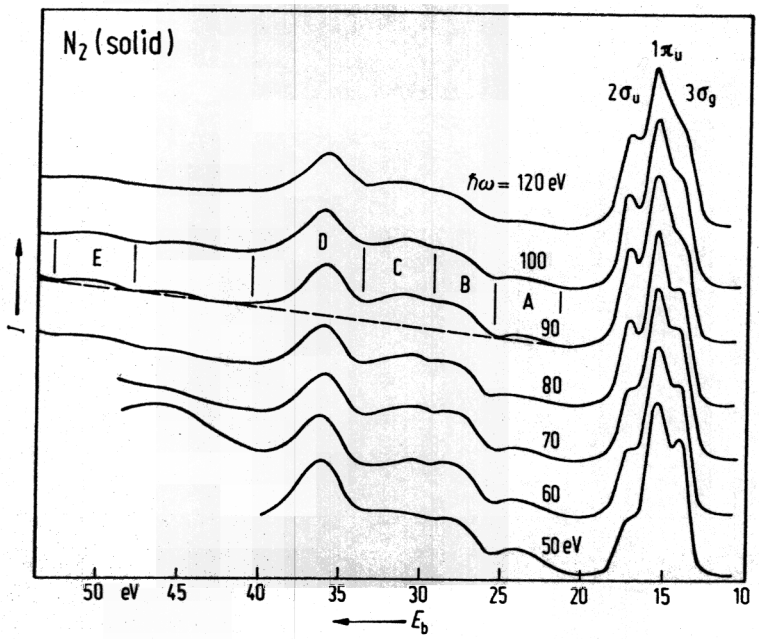

Fig. 6. N_2. Electron distribution curves [83E] of solid N_2 as a function of photon energy. All curves are normalized to show the same intensity for the emission on the $1\pi_u$ orbital. Integration regions for peaks A through E are shown as well as the background correction (dashed curve) for inelastically scattered electrons. The total accumulated counts for the outer valence band vary from $1.0 \cdot 10^6$ (50 eV) to $3.2 \cdot 10^4$ (120 eV).

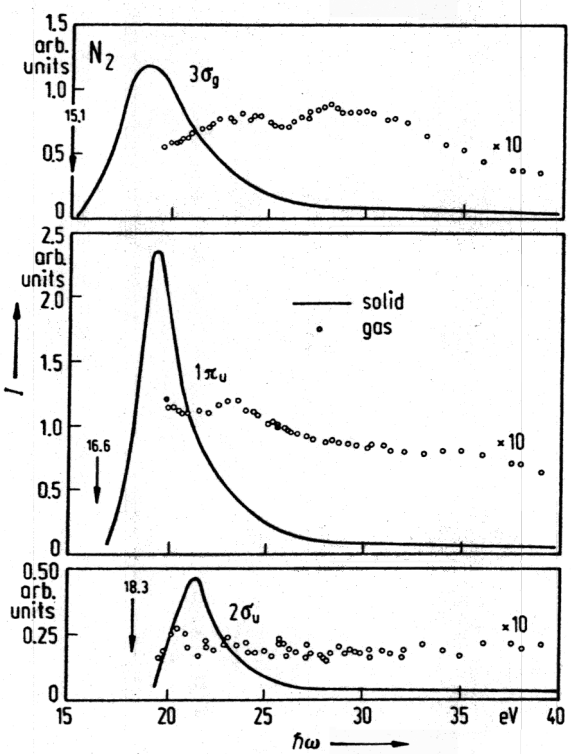

Fig. 7. N_2. Emission intensities of the three outer valence ion states of solid N_2 [83F1] in comparison with gas phase N_2 [77P1]. The arrows indicate the photoemission thresholds.

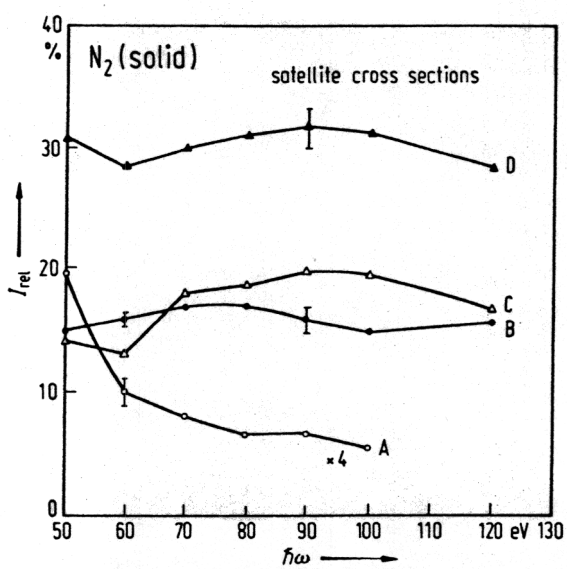

Fig. 8. N_2. Inner valence satellite cross-sections measured relative to the outer valence level emission of solid N_2 [83E]. The integration is carried out for regions A through D after background subtraction (see Fig. 6). Typical errors based on the uncertainty in background subtraction and counting statistics are indicated.

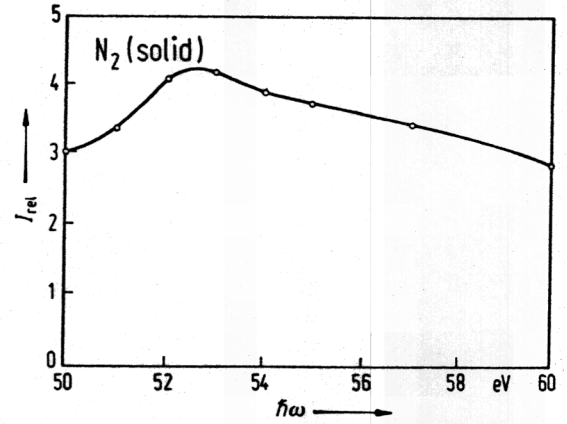

Fig. 9. N_2. Intensity of the N_2 photoemission in solid N_2 signal at 36 eV binding energy measured relative to the $1\pi_u$ emission as a function of photon energy showing the coupling to the σ_u final state shape resonance [83E].

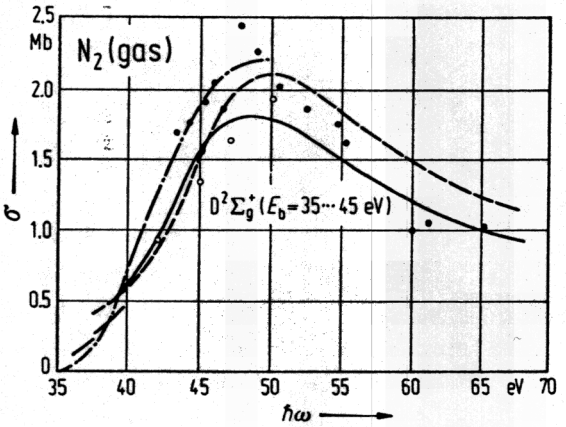

Fig. 11. N_2. Inner-valence-shell D $^2\Sigma_g^+$-band partial-channel photoionization cross-section in gaseous N_2. (●) Synchrotron-radiation measurements [80K]; (○) dipole (e, 2e) measurements [76H]; (–·–) dipole (e, e+ion) measurements [76W]; (——) POLCI and (– – – –) SECI calculations [81L1] and static-exchange orbital transition moments.

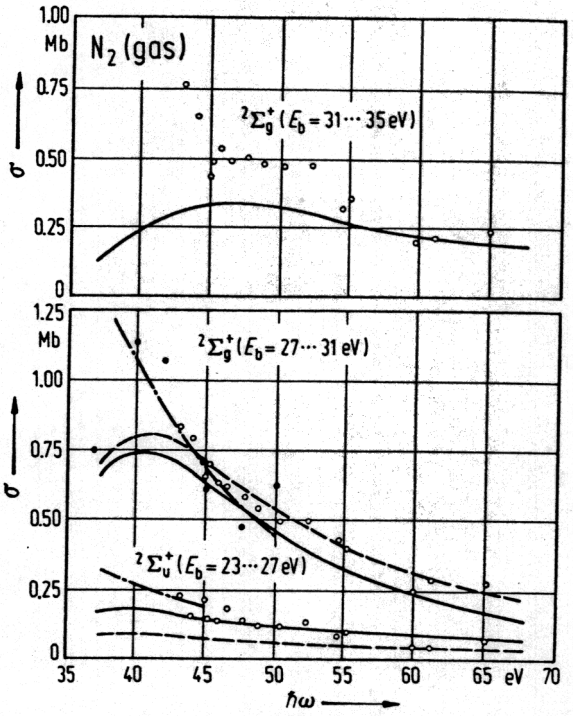

Fig. 10. N_2. Inner-valence-shell $^2\Sigma_u^+$, $^2\Sigma_g^+$, $^2\Sigma_g^+$-band partial-channel photoionization cross-sections in gaseous N_2. (○) Synchrotron-radiation measurements [80K]; (●) dipole (e, 2e) measurements [76H]; (–·–) dipole (e, e+ion) measurements [76W]; (——) POLCI and (– – – –) SECI calculations [81L1] and static-exchange orbital transition moments.

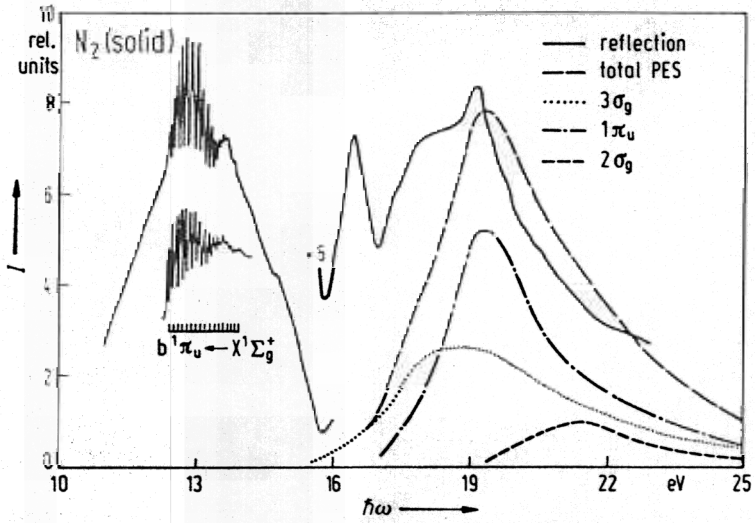

Fig. 12. N_2. Comparison between the optical reflection spectrum [71H2] and photoemission total and partial cross-section (PES) in solid N_2 [83F1].

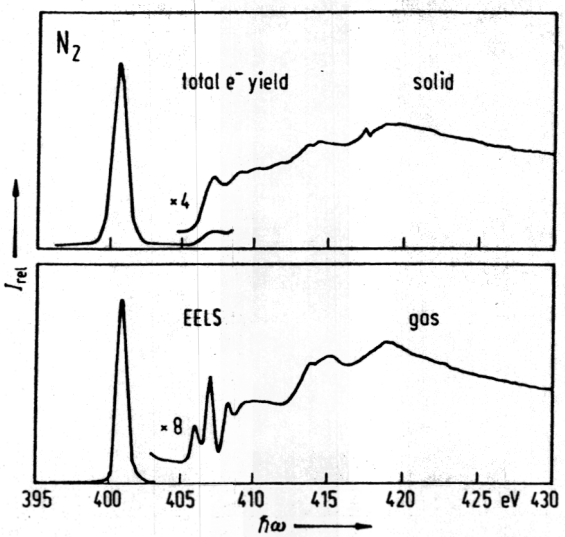

Fig. 13. N_2. e^-photoexcitation-yield spectra of solid N_2 [85R] compared with the EELS spectrum of gaseous N_2 [80H1].

2.3.2 Carbonmonoxide (CO)

Isolated molecule

1: Point group: $C_{\infty v}$
2: Bond length: 1.13 Å
3: Ground state electron configuration:

$^1\Sigma^+$:	$(1\sigma)^2(2\sigma)^2$	$(3\sigma)^2(4\sigma)^2(1\pi)^4(5\sigma)^2$	$(2\pi)^0(6\sigma)^0$
	O(1s) C(1s)	O(2s), C(2s), O(2p), C(2p)	empty

Molecular solid

a) Cubic CO $T<61.5$ K [65W, 75L]
4: Space group: T^4 ($P2_13$)
5: Structure of the solid:

unit cell: $a=5.655$ Å ($T=23$ K) [75L]

Atomic positions:
isomorphic with cubic N_2

b) hexagonal CO 61.5 K $<T<$ melting [65W, 75L]
4: Space group: D^4_{6h} ($P6_3/mmc$)
5: Structure of the solid:

unit cell: $a=4.10$ Å; $c=6.80$ Å ($T=63$ K)

Atomic positions:
isomorphic with hcp N_2

6: Outer valence photoelectron spectrum of the molecular solid [83E] in comparison with the gas phase [75G]: Fig. 14.
7: Inner valence photoelectron spectrum of the molecular solid [83E] in comparison with the gas phase [74G1, 83K1]: Figs. 15, 16.
8: Core photoelectron spectrum of the molecular solid in comparison with the gas phase: not reported.
9: Theoretical assignment of the observed ion states: Table 4.

A computer simulation of the spectra on the basis of the results in Table 4 is shown in Fig. 16.

10: Polarization energies of some ion states: Table 5.
11: Ion state cross-sections as a function of photon energies of solid CO in comparison with gaseous CO: Figs. 17···23.

12: Table of resonance structures in the cross-sections:
not reported.
13: Auger spectrum of the molecular solid in comparison with the gas phase:
not reported.
14: Penning ionization electron spectrum of the molecular solid in comparison with the gas phase:
not reported.
15: Electronic excitation spectrum in the valence electron region:
not reported.
16: Electronic excitation spectrum in the core electron region: Figs. 24, 25.

Table 4. CO. Vertical binding energies E_b and intensity coefficients $(x_p^{(n)})^2$ in CO obtained from 2ph-TDA calculations. States with $(x_p^{(n)})^2 < 0.01$ are omitted except for the first satellites in each symmetry [83S1]. ε_p: Hartree-Fock orbital energies. All energies relative to E_{vac}. 2ph-TDA: 2 particle-hole-Tamm-Dancoff-approximation [a]) [70T], [b]) [83K1], [c]) this state has a small intensity coefficient $(x_p^{(n)})^2$ for the orbital 3σ, [d]) this state has a small orbital coefficient $(x_p^{(n)})^2$ for the orbital 4σ, [e]) these orbitals are not occupied in the Hartree-Fock ground state. Non-vanishing intensity coefficients $(x_p^{(n)})^2$ for the satellite states n arise from ground-state correlation.

Orbital	HF	2ph-DTA		Ext. 2ph-TDA		Experiment	Leading configurations
	$-\varepsilon_p$	E_b [eV]	$(x_p^{(n)})^2$	E_b [eV]	$(x_p^{(n)})^2$	E_b [eV]	
5σ	15.10	13.03	0.87	13.97	0.89	14.0[a])	$5\sigma^{-1}$
1π	17.47	16.45	0.88	16.99	0.90	16.91[a])	$1\pi^{-1}$
		22.96	<0.01	22.98	<0.01		$5\sigma^{-2}2\pi$
		28.70	0.01	28.75	0.01	=27.0[b])	$4\sigma^{-1}5\sigma^{-1}2\pi$
4σ	21.88	18.60	0.87	20.11	0.79	19.68[a])	$4\sigma^{-1}$
		22.84	0.04[c])	22.99	0.11[c])	=23.0[b])	$5\sigma^{-1}1\pi^{-1}2\pi$
		30.03	<0.01	29.81	<0.01		
3σ	41.54						
		33.54	0.20	33.82	0.06[d])		$5\sigma^{-2}6\sigma$
		34.01	0.02	34.08	0.08[d])		$4\sigma^{-1}5\sigma^{-1}6\sigma$
		35.10	0.01	35.12	0.01		$3\sigma^{-1}$
		37.60	0.15	37.75	0.02		
				38.34	0.01		
		38.15	0.18	38.57	0.04		$5\sigma^{-2}n\sigma$
		38.45	0.08				$4\sigma^{-1}5\pi^{-1}n\sigma$
		38.68	0.06	39.01	0.18		$5\sigma^{-1}1\pi^{-1}n\pi$
		39.30	0.05	39.23	0.01		$3\sigma^{-1}$
		39.87	0.01	39.44	0.28		
				39.89	0.05		
		40.11	0.01	40.13	0.03		
		40.31	0.01	40.26	0.02		
				40.42	0.01		
		40.85	0.01	40.83	0.02		
				41.67	0.01		
		41.81	0.01	41.76	0.02		
1δ[e])	−38.19						
		21.91	<0.01	21.91	<0.01		$5\sigma^{-1}1\pi^{-1}2\pi$
		24.57	<0.01	24.57	<0.01		$5\sigma^{-1}1\pi^{-1}2\pi$

Table 5. CO. Vertical binding energies and polarization energies E_{pol}.

State	Vertical binding energies [eV]													E_{pol} [eV]
	Solid					Gas								
	[77N]	[78N]	[79S]	[82L2]	[83E]	[70T]	[74G1]	[74P1]	[74Å1]	[77P1]	[78N]	[79S]	[83K1]	
$X\ ^2\Sigma^+ (5\sigma)$	12.7	13.0	13.0	13.5	12.8	14.01	14.5	14.01		14.0	14.06	14.0	14.5	0.5···1.8
$A\ ^2\Pi (1\pi)$	15.8	15.9	15.95	16.5	15.6	16.91	17.2	16.91		17.0	16.76	16.9	17.2	0.4···1.6
$B\ ^2\Sigma^+ (4\sigma)$	18.6	18.7	18.7	19.2	18.5	19.86	20.1	19.69		19.7	19.71	19.8	20.1	0.5···1.6
$D\ ^2\Pi$				22.3	21.6			22.7	22.73				22.9	0.4···1.1
$C\ ^2\Sigma^+$							23.29	23.4	23.38					
$E\ ^2\Sigma^+$				25.2	24.3		25.9	25.3	25.48				26.9	0.1···1.6
$F\ ^2\Sigma^+$				27.6	27.0		28.6	28.1	28.09				28.0	0.5···1.6
				31.5	30.5		32.1	31.8					31.5	0.3···1.6
					32.5								33.8	1.3
							36.0						36.0	–
$^2\Sigma^+ (3\sigma^{-1})$					37.5		38.6	37.3		38.3			38.3	−0.2···1.1

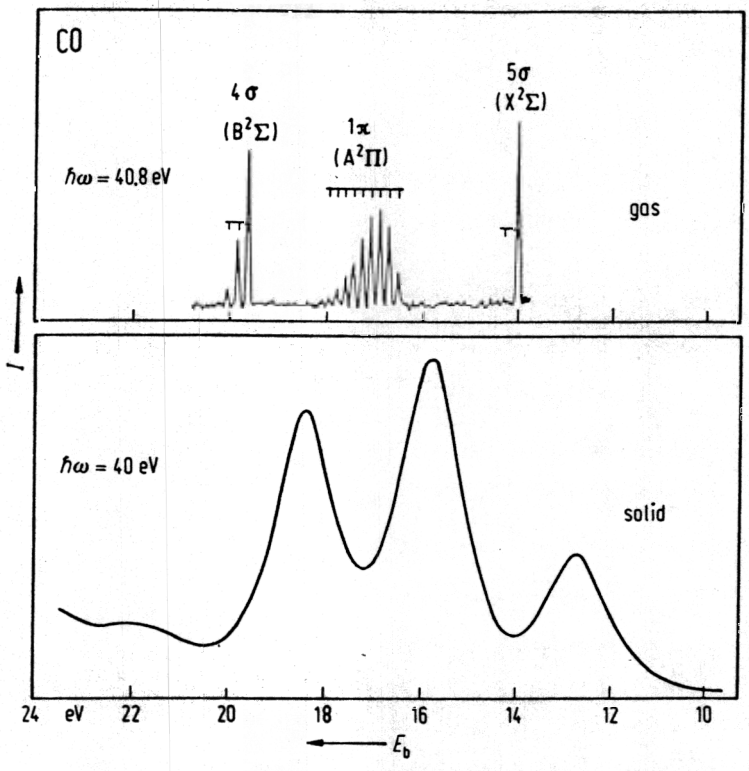

Fig. 14. CO. Photoelectron spectra of gaseous [75G] and solid [83E] CO in the outer valence region (system at $T=20$ K).

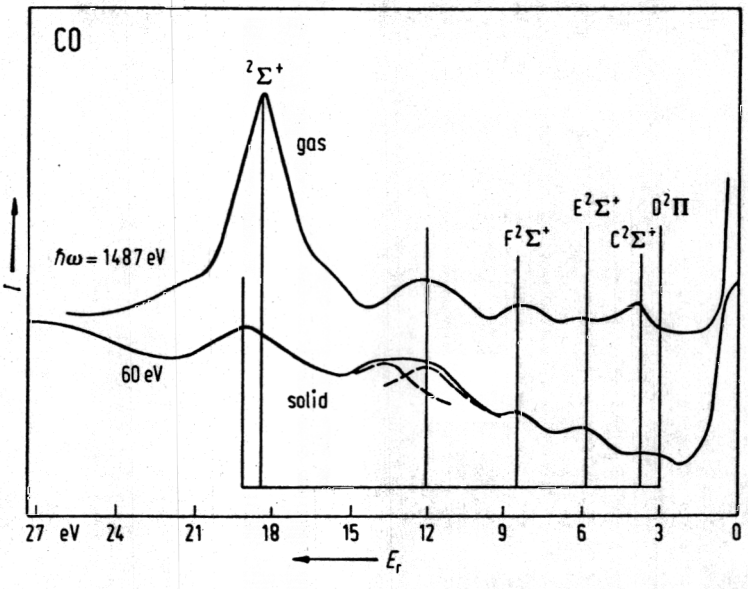

Fig. 15. CO. Photoelectron spectra of gaseous [74G1] and solid [83E] CO in the inner valence region. E_r: energy relative to 4σ.

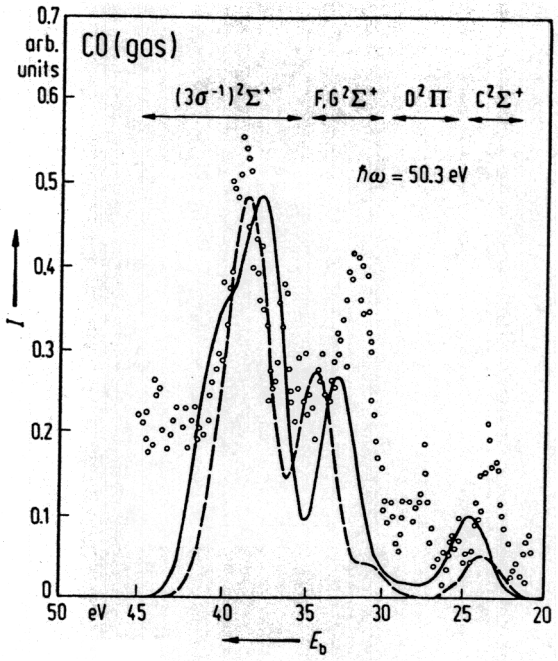

Fig. 16. CO. Inner valence-shell photoelectron spectrum of gaseous CO for $\hbar\omega = 50.3$ eV incident photons; circles: experimental values obtained employing a synchrotron light source and an ≈ 0.2 eV electron monochromator band pass [83K1]; (——) POLCI and (----) SECI calculations [81L1] obtained employing the energies and spectroscopic factors reported in [77S1], and static-exchange orbital transition moments determined from the Stieltjes-Tchebycheff development. SECI: single-excitation CI calculation, POL-CI: polarization CI calculation.

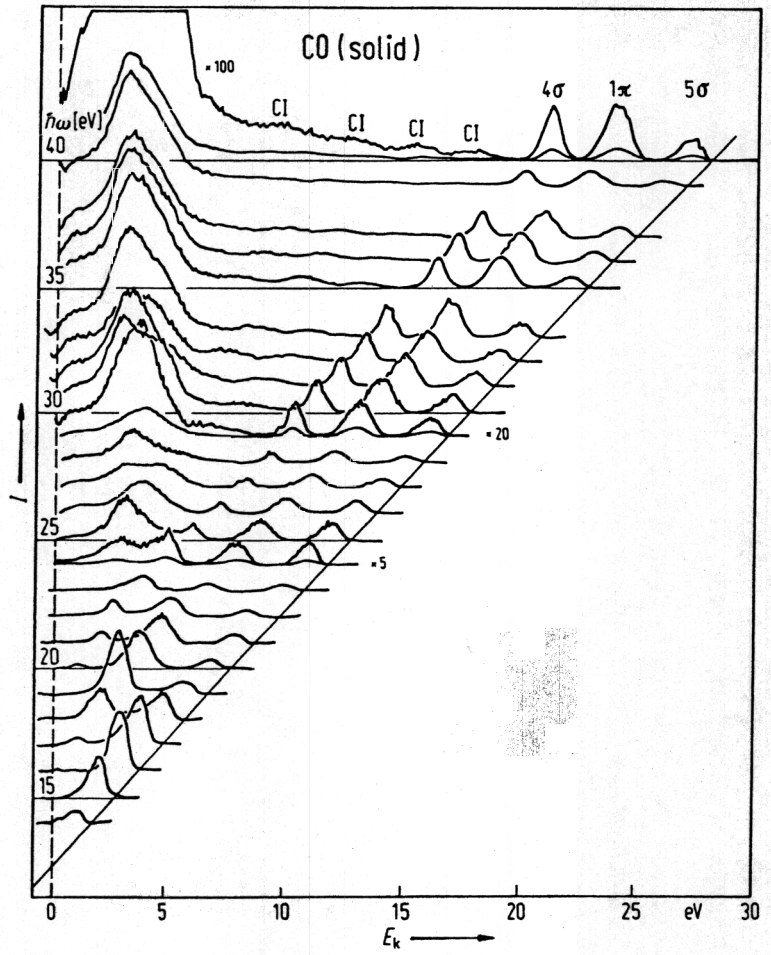

Fig. 17. CO. Electron distribution curves of solid CO as a function of photon energy ($\hbar\omega$: 14 eV···40 eV) [82L2]. CI: configuration interaction structures.

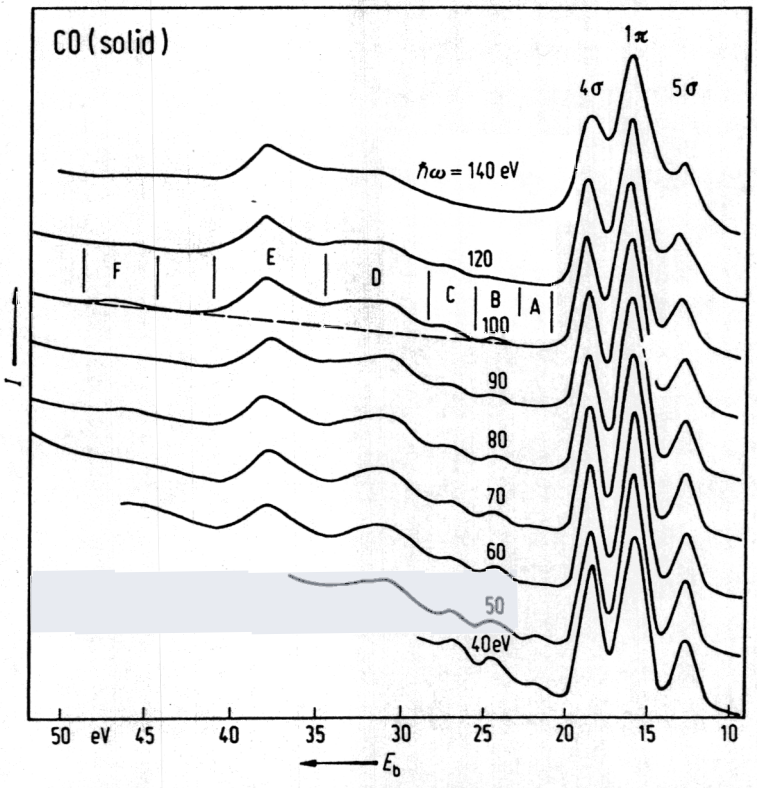

Fig. 18. CO. Electron distribution curves [83E] of solid CO as a function of photon energy. All curves are normalized to show the same intensity for the emission on the $1\pi_u$ orbital. Integration regions for peaks A through F are shown as well as the background correction (dashed curve) for inelastically scattered electrons.

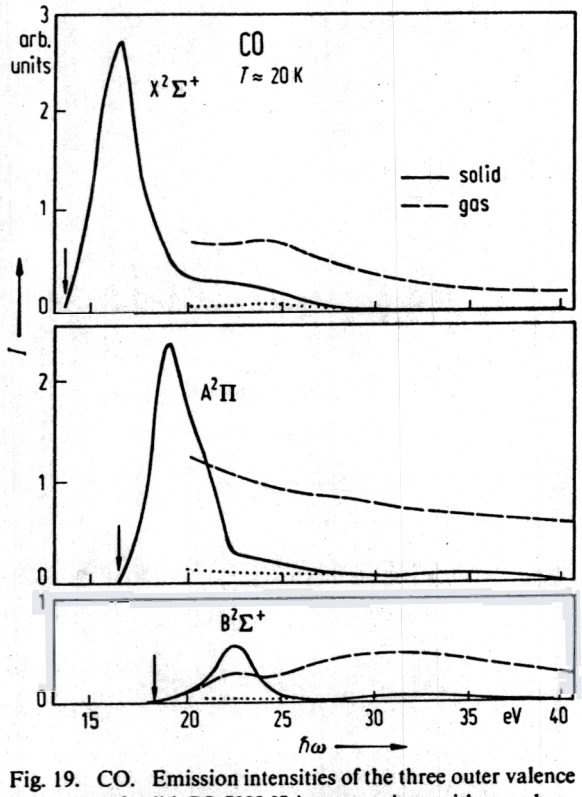

Fig. 19. CO. Emission intensities of the three outer valence ion states of solid CO [82L2] in comparison with gas phase CO [77P1]. Arrows indicate photoemission thresholds.

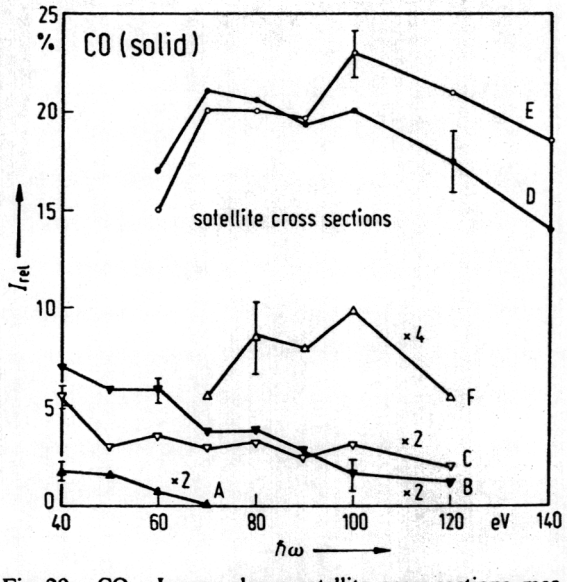

Fig. 20. CO. Inner valence satellite cross-sections measured relative to the outer valence level emission of solid CO [83E]. The integration is carried out for regions A through F (Fig. 18) after background subtraction. Typical errors based on the uncertainty in background subtraction and counting statistics are indicated.

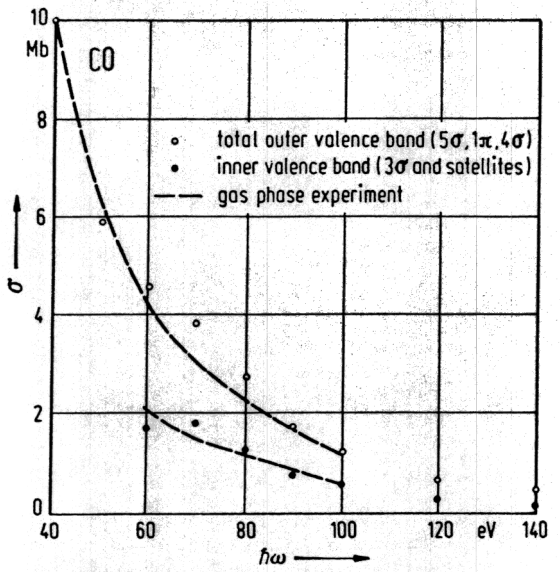

Fig. 21. CO. Partial photoionization cross-section for the inner and outer valence states of CO. The data points are normalized at $\hbar\omega = 40$ eV to the gas phase outer valence results [83K1]. These independently determined data are also shown as dashed lines [83E].

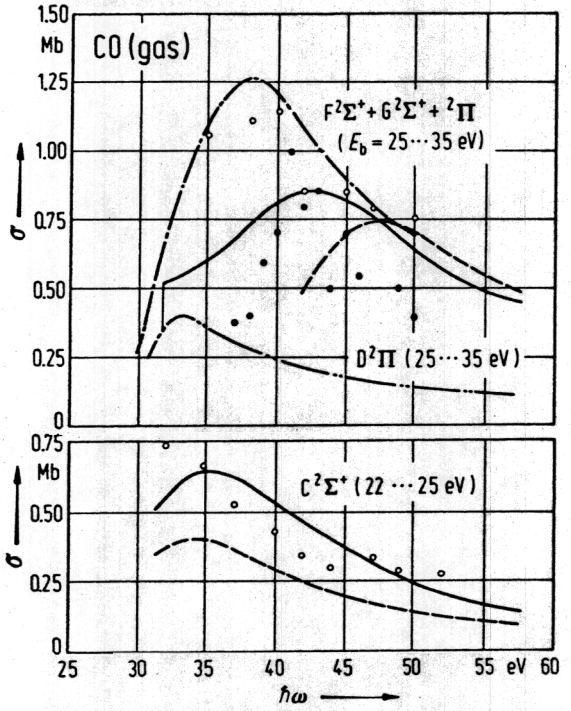

Fig. 22. CO. Inner-valence-shell (A) C $^2\Sigma^+$, (B) D $^2\Pi$, (C) F, G $^2\Sigma^+$-band partial-channel photoionization cross-sections in gaseous CO. (●) synchrotron-radiation measurements [77P1]; (○) dipole (e, 2e) measurements [76H]; (–·–) dipole (e, e+ion) measurements [76W]; (——) POLCI and (– – – –) SECI calculations [81L1] and static-exchange orbital transition moments.

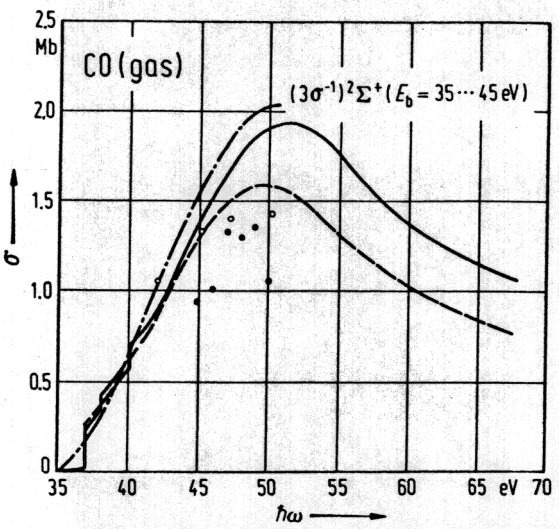

Fig. 23. CO. Inner-valence-shell $^2\Sigma^+$-band partial-channel photoionization cross-section in gaseous CO. (●) synchrotron-radiation measurements [77P1]; (○) dipole (e, 2e) measurements [76H]; (–·–) dipole (e, e+ion) measurements [76W]; (——) POLCI and (– – – –) SECI calculations [81L1] and static-exchange orbital transition moments.

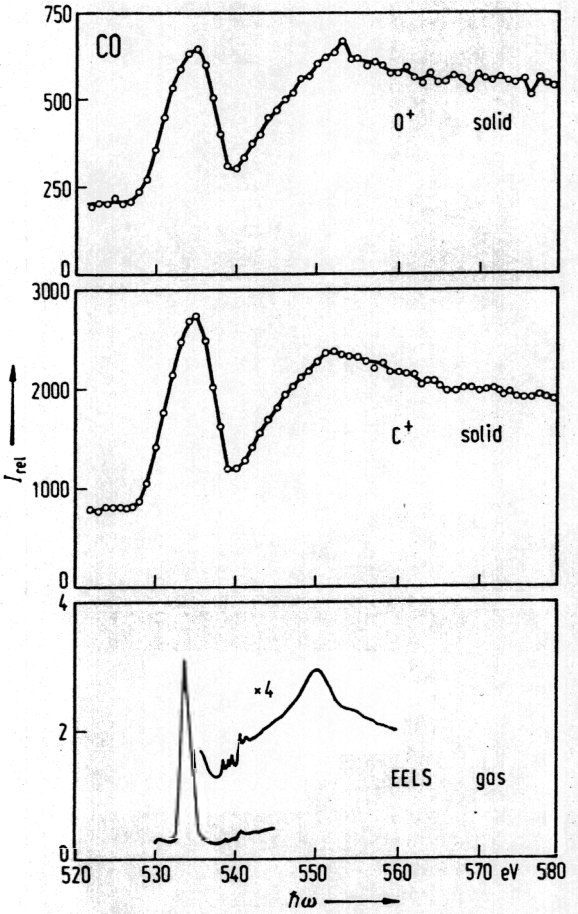

Fig. 24. CO. C^+- and O^+-photoexcitation-yield spectra of solid CO [85R] after O(1s) excitation compared with the EELS spectrum of gaseous CO [80H1].

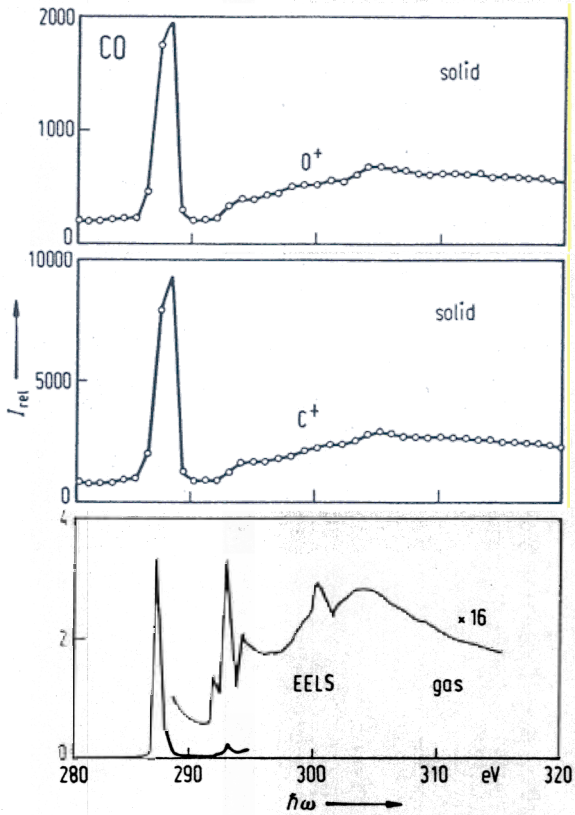

Fig. 25. CO. C^+- and O^+-photoexcitation-yield spectra of solid CO [85R] after C(1s) excitation compared with the EELS spectrum of gaseous CO [80H1].

2.3.3 Oxygen (O_2)

Isolated molecule

1: Point group: $D_{\infty h}$
2: Bond length: 1.208 Å
3: Ground state electron configuration:

$$^3\Sigma_g^-: \quad \underset{O(1s)}{(1\sigma_g)^2\,(1\sigma_u)^2} \;\Big|\; \underset{O(2s),\,O(2p)}{(2\sigma_g)^2\,(2\sigma_u)^2\,(3\sigma_g)^2\,(1\pi_u)^4\,(1\pi_g)^2} \;\Big|\; \underset{\text{empty}}{(3\sigma_u)^0}$$

Molecular solid

a) monoclinic (α) O_2 $T<23$ K [72D1, 85K2]
4: Space group: C2/m (C_{2h}^3)
5: Structure of the solid:

unit cell: monoclinic $a=5.403$ Å, $b=3.429$ Å, $c=5.086$ Å
$\beta=132.53°$

Atomic positions:
(0, 0, 0; 1/2, 1/2, 0) ± X, 0, Z
$X=0.089$ (10), $Z=0.153$ (15)
nearest neighbours: six molecules, 4 at 3.20 (12) Å, 2 at 3.25 (18) Å distance

See also Fig. 26.

b) hexagonal (β) O_2: 24 K < T < 43.6 K [72D1, 85K2]
4: Space group: $R\bar{3}m$
5: Structure of the solid:

unit cell: $a=3.307$ Å, $c=11.256$ Å (at $T<28$ K) [71L1]

Atomic positions:
distorted cubic close packed.
See also Fig. 27.

c) cubic (Γ) O_2 $43.6 < T < 54.4$ K [72D1, 85K2]
4: Space group: Pm3n (O_h^3)
5: Structure of the solid:

unit cell: $a = 6.83$ Å (at 50 K)

Atomic positions:
not reported.

6: Outer valence photoelectron spectrum of the molecular solid [82L2] in comparison with the gas phase [70T]: Fig. 28.
7: Inner valence photoelectron spectrum of the molecular solid in comparison with the gas phase: not reported.
8: Core photoelectron spectrum of the molecular solid in comparison with the gas phase: not reported.
9: Theoretical assignment of the observed ion states [81H]: Table 6.
10: Polarization energies of some ion states: Table 7.
11: Ion state cross-sections as a function of photon energies of solid O_2 in comparison with gaseous O_2: Figs. 29, 30.
12: Table of resonance structures in the cross-sections: not reported.
13: Auger spectrum of the molecular solid in comparison with the gas phase: not reported.
14: Penning ionization electron spectrum of the molecular solid in comparison with the gas phase: not reported.
15: Electronic excitation spectrum in the valence electron region: not reported.
16: Electronic excitation spectrum in the core electron region: Fig. 31.

Table 6. O_2. I. Vertical binding energies E_b (eV), calculated intensities S, and II. weights of important configurations (%) for gaseous O_2 ion states [81H] in comparison with experimental values.

I.

Exp.				Calc. [81H]			
Band no.	Final state[a]	E_b[b] eV	S[b]	State		E_b eV	S
1	$X\ ^2\Pi_g$	12.33	0.15	$^2\Pi_g$	I	12.3	0.08
2	$a\ ^4\Pi_u$	16.70	0.21	$^4\Pi_u$	I	16.5	0.09
3	$A\ ^2\Pi_u$	–	0.23	$^2\Pi_u$	I	17.7	0.01[c]
	$b\ ^4\Sigma_g^-$	18.17		$^4\Sigma_g^-$	I	18.2	0.29
4	$B\ ^2\Sigma_g^-$	20.39	0.15	$^2\Sigma_g^-$	I	20.6	0.13
5	$^2\Pi_u$[b]	23.0	0.14	$^2\Sigma_u^-$	I	24.1	0.03
				$^2\Pi_u$	III	24.3	0.03
6	$c\ ^4\Sigma_u^-$	24.51	1.00	$^4\Sigma_u^-$	I	25.8	1.00
7	$c\ ^2\Sigma_u^-$	27.25	0.35	$^2\Sigma_u^-$	II	29.0	0.23
				$^4\Sigma_u^-$	II	29.0	0.19
8	–	33.6[a]	–	$^2\Sigma_g^-$	V	34.6	0.03
				$^2\Sigma_u^-$	III	34.9	0.22
				$^2\Sigma_u^-$	IV	36.6	0.09
9	$^4\Sigma_g^-$	39.6[a]	–	$^4\Sigma_u^-$	V	41.9	0.07
				$^4\Sigma_g^-$	V	42.2	0.78
				$^2\Sigma_g^-$	VI	42.5	0.08

(continued)

Table 6 (continued)

Exp.				Calc. [81H]		
Band no.	Final state[a])	E_b[b]) eV	S[b])	State	E_b eV	S
10	$^2\Sigma_g^-$	41.6[a])	–	$^2\Sigma_u^-$ VII	44.2	0.05
				$^2\Sigma_u^-$ VIII	46.0	0.03
				$^2\Sigma_g^-$ IX	47.8	0.03
11	–	46[a])	–	$^4\Sigma_g^-$ VIII	50.2	0.06
12	–	48[a])	–	$^2\Sigma_u^-$ IX	51.6	0.03
				$^2\Sigma_g^-$ XI	51.7	0.24
13	–	56[a])	–			

[a]) [71S].
[b]) [76B].

II.

State		Hole configuration		Other configuration (weight ≧ 10%)							
		$2\sigma_g^{-1}$	$3\sigma_g^{-1}$								
$^4\Sigma_g^-$	I		92								
	V	75									
	VIII	6	1	$2\sigma_u^{-1}3\sigma_g^{-1}3\sigma_u$	47	$3\sigma_g^{-2}1\pi_u^{-1}1\pi_g3\sigma_u$	20				
$^2\Sigma_g^-$	I		90								
	V	8		$3\sigma_g^{-1}1\pi_u^{-2}1\pi_g^2$	48	$2\sigma_u^{-1}1\pi_u^{-1}1\pi_g$	34				
	VI	19	1	$2\sigma_u^{-1}1\pi_u^{-1}1\pi_g$	25	$3\sigma_g^{-2}1\pi_u^{-1}1\pi_g3\sigma_u$	20	$3\sigma_g^{-1}1\pi_u^{-2}1\pi_g^2$	18		
	IX	4		$1\pi_u^{-3}1\pi_g3\sigma_u$	75	$3\sigma_g^{-1}1\pi_u^{-2}3\sigma_u^2$	11				
	XI	40		$2\sigma_u^{-1}3\sigma_g^{-1}3\sigma_u$	25	$2\sigma_u^{-1}1\pi_u^{-1}1\pi_g$	16				
		$2\sigma_u^{-1}$									
$^4\Sigma_u^-$	I	71		$3\sigma_g^{-1}1\pi_u^{-1}1\pi_g$	23						
	II	13		$3\sigma_g^{-1}1\pi_u^{-1}1\pi_g$	53	$3\sigma_g^{-2}3\sigma_u$	23				
	V	7		$3\sigma_g^{-2}3\sigma_u$	53	$3\sigma_g^{-1}1\pi_u^{-1}1\pi_g$	11	$2\sigma_u^{-1}3\sigma_g^{-1}1\pi_u^{-1}1\pi_g3\sigma_u$	11		
$^2\Sigma_u^-$	I	3		$3\sigma_g^{-1}1\pi_u^{-1}1\pi_g$	94						
	II	32		$3\sigma_g^{-1}1\pi_u^{-1}1\pi_g$	59						
	III	30		$3\sigma_g^{-2}3\sigma_u$	22	$1\pi_u^{-2}3\sigma_u$	21	$3\sigma_g^{-1}1\pi_u^{-1}1\pi_g$	17		
	IV	11		$1\pi_u^{-2}3\sigma_u$	74						
	VII	5		$3\sigma_g^{-2}3\sigma_u$	37	$2\sigma_u^{-1}1\pi_u^{-2}1\pi_g^2$	20	$2\sigma_g^{-1}1\pi_u^{-1}1\pi_g$	15		
	VIII	7		$2\sigma_g^{-1}1\pi_u^{-1}1\pi_g$ / $3\sigma_g^{-2}1\pi_u^{-2}1\pi_g^2 3\sigma_u$	20 / 13	$3\sigma_g^{-2}3\sigma_u$ / $3\sigma_g^{-1}1\pi_u^{-1}1\pi_g$	16 / 11	$2\sigma_u^{-1}\pi_u^{-2}1\pi_g^2$	16		
	IX	2		$2\sigma_g^{-1}1\pi_u^{-1}1\pi_g$	59	$2\sigma_u^{-1}1\pi_u^{-2}1\pi_g^2$	14	$2\sigma_u^{-1}3\sigma_g^{-1}1\pi_u^{-1}1\pi_g3\sigma_u$	11		
		$1\pi_g^{-1}$									
$^2\Pi_g$	I	87									
		$1\pi_u^{-1}$									
$^4\Pi_u$	I	95									
$^2\Pi_u$	I	93									
	III	61		$3\sigma_g^{-1}1\pi_g^{-1}3\sigma_u$	20	$1\pi_u^{-3}1\pi_g^2$	15				

Table 7. O_2. Vertical binding energies and polarization energies E_{pol}.

State	Vertical binding energies [eV]						E_{pol}**) [eV]
	Solid				Gas		
	[82L2]	[75H1]	[70E1]	[70T]	[71S]	[76B]	
$X\ ^2\Pi_g\ (1\pi_g)$	11.3	10.5*)	12.33	12.01*)	13.1	12.33	1.03···1.9
$a\ ^4\Pi_u\ (1\pi_u)$	15.8	14.5*)	16.7	16.12*)	17.0	16.7	0.9···1.2
$\Delta\ ^2\Pi_u\ (1\pi_u)$			17.73				
$b\ ^4\Sigma_g^-\ (3\sigma_g)$	17.25	16.5*)	18.31	18.17*)	18.8	18.17	0.92···1.55
$B\ ^2\Sigma_g^-\ (3\sigma_g)$	19.4	18.7*)	20.43	20.29*)	21.1	20.39	1.0···1.7
$^2\Pi_u$			24.0			23.0	
$c\ ^4\Sigma_u^-$	23.4	21.5*)	24.58		25.3	24.51	1.11···1.9
$c\ ^2\Sigma_u^-$			27.4		27.9	27.25	

*) Adiabatic binding energies.
**) With respect to E_b (solid) of [82L2].

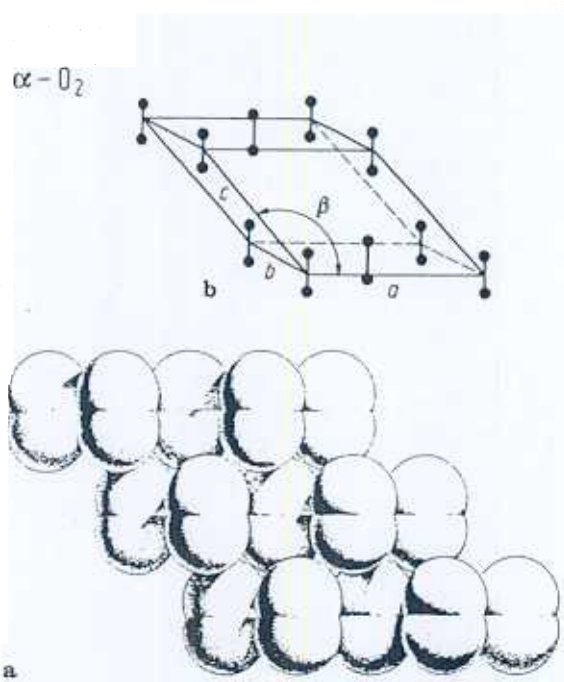

Fig. 26. O_2. (a) Packing drawing of the α-form of solid O_2; (b) schematic of the structure of the α-O_2.

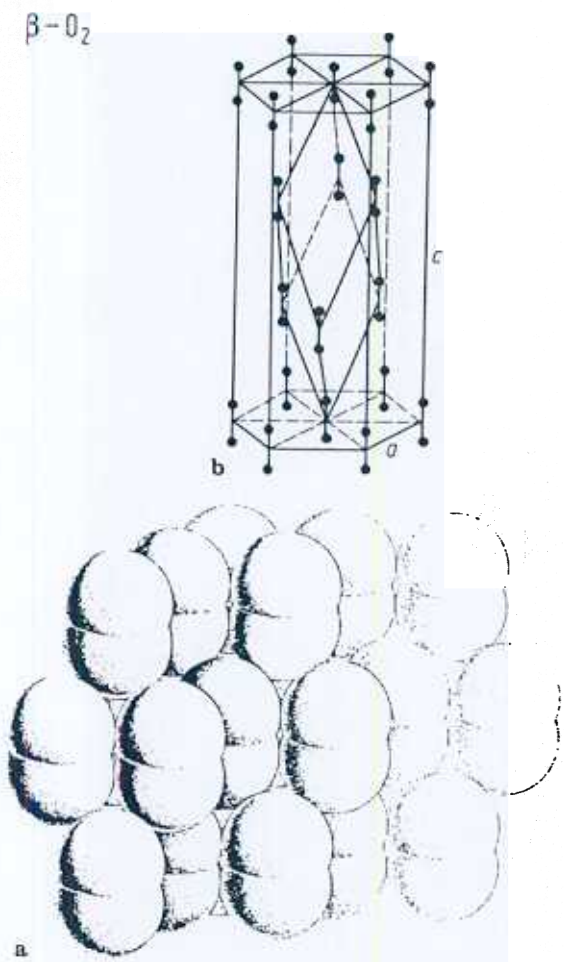

Fig. 27. O_2. (a) Packing drawing of the β-form of solid O_2; (b) schematic of the structure of the β-O_2.

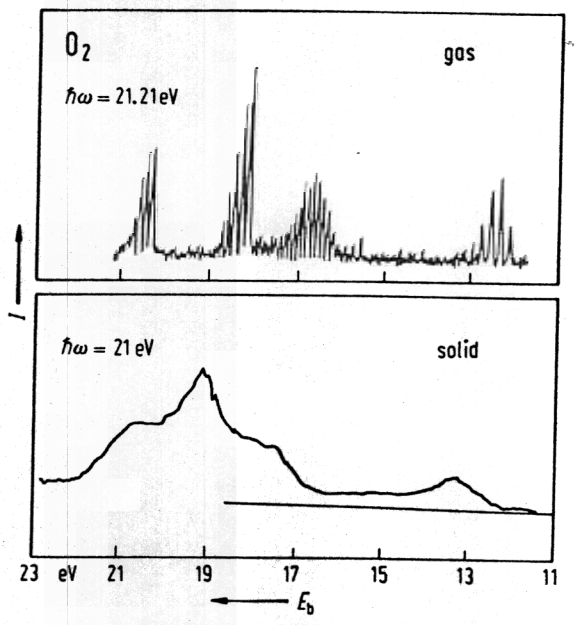

Fig. 28. O_2. Photoelectron spectra of gaseous [70T] and solid [82L2] O_2 in the outer valence region.

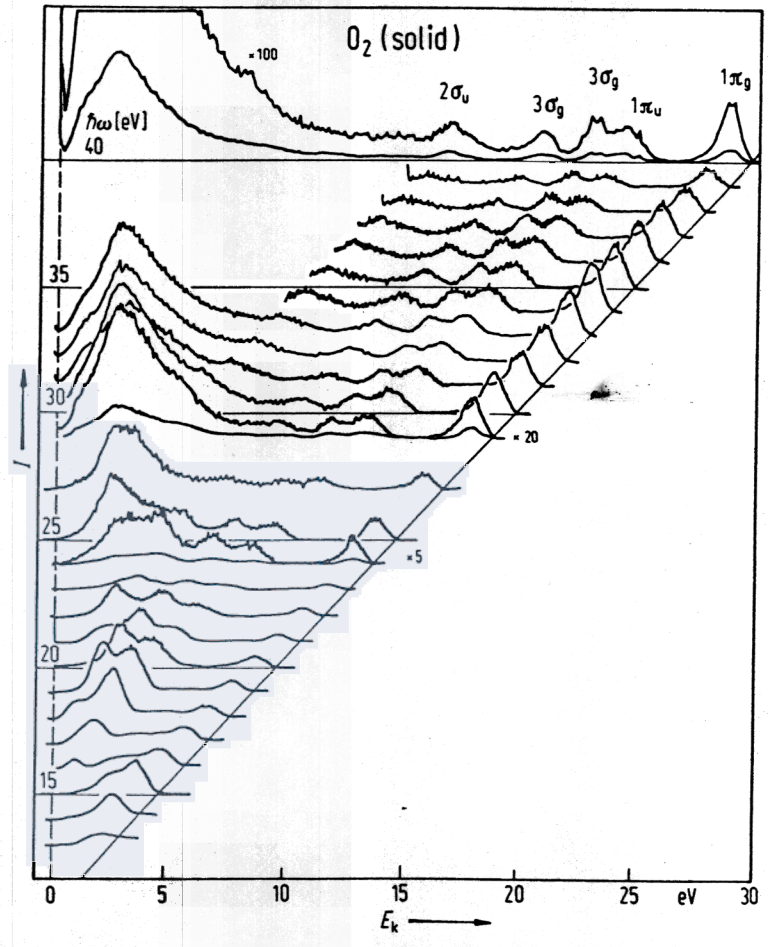

Fig. 29. O_2. Electron distribution curves of solid O_2 as a function of photon energy ($\hbar\omega$: 13···40 eV) [82L2].

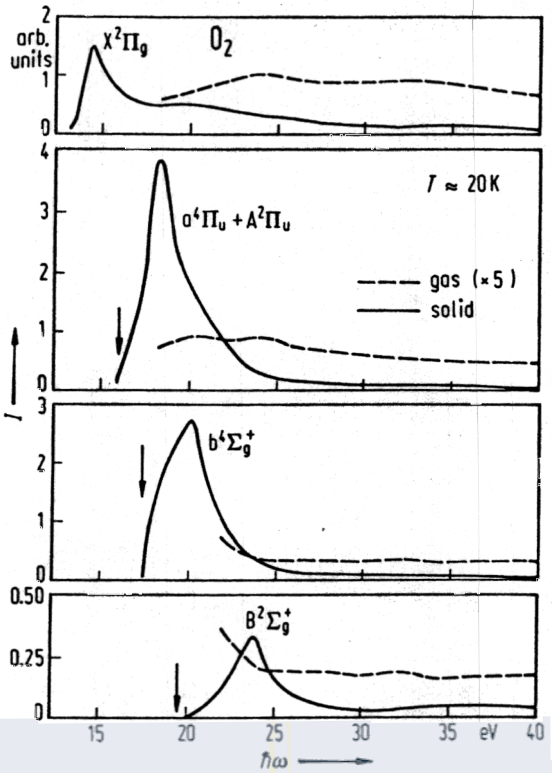

Fig. 30. O_2. Emission intensities of the five outer valence ion states of solid O_2 [82L2] in comparison with gas phase [80G2]. Arrows indicate photoemission thresholds.

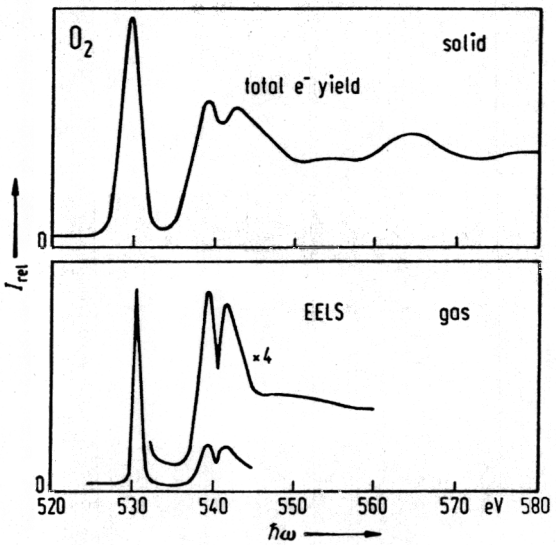

Fig. 31. O_2. e^-photoexcitation-yield spectra of solid O_2 [85R] compared with the EELS spectrum of gaseous O_2 [80H1].

2.3.4 Nitric oxide (NO)

Isolated molecule

1: Point group: $C_{\infty v}$
2: Bond length: 1.12 Å
3: Ground state electron configuration:

$^2\Pi$:	$(1\sigma)^2(2\sigma)^2$	$(3\sigma)^2(4\sigma)^2(1\pi)^4(5\sigma)^2(2\pi)^1$	$(6\sigma)^0$
	O(1s) N(1s)	O(2s), N(2s), O(2p), N(2p)	empty

Molecular solid

Monoclinic NO [61L, 65W]
4: Space group: C_{2h}^5 ($P2_1/a$)
5: Structure of the solid:

unit cell: $a = 6.68$ Å, $b = 3.96$ Å, $c = 6.55$ Å
$\beta = 127°54'$

Atomic positions:
$\pm(x, y, z; x+1/2, 1/2-y, z)$
dimer formation

See also Fig. 32.

6: Outer valence photoelectron spectrum of the molecular solid [84B1] in comparison with the gas phase [70E2, 71E, 82S2, 87F2]: Fig. 33.
7: Inner valence photoelectron spectrum of the molecular solid in comparison with the gas phase: not reported.
8: Core photoelectron spectra of the molecular solid [83T] in comparison with the gas phase [71S]: Figs. 34, 35.
9: Theoretical assignment of the observed ion states [81H]: Table 8.
10: Polarization energies of some ion states: Table 9.
11: Ion state cross-sections as a function of photon energies of solid NO in comparison with gaseous NO: Figs. 36···38.
12: Table of resonance structures in the cross-sections: not reported.
13: Auger spectrum of the molecular solid in comparison with the gas phase: not reported.
14: Penning ionization electron spectrum of the molecular solid in comparison with the gas phase: not reported.
15: Electronic excitation spectrum in the valence electron region: not reported.
16: Electronic excitation spectrum in the core electron region: Fig. 39.

Table 8. NO. I. Vertical binding energies E_b (in eV), calculated intensities S, and II. weights of important configurations (%) for gaseous NO ion states [81H] in comparison with experimental values [71S].

I.

Exp. [71S]			Calc [81H]			
Band no.	Final state	E_b eV	State		E_b eV	S
1	$X\,^1\Sigma^+$	10	$^1\Sigma^+$	I	9.6	0.05
2	$a\,^3\Sigma^+$	14	$^3\Sigma^+$	I	15.0	0.04
3	$^3\Pi$	16.7	$^3\Pi$	I	15.6	0.56
			$^3\Delta$	I	16.8	0.07
4	$A\,^1\Pi$	18.5	$^1\Pi$	I	17.4	0.14
5	$^3\Pi$	21.7	$^3\Pi$	II	21.3	1.00
			$^3\Pi$	III	22.3	0.09
			$^1\Pi$	II	22.4	0.19
6	$^1\Pi$	23.3	$^3\Pi$	IV	24.4	0.40
–	–	–	$^1\Pi$	III	26.4	0.07
			$^1\Pi$	IV	27.1	0.20
7	–	≈31	$^1\Pi$	V	30.3	0.11
			$^3\Pi$	VIII	30.6	0.07
			$^3\Pi$	IX	31.4	0.05
–	–	–	$^1\Pi$	VII	34.0	0.05
			$^3\Pi$	XV	36.4	0.11
8	$^3\Pi$	40.6	$^3\Pi$	XVIII	39.7	0.07
			$^3\Pi$	XIX	40.6	0.04
			$^3\Pi$	XX	41.6	0.22
			$^1\Pi$	XIV	41.7	0.04
			$^3\Pi$	XXI	42.3	0.72
			$^3\Pi$	XXII	42.9	0.12
			$^1\Pi$	XV	44.0	0.17
9	$^1\Pi$	43.8				

(continued)

Table 8 (continued)

II.

State		Hole configuration			Other configuration (weight ≥ 10%)					
		$3\sigma^{-1}$	$4\sigma^{-1}$	$5\sigma^{-1}$						
$^3\Pi$	I		1	84						
	II		52	4	$5\sigma^{-1}1\pi^{-1}2\pi$	33				
	III		5	1	$5\sigma^{-1}1\pi^{-1}2\pi$	86				
	IV		22		$5\sigma^{-1}1\pi^{-1}2\pi$	69				
	VIII		3		$5\sigma^{-1}1\pi^{-1}2\pi$	37	$4\sigma^{-1}1\pi^{-1}2\pi$	19	$5\sigma^{-2}6\sigma$	14
	IX	4		1	$4\sigma^{-1}1\pi^{-1}2\pi$	44	$5\sigma^{-1}1\pi^{-2}2\pi^2$	26		
	XV	6			$4\sigma^{-1}1\pi^{-1}2\pi$	25	$5\sigma^{-1}1\pi^{-2}2\pi^2$	22	$1\pi^{-2}6\sigma$	16
					$4\sigma^{-1}1\pi^{-2}2\pi^2$	14				
	XVIII	1	2		$5\sigma^{-2}6\sigma$	32	$4\sigma^{-1}5\sigma^{-2}2\pi^2$	23		
	XIX	2		1	$4\sigma^{-1}5\sigma^{-2}2\pi^2$	47				
	XX	14			$4\sigma^{-1}5\sigma^{-2}2\pi^2$	13	$4\sigma^{-1}1\pi^{-2}2\pi^2$	12		
	XXI	38	1		$4\sigma^{-1}1\pi^{-2}2\pi^2$	13				
	XXII	6			$4\sigma^{-1}5\pi^{-1}6\sigma$	20	$4\sigma^{-1}1\pi^{-2}2\pi^2$	15	$5\sigma^{-2}1\pi^{-1}2\pi6\sigma$	10
					$3\sigma^{-1}1\pi^{-1}2\pi$	11				
$^1\Pi$	I			85						
	II		26′		$5\sigma^{-1}1\pi^{-1}2\pi$	63				
	III		10		$5\sigma^{-1}1\pi^{-1}2\pi$	78				
	IV		29		$5\sigma^{-1}1\pi^{-1}2\pi$	58				
	V	6	6	3	$4\sigma^{-1}1\pi^{-1}2\pi$	35	$5\sigma^{-1}1\pi^{-2}2\pi^2$	21	$1\pi^{-1}2\pi^{-1}6\sigma$	14
	VII	3	8		$5\sigma^{-1}1\pi^{-1}2\pi$	37	$5\sigma^{-2}6\sigma$	18	$4\sigma^{-1}1\pi^{-1}2\pi$	14
	XIV	2	2		$5\sigma^{-2}6\sigma$	40				
	XV	29	1	1	$4\sigma^{-1}1\pi^{-1}2\pi$	11				
		$1\pi^{-1}$	$2\pi^{-1}$							
$^1\Sigma^+$	I	1	85							
$^3\Sigma^+$	I	91								
$^3\Delta$	I	92								

Table 9. NO. Vertical binding energies and polarization energies E_{pol}.

State		Vertical binding energies [eV]			E_{pol} [eV]
		Solid	Gas		
		[84B1]	[71E, 70E1]	[87F2]	
$X\ ^1\Sigma^+$	(2π)	8.25	9.55	9.7	1.3
$a\ ^3\Sigma^+$	(1π)		16.1	16.1	
$b\ ^3\Pi$	(5σ)	14.6	16.6	16.6	2.0
$w\ ^3\Delta$	(1π)		17.3	17.2	
$b'\ ^3\Sigma^-$	(1π)		17.9	17.9	
$A'\ \Sigma^-$	(1π)	16.0	18.4	18.4	2.4
$w\ ^1\Delta$	(1π)		18.5	18.9	
$A\ ^1\Pi$	(5σ)		18.3	18.3	
$c\ ^3\Pi$	(4σ)			21.7	
$B\ ^1\Pi$	$4\sigma)$	20.5	21.7		1.2
$B'\ ^1\Sigma^+$	(1π)			23.3	
				24.8	
				26.6	
				29.2	
				29.8	

(continued)

Table 9 (continued)

State	Vertical binding energies [eV]			E_{pol} [eV]
	Solid	Gas		
	[84B1]	[71E, 70E1]	[87F2]	
$B'\ ^1\Sigma^+$ (1π)			30.3	
			31.1	
			32.0	
			32.6	
			33.9	
			34.6	
			35.3	
			36.0	
			37.8	
3σ			39.2	
3σ			40.4	
			45.1	

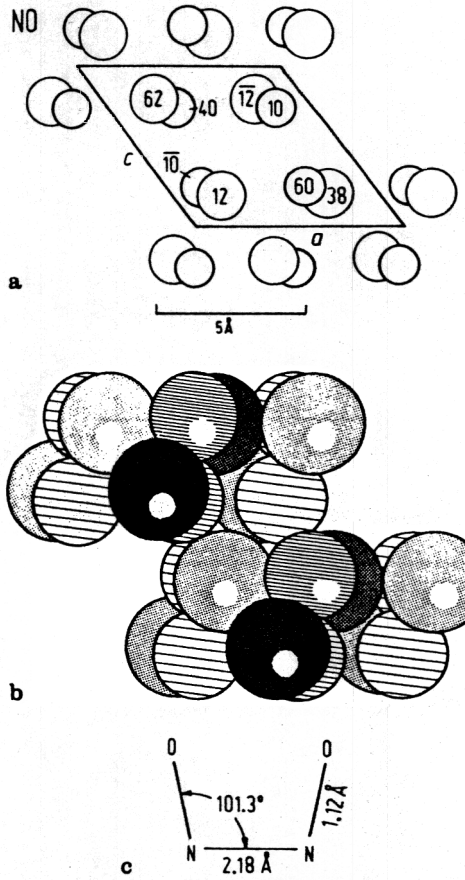

Fig. 32. NO. (a) A projection along *b* of the monoclinic structure of N_2O_2. Nitrogen and oxygen atoms cannot be distinguished experimentally. Origin in lower left [65W]. Fractional *b* coordinates are indicated (× 100). (b) A packing drawing of the monoclinic N_2O_2 structure viewed along the *b* axis. It is not known whether the dotted or the hatched atoms are oxygen [65W]. (c) Geometry of the N_2O_2 dimer [71B].

For Fig. 33 see next page.

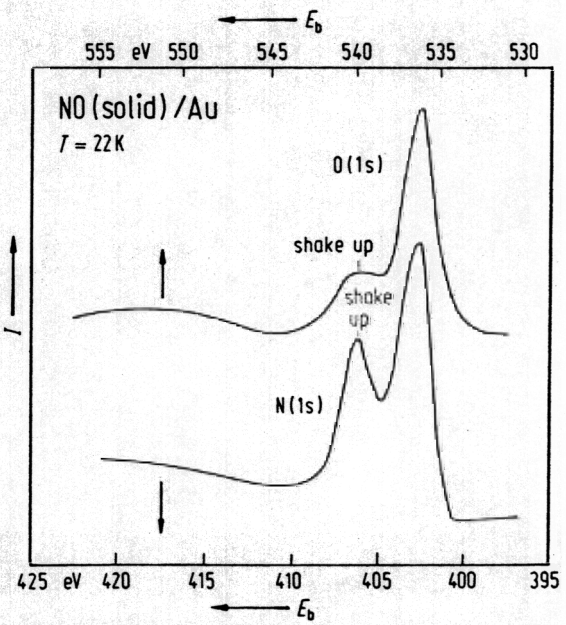

Fig. 34. NO. X-ray induced N(1s) and O(1s) spectra of solid [83T] NO at $T = 22$ K. The binding energy is given relative to the Fermi energy of the substrate (Au).

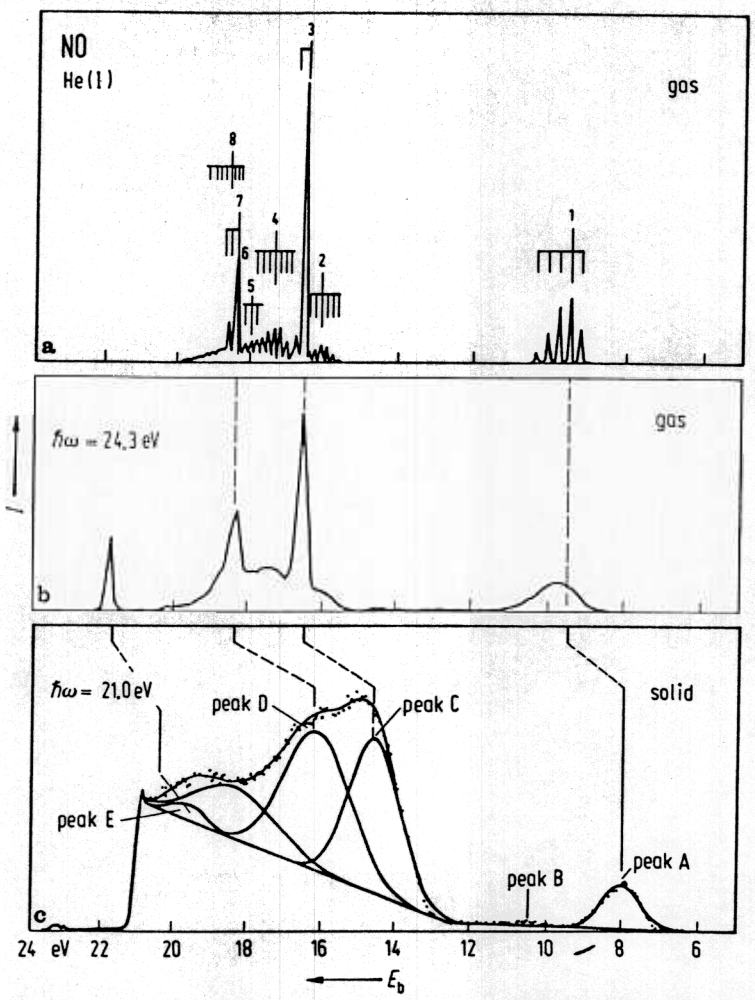

Fig. 33. NO. Photoelectron spectra of gaseous [70E2, 71E, 82S2] and solid [84B1] NO in the outer valence region. Solid lines in (c): Lorentzian fit to the measured spectrum.

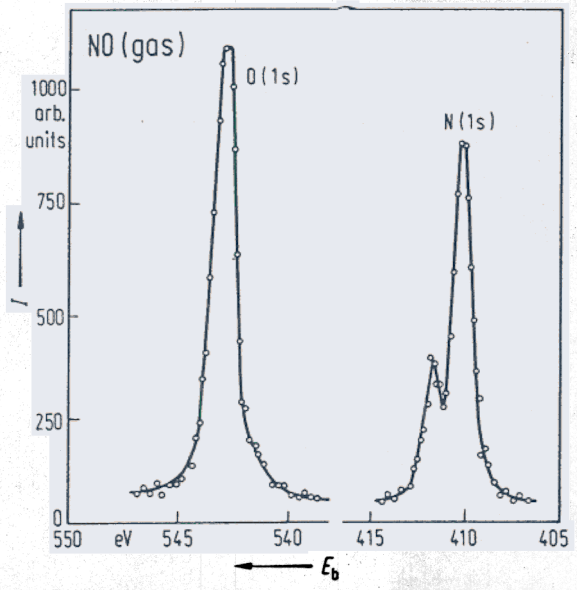

Fig. 35. NO. X-ray induced N(1s) and O(1s) spectra of gaseous NO [71S]. Binding energy relative to E_{vac}.

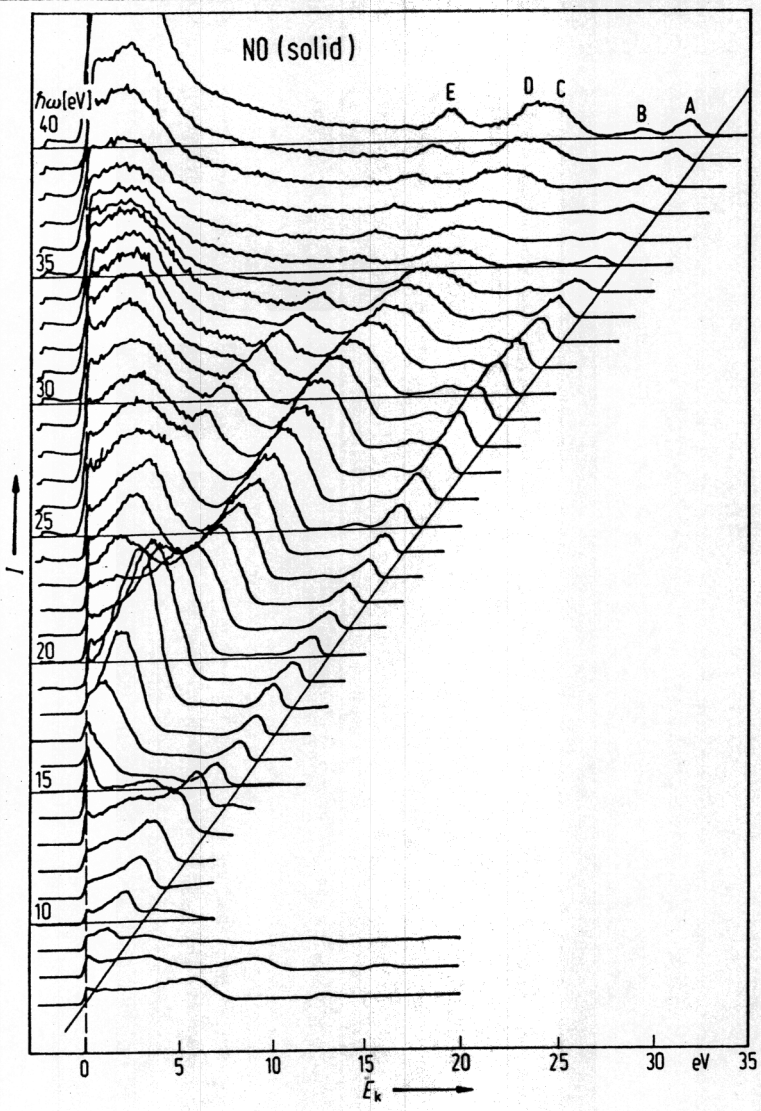

Fig. 36. NO. Electron distribution curves of solid NO as a function of photon energy ($\hbar\omega$: 7···40 eV) [84B1].

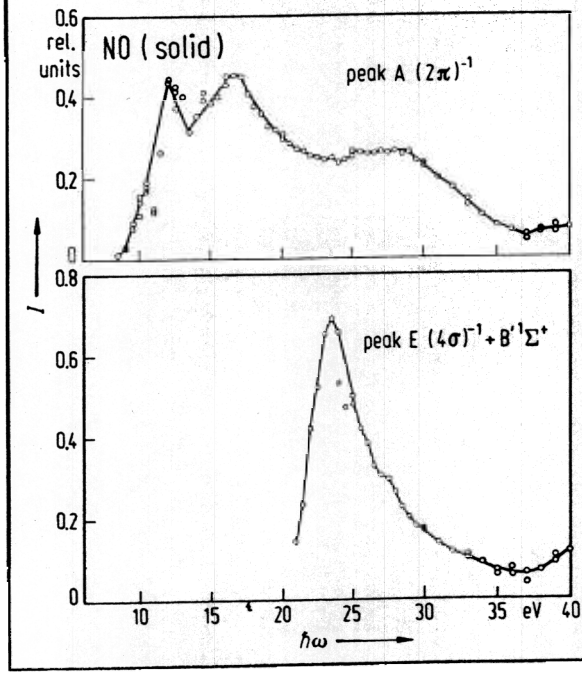

Fig. 37. NO. Emission intensities of some outer valence ion states of solid NO [84B1]. Cf. Fig. 36 for peaks A, E.

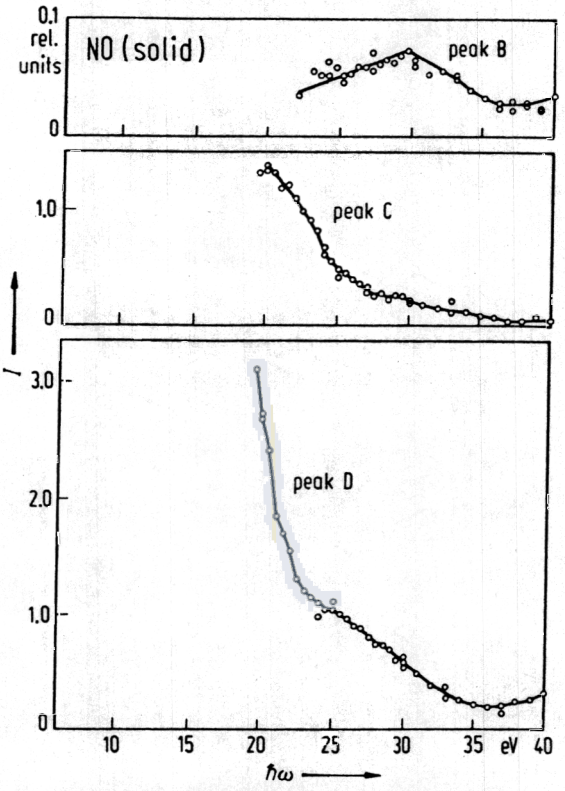

Fig. 38. NO. Emission intensities of some outer valence ion states of solid NO [84B1]. Peaks B, C, D, see Fig. 36.

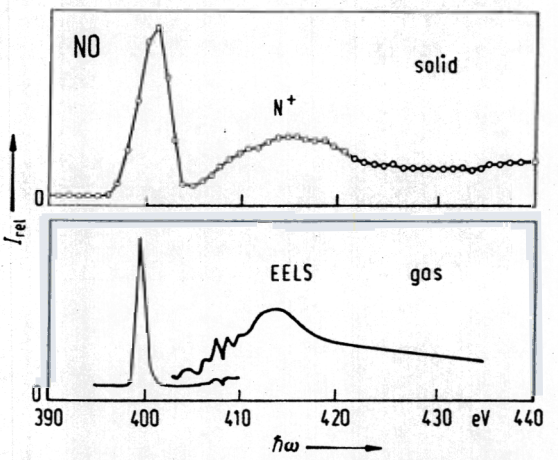

Fig. 39. NO. N^+ photon-ion-yield spectra from solid NO [85R] in the N(1s) region compared with the EELS spectrum of gaseous NO [74W].

2.3.5 Iodine (I_2)

Isolated molecule

1: Point group: $D_{\infty h}$

2: Bond length: 2.70 Å

3: Ground state electron configuration:

$$
{}^1\Sigma_g^+:\quad
\begin{array}{|c|c|c|}
\hline
\begin{array}{c}56\text{ electrons}\\2\text{ Kr-cores}\end{array} & \begin{array}{c}(7\sigma_g)^2(7\sigma_u)^2\\ \text{I(4s)}\end{array} & \begin{array}{c}(8\sigma_g)^2(4\pi_u)^4(4\pi_g)^4(8\sigma_u)^2\\ \text{I(4p)}\end{array}\\
\hline
\multicolumn{3}{|c|}{\begin{array}{c}(9\sigma_g)^2(5\pi_u)^4(2\delta_g)^4(2\delta_u)^4(5\pi_g)^4(9\sigma_u)^2\\ \text{I(4d)}\end{array}}\\
\hline
\multicolumn{3}{|c|}{\begin{array}{c}(10\sigma_g)^2(6\pi_u)^4(3\delta_g)^4(1\Phi_u)^4(1\Phi_g)^4(3\delta_u)^4(6\pi_g)^4(10\sigma_u)^2\\ \text{I(4f)}\end{array}}\\
\hline
\begin{array}{c}(11\sigma_g)^2(11\sigma_u)^2\\ \text{I(5s)}\end{array} & \begin{array}{c}(12\sigma_g)^2(7\pi_u)^4(7\pi_g)^4\\ \text{I(5p)}\end{array} & \begin{array}{c}(11\sigma_u)^0\\ \text{empty}\end{array}\\
\hline
\end{array}
$$

Molecular solid

4: Space group: V_h^{18}(Bmab) [65W]; (Cmca) [71L1]

5: Structure of the solid:

unit cell: orthorhombic; $a=7.27$ Å, $b=9.79$ Å, $c=4.79$ Å ($T=291$ K) [65W, 71L1]

Atomic positions:

$\pm(0, u, v; 1/2, u+1/2, v; 1/2, u, v+1/2; 0, u+1/2, 1/2-v)$

$u=0.1156$, $v=0.1493$

nearest neighbour distance of molecules (center): 3.54 Å

See also Fig. 40.

6: Outer valence photoelectron spectrum of the molecular solid [87Y] in comparison with the gas phase [71C, 71P]: Fig. 41.
7: Inner valence photoelectron spectrum of the molecular solid [81S2] in comparison with the gas phase [71P, 81S1]: Fig. 42.
8: Core photoelectron spectra of the molecular solid in comparison with the gas phase [81S1]: Figs. 43, 44.
9: Theoretical assignment of the observed ion states:
not reported.
10: Polarization energies of some ion states: Table 10.
11: Ion state cross-sections as a function of photon energies of solid I_2 in comparison with gaseous I_2:
not reported.
12: Table of resonance structures in the cross-sections:
not reported.
13: Auger spectrum of the molecular solid in comparison with the gas phase:
not reported.
14: Penning ionization electron spectrum of the molecular solid in comparison with the gas phase:
not reported.
15: Electronic excitation spectrum in the valence electron region:
not reported.
16: Electronic excitation spectrum in the core electron region:
not reported.

Table 10. I_2. Vertical binding energies and polarization energies of some ion states [87Y].

State	Vertical binding energies [eV]		E_{pol} [eV]
	Solid [87Y]	Gas [71P]	
$^2\Pi_{3/2g}$	7.2	9.4	2.2
$^2\Pi_{1/2g}$	7.8	10.0	2.2
$^2\Pi_{3/2u}$	8.8	11.0	2.2
$^2\Pi_{1/2u}$	10.1	11.8	1.7
Σ_g^+	11.4	12.9	1.5

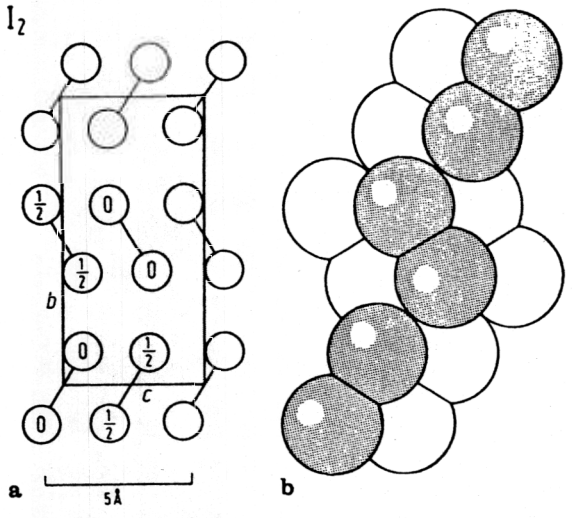

Fig. 40. I_2. (a) Projection drawing of solid I_2 along the *a* direction. (b) Packing drawing of solid I_2 along the *a* direction [65W].

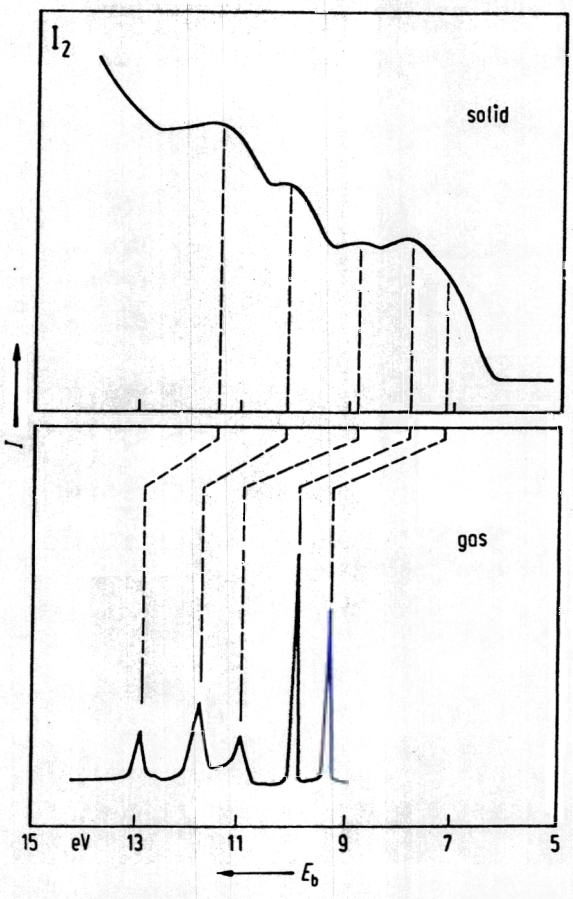

Fig. 41. I_2. Photoelectron spectra of gaseous [71C] and solid [87Y] I_2 in the outer valence electron region.

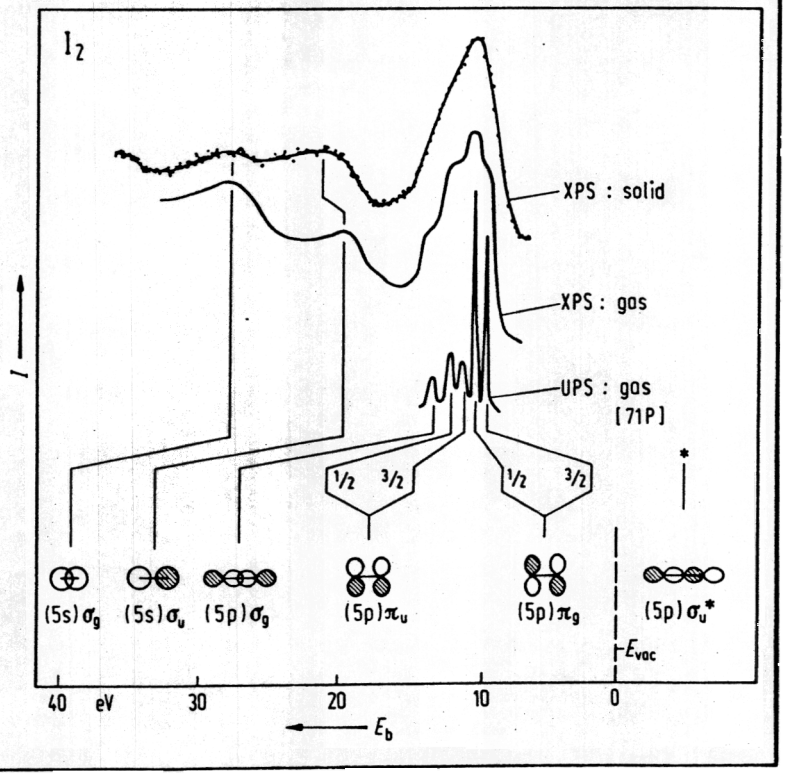

Fig. 42. I_2. Photoelectron spectra of gaseous [81S1, 71P] and solid [81S1] I_2 in the outer and inner valence electron region. Energy scale is that for the gas phase spectra. Schematic atomic-orbital representation of the one-electron inital state giving rise to peak in the spectra is shown.

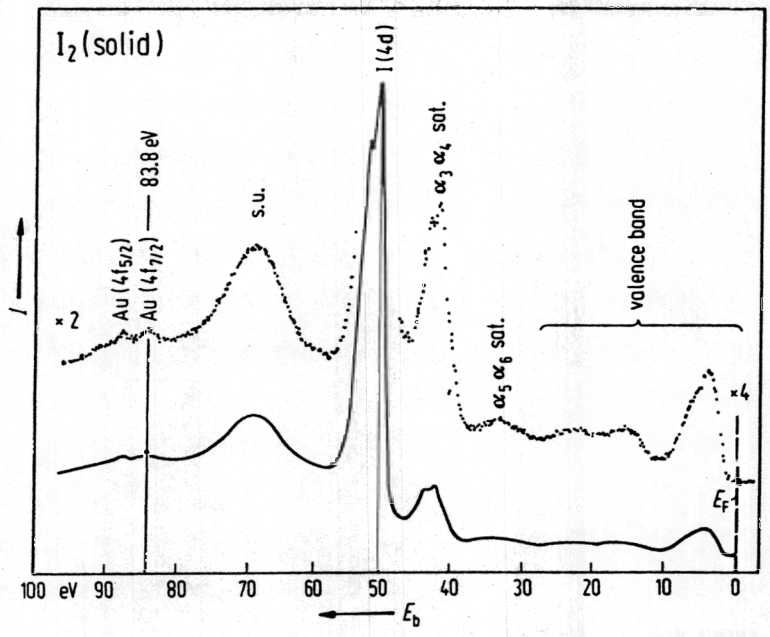

Fig. 43. I_2. Photoelectron spectrum of solid I_2 between 0···90 eV binding energy [81S1]. A weak Au($4f_{5/2,\ 7/2}$) doublet is seen from the substrate and was used to calibrate the E_b-spectrum. s.u. = shake-up satellite. $\alpha_i$sat: satellites due to non-monochromatized radiation.

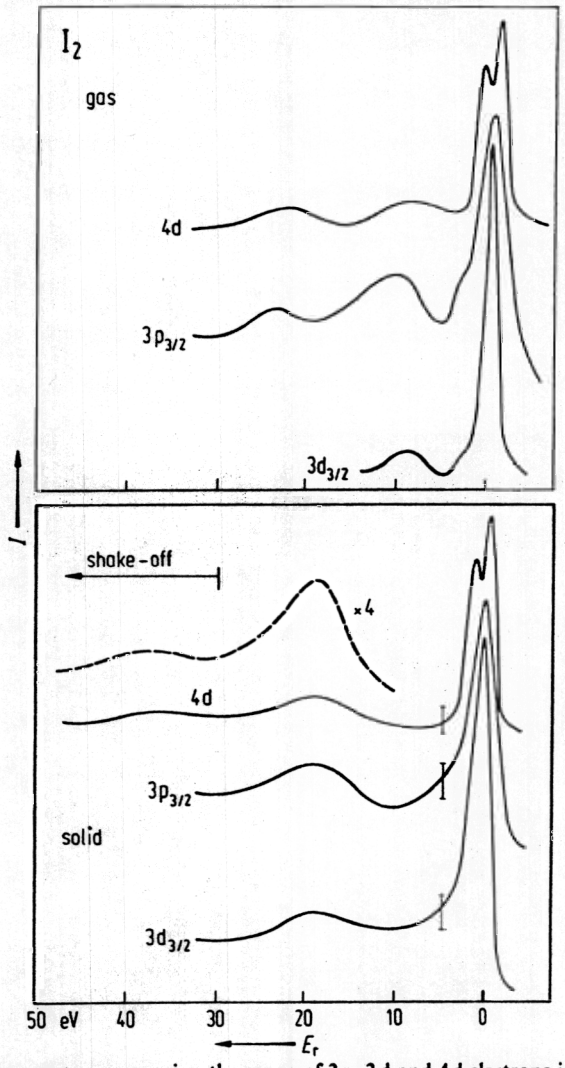

Fig. 44. I_2. Core-photoelectron spectra concerning the range of 3p, 3d and 4d electrons in the gas- and in the solid-phase [81S1]. E_r: relative binding energy.

2.3.6 Water (H_2O)

Isolated molecule

(See also [87L].)

1: Point group: C_{2v}

2: Bond length and bond angles: O–H: 0.976 Å
H–O–H: 107.2°

3: Ground state electron configuration:

$^1A_1$: $(1a_1)^2 \mid (2a_1)^2 (1b_2)^2 (3a_1)^2 (1b_1)^2 \mid (4a_1)^0 (2b_2)^0$

O(1s) O(2s), O(2p), H(1s) empty

Molecular solid

a) Hexagonal ice (I) [65W], [75L]

4: Space group: $D_{6h}^4(P6_3/mmc)$

5: Structure of the solid:

unit cell: $a = 4.5190$ Å, $c = 7.3616$ Å ($T = -10$ °C) [75L]

Atomic positions:
oxygen atoms: $\pm(1/3, 2/3, u; 2/3, 1/3, u+1/2)$
$u = 1/16$ at $T = -20$ °C

See also Fig. 45.

b) Cubic ice (Ic) [65W], [75L]

4: Space group: $O_h^7(Fd3m)$

5: Structure of the solid:

unit cell: $a = 6.35$ Å ($T = -185$ °C) [75L]

Atomic positions:
oxygen atoms: (0, 0, 0; 1/4, 1/4, 1/4; F.C.)

c) Tetragonal ice (III) [65W]; (acc. to [75L] H_2O(IX))

4: Space group: $D_4^{4\cdot 8}(P4_{1,3}2_12)$

5: Structure of the solid:

unit cell: $a = 6.73$ Å, $c = 6.83$ Å, $p = 1$ bar, $T = -175$ °C [75L]

Atomic positions:
oxygen atoms:
$(u, u, 0; \bar{u}, \bar{u}, 1/2; 1/2-u, u+1/2, 1/4; u+1/2, 1/2-u, 3/4)$
$u = 0.392$
each oxygen atom is tetrahedrally surrounded by four others at distances 2.73 ··· 2.90 Å.

See also Fig. 46.

6: Outer valence photoelectron spectrum of the molecular solid [82C1, 79C, 77M] in comparison with the gas phase [82C1, 70T, 77M]: Figs. 47 ··· 49.

7: Inner valence photoelectron spectrum of the molecular solid in comparison with the gas phase [77M]: see Fig. 51.

8: Core photoelectron spectra of the molecular solid [77M] in comparison with the gas phase [77M]: Fig. 50.

9: Theoretical assignment of the observed ion states [72C1, 82C2, 82N]: Tables 11 ··· 13.

10: Polarization energies of some ion states: Table 14.

11: Ion state cross-sections as a function of photon energies of solid H_2O in comparison with gaseous H_2O:
not reported.

12: Table of resonance structures in the cross-sections:
not reported.
13: Auger spectrum of the molecular solid in comparison with the gas phase:
not reported.
14: Penning ionization electron spectrum of the molecular solid [81Y] in comparison with the gas phase [77C]: Fig. 51.
15: Electronic excitation spectrum in the valence electron region:
not reported.
16: Electronic excitation spectrum in the core electron region [70O]: see Fig. 52 in comparison with the core photoelectron spectrum.

Table 11. H_2O. Calculated ion state energies of gaseous H_2O [71M].

Level	E_b [eV]
$1b_1$	12.4
$3a_1$	14.6
$1b_2$	18.7
$2a_1$	32.4
$1a_1$	540.0

For Table 12 see next page.

Table 13. H_2O. Calculated shake-up satellite energies accompanying the O(1s) spectrum of gaseous H_2O [75Å, 76S]. (See Fig. 52 for comparison with experiment.)

Line No.	Calculated vertical binding energies[a][c] eV	Transition[a]
1	15.91	
	17.28	$3a_1$–$4a_1$
	19.83	$1b_1$–$2b_1$
2	20.81	$1b_2$–$2b_2$
	21.22	$3a_1$–$5a_1$
3	21.98	$1b_1$–$2b_1$
4	22.93	$3a_1$–$5a_1$
5	24.60	$1b_2$–$2b_2$
6	[b]	Shake-off
7	34.73	
	36.31	$2a_1$–$4a_1$

[a] From [76S].
[b] From [75Å].
[c] Relative to O(1s).

Table 14. H_2O. Vertical binding energies and polarization energies E_{pol} of some ion states.

Level	Vertical binding energies [eV]		E_{pol}
	Solid [77M]	Gas [77M]	eV
$1b_1$	11.0	12.6	1.6
$3a_1$	13.4	14.7	1.3
$1b_2$	17.3	18.6	1.3
$2a_1$	31.0	32.1	1.1
$1a_1$	538.0	539.9	1.9

Table 12. H_2O. Calculated ion state energies in the inner valence electron region of gaseous H_2O [82N], [80Å].

Peak	[80Å]			[82N] Basis A			[82N] Basis B		
	Transition energy [eV]*)	Relative intensity	Main configuration	Transition energy [eV]*)	Relative intensity	Main configuration	Transition energy [eV]*)	Relative intensity	Main configuration
1	27.24	6.6	0.93 $1b_1^{-2}4a_1^*$	32.39	100	0.84 $2a_1^{-1}$	32.12	100	0.76 $2a_1^{-1}$
2	31.48	100	0.82 $2a_1^{-1}$	34.89	23	1.17 $1b_1^{-2}4a_1^*$	34.04	48	0.62 $1b_1^{-2}6a_1^*$
3	32.29	2.5	0.87 $3a_1^{-2}4a_1^*$				36.68	1.1	0.62 $3a_1^{-2}6a_1^*$
4	35.37	16	0.73 $3a_1^{-1}1b_2^{-1}2b_2^*$				39.32	1.3	0.64 $1b_1^{-1}3a_1^{-1}3b_1^*$
5	35.97	14	0.69 $3a_1^{-1}1b_2^{-1}2b_2^*$				40.42	1.4	0.53 $3a_1^{-1}1b_1^{-1}3b_1^*$
6				40.70	6.6	0.88 $1b_2^{-1}3a_1^{-1}2b_2^*$	40.97	3.5	0.61 $3a_1^{-1}1b_2^{-1}4b_2^*$

*) Transition energy is relative to the ground-state energy, −76.04111 a.u. [80Å], −76.24749 a.u. [82N, Basis A], −76.26128 a.u. [82N, Basis B].

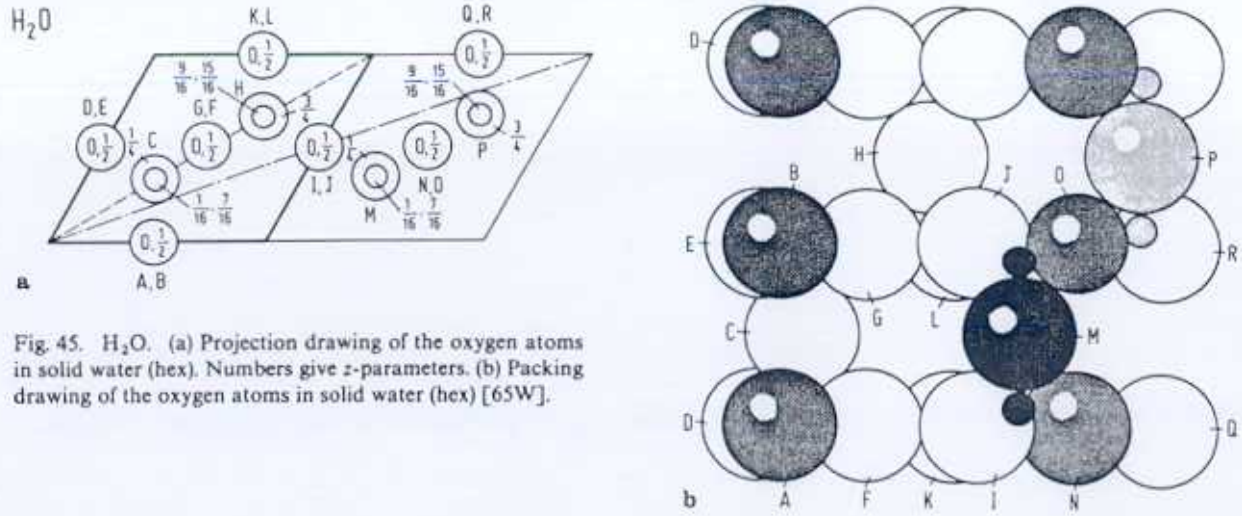

Fig. 45. H_2O. (a) Projection drawing of the oxygen atoms in solid water (hex). Numbers give z-parameters. (b) Packing drawing of the oxygen atoms in solid water (hex) [65W].

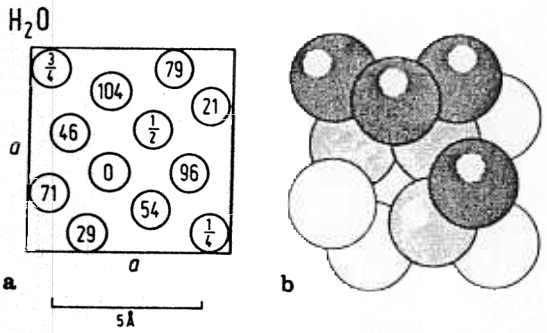

Fig. 46. H_2O. (a) A projection along the c axis showing the distribution of the oxygen atoms in the tetragonal high-pressure modification III of ice. Fractional c coordinates of O atoms are indicated ($\times 100$). (b) A packing drawing of the oxygen atoms of ice III, viewed along the c axis [65W].

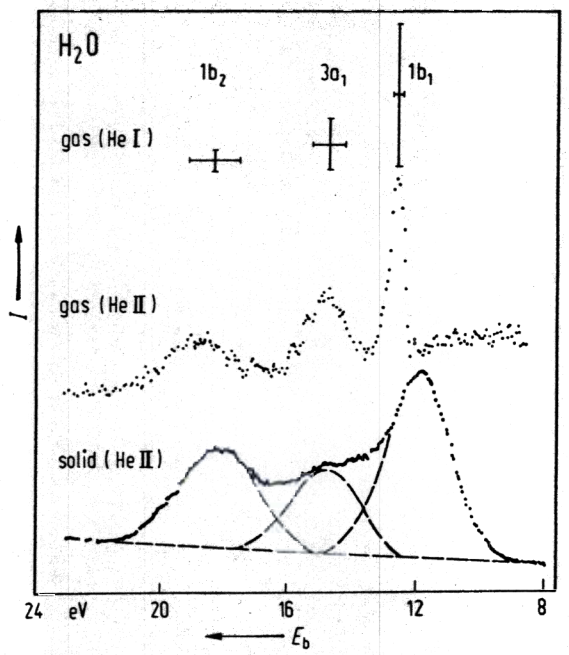

Fig. 47. H_2O. The He II UPS of solid and gas phase H_2O together with the He I gas phase spectrum. Band positions, relative peak heights and FWHM taken from [70T]. The broken curves show the derived peaks as a result of curve fitting.

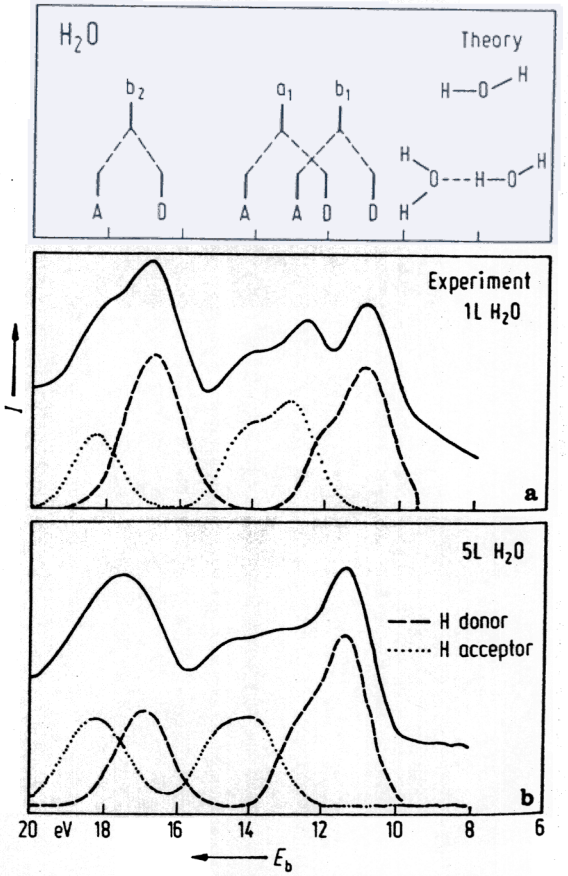

Fig. 48. H_2O. Comparison of the photoelectron spectra of a monolayer of physisorbed water (a) with multilayer (b). The splitting of the three H_2O ion states is explained by comparison with the calculated binding energies for the sketched H_2O-dimer [83S2]. E_b w.r. to E_{vac}.

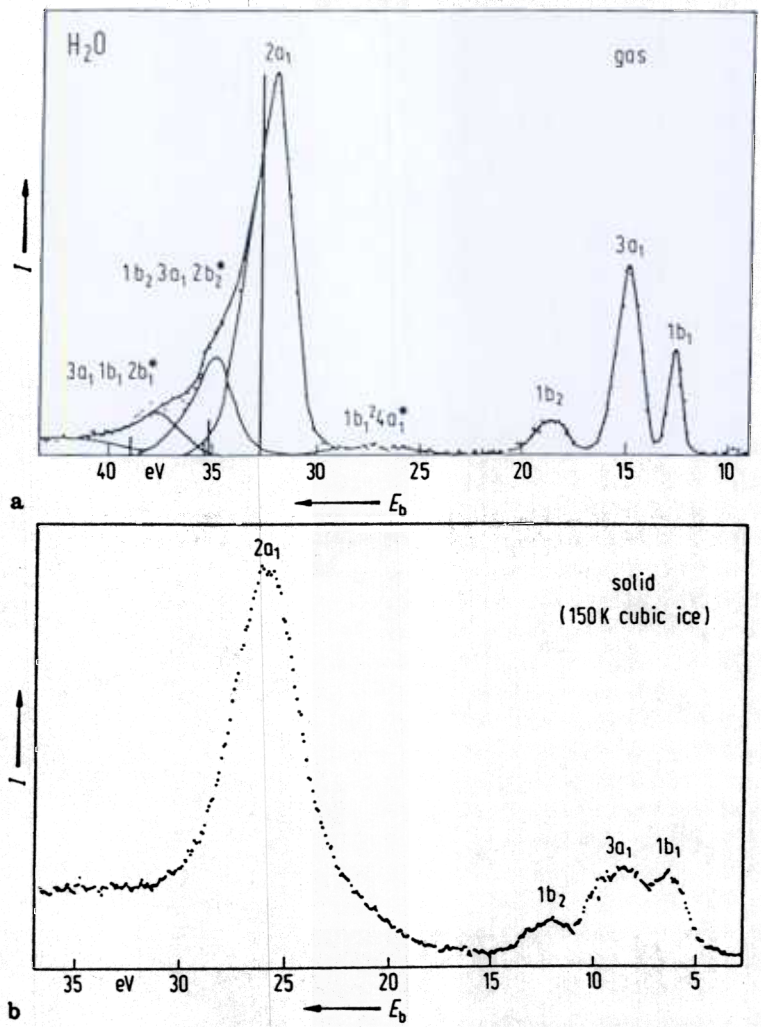

Fig. 49. H_2O. The valence electron spectrum for H_2O in the gas (a) and solid phases (b) [77M]. The figure also marks the poles from a theoretical $2a_1$ excitation spectrum [72C1]. The energy scales are adjusted so that the $1b_1$ lines fall above each other. Fig. (a): E_b w.r. to E_{vac}; Fig. (b): E_b w.r. to E_F.

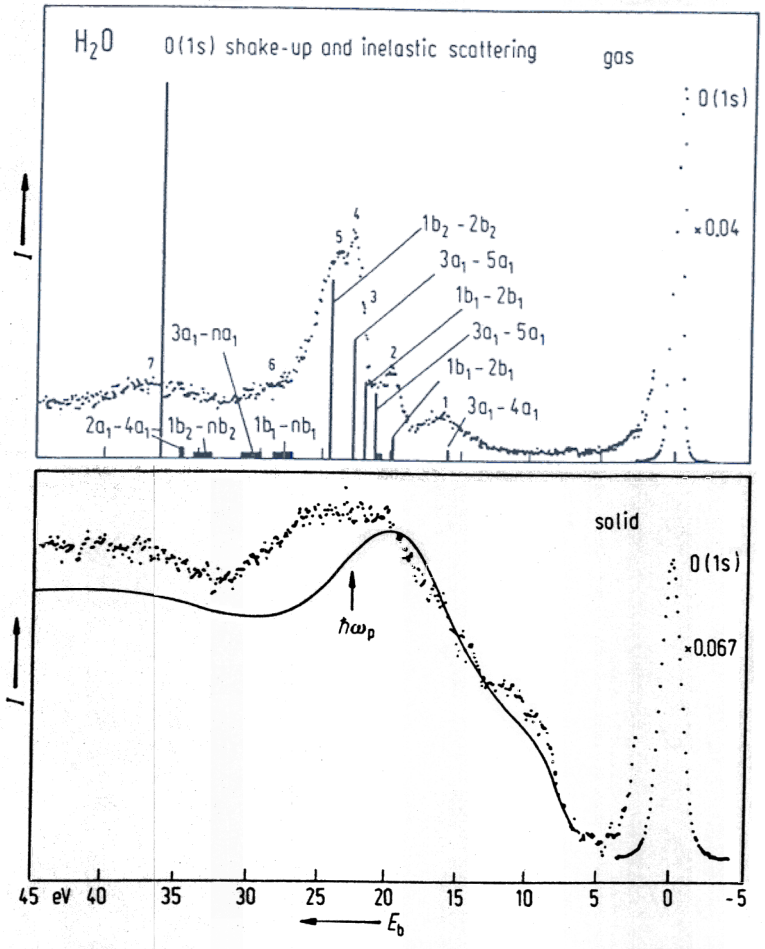

Fig. 50. H_2O. The O(1s) electron spectrum and the corresponding low kinetic energy satellites from H_2O in the gas and solid phases [77M]. The two spectra are comparable on a common intensity scale. The full line represents the electron energy loss spectrum for ice [70O]. The bars have been taken from theoretical calculations [76S, 75A]. For line numbers and transitions, see also Table 13.

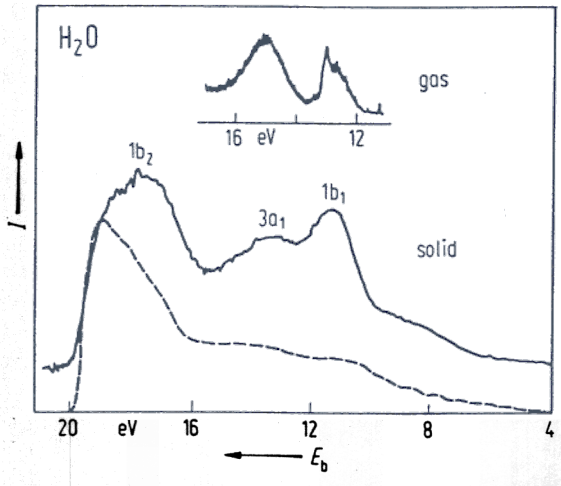

Fig. 51. H_2O. Penning ionization spectrum of solid [81Y] and gaseous [77C] H_2O. Dashed line: background.

2.3.7 Carbondioxide (CO_2)

Isolated molecule

(See also [87L].)

1: Point group: $D_{\infty h}$

2: Bond length and bond angle: C–O: 1.162 Å
O–C–O: 180°

3: Ground state electron configuration:

$$\left|\begin{array}{l}(1\sigma_g)^2(1\sigma_u)^2(2\sigma_g)^2 \\ \quad \text{O(1s), C(1s)}\end{array}\right|$$

$$^1\Sigma_g^+: \left|\begin{array}{l}(3\sigma_g)^2(2\sigma_u)^2(4\sigma_g)^2(3\sigma_u)^2(1\pi_u)^4(1\pi_g)^4 \\ \quad \text{O(2s), O(2p), C(2s), C(2p)}\end{array}\right|$$

$$\left|\begin{array}{l}(2\pi_u)^0(5\sigma_g)^0(4\sigma_u)^0 \\ \quad \text{empty}\end{array}\right|$$

Molecular solid

Cubic CO_2 $T=83$ K [65W], [75L]

4: Space group: $T_h^6(Pa3)$

5: Structure of the solid:

unit cell: $a=5.579$ Å

Atomic positions:

carbon atoms: (0, 0, 0; F. C.)

oxygen atoms: $\pm(u, u, u; u+1/2, 1/2-u, u; u, u+1/2, 1/2-u; 1/2-u, u, u+1/2)$
$u=0.11$

See also Fig. 52.

6: Outer valence photoelectron spectrum of the molecular solid [84F1, 83F1] in comparison with the gas phase [70T]: Fig. 53.

7: Inner valence photoelectron spectrum of the molecular solid in comparison with the gas phase [86F, 72A]: Fig. 54.

8: Core photoelectron spectra of the molecular solid in comparison with the gas phase:
not reported.

9: Theoretical assignment of the observed ion states [79D, 83C]: Table 15.
See Fig. 56 for a graphical representation of the calculational results.

10: Polarization energies of some ion states: Table 16.

11: Ion state cross-sections as a function of photon energies of solid CO_2 in comparison with gaseous CO_2: Figs. 55, 56.

12: Table of resonance structures in the cross-sections [83F1]: Table 17.

13: Auger spectrum of the molecular solid in comparison with the gas phase:
not reported.

14: Penning ionization electron spectrum of the molecular solid in comparison with the gas phase:
not reported.

15: Electronic excitation spectrum in the valence electron region [72K1, 84A]: Figs.: 57, 58; Table 18.

16: Electronic excitation spectrum in the core electron region:
not reported.

Table 15. CO_2. Calculated binding energies (E_b), 2 ph-TDA ionization potential (IP) and pole strengths (P) in the diagonal approximation for gaseous CO_2 obtained with two different basis sets. Only lines with $IP < 50$ eV and $P > 0.01$ are given. All energies in eV [79D].

Orbital	Basis I			Basis II		
	E_b eV	IP eV	P	E_b eV	IP eV	P
$1\pi_g$	14.79	12.65	0.88	14.84	12.63	0.90
		36.73	0.02		38.45	0.01
$1\pi_u$	20.20	17.08	0.79	19.58	16.62	0.83
		21.98	0.02		22.75	0.01
		28.02	0.06		28.33	0.04
		32.80	0.02		32.37	0.03
		33.31	0.03			
$3\sigma_u$	20.11	16.56	0.88	20.27	16.83	0.89
		37.72	0.01			
$4\sigma_g$	21.50	17.51	0.86	21.79	18.12	0.87
		32.84	0.01		33.68	0.01
		35.83	0.02		36.39	0.02
		37.28	0.01			
$2\sigma_u$	41.06	32.22	0.01	40.35	33.07	0.02
		34.68	0.36		34.40	0.03
		36.65	0.03		35.30	0.54
		37.39	0.03		38.30	0.04
		38.18	0.35		38.76	0.03
		39.98	0.02		39.10	0.13
		43.02	0.02		45.25	0.02
		48.74	0.01			
$3\sigma_g$	42.45	34.74	0.19	41.78	33.18	0.01
		36.41	0.11		35.39	0.22
		38.88	0.15		36.84	0.26
		39.13	0.15		37.96	0.01
		40.27	0.20		39.42	0.01
					39.83	0.20
					40.54	0.11

Table 16. CO_2. Vertical binding energies and polarization energies of some ion states.

Level	Vertical binding energies [eV]				E_{pol} eV
	Solid			Gas	
	[83F1]	[77N]	[82C1]	[70T]	
$1\pi_g$	13.0	12.7	14.2	13.78	0.8
$1\pi_u$	16.7	16.5		17.59	0.9
$3\sigma_u$	17.6	17.0	18.5	18.08	0.5
$4\sigma_g$	18.8	18.3		19.4	0.6

Table 17. CO_2. Energy positions of resonance structures in absorption and photoemission cross-sections [83F1].

Orbital	Solid [83F1]		Gas [79B1], [78B2], [78G2]		Assignment
	$\hbar\omega$ eV	E_k eV	$\hbar\omega$ eV	E_k eV	
$1\pi_g$	12 ··· 14	(−1) ··· (+1)	12.5	−1.28	$1\pi_g \rightarrow 2\pi_u$
	18.2	5.2	–	–	
	32.0	19.0	(31 ··· 35)	(16 ··· 20)	$1\pi_g \rightarrow 4\sigma_u$
$1\pi_u + 3\sigma_u$	22.0	4.4 ··· 5.3	–	–	–
	–	–	21.0	3.4	$1\pi_u \rightarrow 5\sigma_g$
	–	–	21.0	2.9	$3\sigma_u \rightarrow 5\sigma_g$
$4\sigma_g$	14 ··· 16	−(2.8 ··· 4.8)	15.5	−3.9	$4\sigma_g \rightarrow 2\pi_u$
	23.0	4.2	–	–	–
	–	–	39 ··· 42	20 ··· 23	$4\sigma_g \rightarrow 4\sigma_u$

Table 18. CO_2. Lower valence and Rydberg vertical excitation energies of gaseous CO_2 (in eV).

State[a])	Orbital picture[b])	[83N][d])	[73W]	[79E]	[83N][e])		Exp. [79E, 73W, 71R, 71H1, 73H1]
					Valence only	Valence plus Rydberg	
$^3\Sigma_u^+$	$1\pi_g \rightarrow 4\pi_u$	7.24	7.35	8.65	8.04	8.15	8.1
$^3\Pi_g$(R)	$1\pi_g \rightarrow 5\sigma_g$(s)	9.31	8.95	8.86	–	8.73	8.3
$^3\Delta_u$	$1\pi_g \rightarrow 4\pi_u$	8.02	7.83	9.02	8.67	8.80	8.8
$^1\Pi_g$(R)	$1\pi_g \rightarrow 5\sigma_g$(s)	9.83	9.23	9.10	–	8.93	8.4 ··· 8.6
$^3\Sigma_u^-$	$1\pi_g \rightarrow 4\pi_u$	8.66	8.24	9.42	9.05	9.19	
$^1\Sigma_u^-$	$1\pi_g \rightarrow 4\pi_u$	8.66	8.27	9.42	9.13	9.27	
$^1\Delta_u$	$1\pi_g \rightarrow 4\pi_u$	8.99	8.38	9.43	9.25	9.32	9.3 ··· 9.4
$^1\Sigma_u^+$(R)	$1\pi_g \rightarrow 2\pi_u(p_\pi)$	12.19	11.07	11.20	–	11.00	11.08 ··· 11.20
$^3\Pi_u$(R)	$1\pi_g \rightarrow 4\sigma_u(p_\sigma)$	12.28	11.49	11.43	–	11.31	
$^1\Pi_u$(R)	$1\pi_g \rightarrow 4\sigma_u(p_\sigma)$	12.46	11.53	11.45	–	11.39	11.4 ··· 11.6
$^3\Sigma_g^+$	$1\pi_u \rightarrow 4\pi_u$	11.04		12.13[c])		11.79	
$^3\Delta_g$	$1\pi_u \rightarrow 4\pi_u$	12.22		12.91[c])		12.44	12.4

[a]) (R) denotes Rydberg excited state.

[b]) In the calculations by the valence plus Rydberg basis, the $2\pi_u$, $3\pi_u$, and $4\pi_u$ MOs are mainly Rydberg orbital on C, Rydberg orbital on C and O, and valence π-antibonding orbital, respectively.

[c]) [77E].

[d]) SECI.

[e]) SACCI.

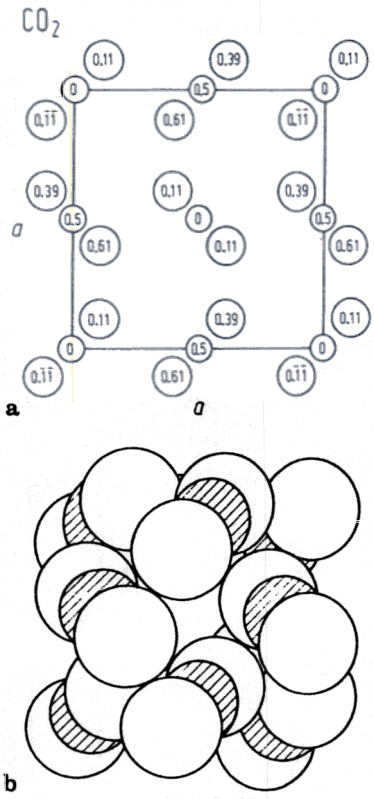

Fig. 52. CO_2. (a) A projection on a cube face of the atomic arrangement in solid CO_2. Both the resemblance to the pyrite structure and the different parameters that make this a molecular crystal are evident. Numbers give fractional coordinates. (b) A packing drawing which shows the way the linear CO_2 molecules pack in the crystalline state. The larger spheres are oxygen atoms, C atoms are hatched [65W].

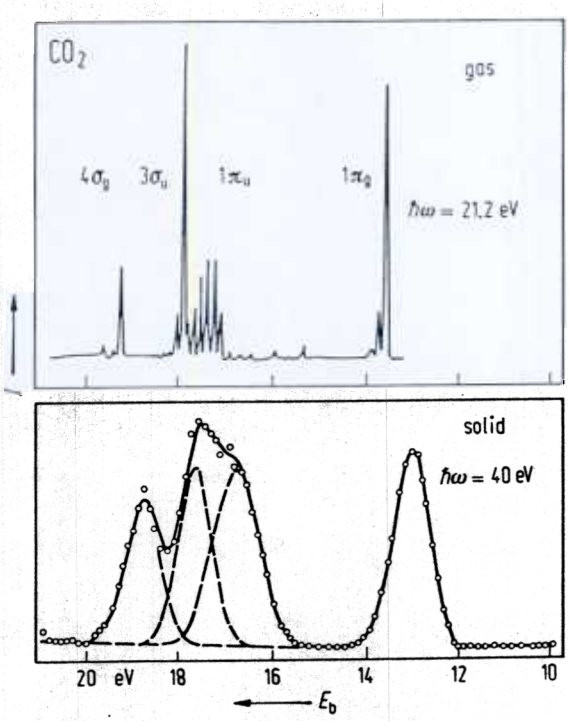

Fig. 53. CO_2. Outer valence photoelectron spectra of solid CO_2 [83F1, 84F1] in comparison with the gas phase [70T]. Dashed lines: Lorentzian fit of four components to the experimental spectrum.

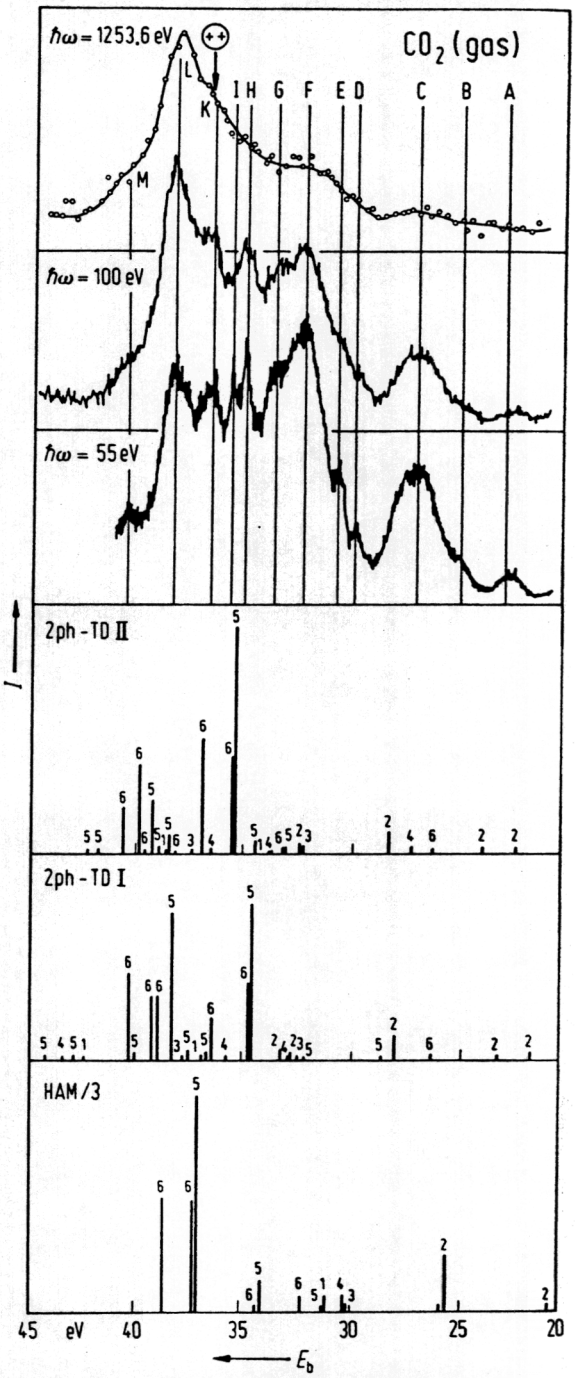

Fig. 54. CO_2. Comparison of inner valence photoelectron spectra of gaseous CO_2 at 55 and 100 eV photon energy with a soft X-ray-induced spectrum (Mg K_α: 1253.6 eV) [72A] and with results of theoretical calculations [79D, 83C]. (1: $1\pi_g$, 2: $1\pi_u$, 3: $3\sigma_u$, 4: $4\sigma_g$, 5: $2\sigma_u$, 6: $3\sigma_g$), [86F]. HAM/3: calculated scheme [83C]. + +: double ionization continuum threshold. 2ph-TD: 2 particle-hole-Tamm-Dancoff approximation.

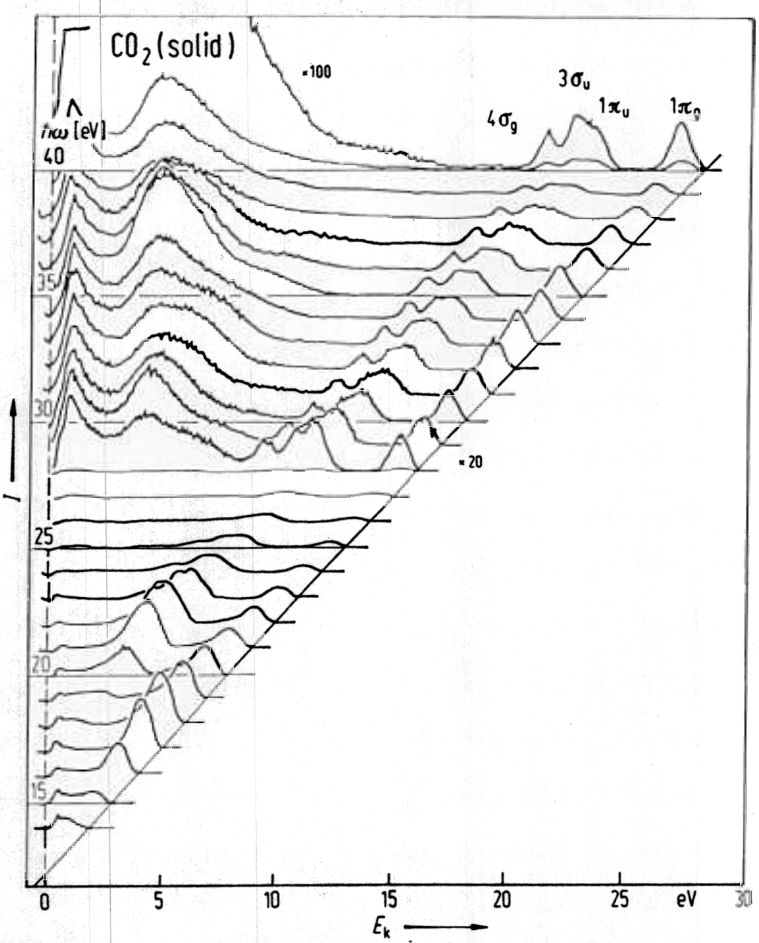

Fig. 55. CO_2. Electron distribution curves of solid CO_2 as a function of photon energy ($14 < \hbar\omega < 40$ eV) [83F1].

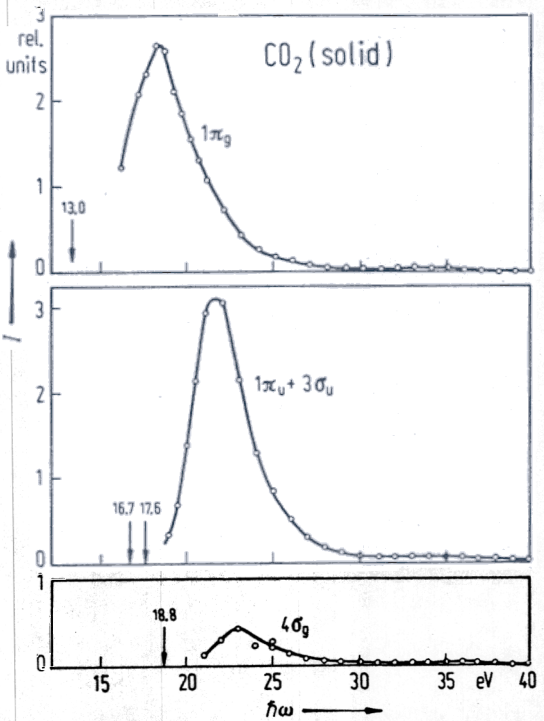

Fig. 56. CO_2. Emission intensities of the four outer valence ion states of solid CO_2 [83F1]. Arrows indicate photoemission thresholds.

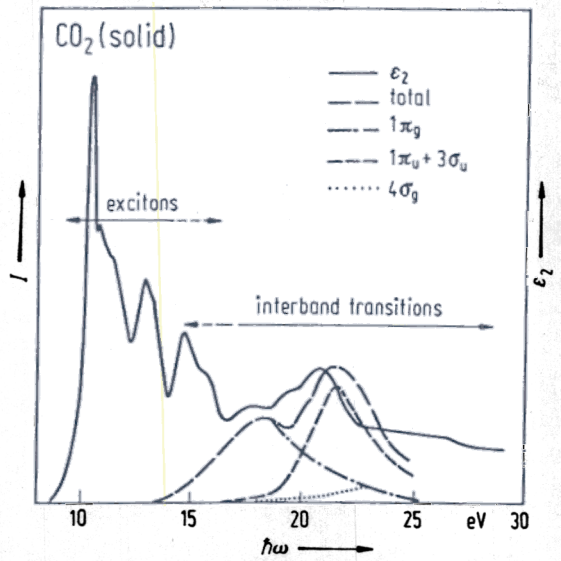

Fig. 57. CO_2. Optical reflection spectrum and photoemission total and partial cross-sections of solid CO_2 at $T=30$ K [83F1, 84F1, 72K1].

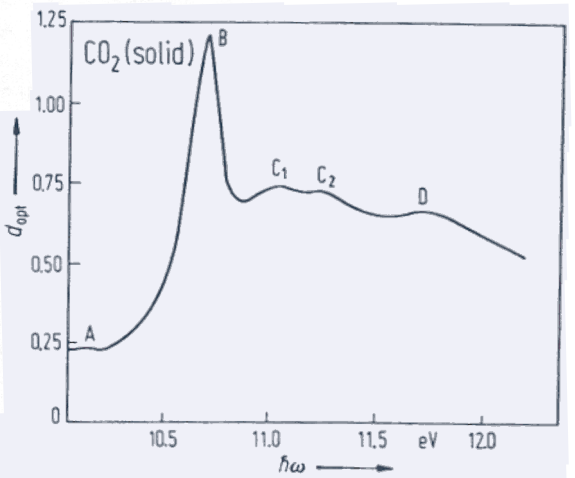

Fig. 58. CO_2. Absorption spectrum of solid CO_2 near the fundamental edge at $T=77$ K (optical density vs. photon energy). The peaks C_1 and C_2 are mainly produced by the Davydow interaction between two degenerate states [84A].

2.3.8 Ammonia (NH_3)

Isolated molecule

(See also [87L].)

1: Point group: C_{3v}

2: Bond length and bond angle: N–H: 1.019 Å
H–N–H: 109.1°

3: Ground state electron configuration:

^1A: $(1a_1)^2 \mid (2a_1)^2 (1e)^4 (3a_1)^2 \mid (4a_1)^0 (2e)^0$

N(1s) N(2s), N(2p), H(1s) empty

Molecular solid

Cubic ammonia $T=77$ K [65W], [78L2]

4: Space group: $T^4(P2_13)$

5: Structure of the solid:

unit cell: $a=5.084$ Å

Atomic positions:

N–N distance: 3.4 Å

See also Fig. 59.

6: Outer valence photoelectron spectrum of the molecular solid [82C1] in comparison with the gas phase [82C1, 70T]: Fig. 60.

7: Inner valence photoelectron spectrum of the molecular solid in comparison with the gas phase: not reported.

8: Core photoelectron spectra of the molecular solid in comparison with the gas phase: not reported.

9: Theoretical assignment of the observed ion states: [78K, 80H2].

10: Polarization energies of some ion states: Table 19.
11: Ion state cross-sections as a function of photon energies of solid NH_3 in comparison with gaseous NH_3:
not reported.
12: Table of resonance structures in the cross-sections:
not reported.
13: Auger spectrum of the molecular solid in comparison with the gas phase:
not reported.
14: Penning ionization electron spectrum of the molecular solid [81Y] in comparison with the gas phase [75Y]: Fig. 61.
15: Electronic excitation spectrum in the valence electron region:
not reported.
16: Electronic excitation spectrum in the core electron region:
not reported.

Table 19. NH_3. Vertical binding energies and polarization energies of some ion states.

Level	Vertical binding energies [eV]		E_{pol} eV
	Solid [82C1]	Gas [82C1, 70T, 75B1]	
$3a_1$	9.7	11.04	1.34
$1e$	14.6	16.74	2.14
$2a_1$		27.74	
$1a_1$		405.6	

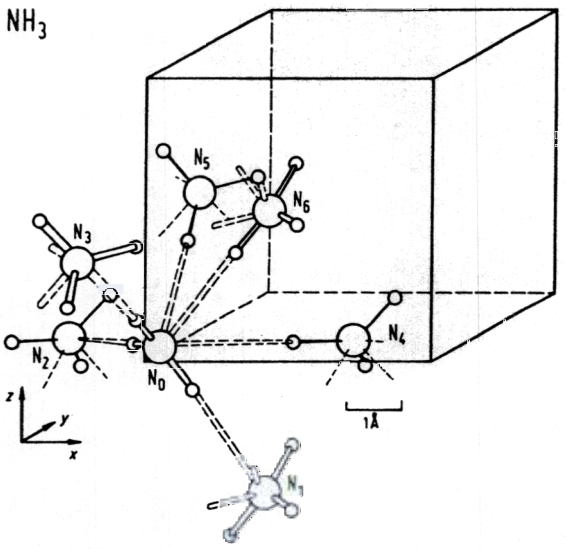

Fig. 59. NH_3. The crystal structure of cubic ammonia. Only the six closest neighbours to the atom N_0 (0.04, 0.04, 0.04) are shown. The hydrogen atoms are for simplicity placed on the lines between the nitrogen atoms, although there is experimental evidence that they are somewhat off these lines [65W].

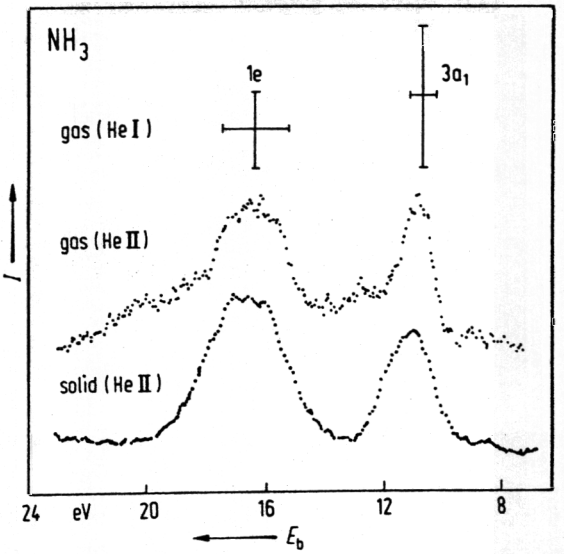

Fig. 60. NH_3. The He II UPS of solid and gas phase NH_3 together with the He I gas phase spectrum. Band positions, relative peak heights and FWHM taken from [70T]. Energies are referred to the vacuum level. The spectra are corrected for an analyser transmission efficiency [82C1].

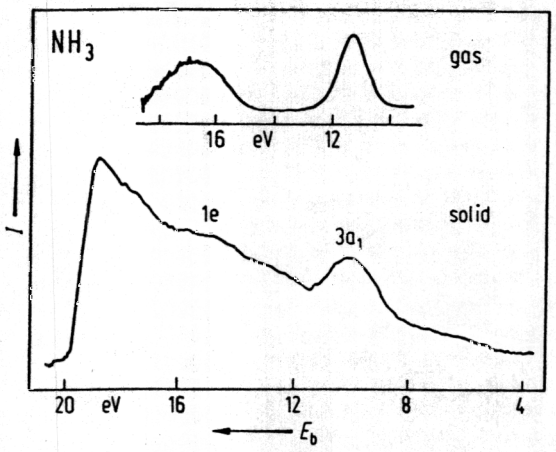

Fig. 61. NH_3. Penning ionization spectra of solid [81Y] and gaseous [75Y] NH_3.

2.3.9 Acetylene (C_2H_2)

Isolated molecule

(See also [87L].)

1: Point group: $D_{\infty h}$

2: Bond length and bond angle: C–C: 1.20 Å
C–H: 1.05 Å
C–C–H: 180°

3: Ground state electron configuration:

$$^1\Sigma_g^+: \left| \begin{array}{c} (1\sigma_g)^2 (1\sigma_u)^2 \\ \text{C(1s)} \end{array} \right| \left| \begin{array}{c} (2\sigma_g)^2 (2\sigma_u)^2 (3\sigma_g)^2 (1\pi_u)^4 \\ \text{C(2s), C(2p), H(1s)} \end{array} \right| \left| \begin{array}{c} (1\pi_g)^0 (4\sigma_g)^0 (3\sigma_u)^0 (4\sigma_u)^0 \\ \text{empty} \end{array} \right|$$

Molecular solid

Cubic acetylene ($-140\,°C < T < -84\,°C$) [66W], [79N2]

4: Space group: T_h^6(Pa3)

5: Structure of the solid

unit cell: $a = 6.14$ Å ($T = -117\,°C$)

Atomic positions:

carbon atoms: $\pm(u, u, u; u+1/2, 1/2-u, \bar{u}; \bar{u}, u+1/2, 1/2-u; 1/2-u, \bar{u}, u+1/2)$
$u = 0.056$

shortest intermolecular distances: C–C: 3.89 Å
H–H: 3.28 Å

See also Fig. 62.

6: Outer valence photoelectron spectrum of the molecular solid [83F1, 84F1] in comparison with the gas phase [80B1, 70T]: Fig. 63.

7: Inner valence photoelectron spectrum of the molecular solid in comparison with the gas phase [82M2]: not reported.

8: Core photoelectron spectra of the molecular solid in comparison with the gas phase [82A, 82M2]: not reported.

9: Theoretical assignment of the observed ion states [80B1]: Table 20.

10: Polarization energies of some ion states: Table 21.
11: Ion state cross-sections as a function of photon energies of solid C_2H_2 in comparison with gaseous C_2H_2: Figs. 64···68.
12: Table of resonance structures in the cross-sections: Table 22.
13: Auger spectrum of the molecular solid in comparison with the gas phase: not reported.
14: Penning ionization electron spectrum of the molecular solid in comparison with the gas phase: not reported.
15: Electronic excitation spectrum in the valence electron region: not reported.
16: Electronic excitation spectrum in the core electron region: not reported.

Table 20. C_2H_2. Calculated vertical electron binding energies E_b and intensity coefficients S for the outer and inner valence electron states of gaseous C_2H_2 (Ref. 44 in [80B1]).

Level	E_b [eV]	S
$1\pi_u$	11.17	–
$3\sigma_g$	17.07	–
$2\sigma_u$	19.10	–
$2\sigma_g$	23.83	0.56
–	28.82	0.20
–	29.41	0.085

Table 21. C_2H_2. Vertical binding energies and polarization energies of some ion states.

Level	Vertical binding energies [eV]		E_{pol} eV
	Solid [84F1]	Gas [70T, 80B1, 82M2]	
$1\pi_u$	11.04	11.49	0.45
$3\sigma_g$	16.24	16.7	0.5
$2\sigma_u$	18.0	18.7	0.7
$2\sigma_g$	22.83	23.5	0.7
–	–	26.7	–
–	–	27.8	–

Table 22. C_2H_2. Energy positions and structures in the partial cross-sections of solid and gaseous C_2H_2.

Orbital	Solid [83F1]		Gas [81L2, 82H2]		Assignment
	$\hbar\omega$ eV	E_k eV	$\hbar\omega$ eV	E_k eV	
$1\pi_u$	13.5	2.5	13.3	1.8	?
	16	5.0	15.3	3.8	autoioniz. $2\pi_u \rightarrow 1\pi_g$
$3\sigma_g$	19	2.8	18	1.3	$3\sigma_g \rightarrow 3\sigma_u$
$2\sigma_u$	16	−2	15.3	−3.4	$2\sigma_u \rightarrow 1\pi_g$

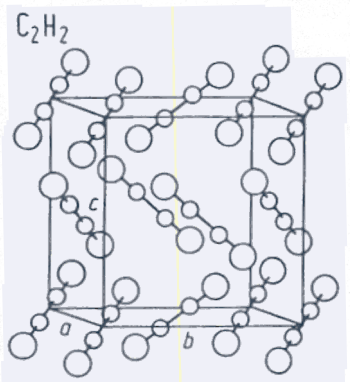

Fig. 62. C_2H_2. Stereoview of the packing of the molecules in the cubic phase of acetylene [79V].

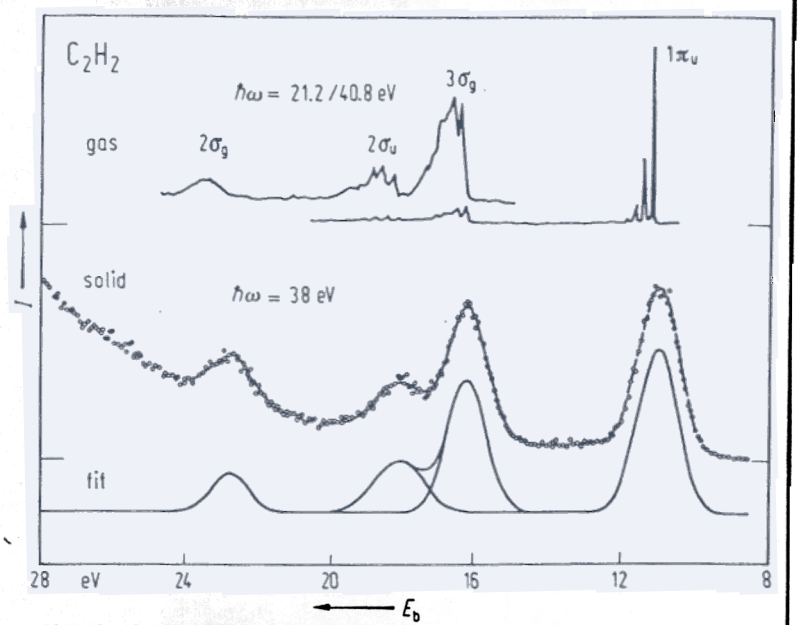

Fig. 63. C_2H_2. The outer valence electron spectra of solid [83F1, 84F2] and of gas phase C_2H_2 [70T, 80B1].

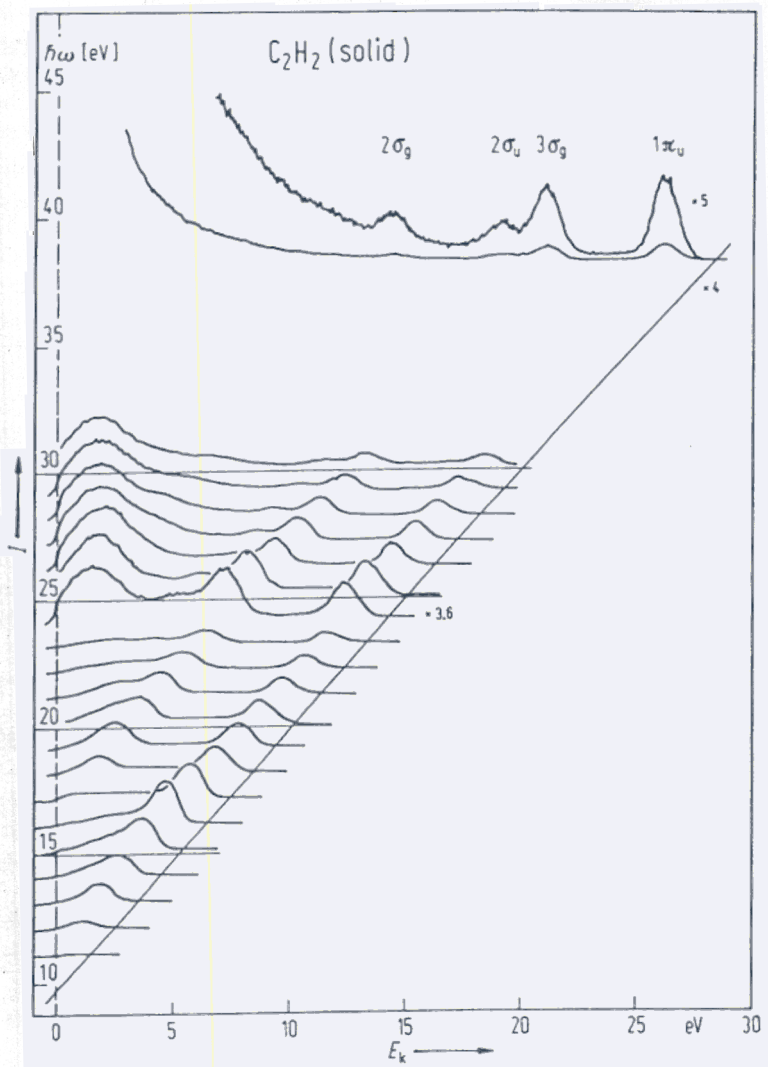

Fig. 64. C_2H_2. The electron distribution curves of the outer valence electron region of solid C_2H_2 as a function of photon energy [83F1].

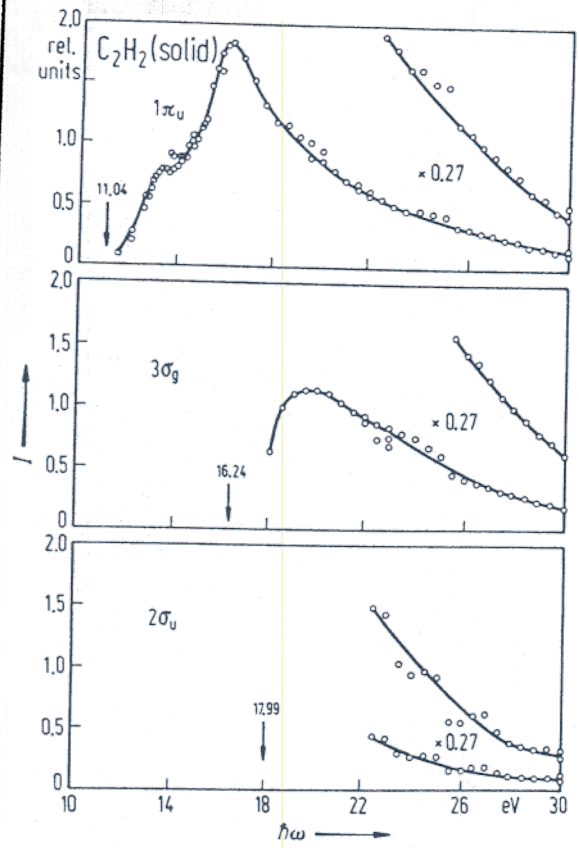

Fig. 65. C_2H_2. The emission intensities of the outer valence electron states of solid C_2H_2 [83F1] as a function of photon energy. Arrows indicate photoemission thresholds.

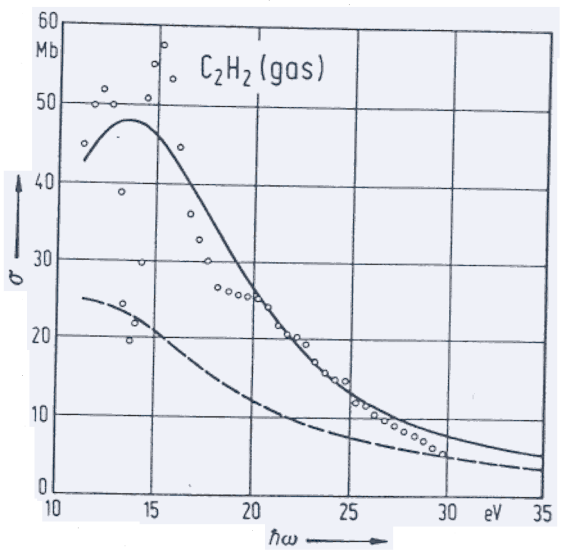

Fig. 66. C_2H_2. Photoionization cross sections for the $X\ ^2\Pi_u$ state of gaseous C_2H_2: (——) dipole length form [84L], (– – – –) dipole velocity form [84L], (circles) normalized to the dipole length cross sections at 24 eV photon energy [81L2].

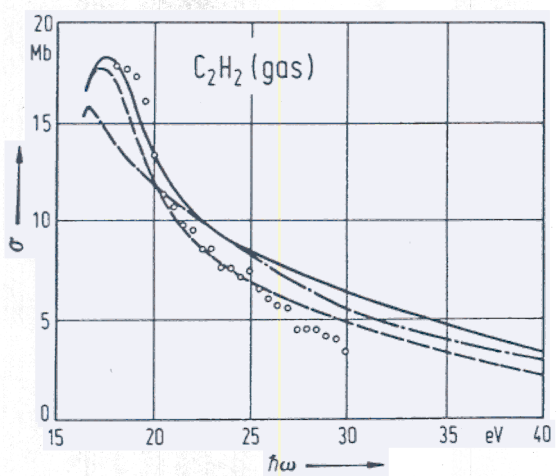

Fig. 67. C_2H_2. Photoionization cross sections for the $A\ ^2\Sigma_g$ state of gaseous C_2H_2: (——) dipole length form [84L], (– – – –) dipole velocity form [84L], (circles) normalized to the dipole length cross sections at 24 eV photon energy [81L2], (–·–) Stieltjes moment theory results [82M1].

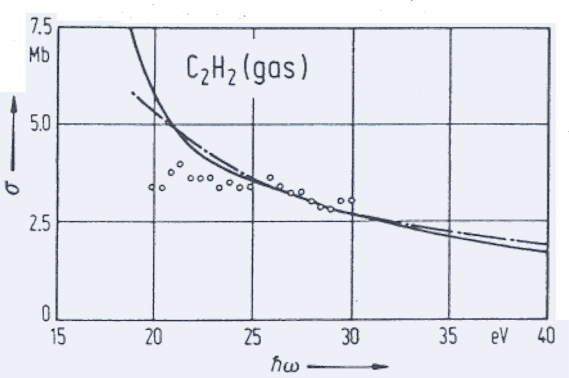

Fig. 68. C_2H_2. Photoionization cross sections for the $B\ ^2\Sigma_u$ state of gaseous C_2H_2: (——) dipole length form [84L], (circles) normalized to the dipole length cross sections at 28 eV photon energy [81L2], (–·–) Stieltjes moment theory results [82M1].

2.3.10 Ethylene (C_2H_4)

Isolated molecule

(See also [87L].)

1: Point group: D_{2h}

2: Bond lengths and bond angles: C–C: 1.3327 Å
C–H: 1.084 Å
H–C–H: 115.5°
H–C–C: 122.25°

3: Ground state electron configuration:

$^1A_{1g}$: $|\ (1a_g)^2(1b_{1u})^2\ |\ (2a_g)^2(2b_{1u})^2(1b_{2u})^2(3a_g)^2(1b_{3g})^2(1b_{3u})^2\ |$
C(1s) C(2s), C(2p), H(1s)
$|\ (1b_{2g})^0(4a_g)^0(3b_{1u})^0(2b_{2u})^0(4b_{1u})^0(2b_{3g})^0\ |$
empty

Molecular solid

Orthorhombic ethylene $T = -175$ °C [66W]

4: Space group: V_h^{12}(Pnnm)

5: Structure of the solid:

unit cell: $a = 4.87$ Å, $b = 6.46$ Å, $c = 4.14$ Å

Atomic positions:
carbon atoms: 4(g) $\pm(u, v, 0; u+1/2, 1/2-v, 1/2)$ with $u = 0.11$, $v = 0.06$

See also Fig. 69.

6: Outer valence photoelectron spectrum of the molecular solid [83F1] in comparison with the gas phase [70T]: Fig. 70.

7: Inner valence photoelectron spectrum of the molecular solid [84M] in comparison with the gas phase [80B1, 74G1, 75B2]: Fig. 71.

8: Core photoelectron spectra of the molecular solid in comparison with the gas phase [74G1, 75B2]: not reported.

9: Theoretical assignment of the observed ion states [80B1, 78C2]: Table 23.

10: Polarization energies of some ion states: Table 24.

11: Ion state cross-sections as a function of photon energies of solid C_2H_4 in comparison with gaseous C_2H_4: Figs. 72 ··· 75.

12: Table of resonance structures in the cross-sections: Table 25.

13: Auger spectrum of the molecular solid in comparison with the gas phase: not reported.

14: Penning ionization electron spectrum of the molecular solid in comparison with the gas phase: not reported.

15: Electronic excitation spectrum in the valence electron region (Ref. 196 in [83F1]): Fig. 76.

16: Electronic excitation spectrum in the core electron region: not reported.

For Table 23 see next page.

Table 24. C_2H_4. Vertical binding energies and polarization energies E_{pol} [83F1].

Level	Vertical binding energies [eV]		E_{pol} eV
	Solid [84F1]	Gas [79B2]	
$1b_{3u}$	10.2	10.51	0.31
$1b_{3g}$	12.3	12.85	0.55
$3a_g$	14.1	14.7	0.6
$1b_{2u}$	16.2	15.87	−0.33
$2b_{1u}$	18.6	19.1	0.5
$2a_g$	22.9	23.68	0.8

Table 23. C_2H_4. Vertical binding energies E_b and intensity coefficients S in gaseous C_2H_4 obtained from 2 ph-TDA calculations. 2 ph-TDA: 2particle-hole-Tamm-Dancoff-approximation. E_b: [80B1], S: [80B1, 78C2].

Level	E_b [eV]	S
$1b_{3u}$	10.44	–
$1b_{3g}$	13.04	–
$3a_g$	14.70	–
$1b_{2u}$	16.07	–
$2b_{1u}$	19.4	–
$2a_g$	23.10	0.36
	23.83	0.27
	26.95	0.07
	28.02	0.08
	30.34	0.04
	30.88	0.01
	33.12	0.01

Table 25. C_2H_4. Energy position of resonance structures in absorption and photoemission cross-sections in gaseous and solid C_2H_4 [83F1].

Orbital	Solid [83F1]		Gas [80G1]		Assignment
	$\hbar\omega$ eV	E_k eV	$\hbar\omega$ eV	E_k eV	
$1b_{3u}$	(15.0)	(4.8)	10.5	0	$1b_{3u} \rightarrow a_g, b_{1g}$
$1b_{3g}$	(15.3)	(3.0)	12.9	0	$1b_{3g} \rightarrow 3b_{1u} + 4b_{1u}$ $1b_{3g} \rightarrow 2b_{2u}$
$3a_g + 1b_{2u}$	19.0	3.7, 4.9	14.7	0	$3a_g \rightarrow 2b_{2u}$
			22.0	7.3	$3a_g \rightarrow 3b_{1u} + 4b_{1u}$
			15.9	0	$1b_{2u} \rightarrow a_g, b_{1g}$
$2b_{1u}$	28.0	9.4	19.1	0	$2b_{1u} \rightarrow a_g$
			25.0	5.9	$2b_{1u} \rightarrow 2b_{3g}$

For Fig. 69, see next page.

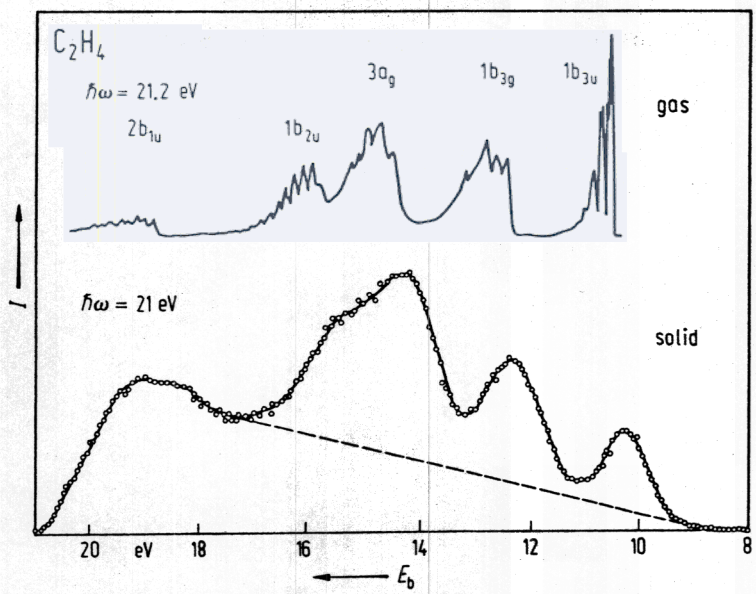

Fig. 70. C_2H_4. Photoelectron spectra of gaseous [70T] and solid [83F1] C_2H_4 in the outer valence region.

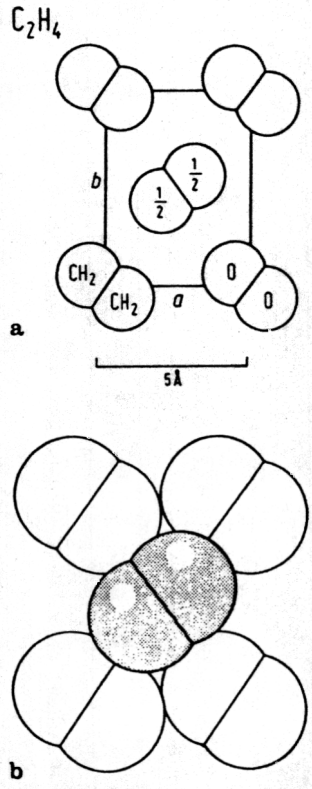

Fig. 69. C_2H_4. (a) A projection down the *c* axis of solid ethylene. (b) A packing drawing of solid C_2H_4 viewed along the *c* axis [66W].

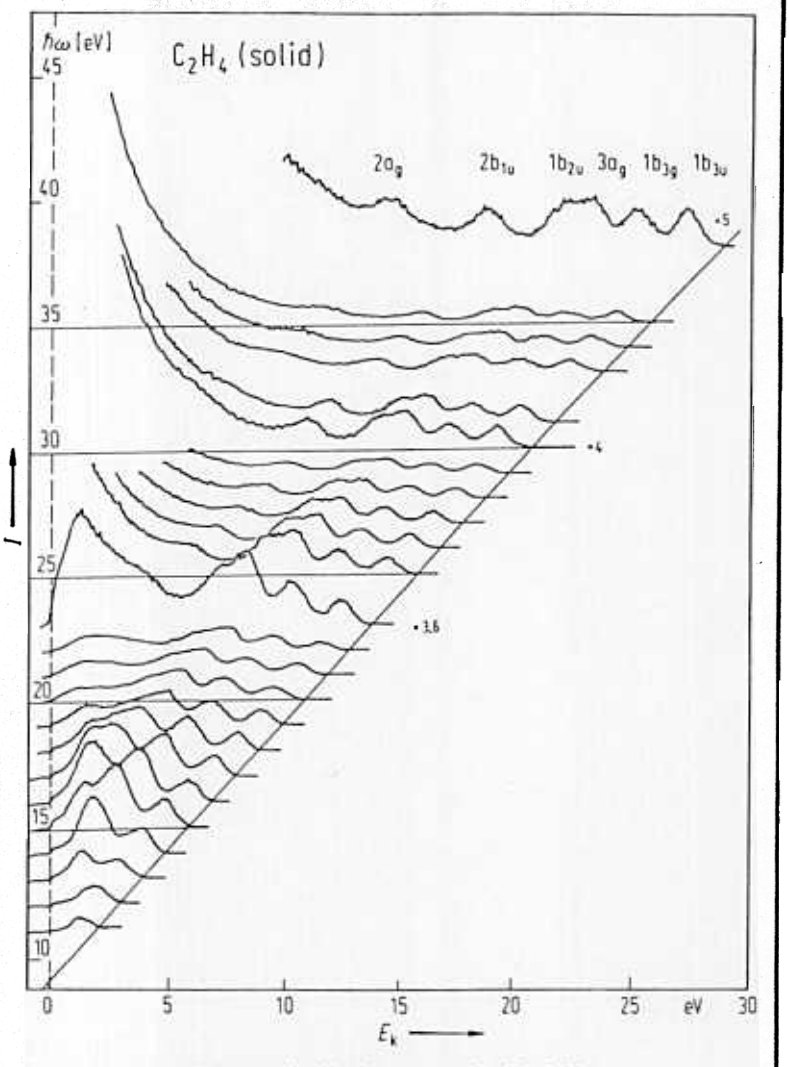

Fig. 72. C_2H_4. Electron distribution curves of solid C_2H_4 as a function of the photon energy ($\hbar\omega = 11 \cdots 40$ eV) [83F1].

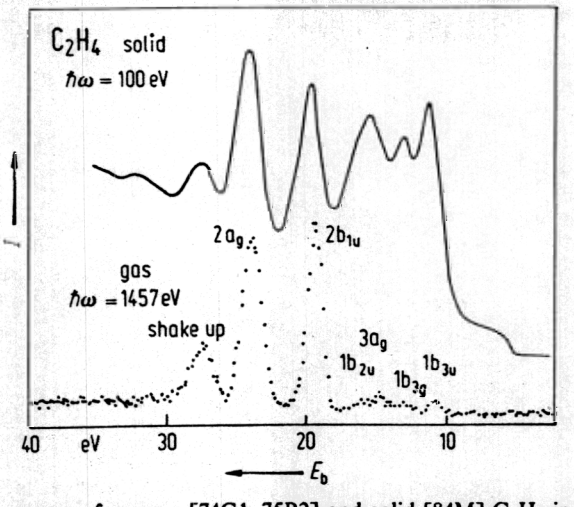

Fig. 71. C_2H_4. Photoelectron spectra of gaseous [74G1, 75B2] and solid [84M] C_2H_4 in the valence region. E_b relative to E_{vac}.

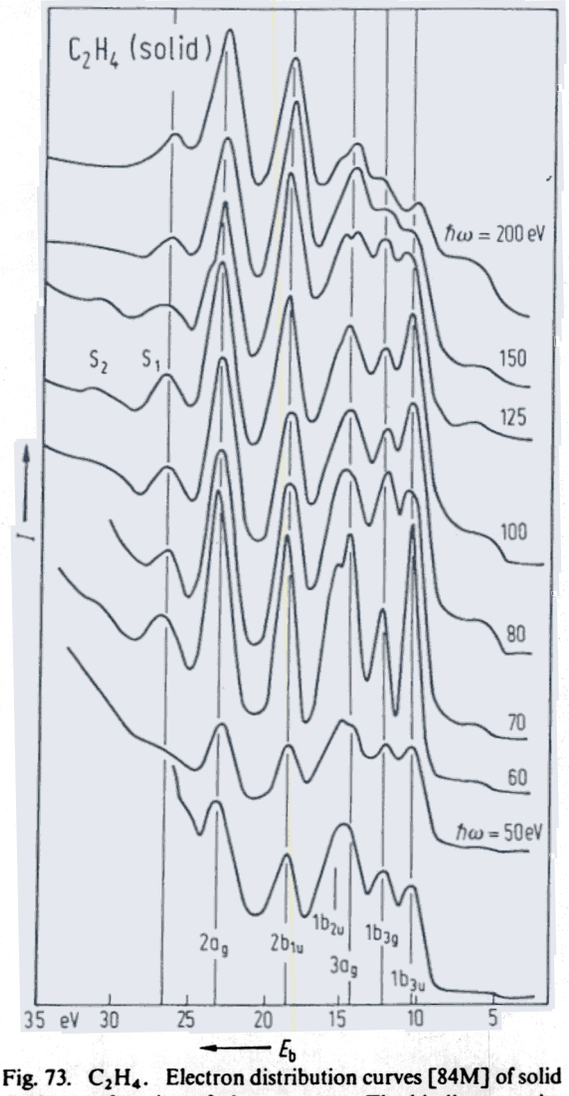

Fig. 73. C_2H_4. Electron distribution curves [84M] of solid C_2H_4 as a function of photon energy. The binding energies are obtained by referencing the $1b_{2u}$ feature to the gas phase results. S_1 and S_2 label satellite features.

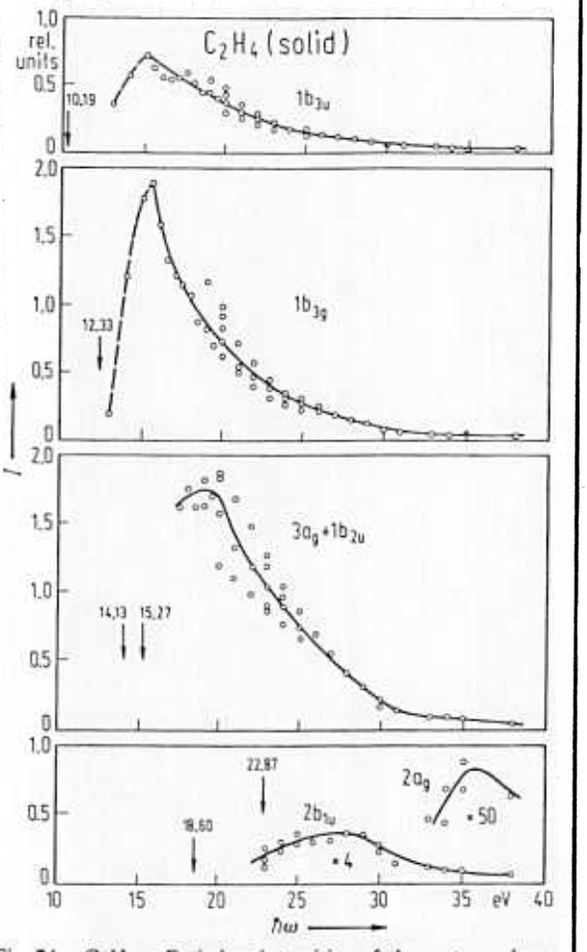

Fig. 74. C_2H_4. Emission intensities of the outer valence ion states of solid C_2H_4 [83F1]. Arrows indicate photoemission thresholds.

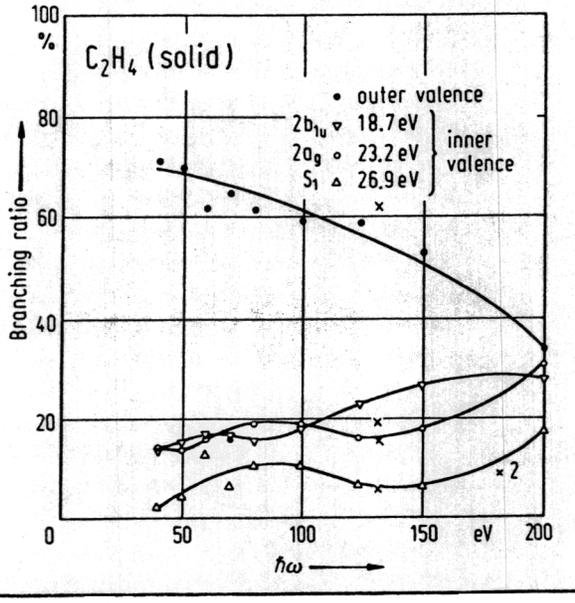

Fig. 75. C_2H_4. Inner valence satellite branching ratios measured relative to the outer valence level of solid C_2H_4 [84M]. The corresponding values for gas phase C_2H_4 [76B] are also shown (crosses).

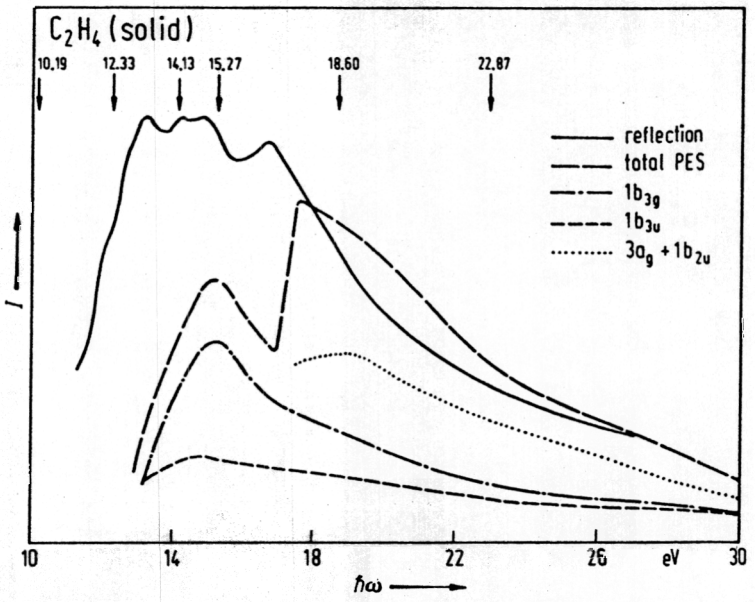

Fig. 76. C_2H_4. Comparison between the optical reflection spectrum and photoemission spectrum (PES) [83F1]. Arrows indicate photoemission thresholds.

2.3.11 Methane (CH_4)

Isolated molecule

(See also [87L])

1: Point group: T_d

2: Bond lengths and bond angle: C—H: 1.107 Å
H—H: 1.811 Å
H—C—H: 109.5°

3: Ground state electron configuration: Fig. 77

Molecular solid

Cubic methane $T<89$ K [66W], [85L]

4: Space group: $P2_13$ in the range 7.8···21 K [85L]

5: Structure of the solid:

unit cell: $a=5.84$ Å ($T=13.9$ K). See also Fig. 78

Atomic positions:
not reported.

6: Outer valence photoelectron spectrum of the molecular solid in comparison with the gas phase [84B1]: Fig. 79.

7: Inner valence photoelectron spectrum of the molecular solid in comparison with the gas phase: not reported.

8: Core photoelectron spectra of the molecular solid in comparison with the gas phase [76P]: not reported.

9: Theoretical assignment of the observed ion states [78C1]: Table 26.

10: Polarization energies of some ion states: Table 27.

11: Ion state cross-sections as a function of photon energies of solid CH_4 in comparison with gaseous CH_4: Figs. 80, 81.

12: Table of resonance structures in the cross-sections: not reported.

13: Auger spectrum of the molecular solid in comparison with the gas phase:
not reported.
14: Penning ionization electron spectrum of the molecular solid in comparison with the gas phase:
not reported.
15: Electronic excitation spectrum in the valence electron region:
not reported.
16: Electronic excitation spectrum in the core electron region:
not reported.

Table 26. CH_4. Calculated vertical binding energies E_b [78C1].

Level	E_b [eV]
$1t_2$	14.05
$2a_1$	23.68

Table 27. CH_4. Vertical binding energies and polarization energies E_{pol}. See also Table 49.

Level	Vertical binding energies [eV]			E_{pol} [eV]
	Solid	Gas		
	[84B1]	[70P]	[84B1]	
		13.6	13.6	
$1t_2$	14.1	14.4	14.3	0.3
		15.0	15.0	
$2a_1$	22.7	22.91	23.0	0.2

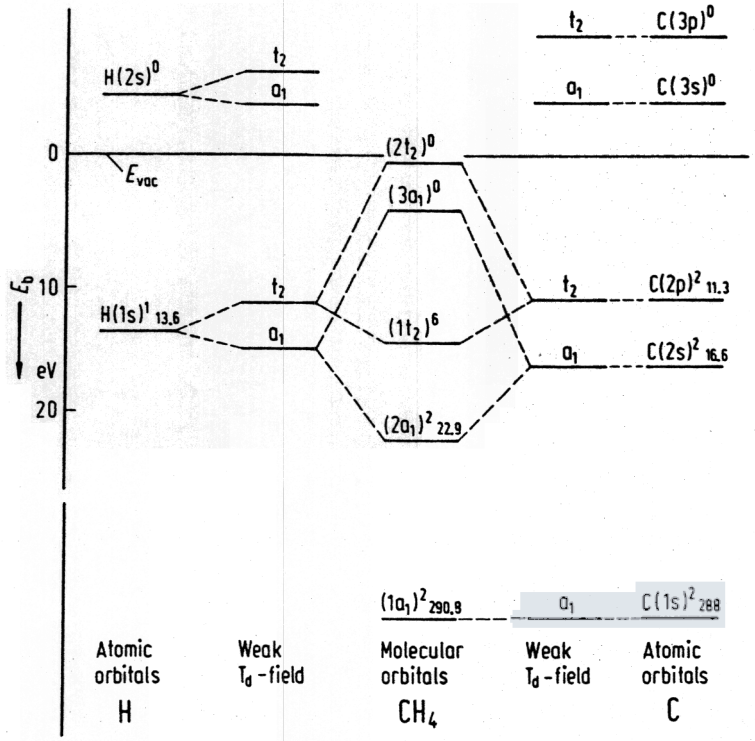

Fig. 77. CH_4. Molecular orbital diagram after [84B1]. Binding energies of various levels are indicated.

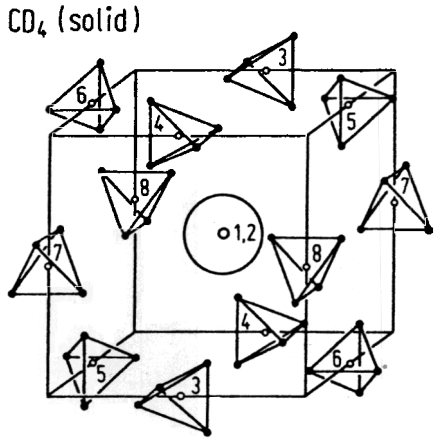

Fig. 78. CD_4. Arrangement of molecules in solid CD_4.

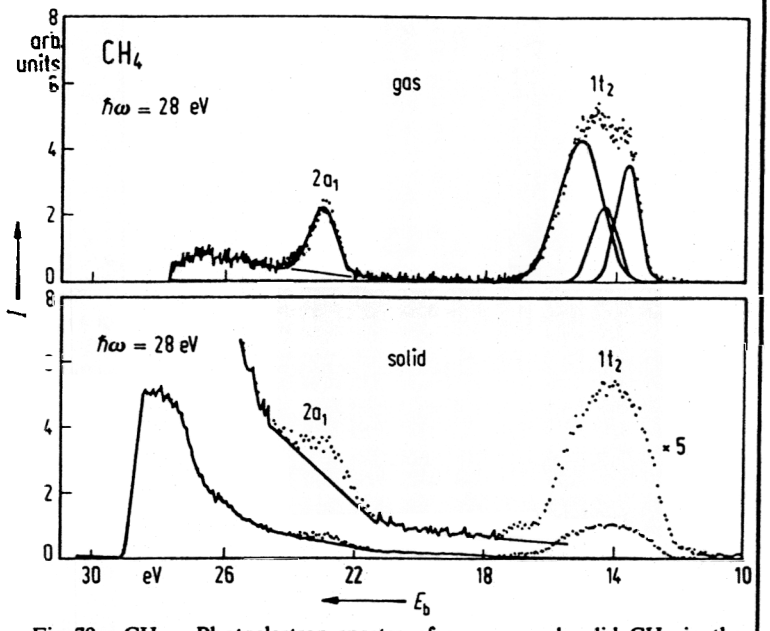

Fig. 79. CH_4. Photoelectron spectra of gaseous and solid CH_4 in the outer valence region [84B1]. Solid curves in the gas spectrum: Gaussian fit. See also Fig. 170.

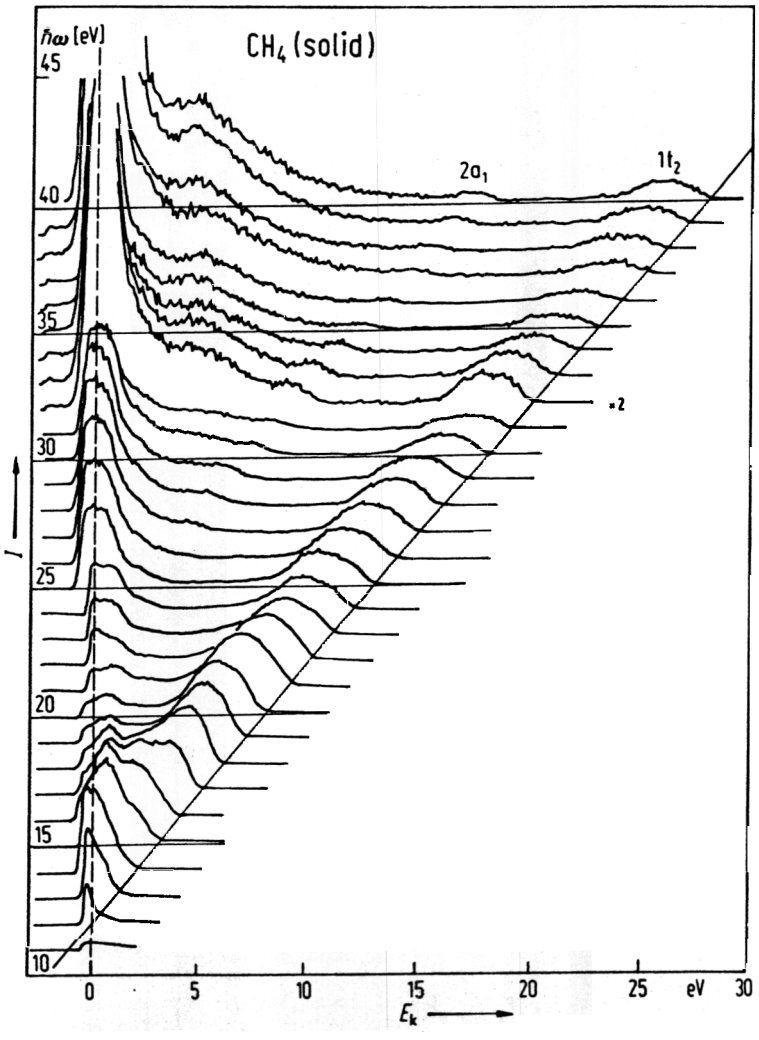

Fig. 80. CH_4. Electron distribution curves of solid CH_4 as a function of photon energy ($\hbar\omega = 11 \cdots 40$ eV) [84B1].

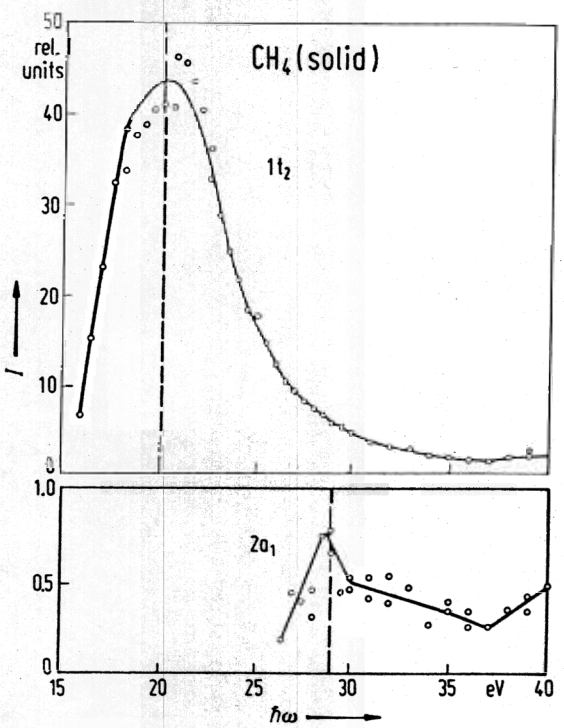

Fig. 81. CH_4. Emission intensities of the first two outer valence ion states of solid CH_4 [84B1]. Solid line: fit to the data.

2.3.12 Carbontetrafluoride (CF_4)

Isolated molecule

1: Point group: T_d
2: Bond length and bond angles: C—F: 1.31 Å
F—C—F: 109.5°
3: Ground state electron configuration: Fig. 82.

Molecular solid

Monoclinic carbontetrafluoride (10 K < T < 70 K) [72S2]

4: Space group: $P2_1/a$ (probably Cc acc. to [85L])
5: Structure of the solid:

unit cell: $a = 8.435$ Å, $b = 4.310$ Å, $c = 8.369$ Å, $\beta = 119.40°$
($a = 8.71$ Å, $b = 4.16$ Å, $c = 12.27$ Å, $\beta = 150.7°$; $T = 40$ K [85L])

Atomic positions:
Intermolecular F ... F-distances: 3.03···3.18 Å ($T = 10$ K)

6: Outer valence photoelectron spectrum of the molecular solid in comparison with the gas phase [84B1]: Fig. 83.
7: Inner valence photoelectron spectrum of the molecular solid in comparison with the gas phase [75B1]: not reported.
8: Core photoelectron spectra of the molecular solid in comparison with the gas phase [76P]: not reported.
9: Theoretical assignment of the observed ion states [80M]: Table 28.
10: Polarization energies of some ion states: Table 29.
11: Ion state cross-sections as a function of photon energies of solid CF_4 in comparison with gaseous CF_4: Figs. 84···86.
12: Table of resonance structures in the cross-sections: Table 30.

13: Auger spectrum of the molecular solid in comparison with the gas phase:
not reported.
14: Penning ionization electron spectrum of the molecular solid in comparison with the gas phase:
not reported.
15: Electronic excitation spectrum in the valence electron region:
not reported.
16: Electronic excitation spectrum in the core electron region of the molecular solid in comparison with the gas phase [73L2, 79T, 78B1]:
not reported.

Table 28. CF_4. Calculated vertical binding energies E_b for gaseous CF_4. [80M].

Level	E_b [eV]
$1t_1$	16.5
$4t_2$	17.51
1e	20.60
$3t_2$	24.00
$4a_1$	27.26
$2t_2$	43.87
$3a_1$	44.54

Table 29. CF_4. Vertical binding energies and polarization energies E_{pol}.

Level	Vertical binding energies [eV]			E_{pol} [eV]
	Solid	Gas		
	[84B1]	[70B]	[84B1]	
$1t_1$	15.8	16.2	16.2	0.4
$4t_2$	16.9	17.4	17.4	0.5
1e	18.1	18.5	18.5	0.4
$3t_2$	21.9	22.1	22.1	0.2
$4a_1$	24.7	25.1	25.1	0.4

Table 30. CF_4. Energy positions of features in photoemission cross-sections of gaseous and solid CF_4 [84B1].

Orbital	Solid		Gas		Assignment
	$\hbar\omega$ eV	E_k eV	$\hbar\omega$ eV	E_k eV	
$1t_1$			17.0	1.2	
	29.0	12.8	27.0	11.2	$1t_1 \rightarrow 6t_2$
			33.0	17.2	$1t_1 \rightarrow t_2$
$4t_2$			18.5	1.7	
			25.0	8.2	
			33.0	16.2	$4t_2 \rightarrow t_2$
1e			20.0	1.9	
	21.7	3.2	7.3		autoioniz.
			24.0	5.9	
	29.5	11.0	28.0	9.9	$1e \rightarrow 6t_2$
			34.0	15.9	$1e \rightarrow t_2$
$3t_3$			24.0	2.2	
			34.0	12.2	$3t_2 \rightarrow 6t_2$
$4a_1$			35.0	10.3	$4a_1 \rightarrow 6t_2$

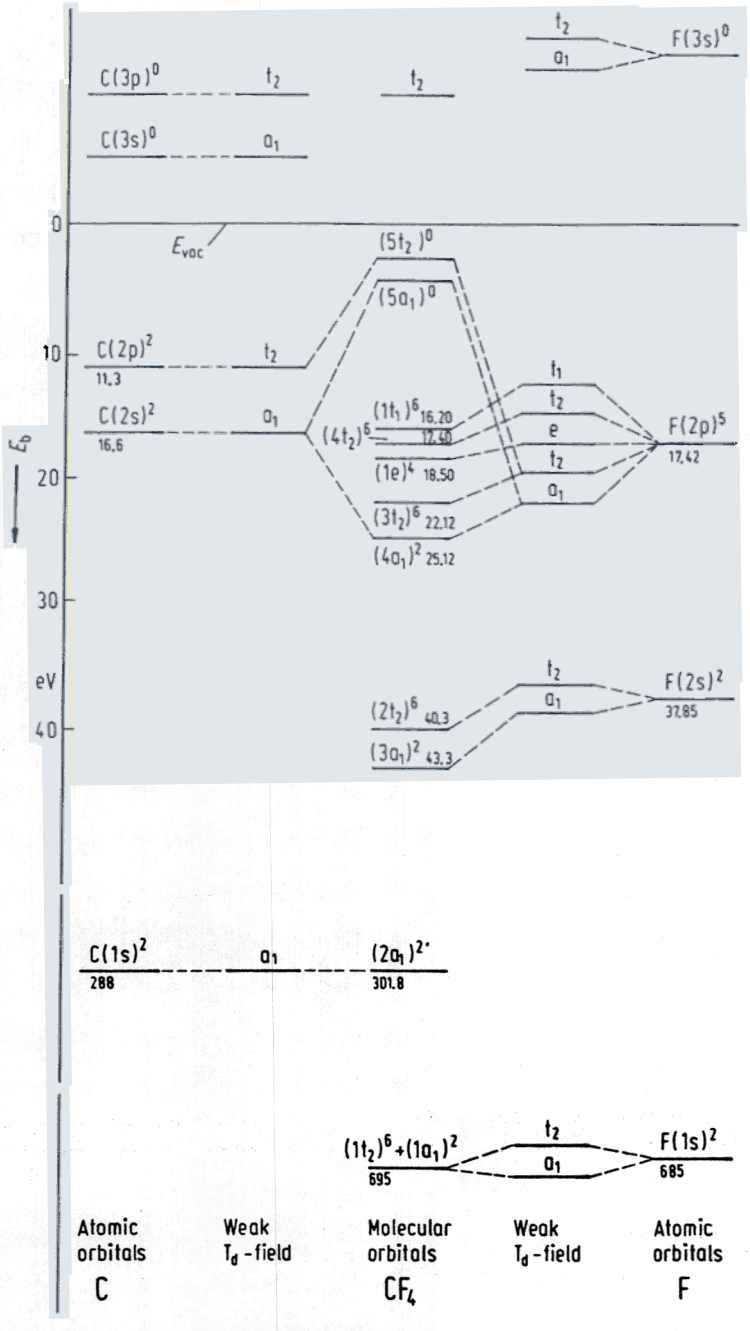

Fig. 82. CF_4. Molecular orbital diagram after [84B1]. Binding energies of various levels are indicated.

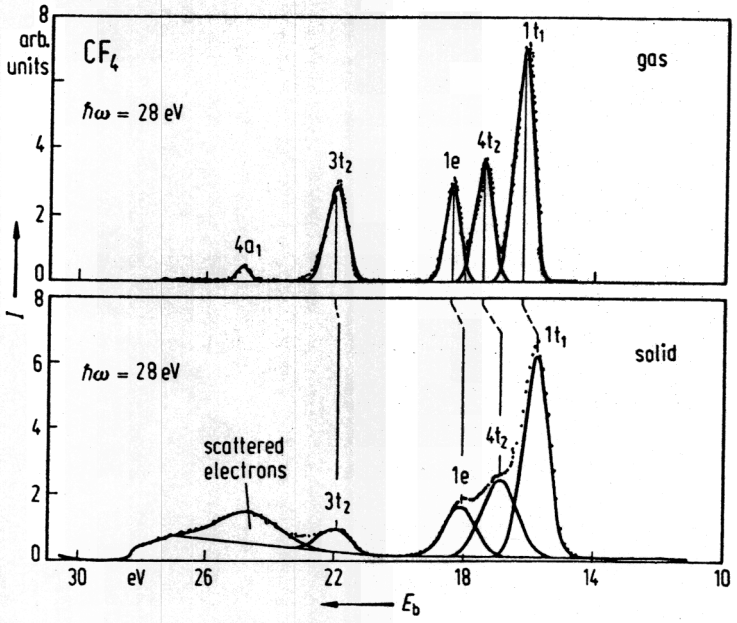

Fig. 83. CF_4. Photoelectron spectra of gaseous and solid CF_4 in the outer valence region [84B1].

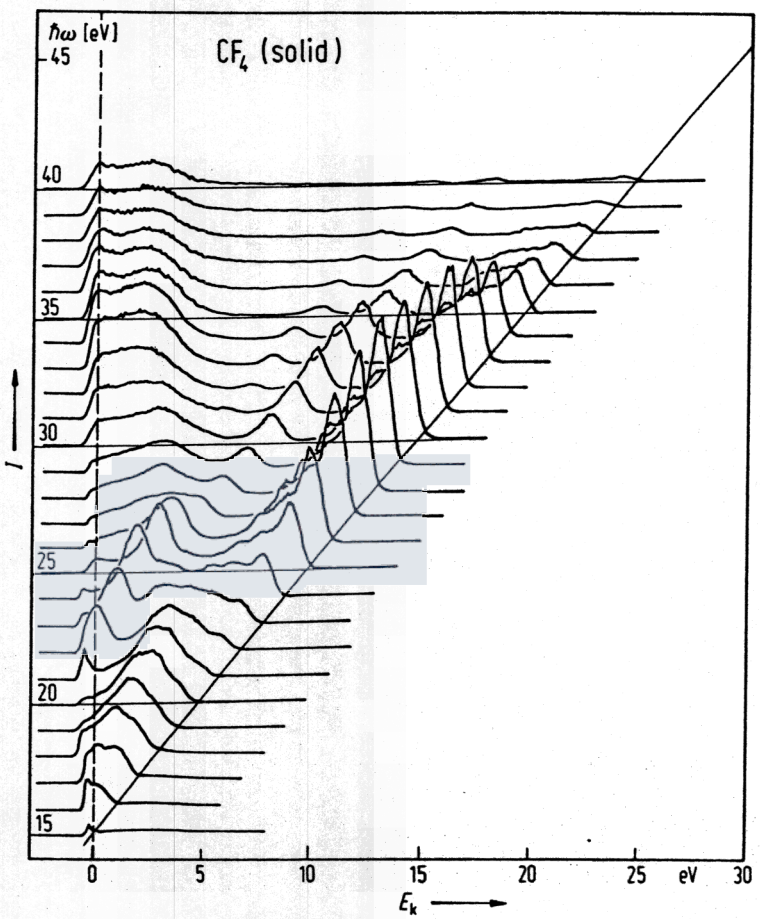

Fig. 84. CF_4. Electron distribution curves of solid CF_4 as a function of photon energy ($\hbar\omega = 15 \cdots 40$ eV) [84B1].

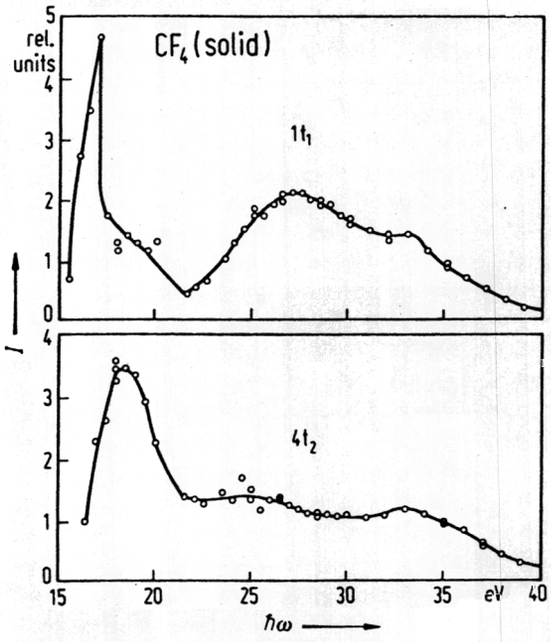

Fig. 85. CF_4. Emission intensities of the first two outer valence ion states of solid CF_4 [84B1].

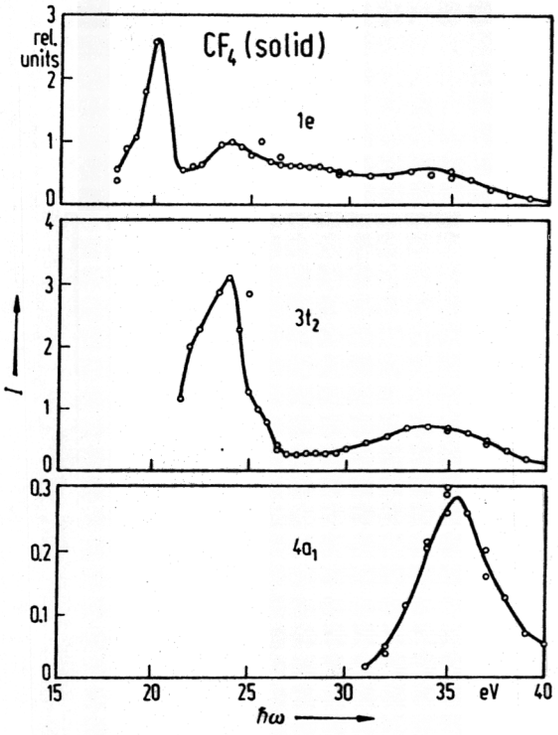

Fig. 86. CF_4. Emission intensities of the outer valence ion states of solid CF_4 [84B1].

2.3.13 Carbontetrachloride (CCl_4)

Isolated molecule

(See also [76L])

1: Point group: T_d
2: Bond length and bond angle: C—Cl: 1.769 Å
Cl—C—Cl: 109.5°
3: Ground state electron configuration: Fig. 87.

Molecular solid

Cubic face-centered carbontetrachloride.
(For various high-pressure forms of CCl_4, see [85L]; see also [71L2])

4: Space group: not reported.
5: Structure of the solid:

unit cell: $a = 8.34$ Å ($T = -35$ °C)

Atomic positions:
not reported.

6: Outer valence photoelectron spectrum of the molecular solid in comparison with the gas phase [85F]: Fig. 88.
7: Inner valence photoelectron spectrum of the molecular solid in comparison with the gas phase: not reported.
8: Core photoelectron spectra of the molecular solid in comparison with the gas phase: not reported.
9: Theoretical assignment of the observed ion states [77P5]: Table 31.
10: Polarization energies of some ion states: Table 32.
11: Ion state cross-sections as a function of photon energies of solid CCl_4 in comparison with gaseous CCl_4: Figs. 89, 90.

12: Table of resonance structures in the cross-sections: Table 33.
13: Auger spectrum of the molecular solid in comparison with the gas phase:
not reported.
14: Penning ionization electron spectrum of the molecular solid in comparison with the gas phase:
not reported.
15: Electronic excitation spectrum in the valence electron region:
not reported.
16: Electronic excitation spectrum in the core electron region of the molecular solid in comparison with the gas phase [68S2, 82O]:
not reported.

Table 31. CCl_4. Vertical binding energies E_b (eV) as calculated via a X_α-MS calculation for gaseous CCl_4 [77P5].

Level	E_b [eV]
$2t_1$	12.8
$7t_2$	13.2
$2e$	13.7
$6t_2$	16.4
$6a_1$	20.6
$5t_2$	25.9
$5a_1$	28.3

Table 32. CCl_4. Vertical binding energies and polarization energies E_{pol}.

Level	Vertical binding energy [eV]		E_{pol}
	Solid [85F]	Gas [81K1, 70P]	eV
$2t_1$	10.27	11.69	1.42
$7t_2$	11.27	12.62	1.35
$2e$	12.22	13.44	1.22
$6t_2$	15.26	16.58	1.32
$6a_1$	18.66	20.00	1.34

Table 33. CCl_4. Energy positions of features in photoemission cross-sections of gaseous and solid CCl_4 [85F].

Orbital	Solid		Gas	Assignment
	$\hbar\omega$ eV	E_k eV	E_k eV	
$2t_1$	13.0	2.7	2.4	$2t_1 \rightarrow t_1$
	15.5	5.2	2.4	$2t_1 \rightarrow e$
$7t_2$	13.5	2.2	4.4	$7t_2 \rightarrow e$
	18.0	6.7	6.4	$7t_2 \rightarrow t_2$
$2e$	14.5	2.3	2.6	$2e \rightarrow t_1$
	23.0	10.8	8.6	$2e \rightarrow t_1$
$6t_2$	18.0	2.7	2.4	$6t_2 \rightarrow e$
	(25.0)	(9.7)	8.4	$6t_2 \rightarrow t_1$

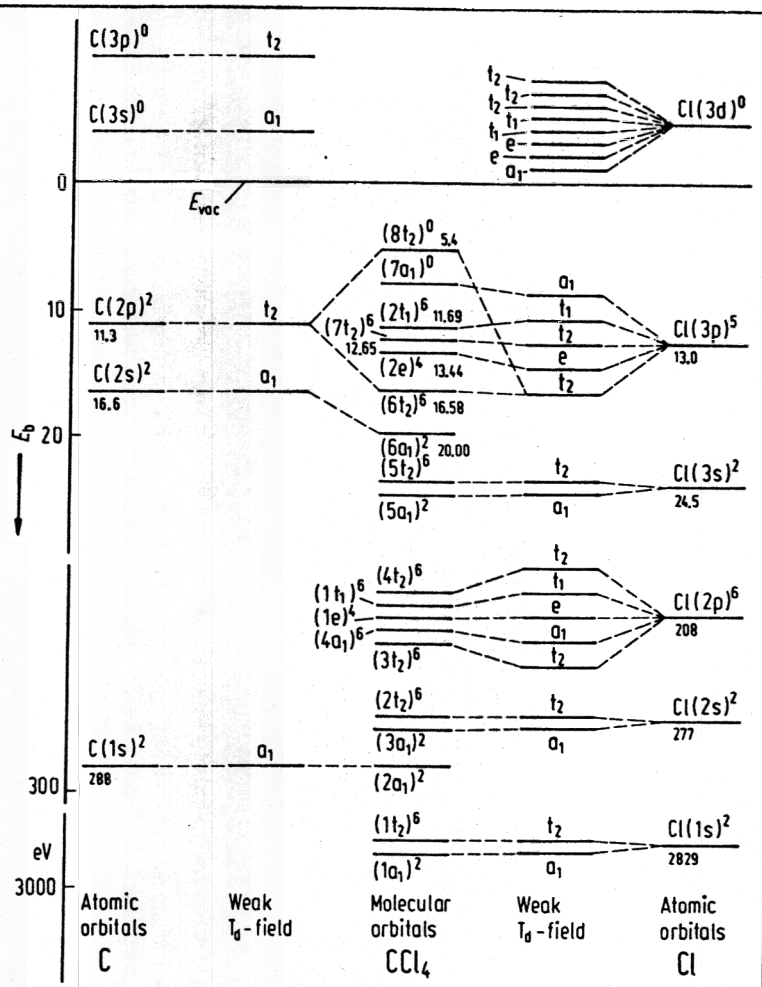

Fig. 87. CCl_4. Molecular orbital diagram after [85F]. The energies have been taken from [81K1, 70P, 78H].

For Fig. 88, see next page.

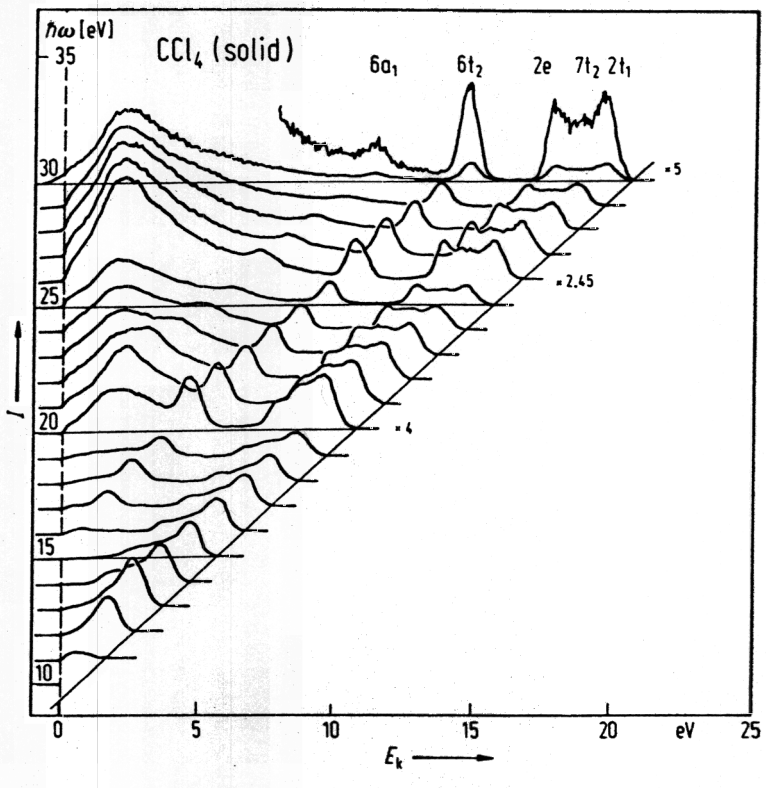

Fig. 89. CCl_4. Electron distribution curves of solid CCl_4 as a function of photon energy ($\hbar\omega = 11 \cdots 30$ eV) [85F].

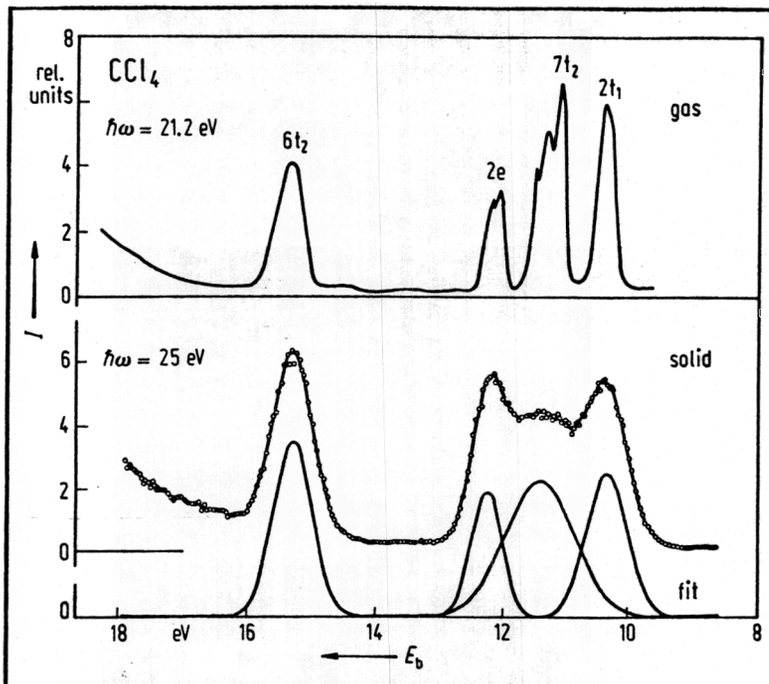

Fig. 88. CCl_4. Photoelectron spectra of gaseous [83K1] and solid [85F] CCl_4 in the outer valence region. Gas phase spectrum is shifted by 1.4 eV (cf. Table 32).

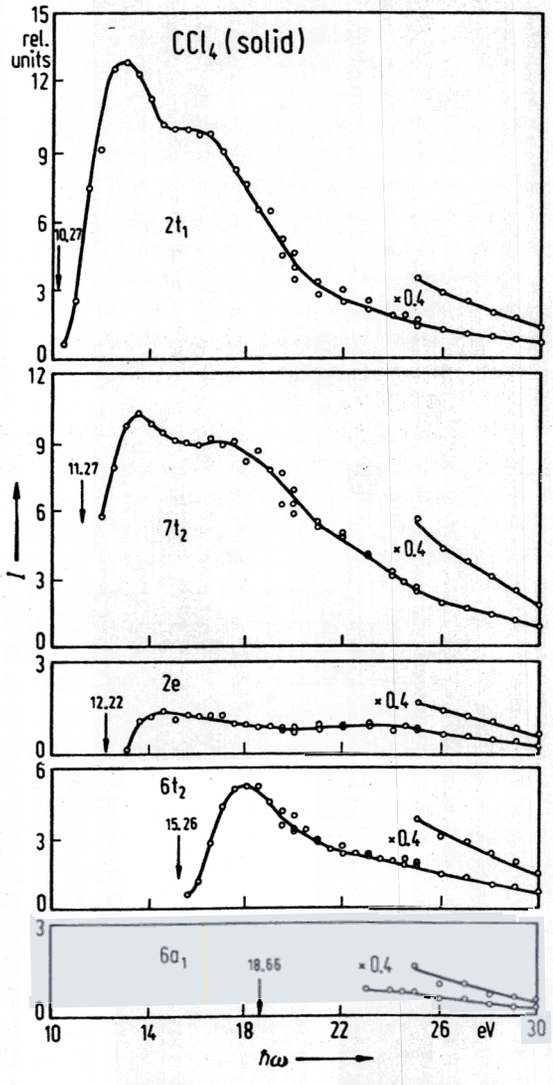

Fig. 90. CCl_4. Emission intensities of the outer valence ion states of solid CCl_4 [85F]. Arrows indicate photoemission thresholds.

2.3.14 Sulfurhexafluoride (SF_6)

Isolated molecule

(See also [87L].)

1: Point group: O_h
2: Bond length and bond angles: S—F: 1.56 Å
F—S—F: 90°
3: Ground state electron configuration: Fig. 91.

Molecular solid

Cubic SF_6

4: Space group: Im3m
5: Structure of the solid:

unit cell: $a = 5.915$ Å ($T = 193$ K)

Atomic positions:
S: (0, 0, 0), (2/3, 1/3, $\bar{z}$), (1/3, 2/3, z)
F: $\pm(x, \bar{x}, z)$, $\pm(x, 2x, z)$, $\pm(2\bar{x}, \bar{x}, \bar{z})$ x, z: S—F bond length

See also Fig. 92.

6: Outer valence photoelectron spectrum of the molecular solid [85F] in comparison with the gas phase [83K2]: Fig. 93.
7: Inner valence photoelectron spectrum of the molecular solid in comparison with the gas phase: not reported.
8: Core photoelectron spectra of the molecular solid in comparison with the gas phase [74G2]: not reported.
9: Theoretical assignment of the observed ion states [75N, 79N1]: Table 34.
10: Polarization energies of some ion states: Table 35.
11: Ion state cross-sections as a function of photon energies of solid SF_6 in comparison with gaseous SF_6: Figs. 94···96.
12: Table of resonance structures in the cross-sections: Table 36.
13: Auger spectrum of the molecular solid in comparison with the gas phase: not reported.
14: Penning ionization electron spectrum of the molecular solid in comparison with the gas phase: not reported.
15: Electronic excitation spectrum in the valence electron region [72B1]: Fig. 97.
16: Electronic excitation spectrum in the core electron region of the molecular solid in comparison with the gas phase [72L, 78A2]: not reported.

Table 34. SF_6. Calculated vertical binding energies E_b (in eV) for various ion states in gaseous SF_6 [75N, 79N1].

Level	E_b [eV]	
	[79N1]	[75N]
$1t_{1g}$	16.22	16.10
$5t_{1u}$	17.43	17.38
$1t_{2u}$	17.52	17.39
$3e_g$	18.44	18.61
$1t_{2g}$	20.32	20.20
$4t_{1u}$	23.02	22.99
$5a_{1g}$	27.41	27.31

Table 35. SF_6. Vertical binding energies and polarization energies E_{pol}.

Level	Vertical binding energies [eV]		E_{pol} [eV]
	Solid [85F]	Gas [76K]	
$1t_{1g}$	15.08	15.67	0.59
$5t_{1u}+1t_{2u}$	16.40	16.93	0.53
$3e_g$	17.82	18.3	0.48
		18.66	0.84
$1t_{2g}$	19.15	19.76	0.61
$4t_{1u}$	21.91	22.7	0.79
$5a_{1g}$	26.16	27.0	0.84

Table 36. SF_6. Energy positions of features in photoemission cross-sections of gaseous and solid SF_6 [85F].

Orbital	Solid [85F]		Gas				Assignment
			[78G1]		[82D]		
	$\hbar\omega$ eV	E_k eV	$\hbar\omega$ eV	E_k eV	$\hbar\omega$ eV	E_k eV	
$1t_{1g}$	17.0	1.9	–	–	17.0	1.3	$1t_{1g}\rightarrow 6t_{1u}$
	20.0	4.9	–	–	20.0	4.3	
	23.0	7.9	23.0	7.3	24.0	8.3	
	27.0	11.9	–	–	–	–	
	29.0	13.9	29.0	13.3	–	–	
$5t_{1u}+1t_{2u}$	20.0	3.6	18.5	1.6	18.0	1.1	
	23.0	6.6	22.5	5.6	23.0	6.1	$5t_{1u}\rightarrow 2t_{2g}$
	29.0	12.6	(29.0	12.1)	–	–	$1t_{2u}\rightarrow 2t_{2g}$
$3e_g$	20.0	2.2	20.0	1.5	19.0	0.5	$3e_g\rightarrow 6t_{1u}$
	22.5	4.7	23.0	4.5	23.5	5.0	
	26.5	8.7	–	–	–	–	
$1t_{2g}$	22.5	3.4	22.5	2.7	23.0	3.2	$1t_{2g}\rightarrow 6t_{1u}$
	27.0	7.9	–	–	–	–	
$4t_{1u}$	23.5	1.6	23.0	0.3	24.0	1.3	
	28.0	6.1	28.0	5.3	28.0	5.3	$4t_{1u}\rightarrow 2t_{2g}$

For Fig. 91, see next page.

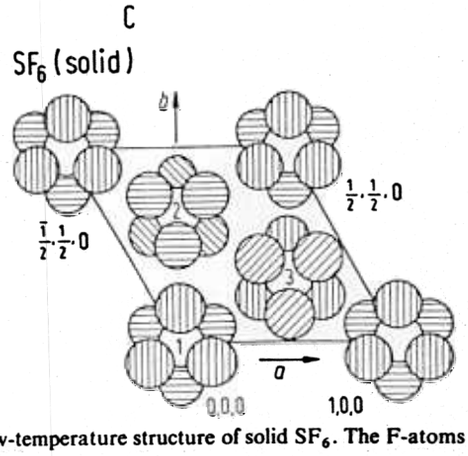

Fig. 92. SF_6. Packing model of low-temperature structure of solid SF_6. The F-atoms are hatched [82R2].

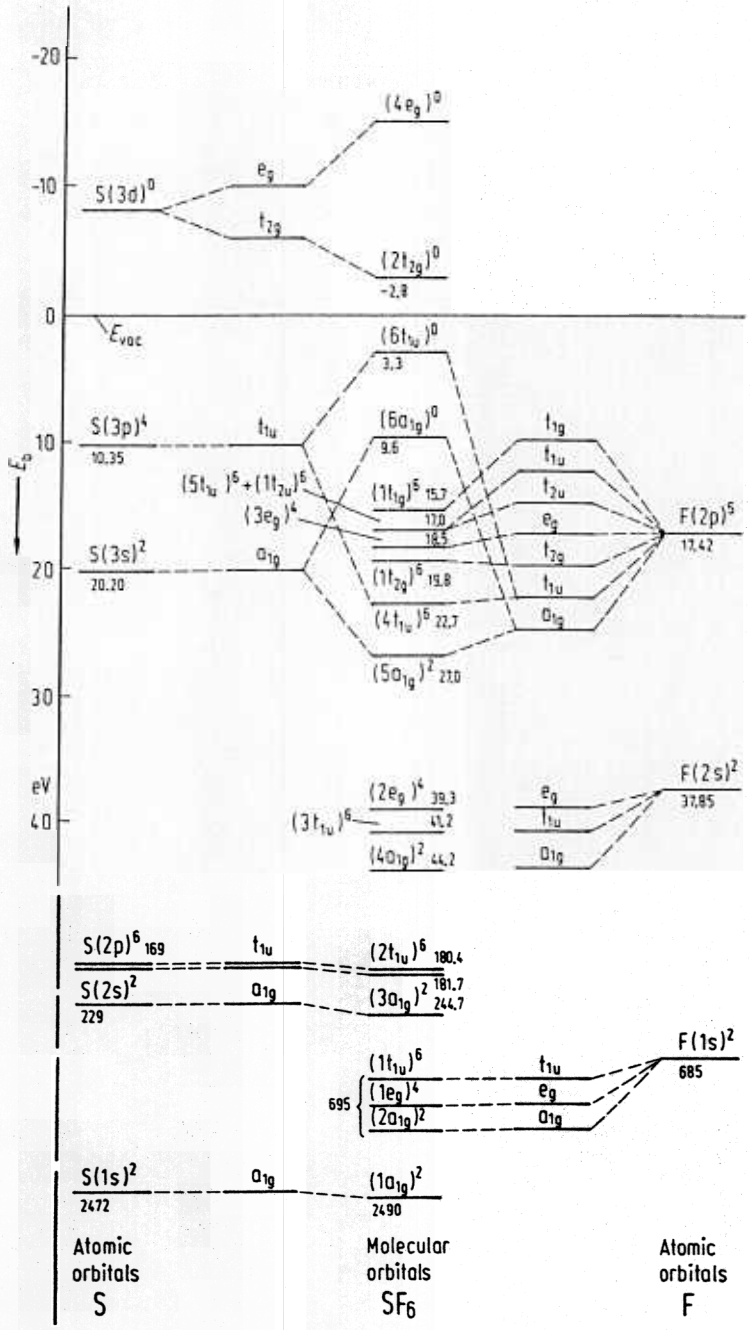

Fig. 91. SF_6. Molecular orbital diagram after [85F]. The energies have been taken from [81K1, 72D2, 72S1].

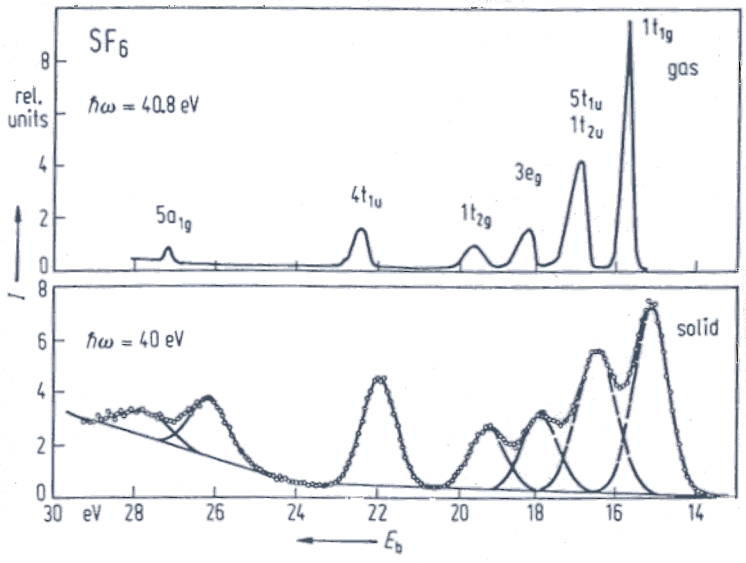

Fig. 93. SF_6. Photoelectron spectra of gaseous [83K2] and solid [85F] SF_6 in the outer valence region.

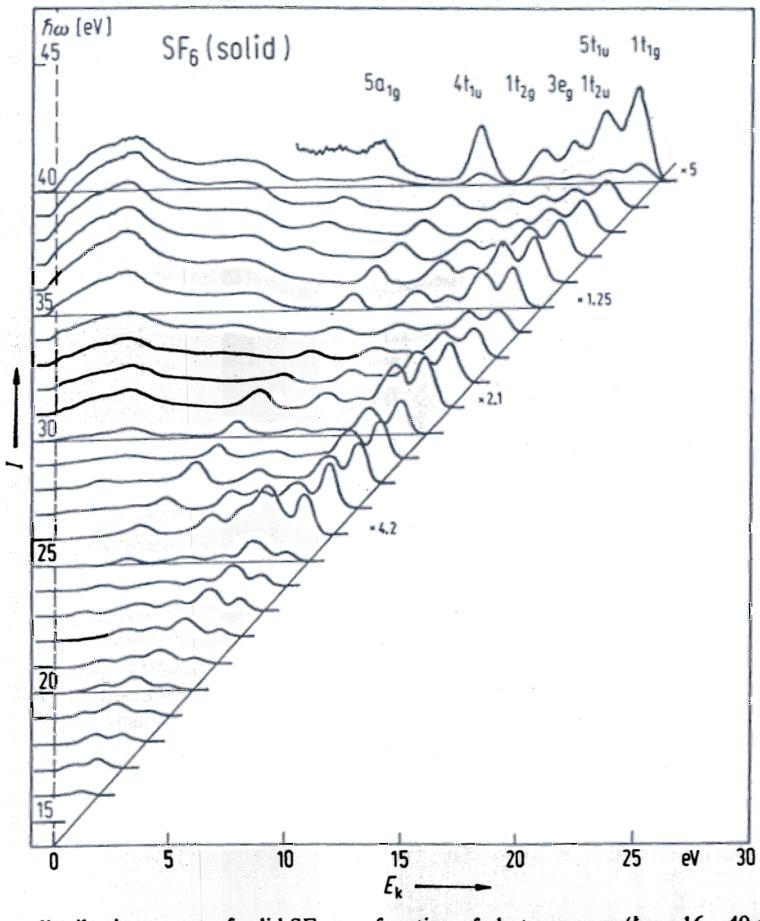

Fig. 94. SF_6. Electron distribution curves of solid SF_6 as a function of photon energy ($\hbar\omega = 16 \cdots 40$ eV) [85F].

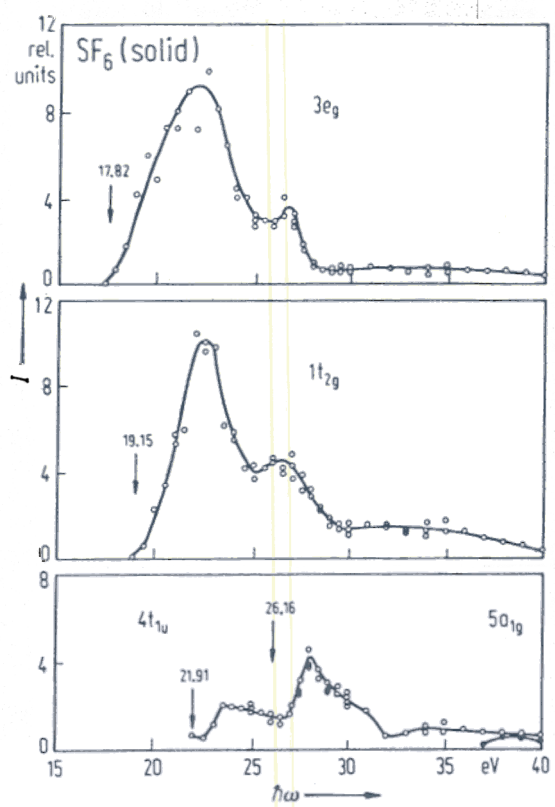

Fig. 95. SF_6. Emission intensities of the outer valence $3e_g$, $1t_{2g}$, and $4t_{1u}$ ion states of solid SF_6 [85F]. Arrows indicate photoemission thresholds.

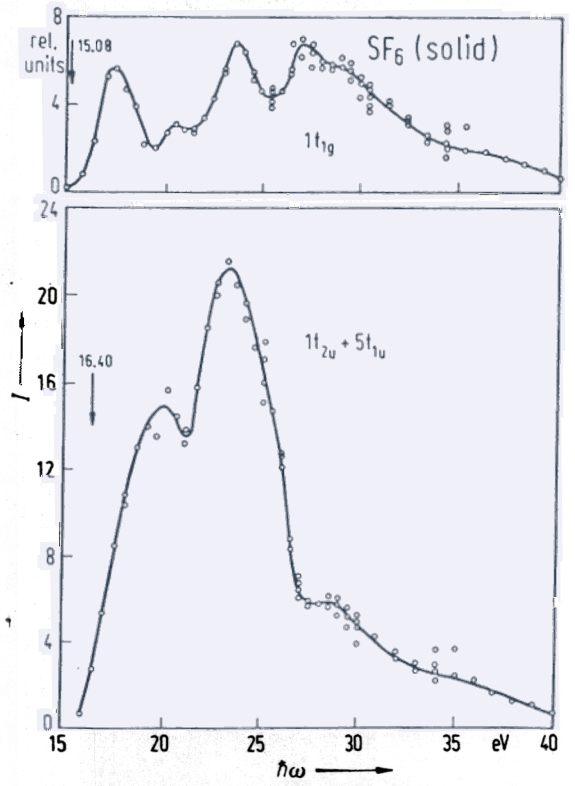

Fig. 96. SF_6. Emission intensities of the outer valence $1t_{1g}$ and combined $1t_{2u}+5t_{1u}$ ion states of solid SF_6 [85F]. Arrows indicate photoemission thresholds.

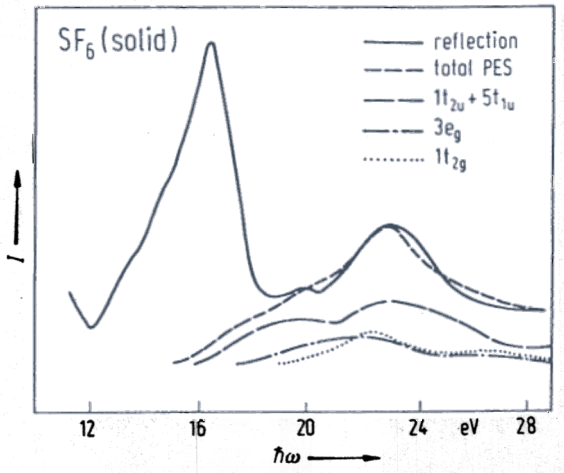

Fig. 97. SF_6. Optical reflection spectrum of the solid SF_6 [72B1] in comparison with total and partial photoemission intensities [85F].

2.3.15 Sulfur (S_8)

(Data on physical properties of sulfur are also given in [83L])

Isolated molecule

1: Point group: D_{4d}

2: Bond length and bond angle: S—S: 2.048 Å
S—S—S: 108.2° [83L]

3: Ground state electron configuration:

80 electrons	$(a_1)^2 (e_1)^4 (e_2)^4 (e_3)^4 (b_2)^2$
8 Ne-cores	S(3s)

$^1A_1$:

$(e_3)^4 (a_1)^2 (e_2)^4 (b_1)^2 (e_1)^4 (b_2)^2 (e_1)^4 (e_2)^4 (a_1)^2 (e_3)^4$
S(3p)

Molecular solid

Orthorhombic sulfur (α-S) [65W], [83L]. (For further S-modifications, see [83L].)

4: Space group: V_h^{24} (Fddd)

5: Structure of the solid:

unit cell: $a = 10.4633$ Å, $b = 12.8786$ Å, $c = 24.4784$ Å ($T = 298$ K) [83L]

Atomic positions:

$\pm(x, y, z; x, 1/4-y, 1/4-z; 1/4-x, y, 1/4-z; 1/4-x, 1/4-y, z)$

F.C.

Atom	x	y	z
S(1)	0.8554	0.9526	0.9516
S(2)	0.7844	0.0301	0.0763
S(3)	0.7069	0.9795	0.0040
S(4)	0.7862	0.9073	0.1290

Closest contact: 3.69 Å

See also Fig. 98.

6: Outer valence photoelectron spectrum of the molecular solid [77S2] in comparison with the gas phase [73B]: Fig. 99.

7: Inner valence photoelectron spectrum of the molecular solid [77S2]: Fig. 100.

8: Core photoelectron spectra of the molecular solid in [75S]: Fig. 101.

9: Theoretical assignment of the observed ion states [75S, 77S2], see also [77G]: Table 37.

10: Polarization energies of some ion states:
not reported.

11: Ion state cross-sections as a function of photon energies of solid S_8 in comparison with gaseous S_8:
not reported.

12: Table of resonance structures in the cross-sections:
not reported.

13: Auger spectrum of the molecular solid in comparison with the gas phase:
not reported.

14: Penning ionization electron spectrum of the molecular solid in comparison with the gas phase:
not reported.

15: Electronic excitation spectrum in the valence electron region [75E]: Fig. 102.

16: Electronic excitation spectrum in the core electron region of the molecular solid in comparison with the gas phase:
not reported.

Table 37. S_8. Orbital energies in the occupied and unoccupied valence region of S_8 (a, antibonding; n, nonbonding; b, bonding orbitals) [77S2].

Symmetry		E [eV]
Unoccupied	e_1	0.82 (a)
	b_2	0.78 (a)
	e_2	0.50 (a)
	b_2	0.17 (a)
	e_2	0.19 (a)
Occupied	e_3	9.11 (n)
	a_1	9.38 (n)
	e_2	9.63 (n)
	e_1	10.13 (n)
	b_2	11.65 (b)
	e_2	12.35 (b)
	b_1	12.46 (b)
	e_1	12.58 (b)
	e_3	14.16 (b)
	a_1	14.34 (b)
	b_2	16.73 (b)
	e_3	17.52 (b)
	e_2	21.53 (b)
	e_1	25.85 (b)
	a_1	28.27 (b)

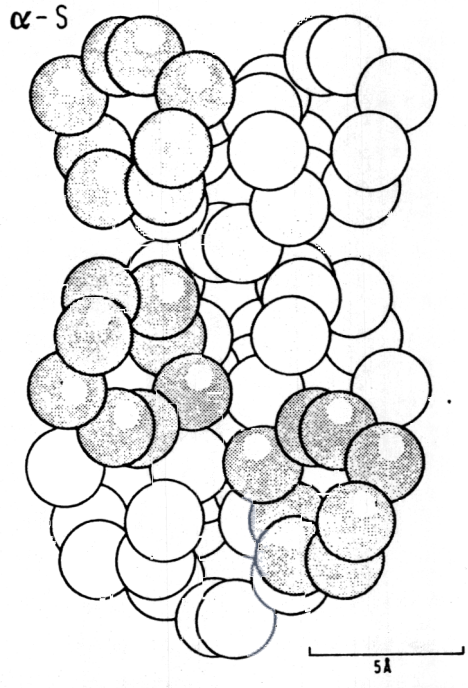

Fig. 98. S_8. A packing drawing of the portion of the structure of rhombic sulfur as viewed along its *a* axis. The nature of the S_8 molecules is apparent in this drawing [65W].

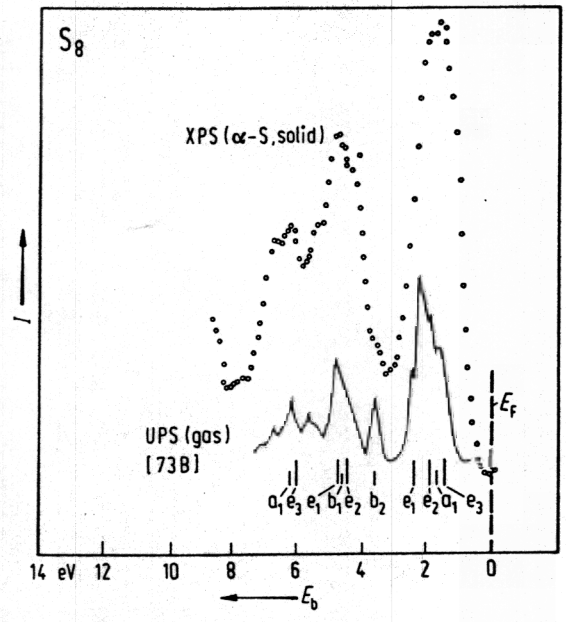

Fig. 99. S_8. Photoelectron spectra of gaseous [73B] and solid [77S2] S_8 in the outer valence region. Results of molecular orbital calculation are shown at the bottom with the states labelled according to the symmetry of the S_8-molecule. E_b w.r. to E_F.

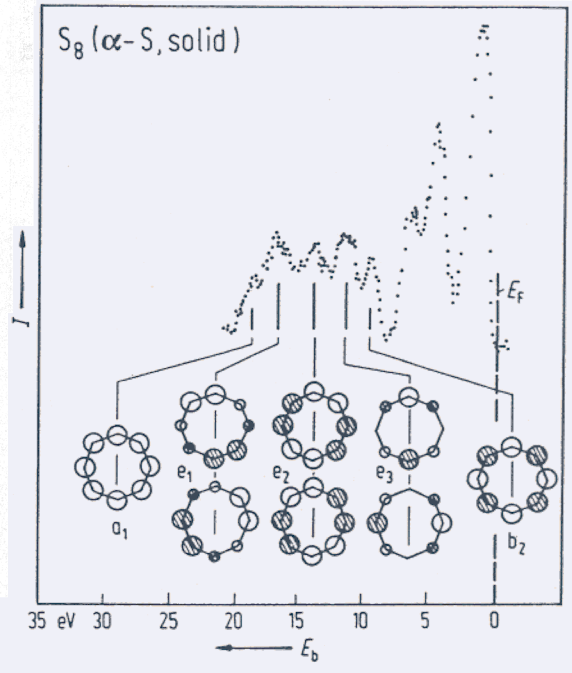

Fig. 100. S_8. High resolution XPS valence-electron photoemission spectra of sulfur in the inner valence region. The 3s-electron derived ring-quantized molecular orbitals are indicated in the figure as are their D_{4d} symmetry labels. The shape of the circles represents amplitude and sign of the wave function [77S2]. E_b w.r. to E_F.

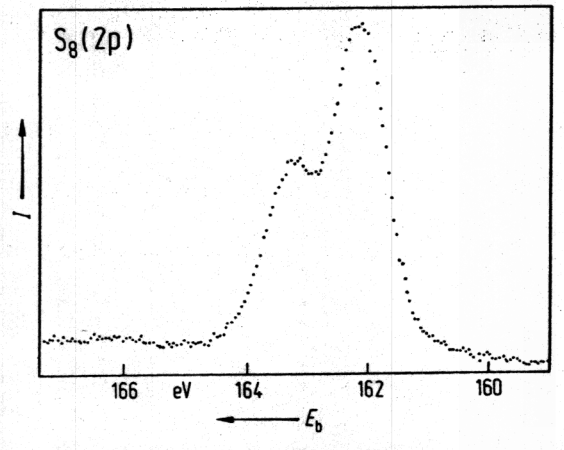

Fig. 101. S_8. The XPS spectrum of the S(2p) core level. The binding energy of the $S(2p_{3/2})$ line, 162.25(15) eV, is an average value for five separate samples. The sample-to-sample variation is within the +0.15 eV limits. The $S(2p_{3/2})$ splitting is 1.15+0.05 eV. The energy referenced to the $Au(4f_{7/2})$ line 83.8 eV [75S].

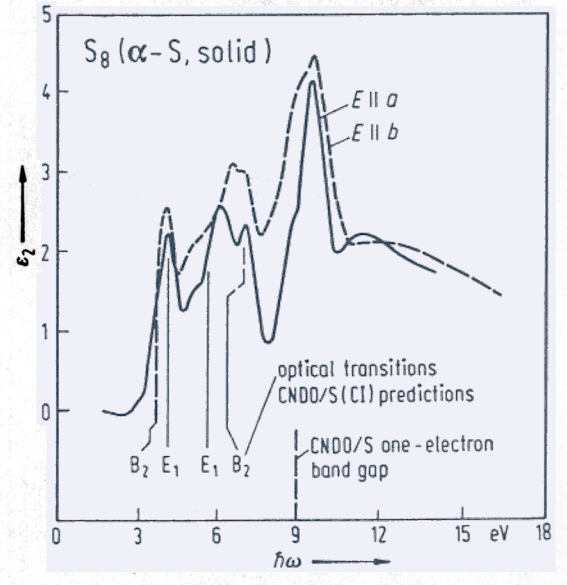

Fig. 102. S_8. Comparison of the imaginary part of the optical dielectric function for orthorhombic sulfur with calculated dipole allowed transitions [75E]. Two polarizations E of light.

2.3.16 Benzene (C_6H_6)

(Data on physical properties of benzene may also be found in [85K1])

Isolated molecule

(See also [87L] and [76L])

1: Point group: D_{6h}

2: Bond length and bond angles: C—C: 1.398 Å
C—H: 1.077 Å
H—C—C: 120°

3: Ground state electron configuration:

$$\left|\begin{array}{c}(1a_{1g})^2(1e_{1u})^4(1e_{2g})^4(1b_{1u})^2\\ C(1s)\end{array}\right|$$

^1A_g:

$$\left|\begin{array}{c}(2a_{1g})^2(2e_{1u})^4(2e_{2g})^4(3a_{1g})^2(2b_{1u})^2\\ C(2s),\ C(2p),\ H(1s)\end{array}\right|$$

$$\left|\begin{array}{c|c}(1b_{2u})^2(3e_{1u})^4(1a_{2u})^2(3e_{2g})^4(1e_{1g})^4 & (1e_{2u})^0(1b_{2g})^0\\ C(2s),\ C(2p),\ H(1s) & \text{empty}\end{array}\right|$$

See also Fig. 103.

Molecular solid

Orthorhombic benzene [58C, 71W]

4: Space group: D_{2h}^{15} (Pbca)

5: Structure of the solid:

unit cell: $a=7.46$ Å, $b=9.666$ Å, $c=7.034$ Å (at $T=270$ K)
unit cell: $a=7.292$ Å, $b=9.471$ Å, $c=6.742$ Å (at $T=78$ K)

Atomic positions: ($T=218$ K):

	x	y	z
C(1)	−0.0569	0.1387	−0.0054
C(2)	−0.1335	0.0460	0.1264
C(3)	−0.0774	−0.0925	0.1295
H(1)	−0.0976	0.2447	−0.0177
H(2)	−0.2409	0.0794	0.2218
H(3)	−0.1371	−0.1631	0.2312

See also Fig. 104.

6: Outer valence photoelectron spectra of the molecular solid [79G] in comparison with the gas phase [70T]: Fig. 105.

7: Inner valence photoelectron spectra of the molecular solid [77R] in comparison with the gas phase [74G1]: Fig. 106.

8: Core photoelectron spectra of the molecular solid [81R, 84R2] in comparison with the gas phase [78L]: Figs. 107, 108.

9: Theoretical assignment of the observed ion state [82B3]: Table 38.

10: Polarization energies of some ion states: Table 39.

11: Ion state cross-sections as a function of photon energies of solid benzene: not reported.

12: Table of resonance structures in the cross-sections: not reported.

13: Auger spectrum of the molecular solid in comparison with the gas phase [84R2]: Fig. 109.

14. Penning ionization electron spectrum of the molecular solid [81K2] in comparison with the gas phase: [79M]: Fig. 110.

15: Electronic excitation spectra in the valence electron region:
not reported.

16: Electronic excitation spectra in the core electron region of the molecular solid in comparison with the gas phase:
not reported.

Table 38. C_6H_6. Calculated vertical binding energies E_b of gaseous benzene [76N]. For different assignment of levels, see [76N].

Level	E_b [eV]
$1e_{1g}$ (Π)	9.1
$2e_{2g}$	11.95
$1a_{2u}$ (Π)	12.26
$2e_{1u}$	14.46
$1b_{2u}$	14.83
$1b_{1u}$	15.75
$2a_{1g}$	17.48
$1e_{2g}$	20.01

Table 39. C_6H_6. Vertical binding energies of gaseous and solid benzene and polarization energies.

State	Vertical binding energies [eV]				E_{pol} [eV]
	XPS (gas) [78L]	XPS (solid) [77R]	UPS (gas) [70T]	UPS (solid) [79G]	
$1e_{1g}$	9.5	7.9	9.3	8.0	1.6
$3e_{2g}$	12.0	10.5	11.8	11.9	1.5
$1a_{2u}$			12.5		
$3e_{1u}$	14.0	(12.3)	14.0	13.1	(1.7)
$1b_{2u}$	15.2	14.0	14.9		(1.2)
$2b_{1u}$			15.5	14.0	1.5
$3a_{1g}$			17.0	15.5	1.5
$2e_{2g}$	19.0	17.7	19.2	17.7	1.5
$2e_{1u}$	22.7	21.2	22.6		1.5
$2a_{1g}$	25.7	24.5	25.8		1.2
C(1s)	290.42	288.1			2.3
su*)	296.32	294.0			2.3
su	297.42	295.4			2.0
su	298.72	296.7			2.0
su	301.12	299.2			1.9
su		301.9			
su		303.7			
su		307.4			
su		313.4			

*) su: shake up satellites.

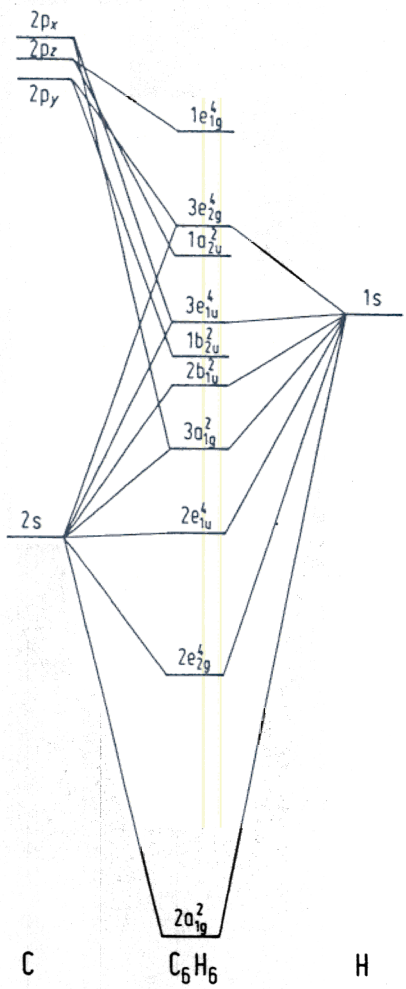

Fig. 103. C_6H_6. Molecular orbitals of benzene in the valence electron region.

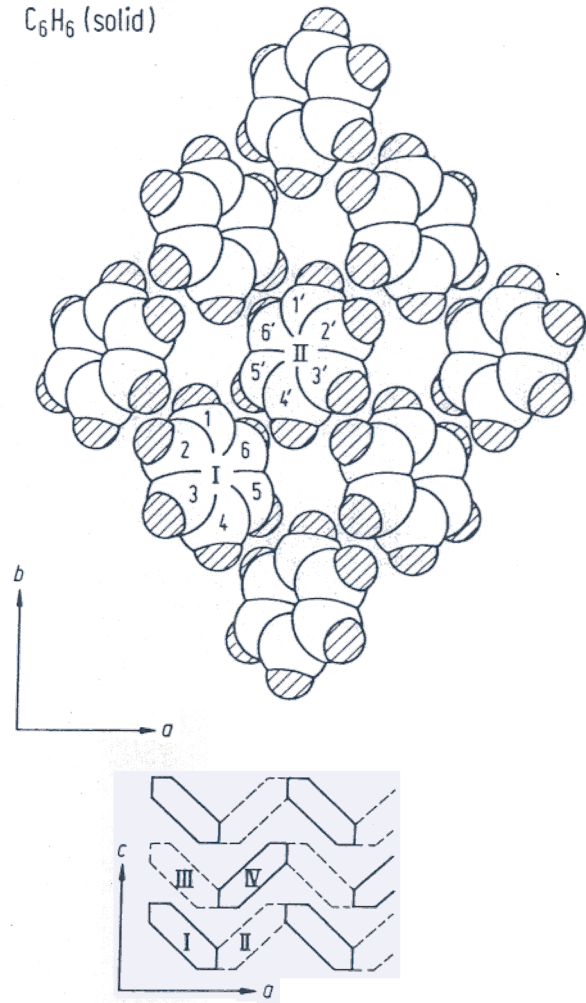

Fig. 104. C_6H_6. Packing drawing of a projection along c in solid benzene [58C].

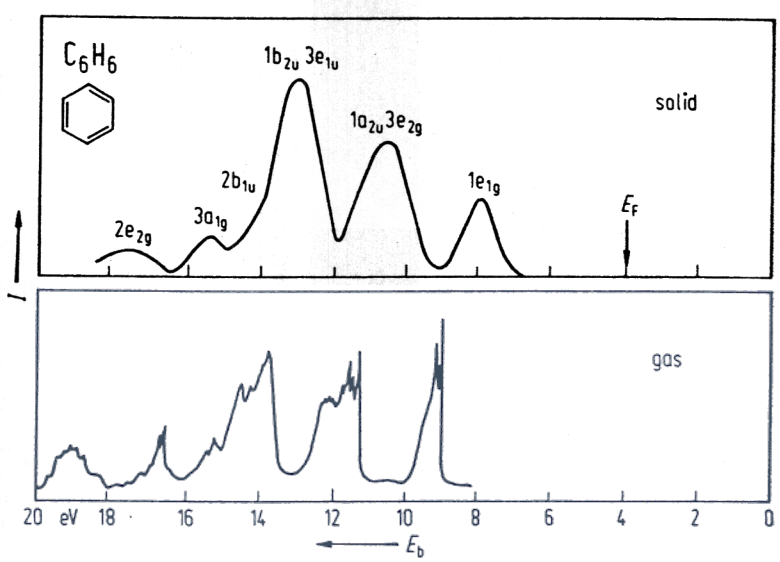

Fig. 105. C_6H_6. Outer valence photoelectron spectrum of solid [79G] benzene (HeI) in comparison with the gas phase (HeI) [70T].

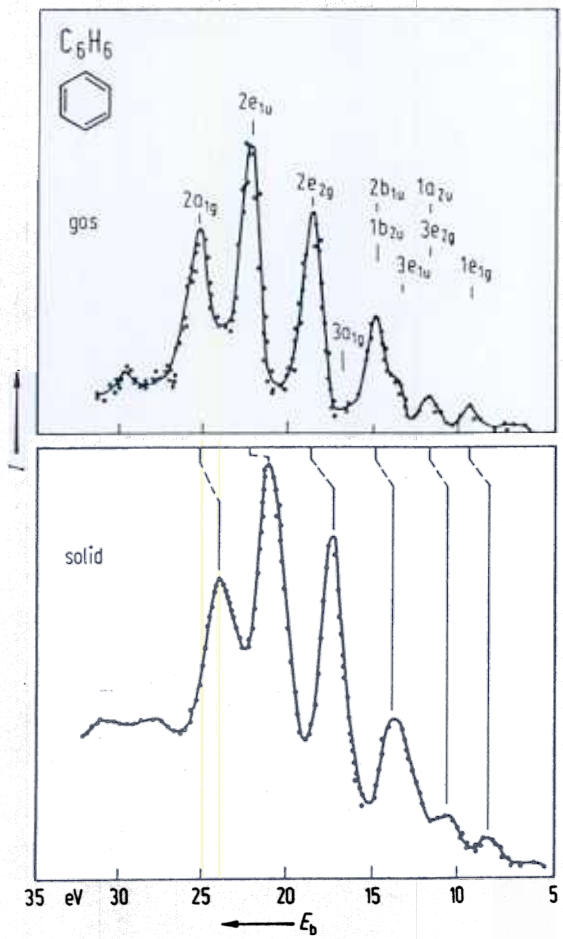

Fig. 106. C_6H_6. Complete valence electron spectrum taken with $\hbar\omega = 1475$ eV in the solid [77R] and in the gas phase of benzene [74G2].

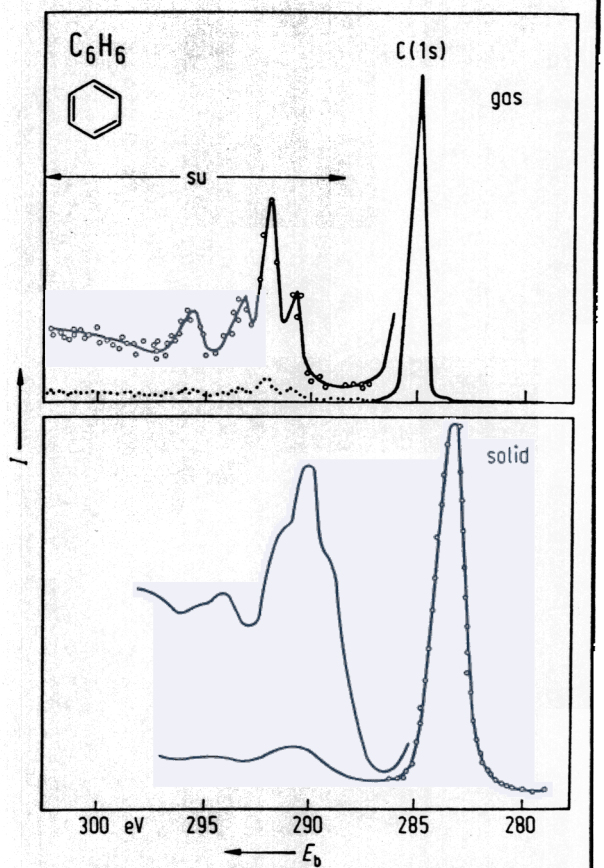

Fig. 108. C_6H_6. Core photoelectron spectra of solid [81R, 84R2] and gaseous [78L] benzene. su: shake up satellites.

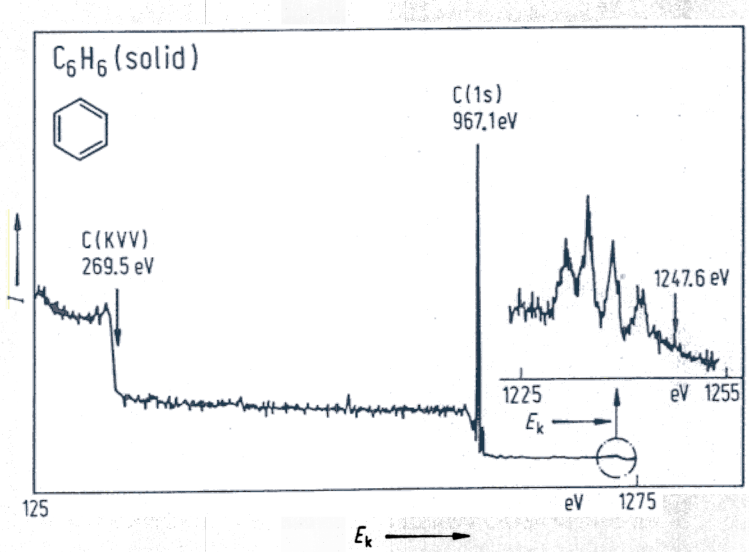

Fig. 107. C_6H_6. Complete ESCA spectrum of solid benzene [84R2].

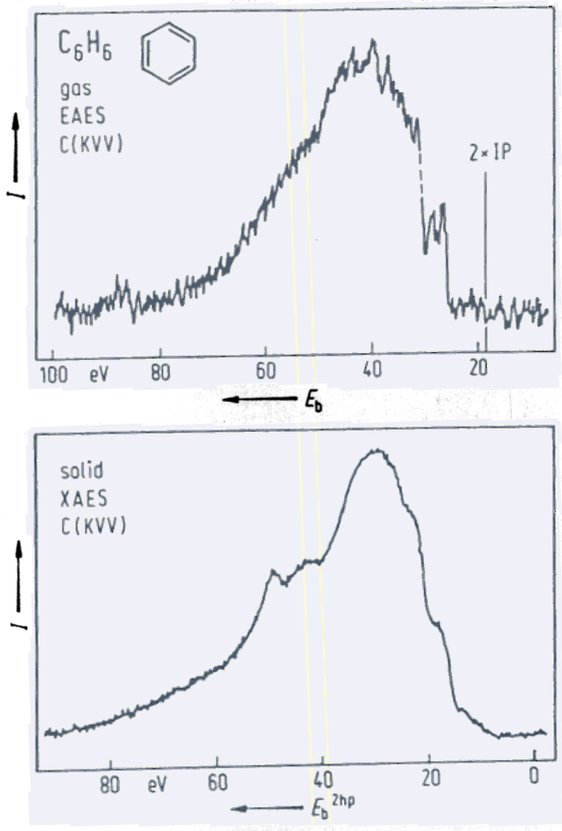

Fig. 109. C_6H_6. Auger spectra of solid and gaseous benzene [84R2]. E_b^{2hp}: two-hole binding energy. IP: ionization potential. EAES: electron excited AES; XAES: X-ray excited AES. $E_b=0$ at E_{vac} for gaseous C_6H_6, $E_b=0$ at E_F (Au) for solid C_6H_6.

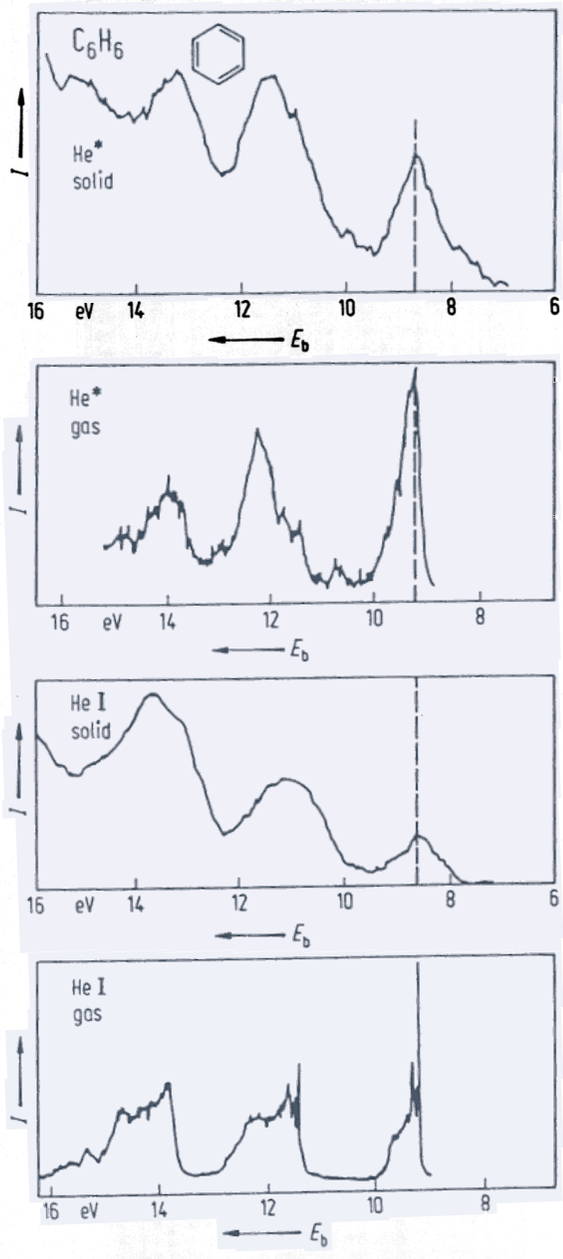

Fig. 110. C_6H_6. The first three valence states of the Penning ionization spectrum of solid [81K2] and gaseous [79M] benzene in comparison with the corresponding He I spectra. E_b: binding energy (=ionization potential).

2.3.17 Pyridine (NC_5H_5)

Isolated molecule

(See also [87L])

1: Point group: C_{2v}
2: Bond lengths and bond angles: Fig. 111
3: Ground state electron configuration: Fig. 112

Molecular solid

Orthorhombic pyridine $T = 153$ K [81M]
4: Space group: $Pna2_1$
5: Structure of the solid:

unit cell: $a = 17.524$ Å, $b = 8.969$ Å, $c = 11.352$ Å

Atomic positions: [81M]: Fig. 113.

6: Outer valence photoelectron spectrum of the molecular solid [84E1] in comparison with the gas phase [82R1]: Fig.114.
7: Inner valence photoelectron spectra of the molecular solid [84E1]: see Fig. 114.
8: Core photoelectron spectra of the molecular solid [81E] gas phase, [80B2]: Fig. 115.
9: Theoretical assignment of the observed ion states: Table 40.
10: Polarization energies of some ion states: see Table 40.
11: Ion state cross-sections as a function of photon energies of solid pyridine [84E1]: Fig. 116.
12: Table of resonance structures in the cross-sections: not reported.
13: Auger spectrum of the molecular solid in comparison with the gas phase: not reported.
14: Penning ionization electron spectrum of the molecular solid in comparison with the gas phase: not reported.
15: Electronic excitation spectra of the solid in the valence electron region: not reported.
16: Electronic excitation spectrum in the core electron region of the molecular solid in comparison with the gas phase: not reported.

Table 40. NC_5H_5. Assignment of valence ion states of gaseous and solid pyridine on the basis of many-body-ab-initio calculations [79N1]. Energy values in eV.

Assignment	Experiment				MO calculation [79N1]
	Gas [82R1]	Solid [84F1]		E_{pol}	
	E_b	E_b			E_b
$7a_1(n)$	9.66	9.6	A		9.59
$1a_2(\pi)$	9.85				9.57
$2b_1(\pi)$	10.51				10.24
$5b_2$	12.45		B		12.87
$1b_1(\pi)$	13.2				13.43
$6a_1$	13.8				14.18
$4b_2$	14.5				15.11
$5a_1$	15.84	15.3		0.54	16.32
$3b_2$					16.31 and 16.05
$4a_1$	17.1	16.8		0.3	17.94 and 18.40
$3a_1$		19.4	C		21.32 and 21.16
$2b_2$					21.29
$1b_2$		23.5	D		26.1 and 26.2[a])
$2a_1$					27.50[a])
$1a_1$		27.8	E		32.3[a])

[a]) Values are taken from a figure in [79N1].

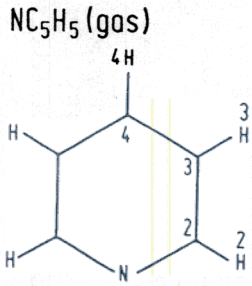

Fig. 111. NC_5H_5. Schematic structure of gaseous pyridine with bond lengths and bond angles as determined by microwave spectra [58B].
Bond lengths in Å:
N–C(2): 1.3402; C(2)–H(2): 1.0843
C(2)–C(3): 1.3945; C(3)–H(3): 1.0805
C(3)–C(4): 1.3944; C(4)–H(4): 1.0773
Bond angles:
C(6)–N–C(2); 116° 50′
N–C(2)–C(3); 123° 53′
C(2)–C(3)–C(4): 118° 32′
C(3)–C(4)–C(5): 118° 20′
N–C(2)–H(2): 115° 53′
C(4)–C(3)–H(3): 121° 18′.

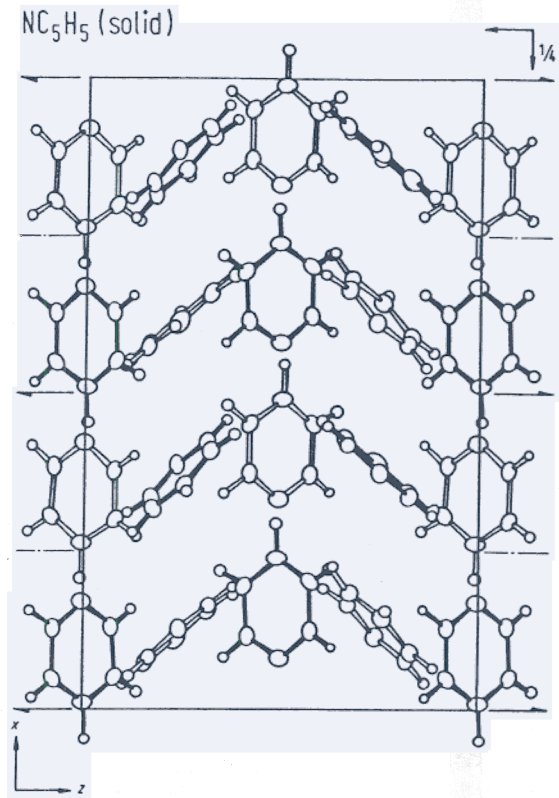

Fig. 113. NC_5H_5. Crystal structure of solid pyridine down to basis [81M].

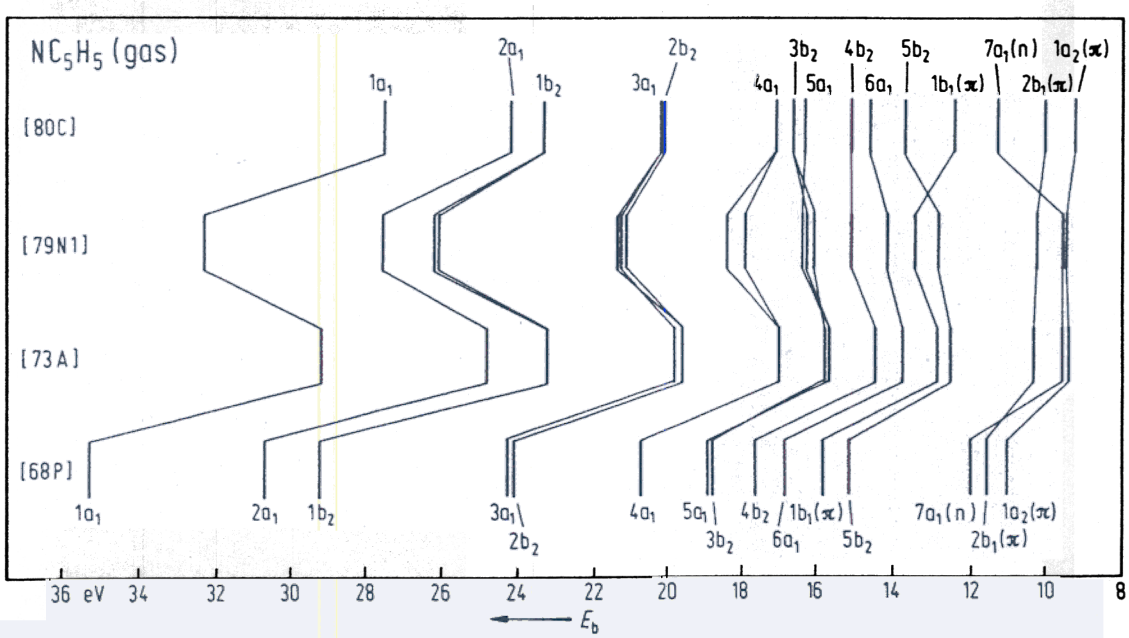

Fig. 112. NC_5H_5. Molecular orbital diagrams of pyridine according to various calculations [80C, 79N1, 73A, 68P].

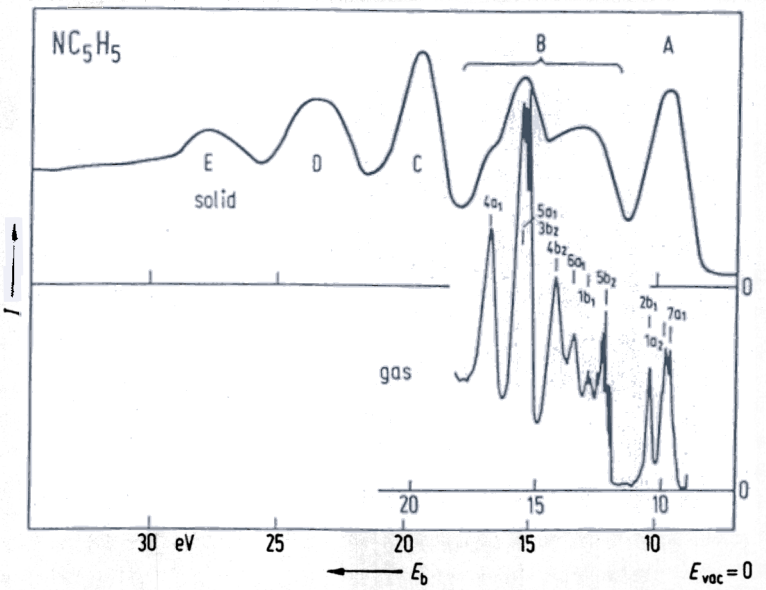

Fig. 114. NC_5H_5. Comparison of the valence photoelectron spectrum of solid pyridine ($\hbar\omega = 170$ eV) with the gas phase spectrum ($\hbar\omega = 21.21$ eV) [84F1, 82R1].

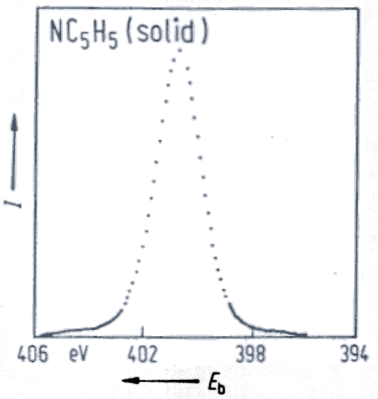

Fig. 115. NC_5H_5. N(1s) X-ray photoelectron spectrum of solid pyridine ($\hbar\omega = 1253.4$ eV) [81E].

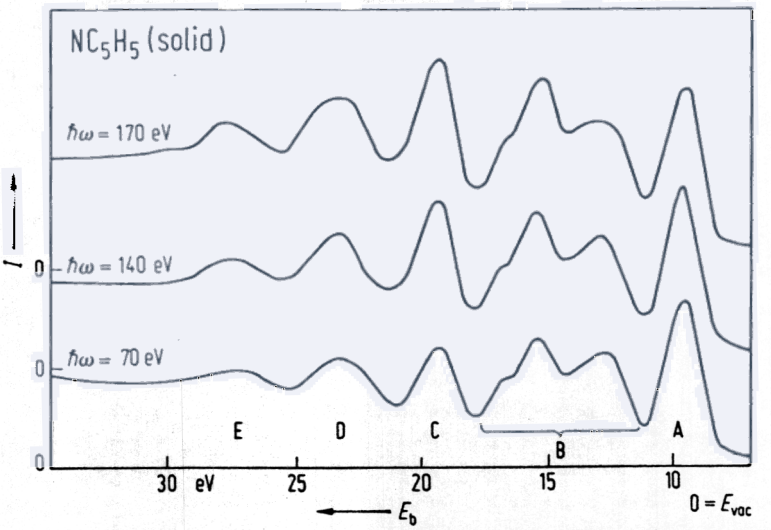

Fig. 116. NC_5H_5. Angle integrated photoelectron spectra of solid pyridine at 120 K for photon energies 70, 140, 170 eV [84F1].

2.3.18 Naphthalene ($C_{10}H_8$)

(For further data on naphthalene, see also [85K1])

Isolated molecule

1: Point group: D_{2h}
2: Bond lengths and bond angles (see also [87L]): Fig. 117
3: Ground state electron configuration: Fig. 118

Molecular solid

Monoclinic naphthalene [49S, 71W, 85K1]

4: Space group: $C_{2h}^5(P2_1/a)$
5: Structure of the solid:

unit cell: $a=8.2606$ Å, $b=5.9872$ Å, $c=8.6816$ Å, $\beta=122.67°$ ($T=296$ K) [85K1]

Atomic positions:

Atom	x	y	z
C(A)	0.0856	0.0186	0.3251
C(B)	0.1148	0.1588	0.2200
C(C)	0.0472	0.1025	0.0351
C(D)	0.0749	0.02471	−0.0784
C(E)	0.0116	0.1869	−0.2541

See also Fig. 119.

6: Outer valence photoelectron spectra of the molecular solid [79G] in comparison with the gas phase [74B, 72B2]: Fig. 120.
7: Inner valence photoelectron spectra of the molecular solid [77R]: Fig. 121.
8: Core photoelectron spectra of the molecular solids [77R]: Fig. 122.
9: Theoretical assignment of the observed ion state: Table 41.
10: Polarization energies of some ion states:
not reported.
11: Ion state cross-sections as a function of photon energies of solid naphthalene:
not reported.
12: Table of resonance structures in the cross-sections:
not reported.
13: Auger spectrum of the molecular solid in comparison with the gas phase:
not reported.
14: Penning ionization electron spectrum of the molecular solid in comparison with the gas phase:
not reported.
15: Electronic excitation spectra of the solid in the valence electron region [78A1] in comparison with gas phase spectra: Fig. 123.
16: Electronic excitation spectrum in the core electron region of the molecular solid in comparison with the gas phase:
not reported.

Table 41. $C_{10}H_8$. Theoretical assignment of some ion states of gaseous naphthalene [82V].

Level	E_b [eV]
a_u (π)	8.56
b_{1u}(π)	9.26
b_{3g}(π)	11.05
b_{2g}(π)	12.61
b_{1g}	12.80
a_g	13.30
b_{3u}	14.89
b_{1u}(π)	15.64
b_{3u}	15.94
b_{2u}	16.17
b_{1g}	16.95

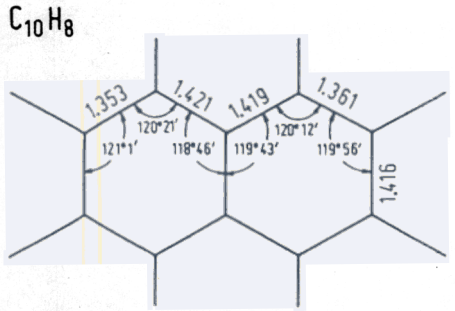

Fig. 117. $C_{10}H_8$. Schematic drawing of the molecular structure. Distances in Å [71W].

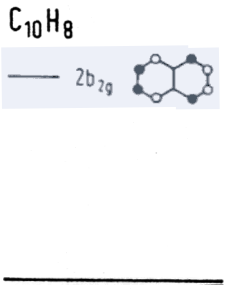

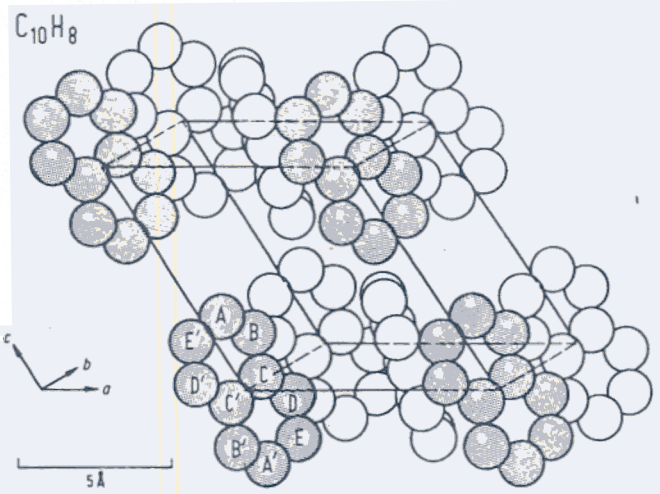

Fig. 119. $C_{10}H_8$. Packing drawing of the unit cell of solid naphthalene [71W, 49S].

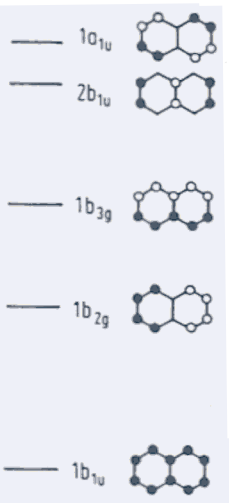

Fig. 118. $C_{10}H_8$. π-electron orbitals of naphthalene. The σ-orbitals have been omitted [84R1].

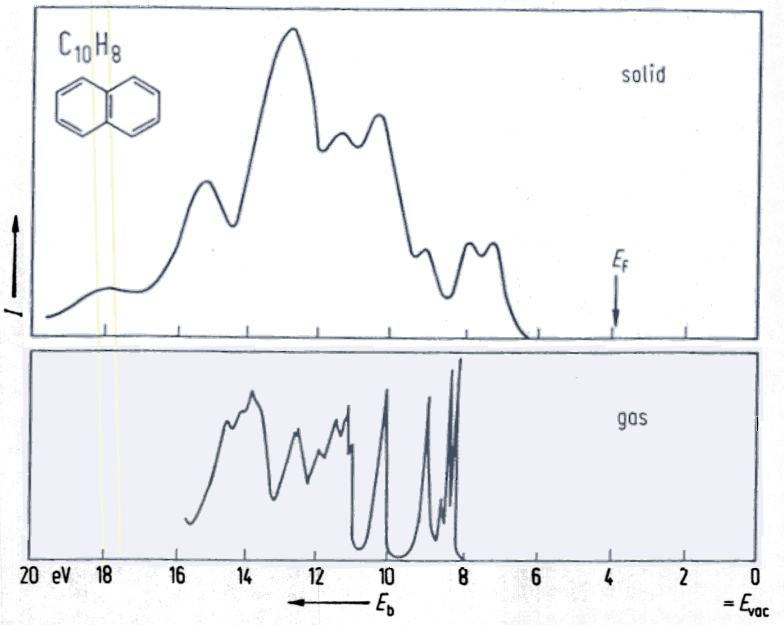

Fig. 120. $C_{10}H_8$. Outer valence photoelectron spectrum of solid naphthalene (He I) [79G] in comparison with the gas phase (He I) [72B2].

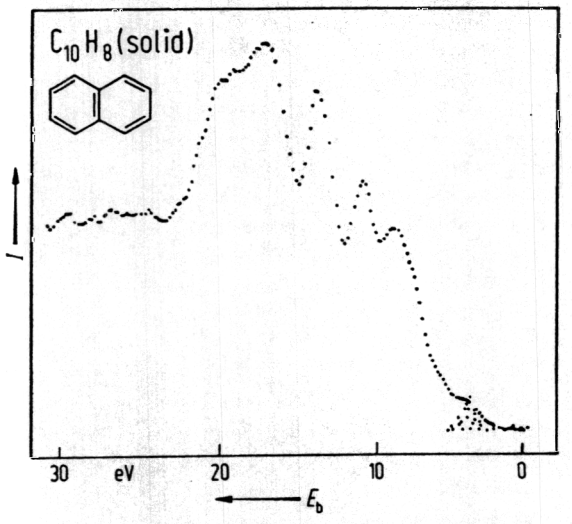

Fig. 121. $C_{10}H_8$. Complete valence electron spectrum taken with $\hbar\omega = 1457$ eV in solid naphthalene [77R].

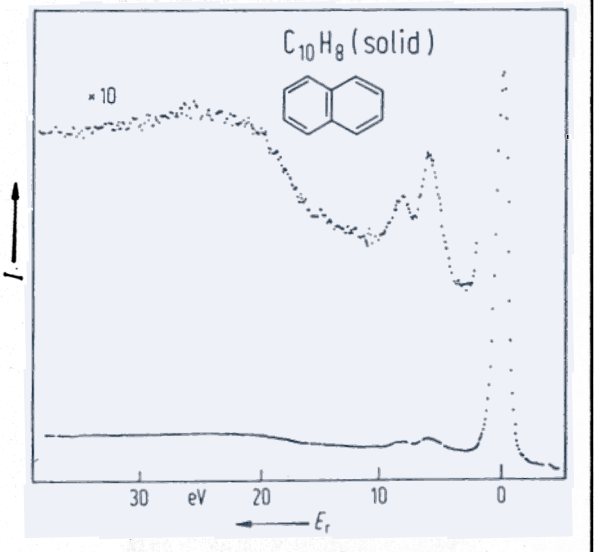

Fig. 122. $C_{10}H_8$. Core photoelectron spectra of solid naphthalene [77R]. E_r: binding energy relative to C(1s) mainpeak.

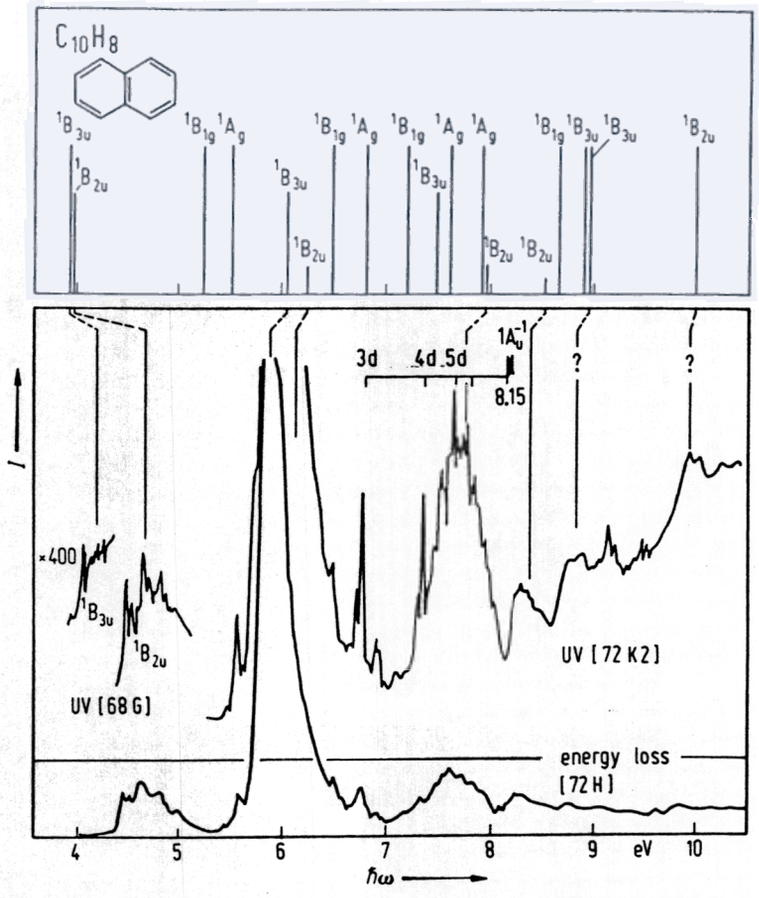

Fig. 123. $C_{10}H_8$. Valence electron excitation spectrum of naphthalene including a theoretical assignment [68G, 72H, 72K2, 78A1].

2.3.19 Anthracene ($C_{14}H_{10}$)

(Data on physical properties (also photoemission) are given in great detail in [85K1])

Isolated molecule

1: Point group: D_{2h}
2: Bond lengths and bond angles (see also [87L]): Fig. 124
3: Ground state electron configuration: Fig. 125

Molecular solid

Monoclinic solid anthracene [50S], [85K1]

4: Space group: $C_{2h}^5(P2_1/a)$
5: Structure of the solid

unit cell: $a=8.562$ Å, $b=6.038$ Å, $c=11.184$ Å; $\beta=124°\ 42'$ ($T=290$ K)
$a=8.443$ Å, $b=6.002$ Å, $c=11.123$ Å; $\beta=125°\ 36'$ ($T=95$ K)

Atomic positions: Table 42 and Fig. 126

6: Outer valence photoelectron spectra of the molecular solid [79G] in comparison with the gas phase [74B]: Figs. 127 ··· 129.
7: Inner valence photoelectron spectra of the molecular solid [77R]: Fig. 130.
8: Core photoelectron spectra of the molecular solid [77R]: Fig. 131.
9: Theoretical assignment of the observed ion state: Table 43.
10: Polarization energies of some ion states:
not reported.

11: Ion state cross-sections as a function of photon energies of solid anthracene [82K]: Fig. 132.
12: Table of resonance structures in the cross-sections:
not reported.
13: Auger spectrum of the molecular solid in comparison with the gas phase.
14: Penning ionization electron spectrum of the molecular solid in comparison with the gas phase:
not reported.
15: Electronic excitation spectra in the valence electron region [79G], [71K]: Figs. 133, 134.
16: Electronic excitation spectrum in the core electron region of the molecular solid in comparison with the gas phase:
not reported.

Table 42. $C_{14}H_{10}$. Atomic positions of solid anthracene [84R1].

Atom	x	y	z
C(1)(A)	0.0873(6)	0.0271(10)	0.3656(5)
C(2)(B)	0.1187(6)	0.1578(8)	0.2807(4)
C(3)(C)	0.0586(5)	0.0803(7)	0.1382(4)
C(4)(D)	0.0879(5)	0.2094(8)	0.0474(4)
C(5)(E)	0.0304(5)	0.1307(7)	−0.0899(4)
C(6)(F)	0.0606(6)	0.2594(8)	−0.1835(4)
C(7)(G)	0.0034(6)	0.1806(9)	−0.3166(5)
H(1)	0.131(6)	0.108(8)	0.472(4)
H(2)	0.196(6)	0.325(8)	0.317(4)
H(4)	0.155(6)	0.376(8)	0.085(4)
H(6)	0.121(6)	0.430(8)	−0.143(4)
H(7)	0.024(6)	0.324(9)	−0.379(4)

Table 43. $C_{14}H_{10}$. Calculated vertical binding energies E_b of some ion states of gaseous anthracene [82V].

Level	E_b [eV]
$b_{3g}(\pi)$	7.83
$b_{2g}(\pi)$	9.47
$a_u(\pi)$	9.93
$b_{3g}(\pi)$	11.50
$b_{1u}(\pi)$	11.62
b_{1g}	12.24
a_g	13.19
b_{3u}	13.86
$b_{2g}(\pi)$	14.19
b_{2u}	14.74
b_{3u}	15.04
a_g	15.64
$b_{1u}(\pi)$	16.14

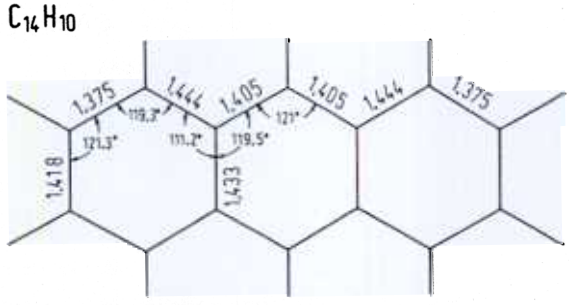

Fig. 124. $C_{14}H_{10}$. Schematic drawing of the molecular structure. Distances in Å [84R1].

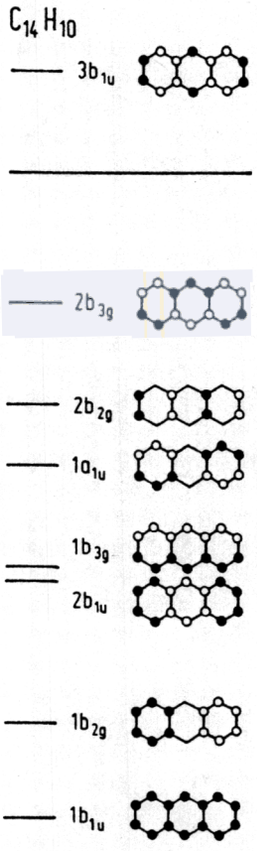

Fig. 125. $C_{14}H_{10}$. π-electron orbitals of anthracene. The σ-orbitals have been omitted [84R1].

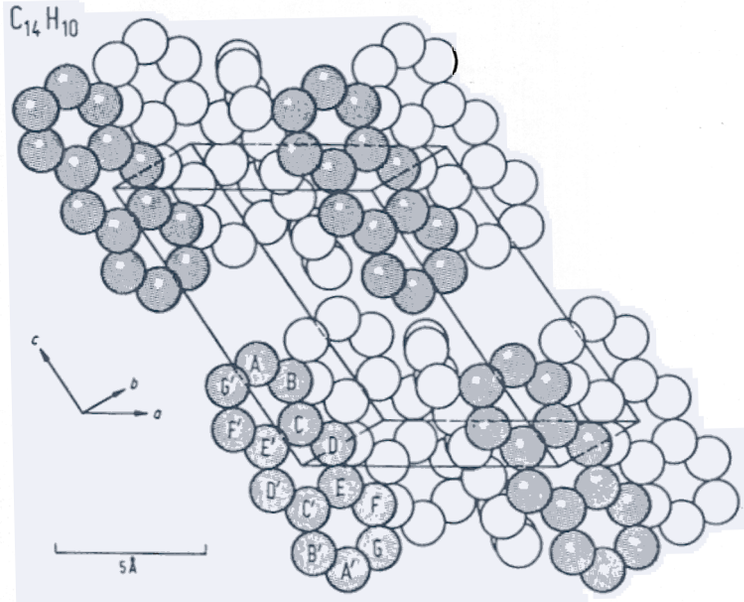

Fig. 126. $C_{14}H_{10}$. Packing drawing of the unit cell of solid anthracene [50S]. See also [71W].

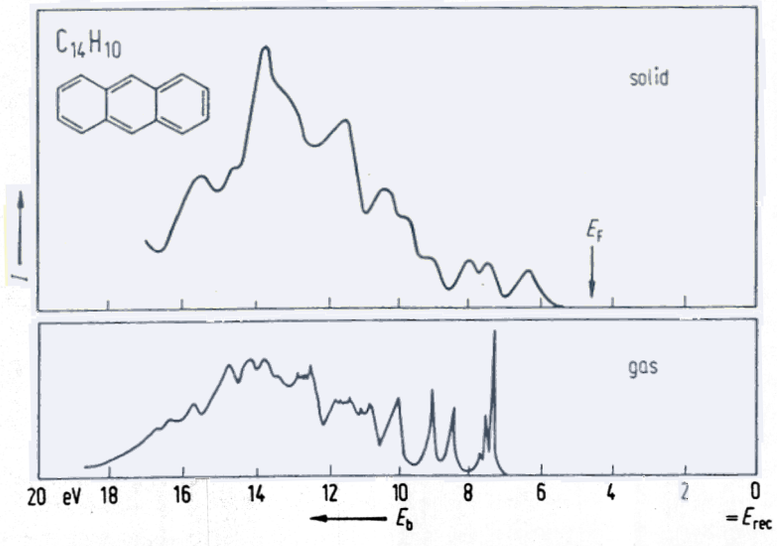

Fig. 127. $C_{14}H_{10}$. Outer valence photoelectron spectrum of solid anthracene (He I) [79G] in comparison with the gas phase (He I) [74B].

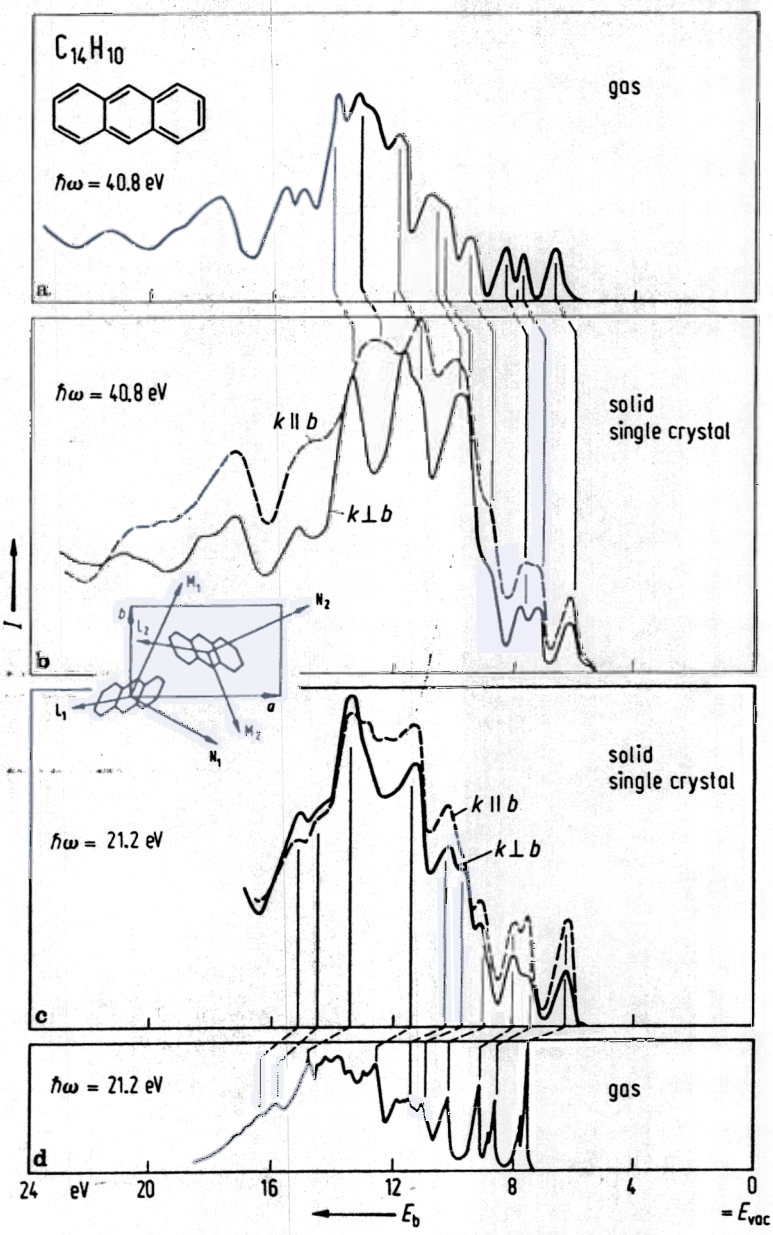

Fig. 128. $C_{14}H_{10}$. He I and He II spectra of single crystalline anthracene in comparison with the corresponding gas phase data. The solid and the dashed lines refer to the orientation of the *b* axis of the single crystal relative to the light propagation direction [79G]. $M_{1,2}$, $L_{1,2}$: short and long axes of the two crystallographic equivalent molecules in the unit cell.

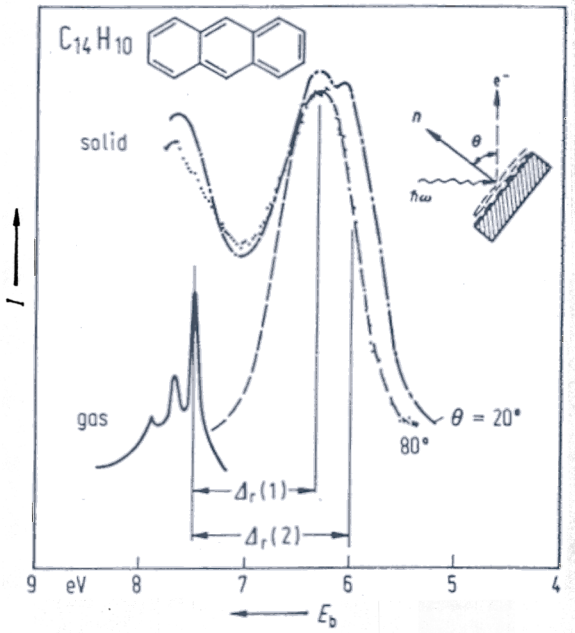

Fig. 129. $C_{14}H_{10}$. He I spectra of the first ion state of solid anthracene taken at two extreme electron emission angles in comparison with gas phase [74B] results. A surface chemical shift for the first layer of 0.3 eV is found [78S]. $\Delta_r(1) = E_{pol}$. E_b w.r. to E_{vac}.

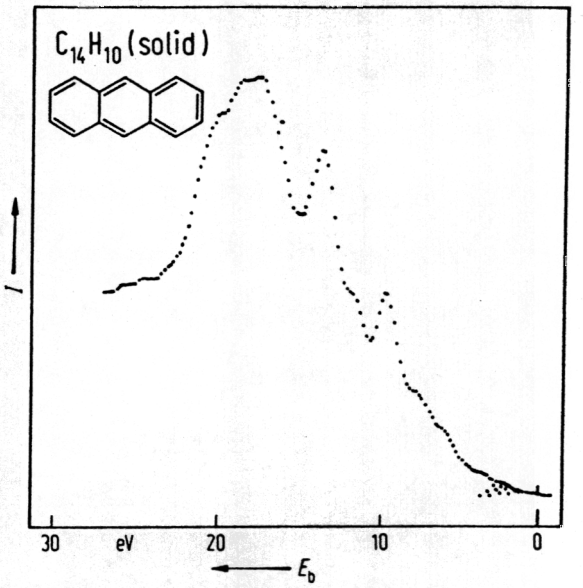

Fig. 130. $C_{14}H_{10}$. Complete valence electron spectrum taken with $\hbar\omega = 1457$ eV in the solid anthracene [77R].

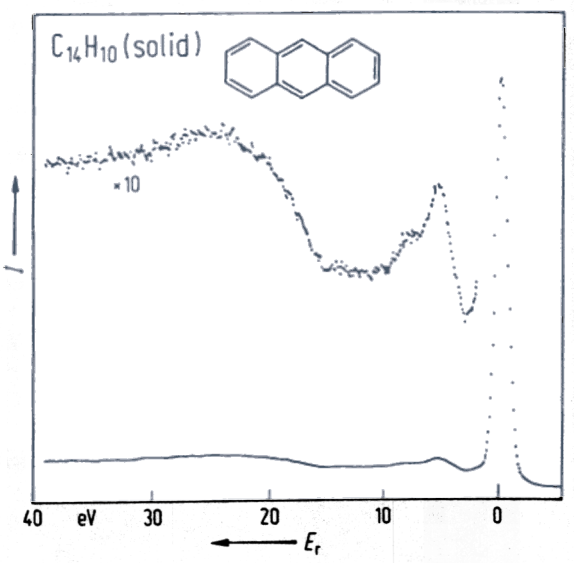

Fig. 131. $C_{14}H_{10}$. Core photoelectron spectra of solid anthracene [77R].

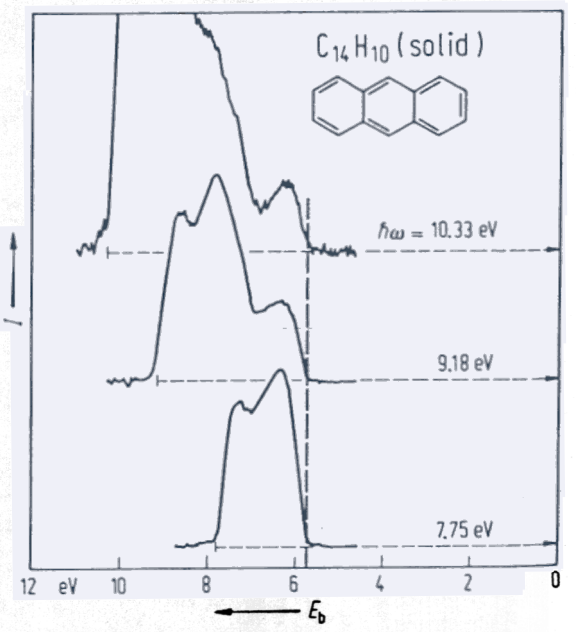

Fig. 132. $C_{14}H_{10}$. Photoelectron spectra of solid anthracene at different photon energies [82K]. $E_b = 0$ at E_{vac}. Vertical line: photoemission threshold.

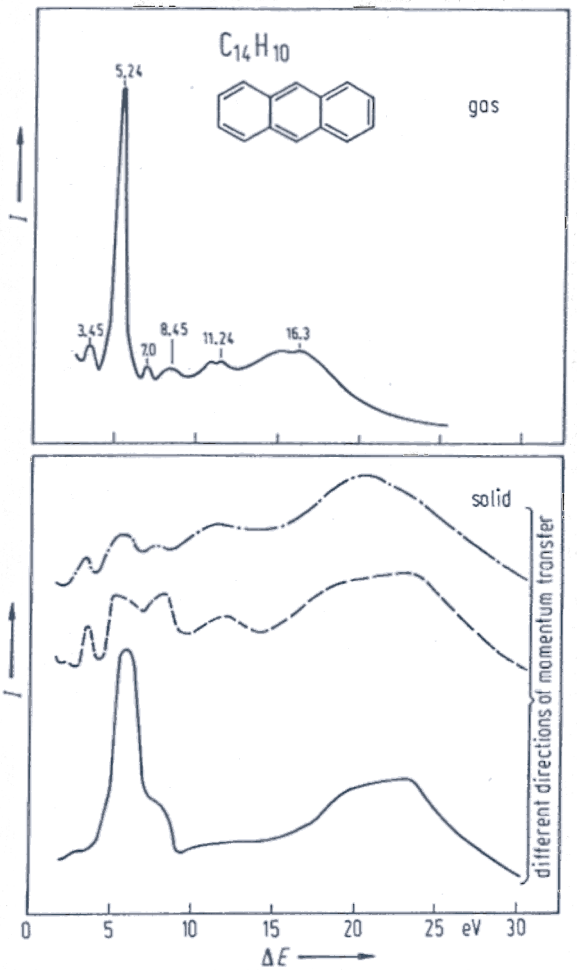

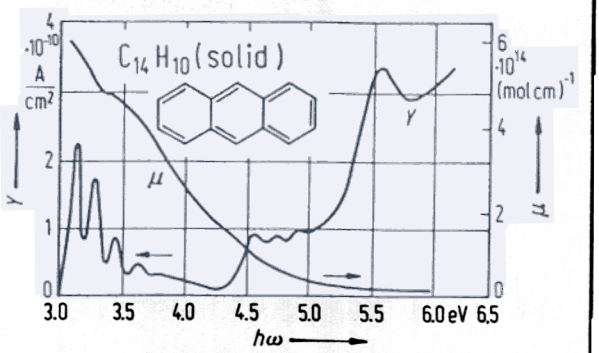

Fig. 133. $C_{14}H_{10}$. Unpolarized absorption and quantum yield of crystalline anthracene in the valence electron region [79G].

◀

Fig. 134. $C_{14}H_{10}$. Electron energy loss spectra of 30 eV electrons in anthracene vapour (top) and solid (bottom) [71K].

2.3.20 Naphthacene or tetracene ($C_{18}H_{12}$)

(For data on physical properties, see also [85K1])

Isolated molecule

1: Point group: D_{2h}
2: Bond lengths and bond angles: Fig. 135
3: Ground state electron configuration: Fig. 136

Molecular solid

Triclinic tetracene [61S, 71W, 85L]

4: Space group: $C_i^1(P\bar{1})$
5: Structure of the solid:

unit cell: $a = 7.90$ Å, $b = 6.03$ Å, $c = 13.53$ Å
$\alpha = 100.3°$, $\beta = 113.2°$, $\gamma = 86.3°$(RT)

Atomic positions: Table 44 and Fig. 137.

6: Outer valence photoelectron spectra of the molecular solid [79G, 81S2] in comparison with the gas phase [74B]: Fig. 138.
7: Inner valence photoelectron spectra of the molecular solid [77R, 75U]: Figs. 139, 140.
8: Core photoelectron spectra of the molecular solid [77R]: Fig. 141.

9: Theoretical assignment of the observed ion state [82V]: Table 45.
10: Polarization energies of some ion states [73S]: Table 46.
11: Ion state cross-sections as a function of photon energies of solid tetracene [73S]: Fig. 142.
12: Table of resonance structures in the cross-sections:
not reported.
13: Auger spectrum of the molecular solid in comparison with the gas phase:
not reported.
14: Penning ionization electron spectrum of the molecular solid in comparison with the gas phase: Fig. 143.
15: Electronic excitation spectra in the valence electron region [75U]: Fig. 144.
16: Electronic excitation spectrum in the core electron region of the molecular solid in comparison with the gas phase:
not reported.

Table 44. $C_{18}H_{12}$. (Tetracene). Atomic positions and deviations (Δ) from the mean planes of the molecules [61S, 71W].

Atom	x	y	z	Δ [Å]
C(1)	0.1194	0.0331	0.3890	−0.002
C(2)	0.1494	0.1564	0.3219	+0.011
C(3)	0.0811	0.0724	0.2040	−0.017
C(4)	0.1094	0.1899	0.1360	+0.002
C(5)	0.0467	0.1089	0.0211	−0.002
C(6)	−0.0691	−0.2228	0.0516	+0.006
C(7)	−0.0035	−0.1405	0.1637	+0.032
C(8)	−0.0378	−0.2646	0.2355	−0.019
C(9)	0.0267	−0.1832	0.3483	−0.001
C(1')	0.5428	0.5680	0.3787	+0.036
C(2')	0.4799	0.6861	0.2930	−0.011
C(3')	0.4997	0.5864	0.1947	−0.008
C(4')	0.4425	0.7007	0.1048	−0.022
C(5')	0.4638	0.6140	0.0052	+0.025
C(6')	0.5948	0.2758	0.0832	+0.010
C(7')	0.5758	0.3649	0.1811	−0.012
C(8')	0.6306	0.2568	0.2685	+0.002
C(9')	0.6148	0.3374	0.3645	−0.017

$\sigma(x)=\sigma(y)=\sigma(z)=0.020$ Å (mean value).

Table 45. $C_{18}H_{12}$. Theoretical assignment of some ion states in gaseous tetracene [82V].

Level	E_b [eV]
a_u (π)	7.39
b_{3g} (π)	9.12
b_{1u} (π)	9.38
a_u (π)	10.66
b_{2g} (π)	11.00
b_{3g} (π)	11.71
b_{1g}	11.93
a_g	13.07
b_{1u} (π)	13.13
b_{3u}	13.46
b_{2u}	13.79
a_g	14.43
b_{3u}	14.57

Table 46. $C_{18}H_{12}$. Vertical binding energies and polarization energies of some ion states of tetracene.

Vertical binding energies [eV]				E_{pol} [eV]
Solid			Gas	
[73S]	[73H2]	[72Z]	[72C2]	
5.9	5.83	5.76	7.01	1.1
7.3	7.28	7.15	8.41	1.1
	8.29	8.25	9.56	
8.7	8.70	8.60	9.7	1.0
9.2	9.40	9.50	10.25	1.1
10.0			11.1	1.1
10.9		10.7	12.0	1.1
12.3		11.9	13.4	1.1
13.2			14.1	0.9
14.4			15.7	1.3
15.3				
16.2				

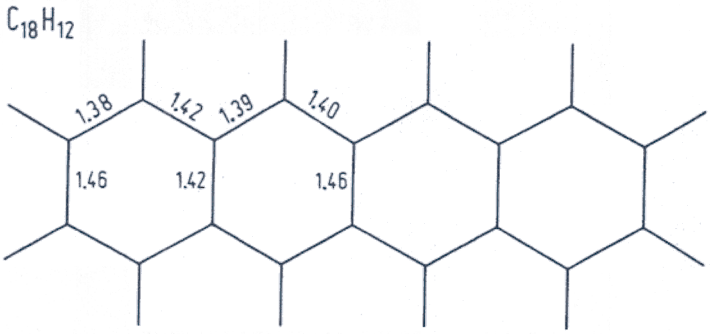

Fig. 135. $C_{18}H_{12}$. Schematic drawing of the molecular structure of tetracene. Distances in Å [71W].

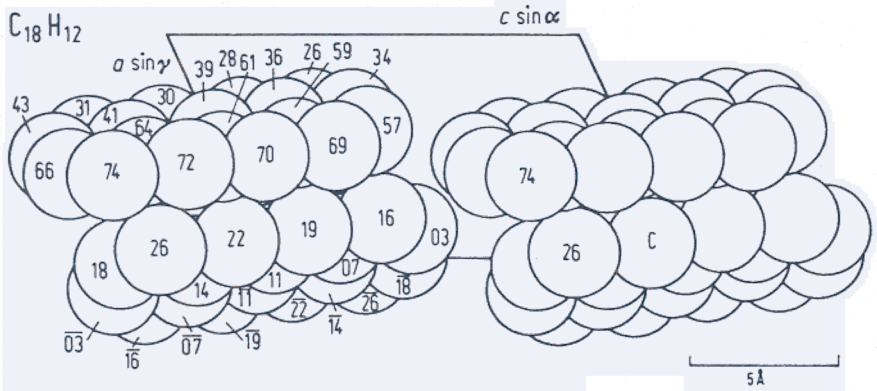

Fig. 137. $C_{18}H_{12}$. Packing drawing of the unit cell of solid tetracene along [010]. Fractional b coordinates of the carbon atoms are indicated (× 100) [71W].

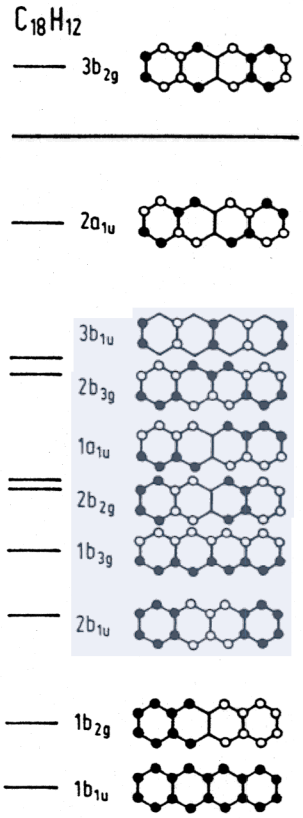

Fig. 136. $C_{18}H_{12}$. π-electron orbitals of tetracene. The σ-orbitals have been omitted [84R1].

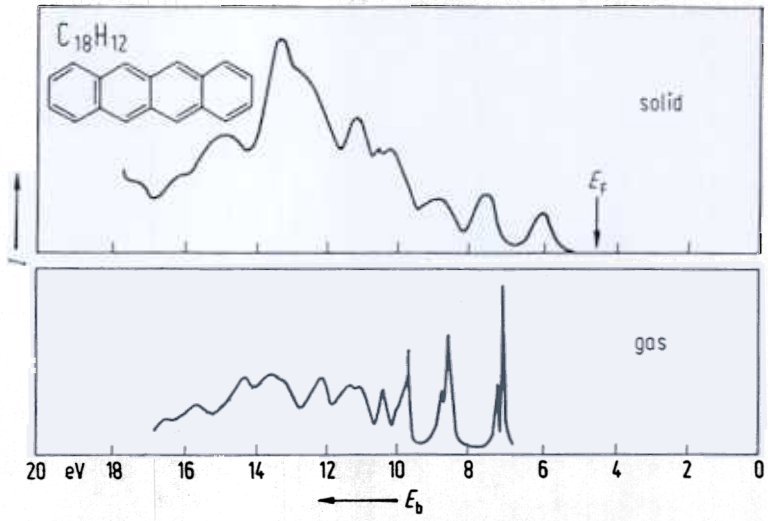

Fig. 138. $C_{18}H_{12}$. Outer valence photoelectron spectrum of solid tetracene (He I) [79G] in comparison with the gas phase (He I) [74B].

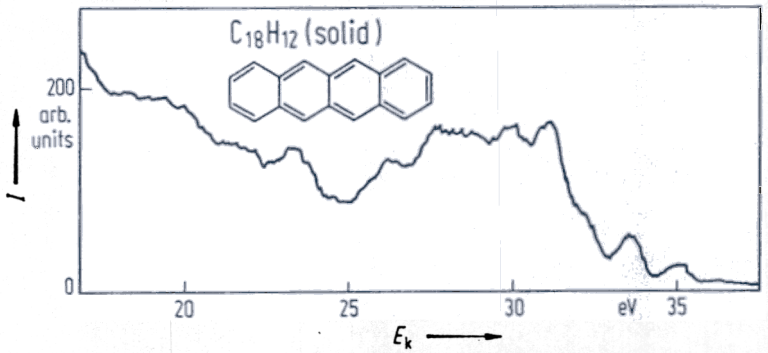

Fig. 140. $C_{18}H_{12}$. Photoelectron spectrum of tetracene polycrystal excited with He II radiation [75U].

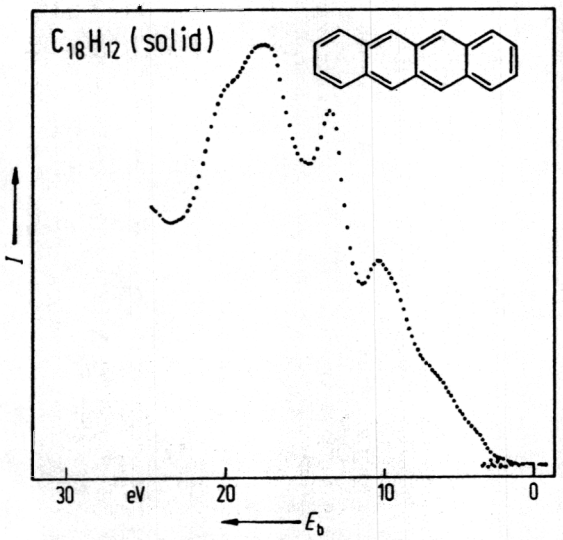

Fig. 139. $C_{18}H_{12}$. Complete valence electron spectrum of tetracene taken with $\hbar\omega = 1457$ eV in the solid [77R].

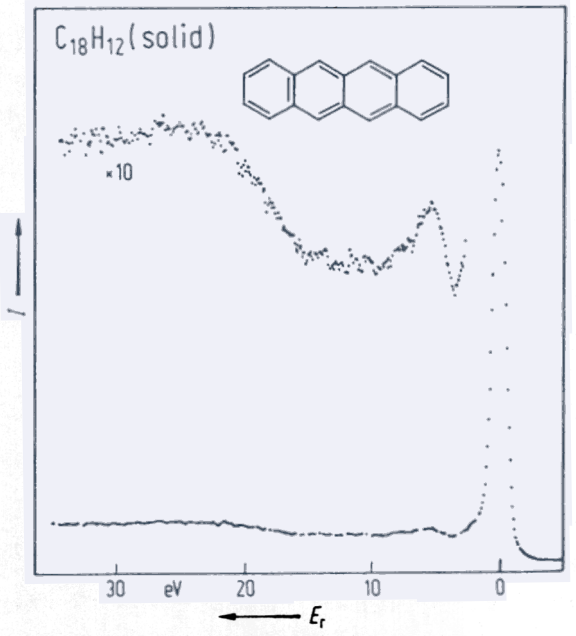

Fig. 141. $C_{18}H_{12}$. Core photoelectron spectra of solid tetracene [77R]. $\hbar\omega = 1457$ eV.

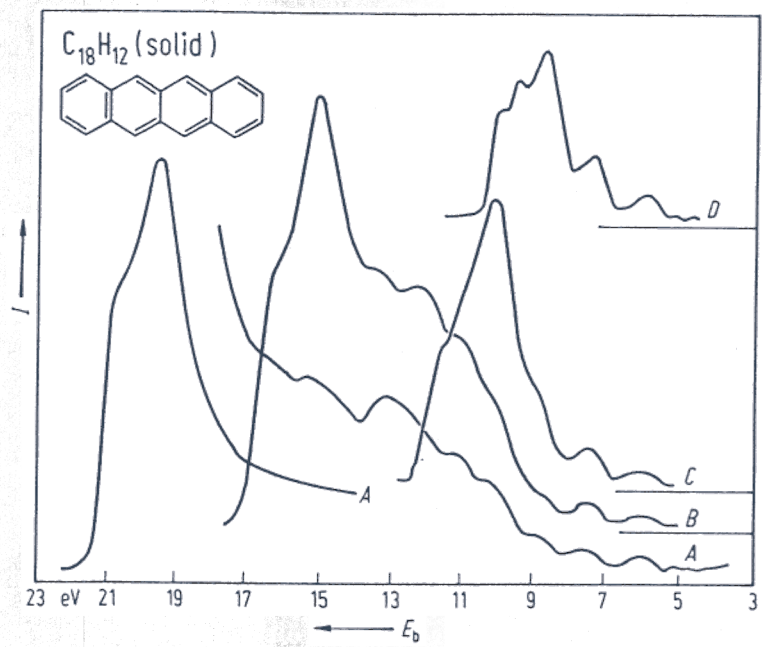

Fig. 142. $C_{18}H_{12}$. The energy distribution curves for solid tetracene taken with different photon energies. *A*: 21.22 eV, *B*: 16.67 eV and 16.85 eV, *C*: 11.62 eV and 11.83 eV, *D*: 10.33 eV [73S].

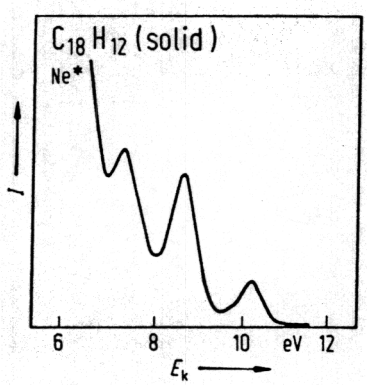

Fig. 143. $C_{18}H_{12}$. Penning ionization spectra of tetracene excited by Ne* [85H].

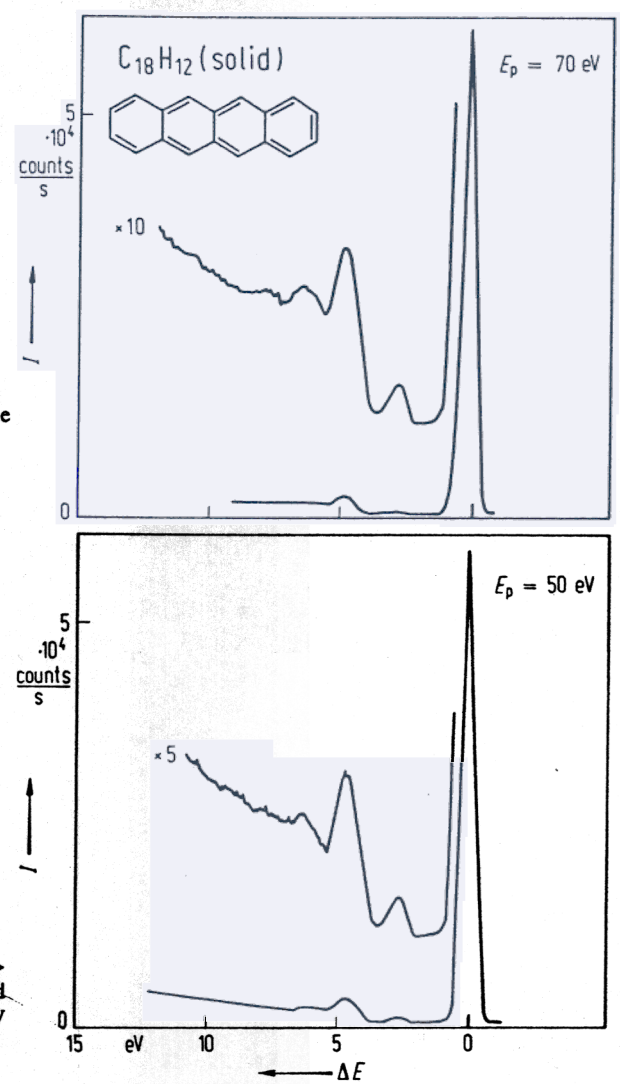

Fig. 144. $C_{18}H_{12}$. Electron energy loss spectra of solid tetracene in the valence electron region measured with 50 eV and 70 eV primary energy (E_p) [75U].

2.3.21 Glycine ($HOOC-CH_2-NH_2$)

Isolated molecule

1: Point group: C_1
2: Bond lengths and bond angles: Fig. 145

Ground state configuration: Fig. 146

Molecular solid

a) Monoclinic α-glycine [72S2, 66W]
4: Space group: $C_{2h}^5(P2_1/n)$
5: Structure of the solid:

unit cell: $a=5.1054$ Å, $b=11.9688$ Å, $c=5.4645$ Å, $\beta=111.697°$ ($T=298$ K)

Atomic positions: Table 47 and Fig. 147.

b) Monoclinic β-glycine [60S2, 66W]
4: Space group: $C_2^2(P2_1)$
5: Structure of the solid:

unit cell: $a=5.077$ Å, $b=6.268$ Å, $c=5.380$ Å, $\beta=113°\ 12'$

Atomic positions: Table 48 and Figs. 148, 149.

c) trigonal Γ-glycine [66W]
4: Space group: $C_3^3(P3_2)$
5: Structure of the solid:

unit cell (hexagonal setting): $a=7.037$ Å, $c=5.483$ Å

Atomic positions:

Atom	x	y	z
N	0.3522	−0.0440	−0.2619
O(1)	0.3772	0.0270	0.2420
O(2)	−0.0896	0.0773	0.0970
C(1)	0.1378	0.0532	0.0633
C(2)	0.1145	0.0719	−0.2265
H(N, 1)	0.540	0.012	−0.135
H(N, 2)	0.340	−0.031	−0.449
H(N, 3)	0.337	−0.203	−0.216
H(C, 1)	0.125	0.241	−0.274
H(C, 2)	−0.091	0.008	−0.362

See also Fig. 150.

6: Outer valence photoelectron spectra of the molecular solid [82B2] in comparison with the gas phase [74D]: Fig. 151.
7: Inner valence photoelectron spectra of the molecular solid [84S1]: Fig. 152.
8: Core photoelectron spectra of the molecular solid [84S1, 76C]: Fig. 153.
9: Theoretical assignment of the observed ion state: (see Fig. 146 and Fig. 151).
10: Polarization energies of some ion states:
not reported.
11: Ion state cross-sections as a function of photon energies of solid glycine:
not reported.
12: Table of resonance structures in the cross-sections:
not reported.
13: Auger spectrum of the molecular solid in comparison with the gas phase.
14: Penning ionization electron spectrum of the molecular solid in comparison with the gas phase:
not reported.

15: Electronic excitation spectra in the valence electron region:
not reported.

16: Electronic excitation spectrum in the core electron region of the molecular solid in comparison with the gas phase:
not reported.

Table 47. Atomic positions in α-glycine [72S, 66W].

Atom	x	y	z	Atom	x	y	z
C(1)	0.07542	0.12478	0.06605	H(1)(N)	0.286	0.100	0.570
C(2)	0.06536	0.14499	0.78711	H(2)(N)	0.457	0.119	0.837
N	0.30135	0.08980	0.74113	H(3)(N)	0.298	0.020	0.763
O(1)	0.30583	0.09427	0.23553	H(4)(C)	0.080	0.220	0.771
O(2)	0.85224	0.14154	0.10711	H(5)(C)	0.898	0.118	0.671

Table 48. Atomic positions in β-glycine [60S2, 66W].

Atom	x	y	z	Atom	x	y	z
N	0.3522	−0.0440	−0.2619	H(1)(NH_3^+)	0.540	0.012	−0.135
O(1)	0.3772	0.0270	0.2420	H(2)(NH_3^+)	0.340	−0.031	−0.449
O(2)	−0.0896	0.0773	0.0970	H(3)(NH_3^+)	0.337	−0.203	−0.216
C(1)	0.1378	0.0532	0.0633	H(1)(CH_2)	0.125	0.241	−0.274
C(2)	0.1145	0.0719	−0.2265	H(2)(CH_2)	−0.091	0.008	−0.362

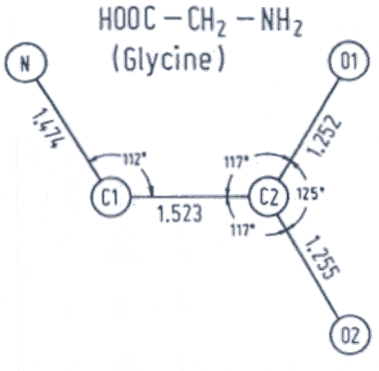

Fig. 145. Glycine ($HOOC—CH_2—NH_2$). Schematic drawing of the molecular structure of glycine. Distances in Å [66W].

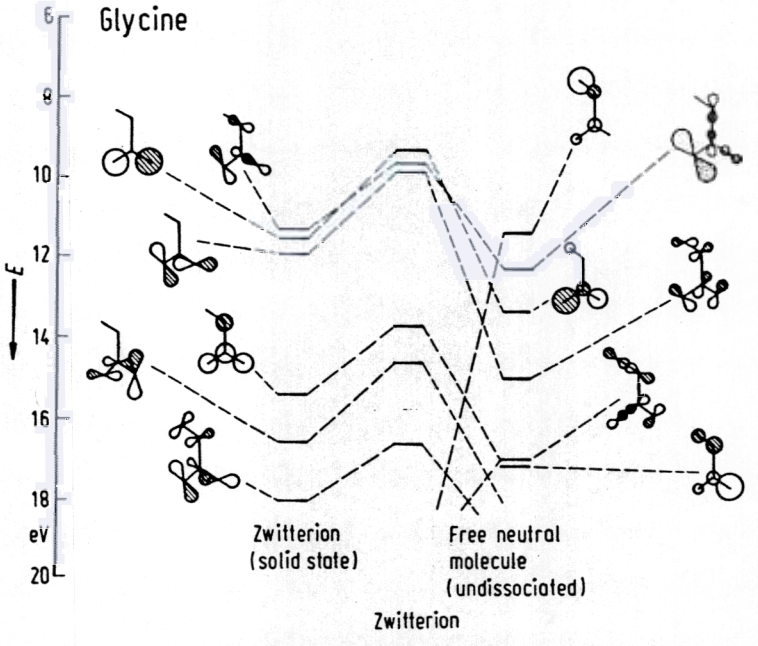

Fig. 146. Glycine. Orbital energy diagram [82B].

Fig. 148. Glycine. (a) The monoclinic structure of the β-glycine modification projected along its *b* axis. Fractional coordinates of the atoms are indicated (× 100). (b) A packing drawing of the monoclinic β-glycine structure along its *b* axis. The oxygen atoms are dark shaded, the carbon atoms light shaded, and the nitrogens are not shaded [66W, 72S2].

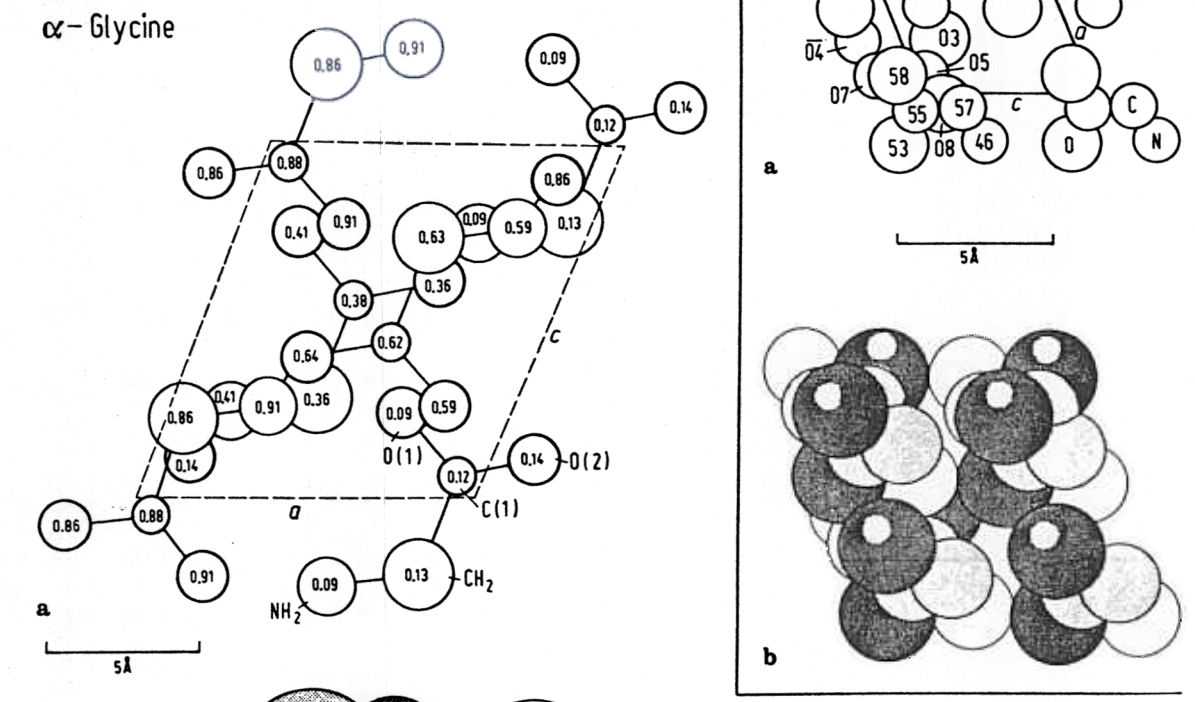

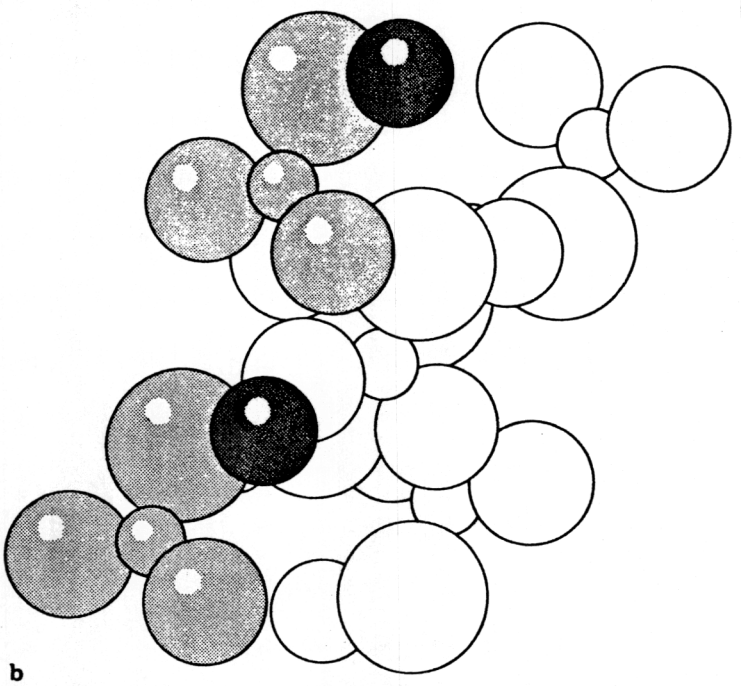

Fig. 147. Glycine. (a) The monoclinic structure of α-glycine projected along its *b* axis. The larger, heavily ringed circles are oxygen; the smaller are the carboxyl carbon atoms. The largest, lightly outlined circles are CH_2; those that are somewhat smaller are NH_2. Fractional coordinates of the atoms are indicated. (b) A packing drawing of the monoclinic structure of α-glycine seen along the *b* axis [66W], [72S2].

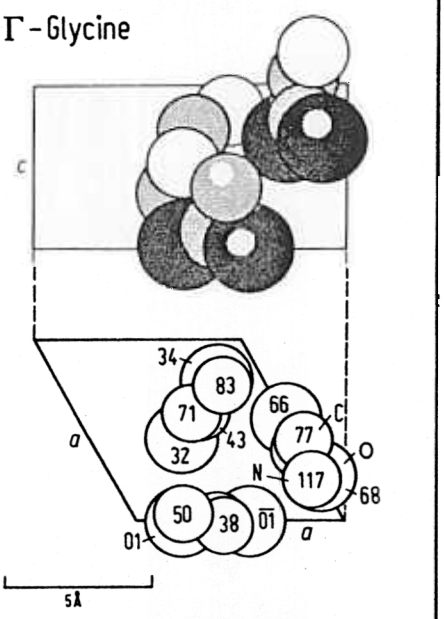

Fig. 150. Glycine. Two packing drawings of the hexagonal Γ-modification of glycine along two different projection directions. Fractional coordinates of the atoms are indicated (× 100) [66W], [72S2].

For Fig. 149, see next page.

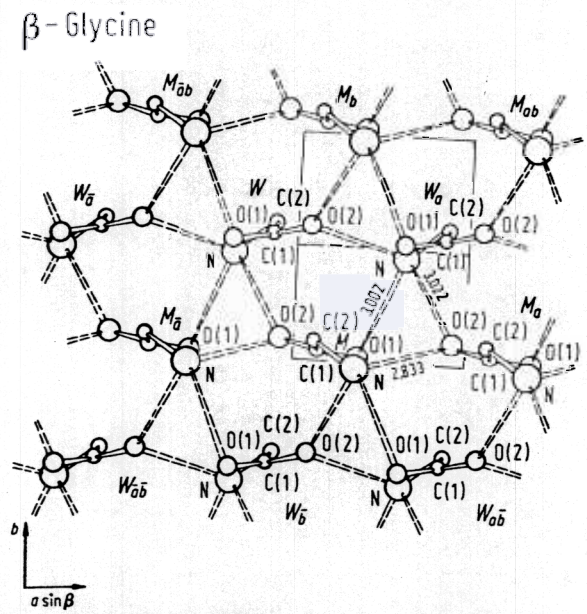

Fig. 149. Glycine. Intermolecular contacts in β-glycine. Distances in Å [60S1].

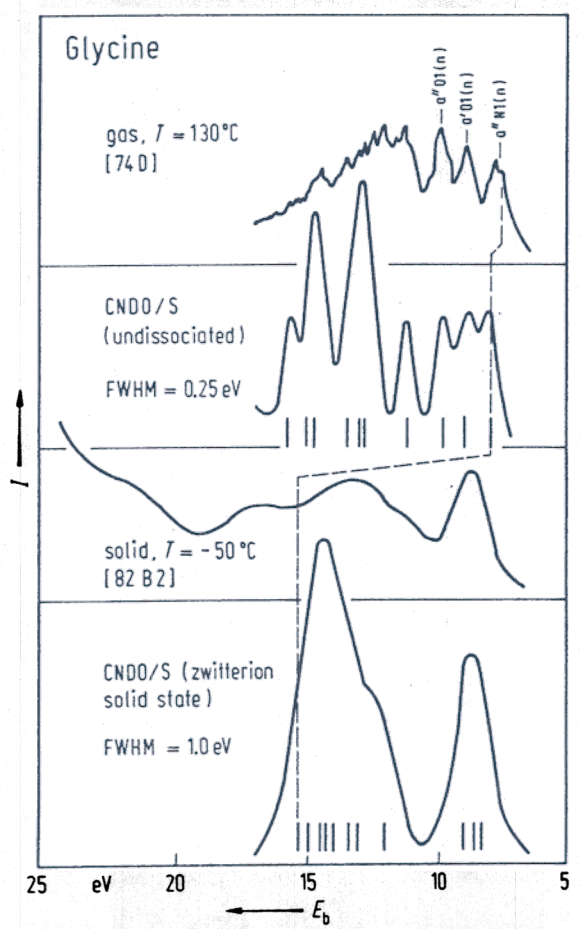

Fig. 151. Glycine. Outer valence photoelectron spectrum of solid glycine (He I) [82B2] in comparison with the gas phase (He I) [74D] and calculated results (CNDO/S method) for the isolated molecule and a model for the solid state. E_b: binding energy of solid phase spectrum, relative to E_{vac}.

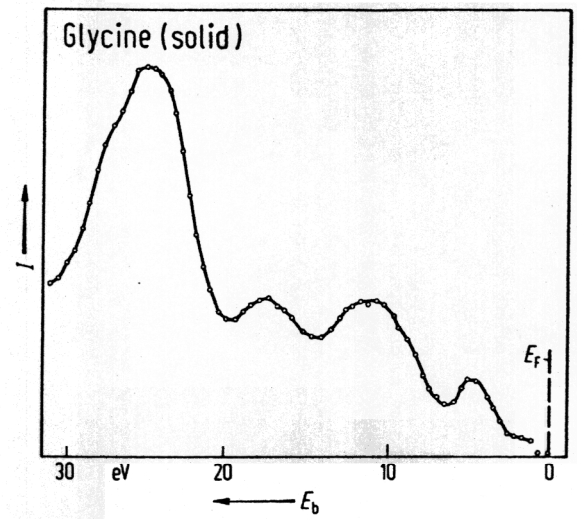

Fig. 152. Glycine. Complete valence electron spectrum taken with $\hbar\omega = 1457$ eV in the solid [84S1].

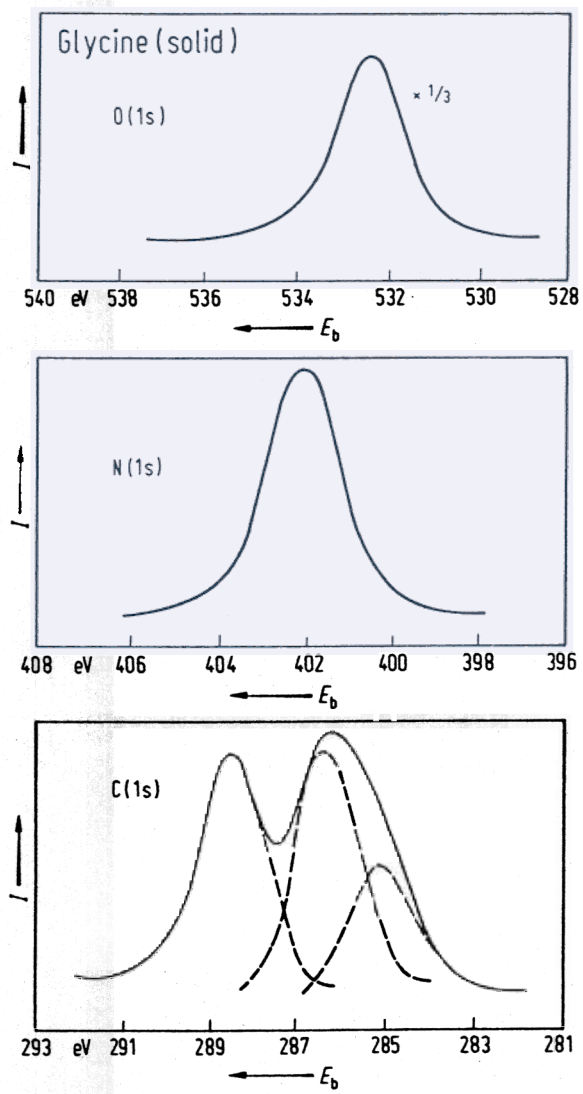

Fig. 153. Glycine. Core photoelectron spectra of solid glycine [76C].

2.3.22 *p*-Oligophenyls ($C_6H_5-(C_6H_4)_n-C_6H_5$; n=0, 1, 2(3, 4))

(For physical properties see also [85K1])

Isolated molecules

1: Point groups: not reported
2: Bond lengths and bond angles: Figs. 154, 155.
3: Ground state electron configurations: Fig. 156.

Molecular solids

a) monoclinic biphenyl $(C_6H_5)_2$ [85L, 71L2, 71W]
4: Space group: $C_{2h}^5(P2_1/a)$
5: Structure of the solid:

unit cell: $a=8.12$ Å, $b=5.63$ Å, $c=9.51$ Å; $\beta=95.1°$(RT)

Atomic positions:

Atom	x	y	z
C(1)	0.0355	−0.0042	0.0759
C(2)	−0.0093	0.1694	0.1707
C(3)	0.0592	0.1636	0.3130
C(4)	0.1665	−0.0161	0.3569
C(5)	0.2119	−0.1825	0.2666
C(6)	0.1420	−0.1792	0.1241

See also Fig. 157.

b) monoclinic terphenyl $C_6H_5-C_6H_4-C_6H_5$ [70S], [85K1]
4: Space group: $C_{2h}^5(P2_1/a)$
5: Structure of the solid:

unit cell: $a=8.119$ Å, $b=5.615$ Å, $c=13.618$ Å; $\beta=92.07°$(RT) [85K1].

Atomic positions:

Atom	x	y	z
C(1)	0.059	0.182	0.064
C(2)	−0.046	0.000	0.100
C(3)	−0.105	−0.182	0.036
C(4)	−0.094	0.000	0.204
C(5)	−0.036	0.182	0.268
C(6)	−0.082	0.182	0.368
C(7)	−0.187	0.000	0.402
C(8)	−0.246	−0.182	0.339
C(9)	−0.200	−0.182	0.239

See also Fig. 158.

c) monoclinic quaterphenyl $C_6H_5-(C_6H_4)_2-C_6H_5$ [71L2]
4: Space group: $C_{2h}^5(P2_1/a)$
5: Structure of the solid:

unit cell: $a=8.05$ Å, $b=5.55$ Å, $c=17.81$ Å; $\beta=95°$(RT) [71L2]

Atomic positions:

Atom	x	y	z
C(1)	−0.018	0.000	0.040
C(2)	0.043	0.186	0.089
C(3)	0.009	0.186	0.165
C(4)	−0.087	0.000	0.192
C(5)	−0.149	−0.186	0.144
C(6)	−0.115	−0.186	0.067
C(7)	−0.123	0.000	0.272
C(8)	−0.061	0.186	0.321
C(9)	−0.096	0.186	0.398
C(10)	−0.192	0.000	0.425
C(11)	−0.254	−0.186	0.376
C(12)	−0.220	−0.186	0.300

See also Fig. 159.

6: Outer valence photoelectron spectra of the molecular solids [81R] in comparison with the gas phase [84S2]: Figs. 160···163.
7: Inner valence photoelectron spectra of the molecular solids: see Figs. 160, 161.
8: Core photoelectron spectra of the molecular solids [81R]: Figs. 164(a, b).
9: Theoretical assignment of the observed ion state:
not reported.
10: Polarization energies of some ion states: see [85L].
11: Ion state cross-sections as a function of photon energies of solid terphenyl [75H2]: Figs. 165, 166.
12: Table of resonance structures in the cross-sections:
not reported.
13: Auger spectrum of the molecular solid in comparison with the gas phase:
not reported.
14: Penning ionization electron spectrum of the molecular solid in comparison with the gas phase:
not reported.
15: Electronic excitation spectra in the valence electron region: [82H1]: Fig. 167.
16: Electronic excitation spectrum in the core electron region of the molecular solid in comparison with the gas phase:
not reported.

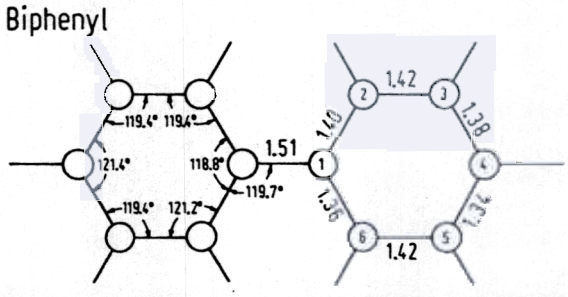

Fig. 154. Biphenyl. Bond lengths and bond angles in the isolated biphenyl molecule [71W]. Distances in Å.

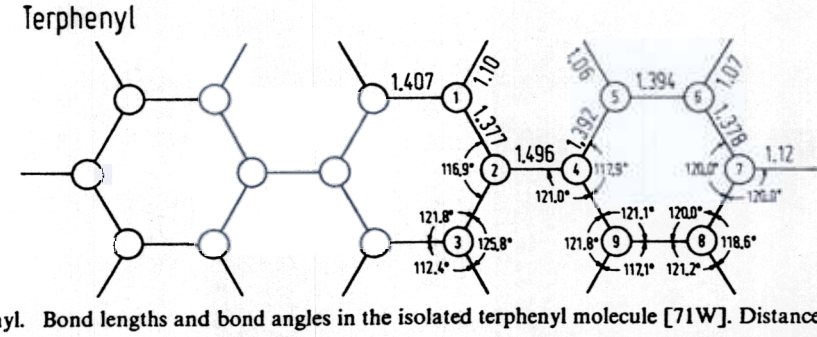

Fig. 155. Terphenyl. Bond lengths and bond angles in the isolated terphenyl molecule [71W]. Distances in Å.

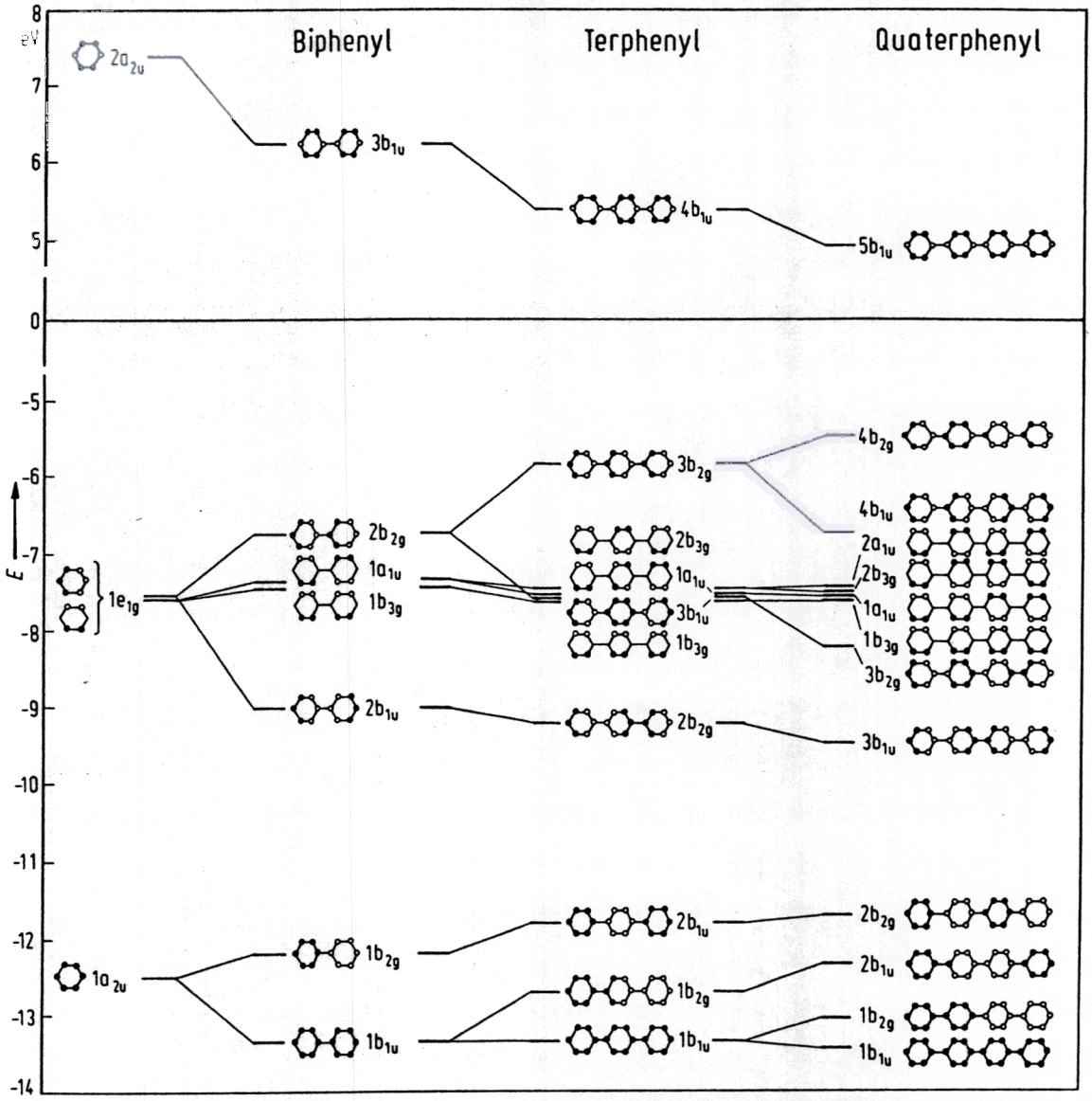

Fig. 156. *p*-Oligophenyls. Molecular orbital diagram of *p*-oligophenyls after [84B2]. σ-orbitals have been omitted. Only π-orbitals are shown.

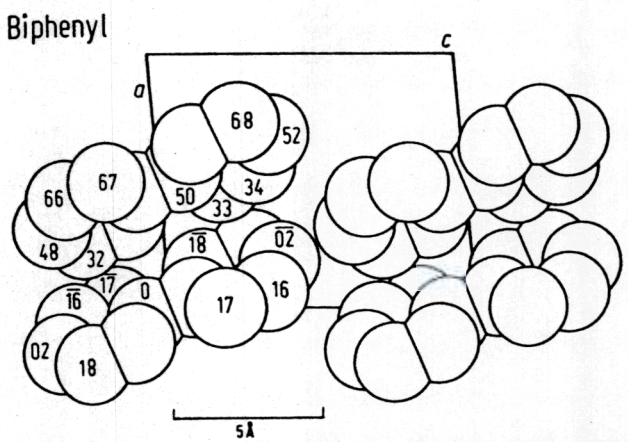

Fig. 157. Biphenyl. The monoclinic structure of biphenyl projected along its *b* axis. Fractional coordinates of the *C* atoms are indicated (×100) [71W].

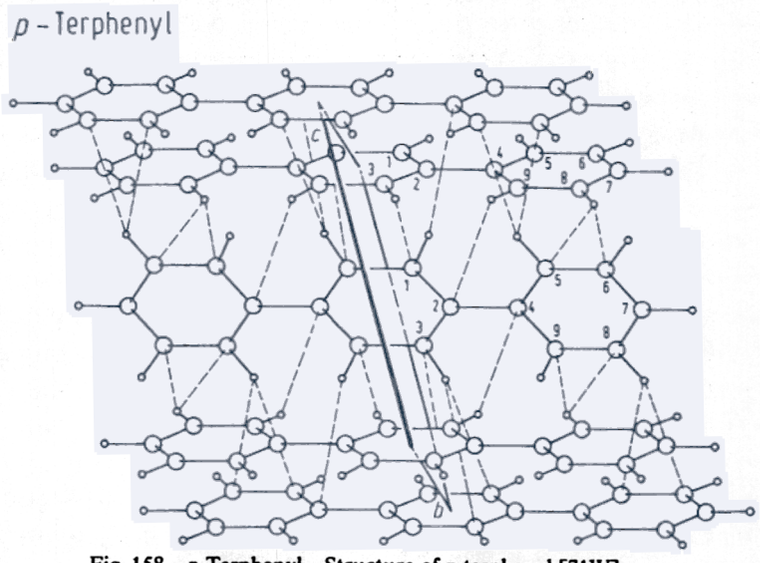

Fig. 158. *p*-Terphenyl. Structure of *p*-terphenyl [71W].

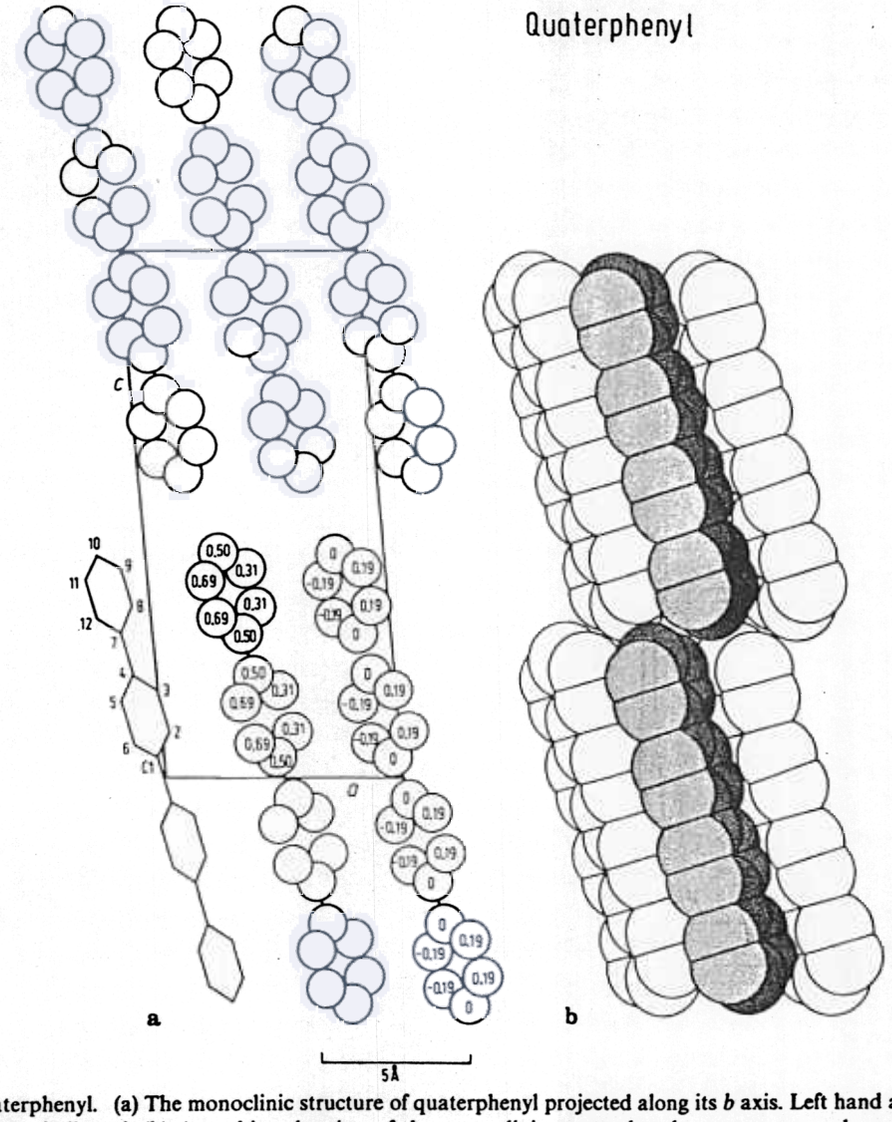

Fig. 159. Quaterphenyl. (a) The monoclinic structure of quaterphenyl projected along its *b* axis. Left hand axis. Fractional *b* coordinates are indicated. (b) A packing drawing of the monoclinic quaterphenyl structure seen along its *b* axis. Left hand axis [71W].

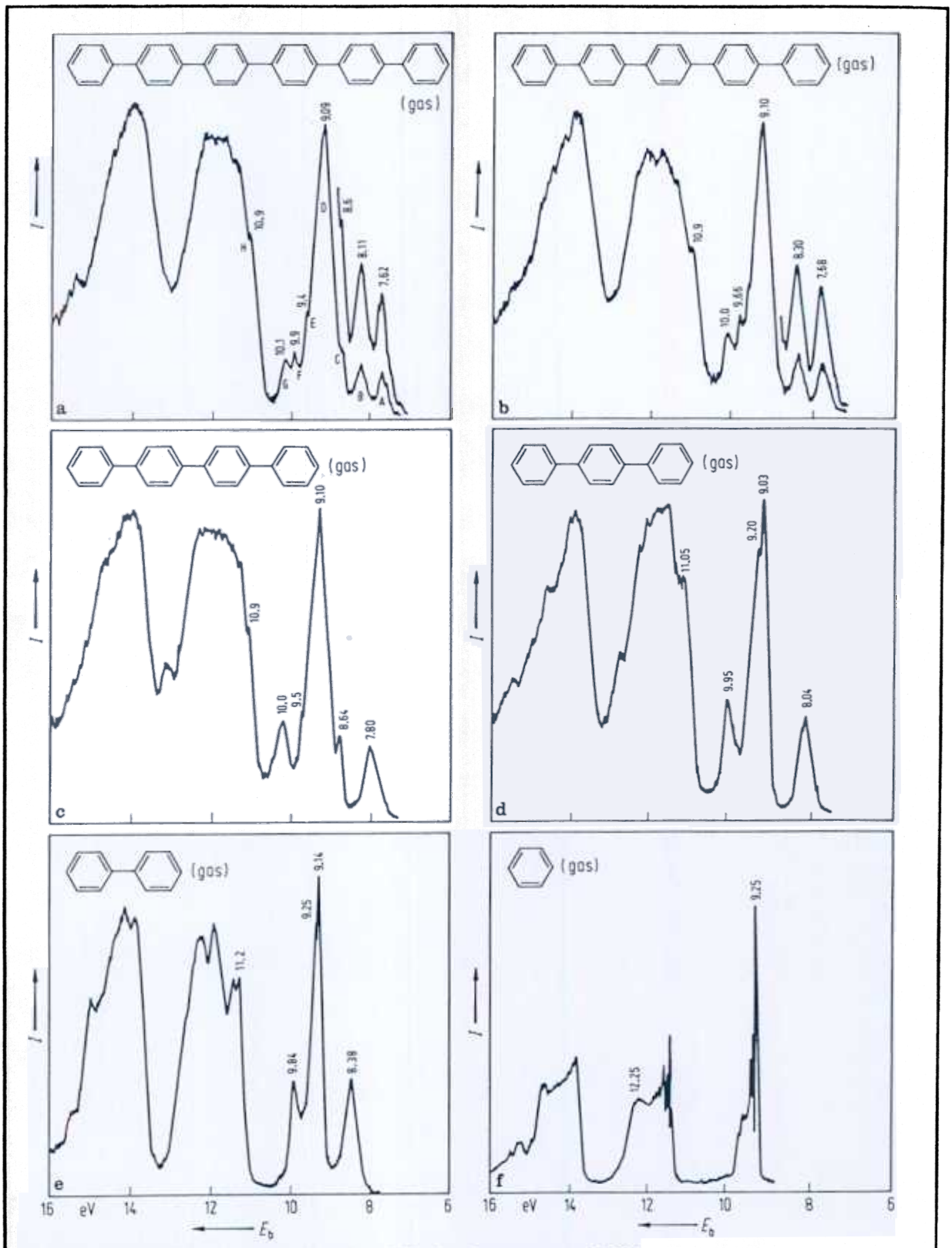

Fig. 160. *p*-Oligophenyl compounds. Gas-phase He I photoelectron spectra [84S2].

For Fig. 161, see next page.

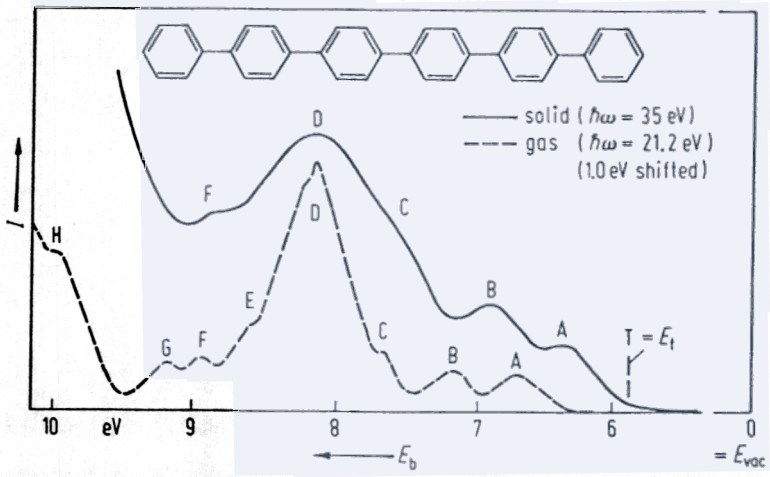

Fig. 162. Sexiphenyl. Comparison between gas and solid phase spectra in the outer valence electron region [84S2]. E_b: binding energy for solid; E_t = photoemission threshold.

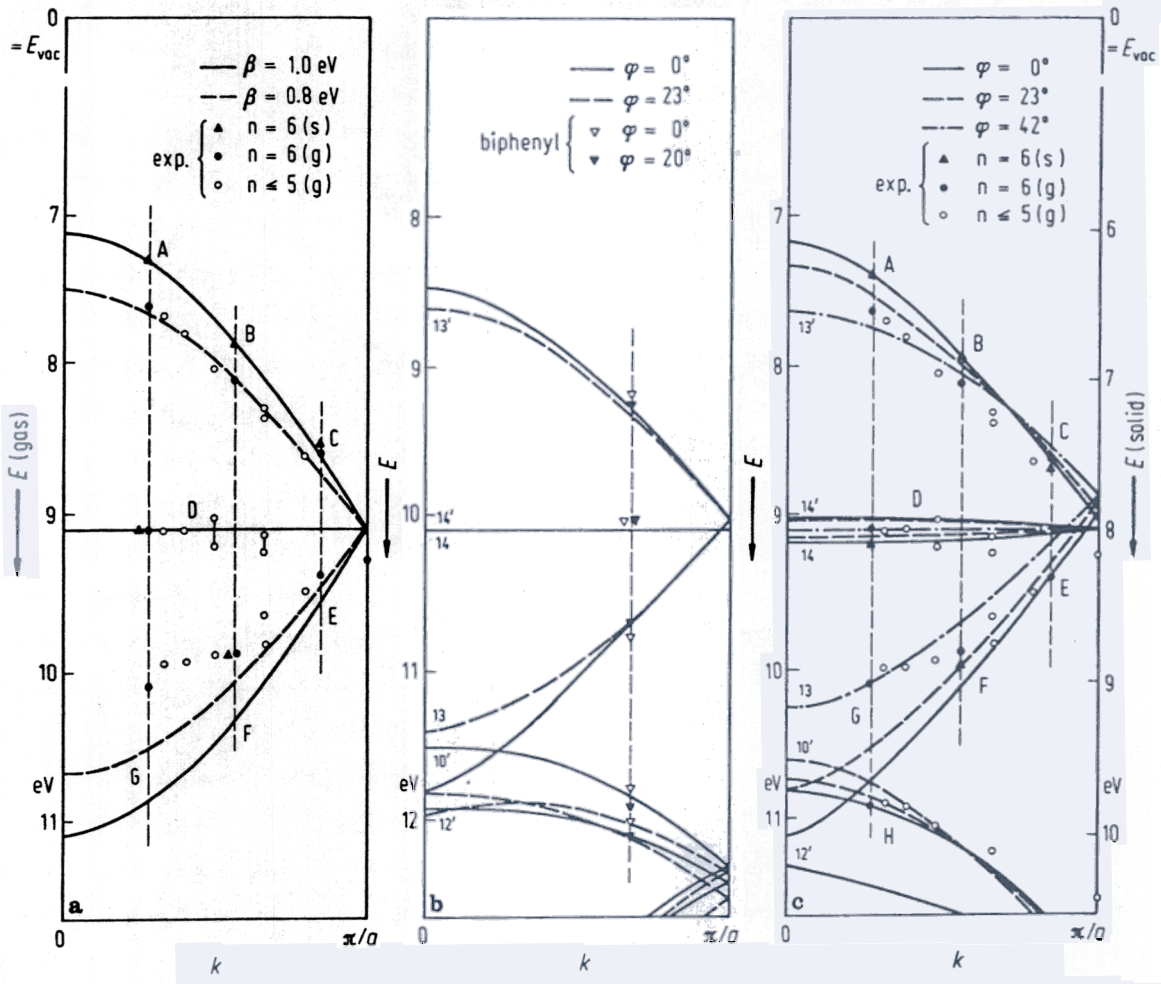

Fig. 163. Polyphenylenes. Experimental and theoretical $E = E(k)$ energy band-dispersion relation for polyphenylenes. (a) Comparison of the experimental data with a simple model [84S2]. Parameters $\alpha = 9.1$ eV and $\beta = 1.0$ eV (gas) are used. (b) CNDO/S3 calculation for the polyparaphenylene (PPP) polymer and a biphenyl molecule [81D, 83F2]. (c) Comparison of the experimental data with the valence electron Hamiltonian (VEH) calculation for PPP chain [82B1].

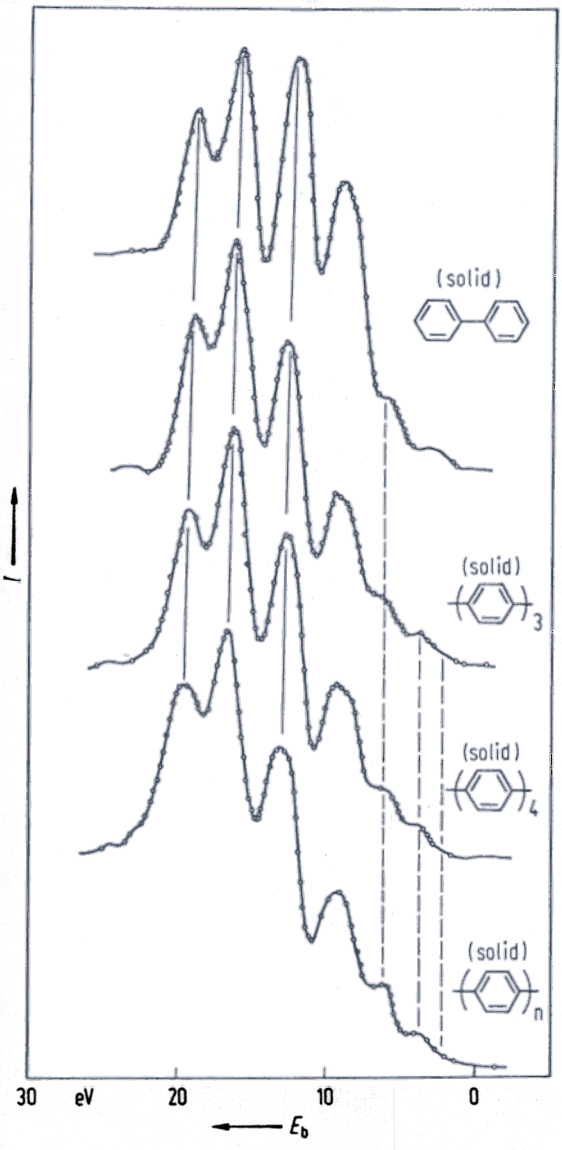

◀ Fig. 161. *p*-Oligophenyl compounds. X-ray induced outer and inner valence electron spectra of bi-, ter-, and quaterphenyl in the solid phase [81R]. Polyphenyl is shown for comparison.

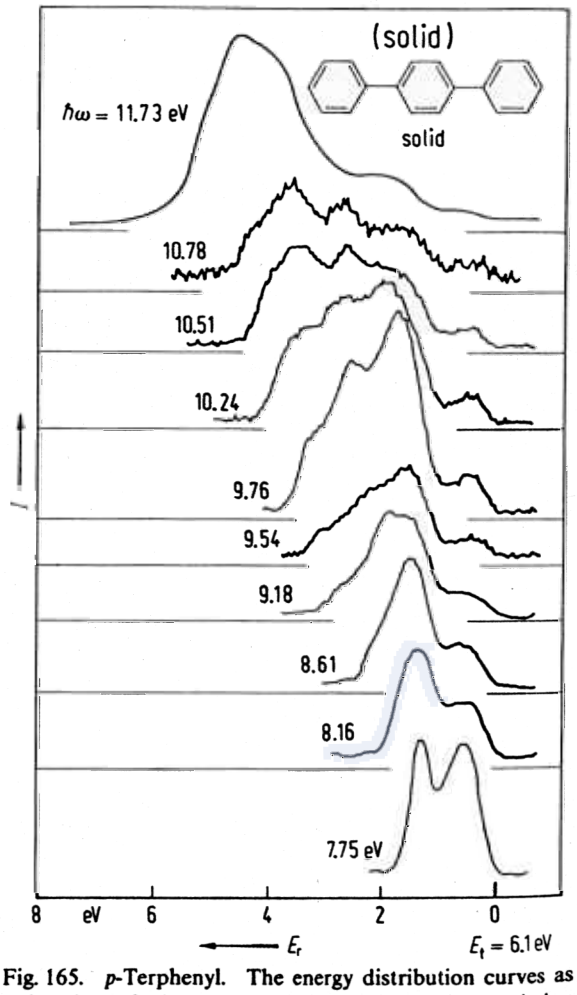

Fig. 165. *p*-Terphenyl. The energy distribution curves as a function of photon energy [75H2]. E_t: photoemission threshold energy.

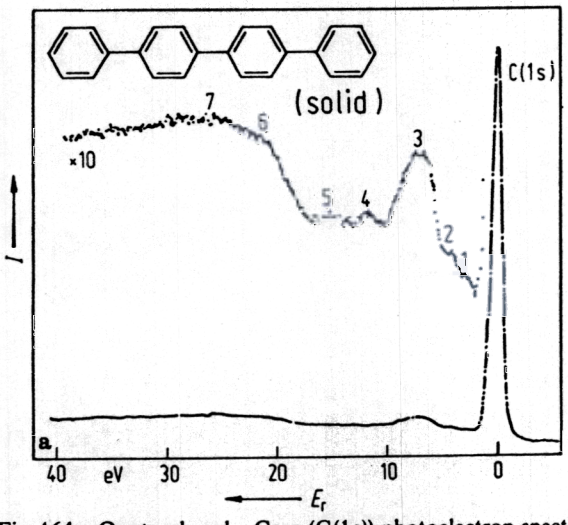

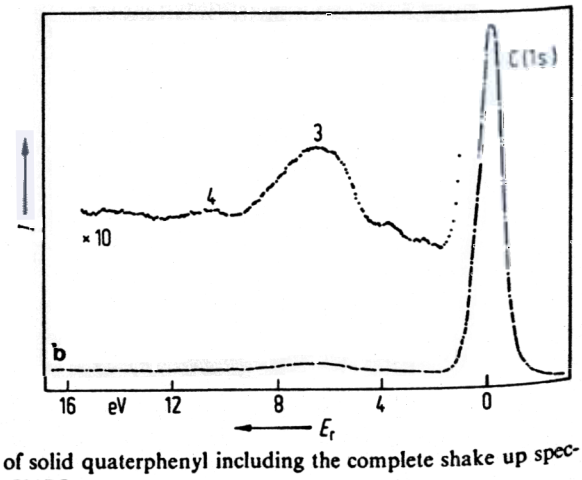

Fig. 164. Quaterphenyl. Core (C(1s)) photoelectron spectra of solid quaterphenyl including the complete shake up spectrum (a); (b) detailed view of the low energy shake up spectrum [81R].

Landolt-Börnstein New Series III/23a

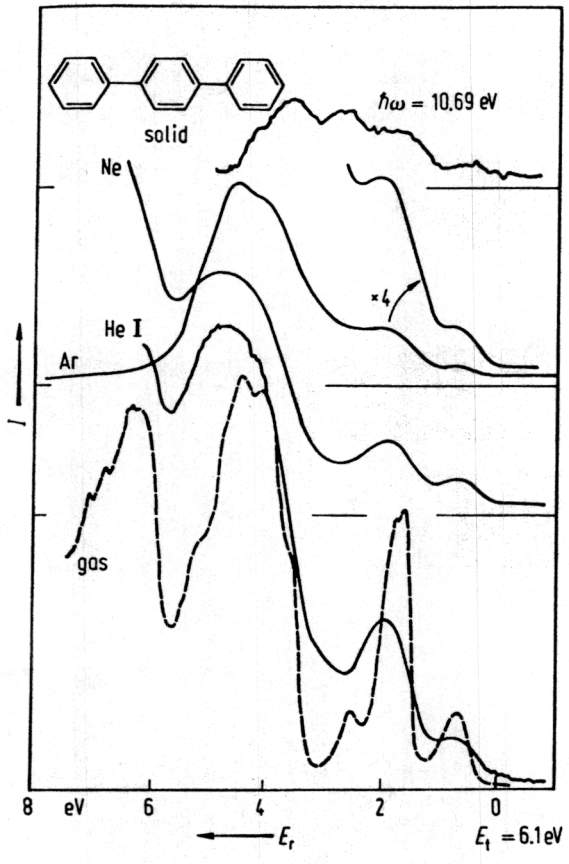

◀ Fig. 166. *p*-Terphenyl (solid). Energy distribution curves obtained by photoemission with line sources in comparison with gaseous terphenyl [75H2]. The spectra have been lined up artificially.

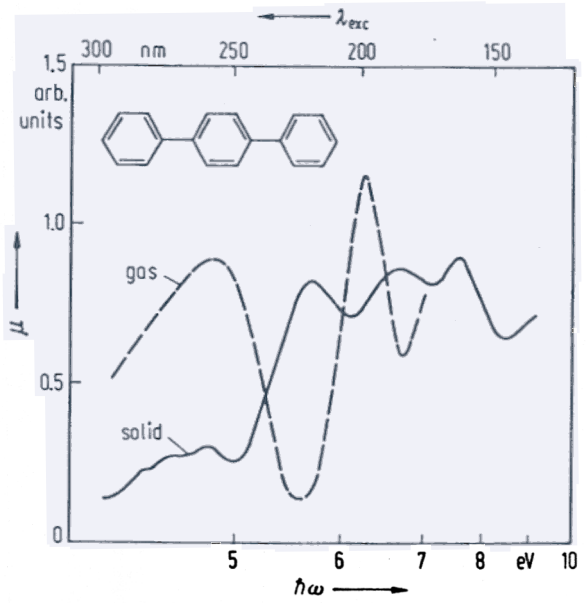

Fig. 167. *p*-Terphenyl. Absorption of solid *p*-terphenyl in the valence electron region (solid line) in comparison with the gas phase (dashed line) [82H1]. λ_{exc}: excitation wavelength.

2.3.23 Saturated hydrocarbons (C_nH_{2n+2}; n = 2 ··· 10, 13, 36)

Isolated molecules

a) ethane (C_2H_6) [68S1], [87L]

1: Point group: D_{3d}

2: Bond lengths and bond angles [87L]: C—C: 1.5351 Å
C—H: 1.0940 Å
C—C—H: 111.17°

3: Ground state electron configuration:

$$\left| \underset{\text{C(1s)}}{(1a_{1g})^2 (1a_{2u})^2} \right| \left| \underset{\text{C(2s), C(2p), H(1s)}}{(2a_{1g})^2 (2a_{2u})^2 (1e_u)^4 (3a_{1g})^2 (1e_g)^4} \right|.$$

$^1A_{1g}$:

$$\left| \underset{\text{empty}}{(3a_{2u})^0 (2e_u)^0} \right|$$

b) propane (C_3H_8) [60S1], [76L]

1: Point group: C_{2v}

2: Bond lengths and bond angles: C—C: 1.526 Å
C—H: 1.096 Å (CH_2 group)
C—H: 1.091 Å (CH_3 group)
C—C—C: 112.4°
H—C—H: 106.1°
H—C—H: 107.7°

3: Ground state electron configuration:

$$\left| \underset{\text{C(1s)}}{(1a_1)^2 (1b_2)^2 (2a_1)^2} \right| \left| \underset{\text{C(2s)}}{(3a_1)^2 (2b_2)^2 (4a_1)^2} \right|$$

$^1A_1$:

$$\left| \underset{\text{C(2p), H(1s)}}{(1b_1)^2 (5a_1)^2 (3b_2)^2 (1a_2)^2 (2b_1)^2 (6a_1)^2 (4b_2)^2} \right| \left| \underset{\text{empty}}{(3b_1)^0 (7a_1)^0} \right|$$

c) *n*-Butane (C_4H_{10}), *n*-Pentane (C_5H_{12}),
n-Hexane (C_6H_{14}), *n*-Heptane (C_7H_{16}), *n*-Octane (C_8H_{18}) [59S], [87L], [76L]

1: Point groups: C_4H_{10}: C_{2h}(*trans*), C_2(*gauche*) [87L]

2: Bond lengths and bond angles (see also [87L] and [76L]):

	n-Butane	*n*-Pentane	*n*-Hexane	*n*-Heptane	*n*-Octane
C–H [Å]	1.108	1.118	1.118	1.121	–
C–C [Å]	1.533	1.531	1.533	1.534	1.525
C–C–C	112.4°	112.9°	111.9°	112.6°	113.3°
C–C–H	110.5°	110.4°	109.5°	109.8°	–

3: Ground state electron configuration:
not reported.

Molecular solids

a) hexagonal ethane [66W]

4: Space group: $D_{6h}^4(P6_3/mmc)$

5: Structure of the solid:

unit cell: $a = 4.46$ Å, $c = 8.19$ Å ($T = -185$ °C)

Atomic positions:

carbon atoms: 4(f), $\pm(1/3, 2/3, u; 2/3, 1/3, u+1/2)$
with u between 0.15 and 0.16

CH_3-CH_3 separation between adjacent molecules: 3.6 Å

See also Fig. 168.

c) orthorhombic *n*-pentane [67S]
triclinic *n*-octane [67S]

4: Space groups: *n*-pentane: $D_{2h}^{14}(Pbcn)$
n-octane: $C_i^1(P\bar{1})$ or $C_i^1(P\bar{1})$

5: Structure of the solids:

unit cells: *n*-pentane: $a = 4.10$ Å, $b = 9.076$ Å, $c = 14.859$ Å
n-octane: $a = 4.22$ Å, $b = 4.79$ Å, $c = 11.02$ Å,
$\alpha = 94.7°$, $\beta = 84.3°$, $\gamma = 105.8°$

Atomic positions:

n-pentane:

	x	*y*	*z*
C(1)	−0.1959	0.1325	0.0878
C(2)	−0.0923	0.0374	0.1685
C(3)	0.0	0.1313	0.25

n-octane:

	x	*y*	*z*
C(1)	0.2998	0.2462	0.3803
C(2)	0.1717	0.0183	0.2781
C(3)	0.1378	0.1548	0.1618
C(4)	0.0182	−0.0687	0.0576

6: Outer valence photoelectron spectra of the molecular solids in comparison with the gas phase [77P2, 82S1]: Figs. 169 ··· 174.

7: Inner valence photoelectron spectra of the molecular solids: see Figs. 169 ··· 175.

8: Core photoelectron spectra of the molecular solids [76P]: Figs. 175, 176.

9: Theoretical assignment of the observed ion state: see Fig. 160.

10: Polarization energies of some ion states: Table 49.

11: Ion state cross-sections as a function of photon energies of solid alkanes [77S3]: Figs. 177, 178.
12: Table of resonance structures in the cross-sections:
not reported.
13: Auger spectrum of the molecular solid in comparison with the gas phase:
not reported.
14: Penning ionization electron spectrum of the molecular solid in comparison with the gas phase:
not reported.
15: Electronic excitation spectra in the valence electron region:
not reported.
16: Electronic excitation spectrum in the core electron region of the molecular solid in comparison with the gas phase:
not reported.

Table 49. Vertical binding energies and polarization energies of saturated hydrocarbons. G: gas, S: solid [74P2, 76P, 77P2, 77P3, 77P4].

Vertical binding energies [eV]

		C(1s)	C(2s)-derived levels					C(2p)-derived levels		
CH_4	G	290.76	22.93					(15.0)	14.45	(13.6)
	S	–	22.70						14.01	
	E_{pol}		0.2						0.3	
C_2H_6	G	290.64	23.91	20.42				15.35		12.69
	S	–		–					–	
	E_{pol}	–		–					–	
C_3H_8	G	290.52	24.60	22.08	19.57			15.64	13.70	12.04
	S	–		–					–	
	E_{pol}	–		–					–	
C_4H_{10}	G	290.44	24.73	23.00	20.81	19.11		(15.72)	15.0	(14.46)
								(12.67)	12.1	(11.36)
	S	–		–					–	
	E_{pol}	–		–					–	
C_5H_{12}	G	290.36	25.0	23.6	21.79					
			19.9	18.7				15.7	14.1	12.4
	S	284.70	19.5	18.2	16.6	14.2			broad	
	E_{pol}	5.72	5.5	5.4	5.2	5.1			–	
C_6H_{14}	G	290.31		–					broad	
	S	284.58	20.0	18.5	16.4	14.9			broad	
	E_{pol}	5.78		–					–	
C_7H_{16}	G	–		–					broad	
	S	–	19.5	16.4	14.1				broad	
	E_{pol}	–		–					–	
C_8H_{18}	G	290.23		–					broad	
	S	284.47	20.0	17.8	16.1	14.2				
	E_{pol}	5.72		–					–	
C_9H_{20}	G	–	24.5	22.7	21.4	20.2	18.8		broad	
	S	284.60	19.6	18.1	16.8	15.2	14.2		broad	
	E_{pol}	–	4.9	4.6	4.6	5.0	4.6		–	
$C_{10}H_{22}$	G	290.19		–					–	
	S	284.47		–					broad	
	E_{pol}	5.80		–					–	
$C_{13}H_{28}$	G	290.15	24.3		18.7				broad	
	S	284.60	19.5		14.0				broad	
	E_{pol}	5.66	4.8		4.7				–	
$C_{36}H_{74}$	S		21.2		15.1				broad	

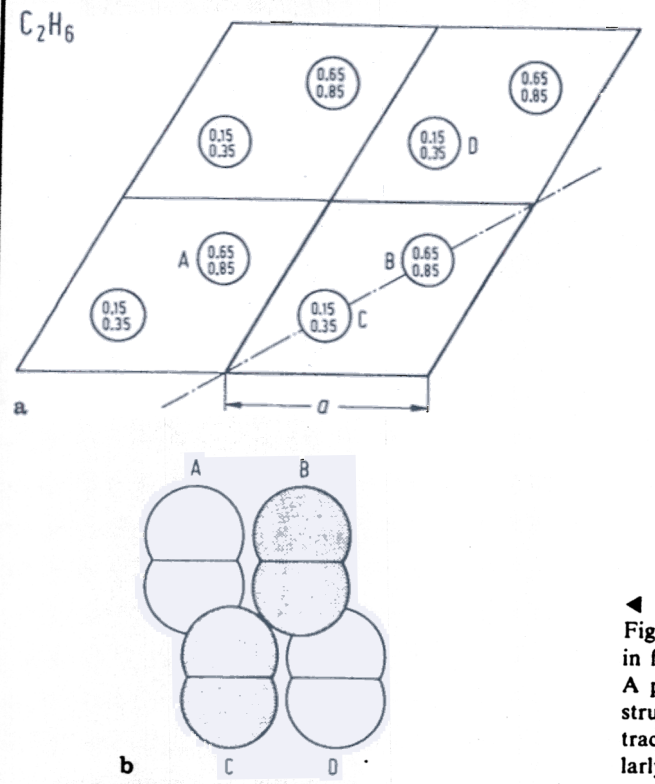

Fig. 168. C_2H_6. (a) A basal projection of the carbon atoms in four unit cells of the hexagonal structure of ethane. (b) A packing drawing of several molecules in the hexagonal structure of ethane as projected on a vertical plane whose trace is the dot-and-dash line in Fig. (a). Molecules are similarly lettered in the two drawings [66W].

For Figs. 169, 170, see pages 269, 270.

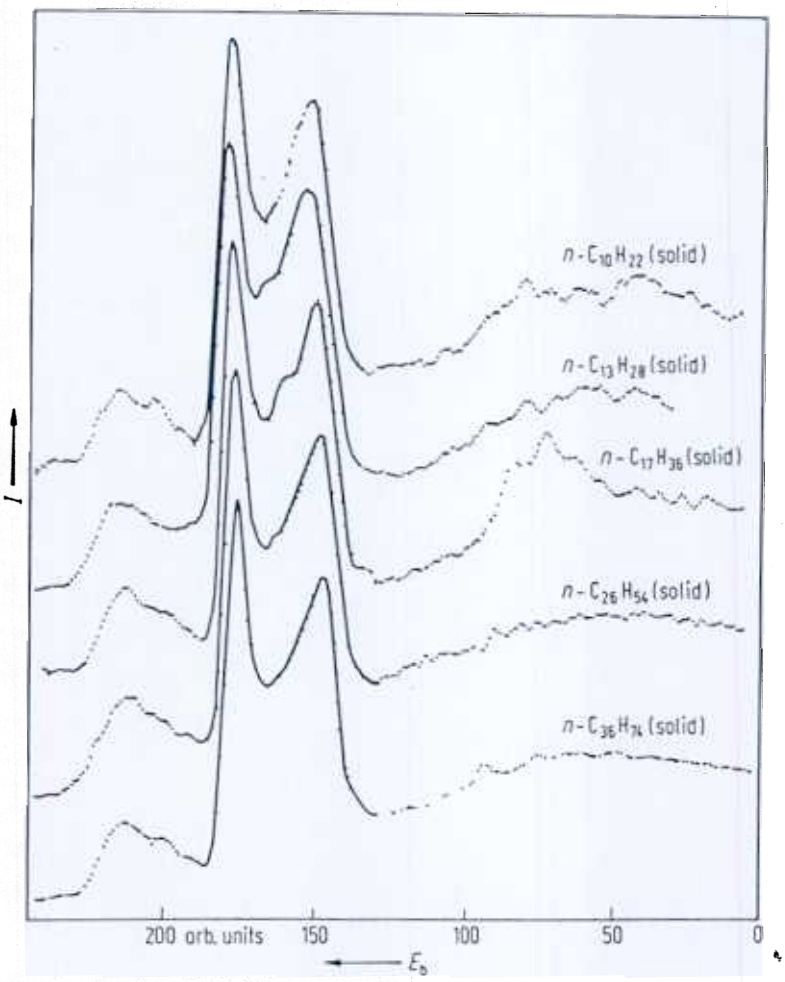

Fig. 171. C_nH_{2n+2}. Complete electron spectrum taken with $\hbar\omega = 1457$ eV of several saturated hydrocarbons (from C_{10} to C_{36}) in the solid phase [77P2].

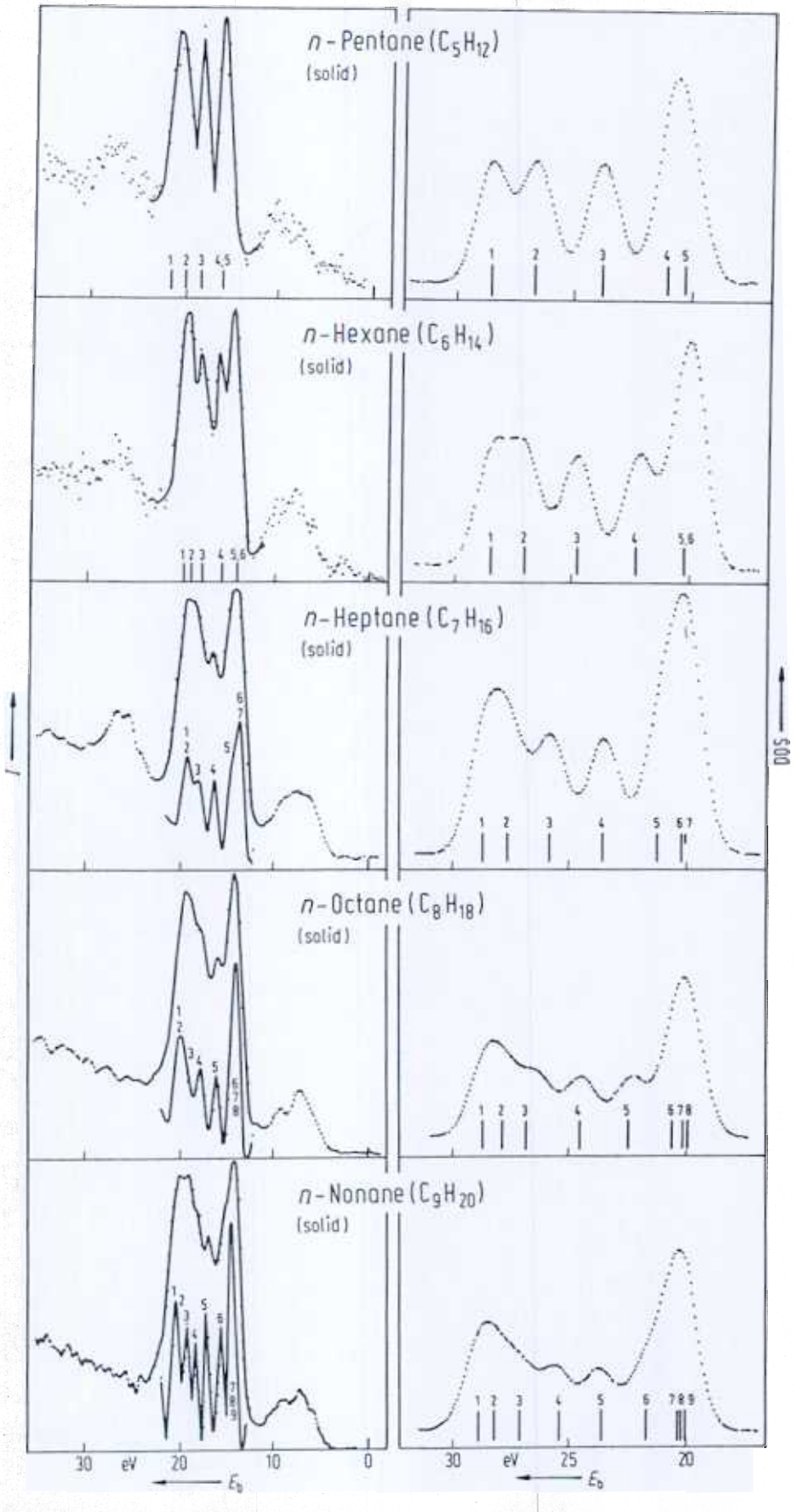

Fig. 169. C_nH_{2n+2}. ▶ Complete valence electron spectra of solid saturated hydrocarbons [77P2] (left) in comparison with calculated densities of states in the C(2s) region (right). For molecules of $n \geqq 7$ the second derivative of each spectrum is also shown. E_b (solid) relative to E_F (Au).

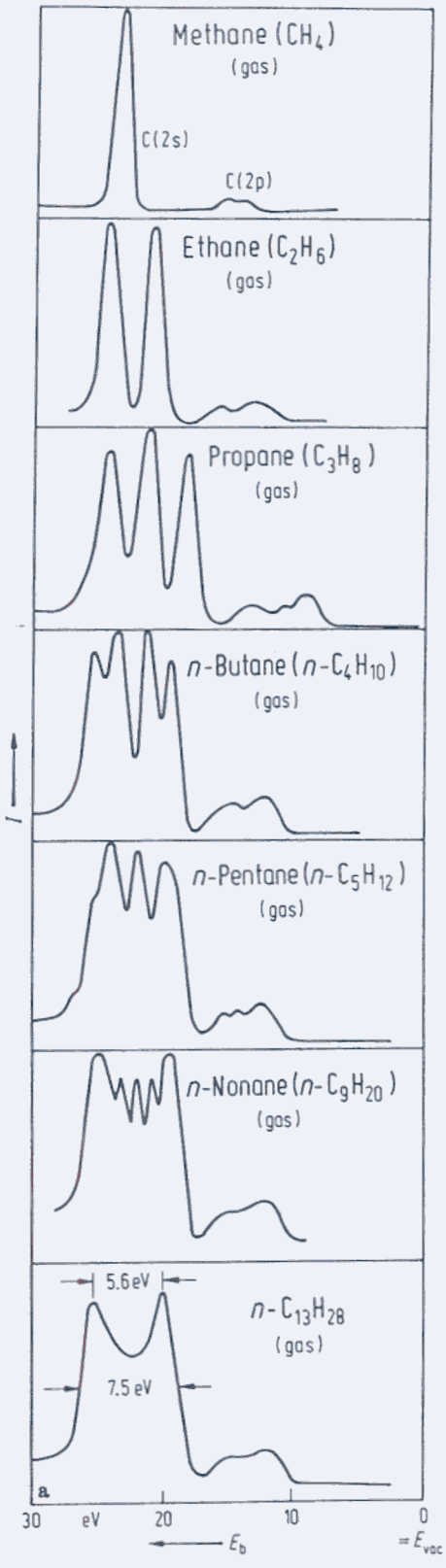

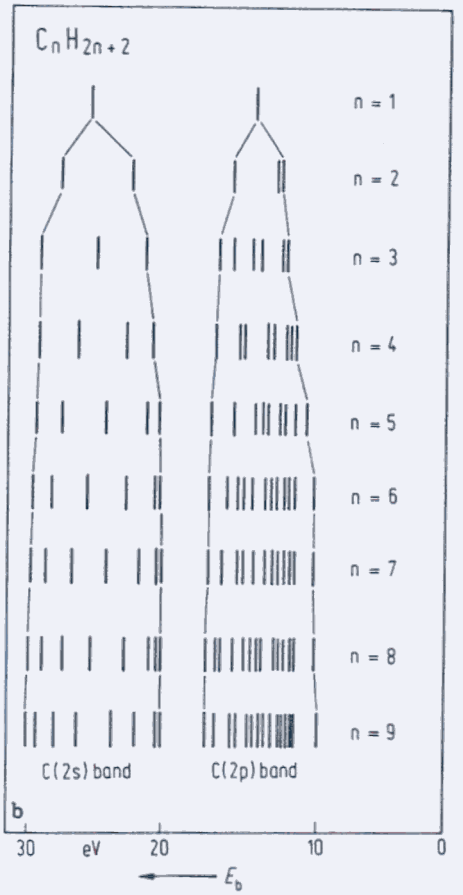

Fig. 170. C_nH_{2n+2}. Complete valence electron spectrum taken with $\hbar\omega = 1457$ eV of several saturated hydrocarbons (up to C_9, C_{13}) in the gas phase (Fig. (a)) [76P]. Calculated orbital energy diagrams are given for comparison (Fig. (b)).

Fig. 173. n-$C_{36}H_{74}$. Normal emission spectra of n-$C_{36}H_{74}$ ▶ as a function of photon energy in valence region [86S]. E_b w.r. to E_{vac}.

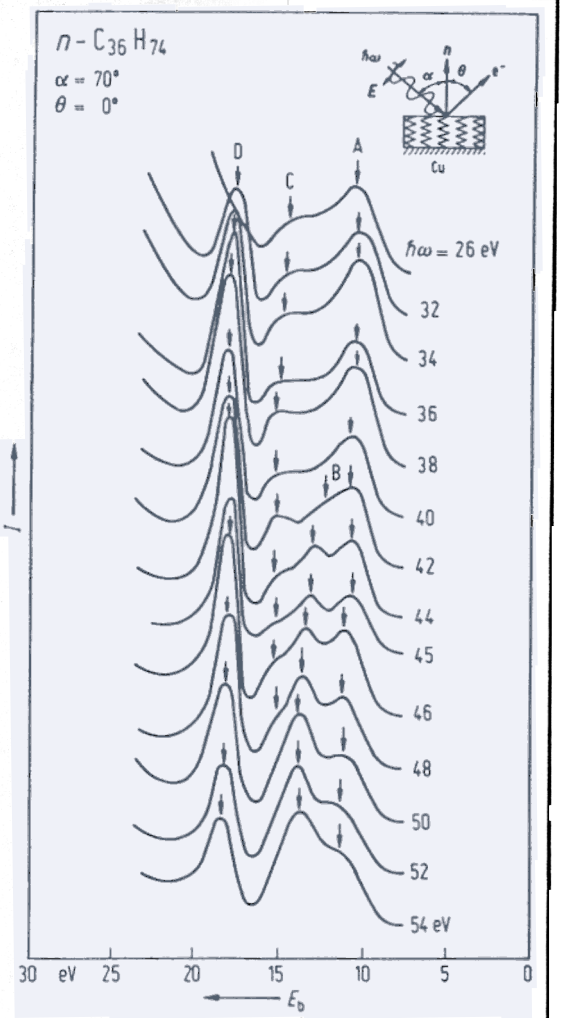

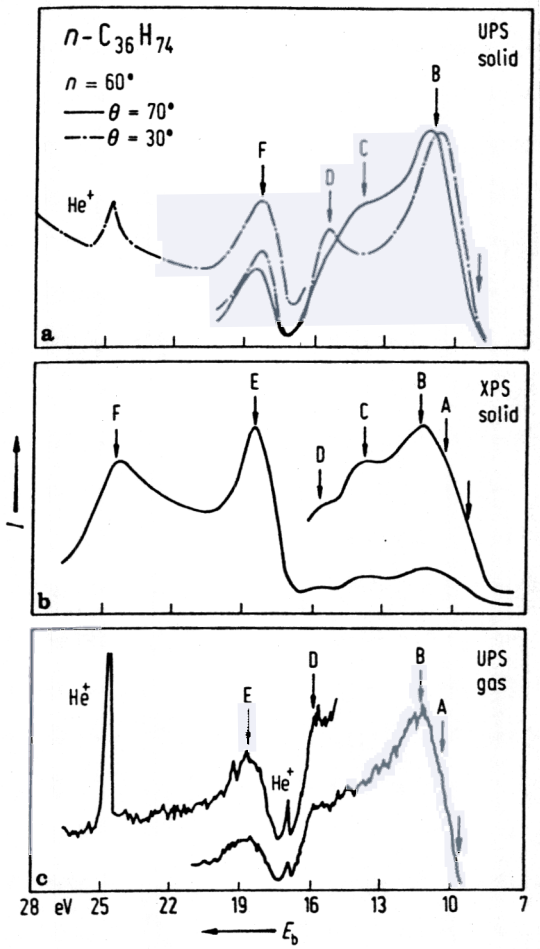

Fig. 172. n-$C_{36}H_{74}$. Comparison of the photoelectron spectra in the solid and gaseous phases [82S1]. (a) He II spectrum of the solid. (b) XPS valence electron spectrum of the solid. (c) He II spectrum of the gas. Peaks assigned to He^+ are due to the ionization of He gas from the light source by He II β (48.4 eV) and He II α (40.8 eV), respectively. The intensity of the spectra in (a) is normalized at peak B. Arrow without letter: photoemission threshold.

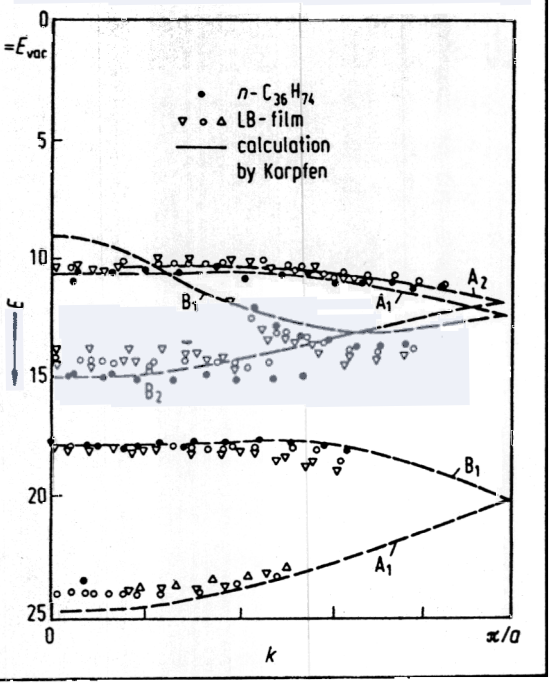

Fig. 174. n-$C_{36}H_{74}$. Measured band structure $E(k)$ of ▶ n-$C_{36}H_{74}$ in comparison with data from Langmuir-Blodgett-films and theoretical calculations [86S and literature therein]. Energy in eV.

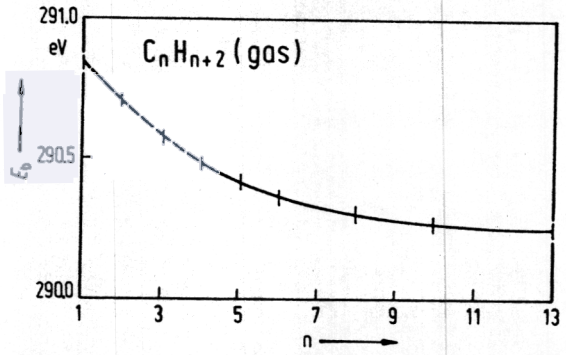

Fig. 175. C_nH_{2n+2}. Binding energies from core photoelectron spectra of saturated hydrocarbons in the gas phase as a function of the number of C-atoms in the chain (n) [76P].

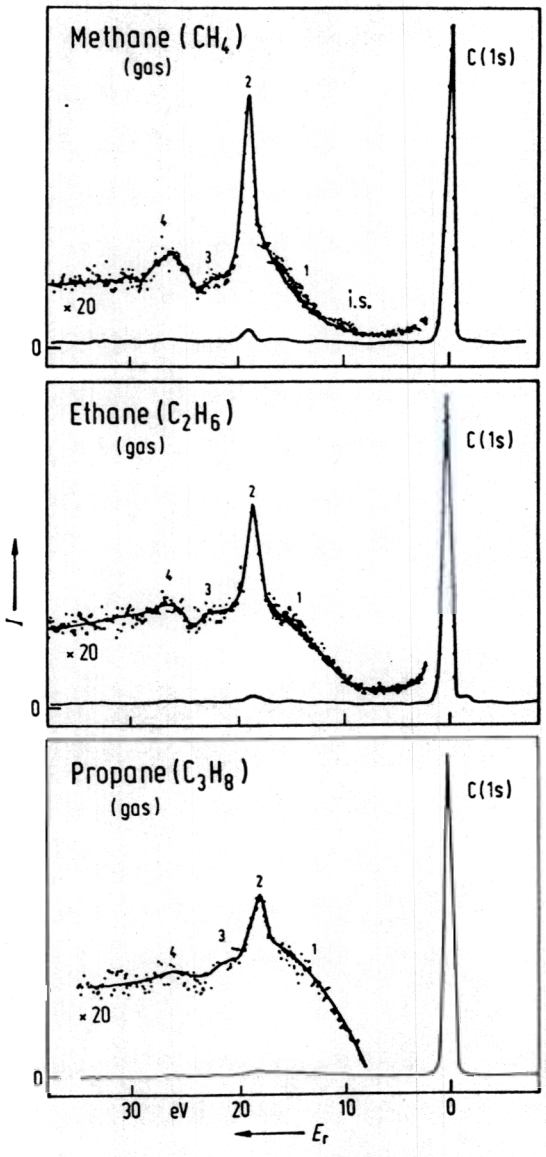

Fig. 176. C_nH_{2n+2}. Core photoelectron spectra of gaseous alkanes [76P]. I.S.: contribution from inelastic scattering.

For Fig. 177, see next page.

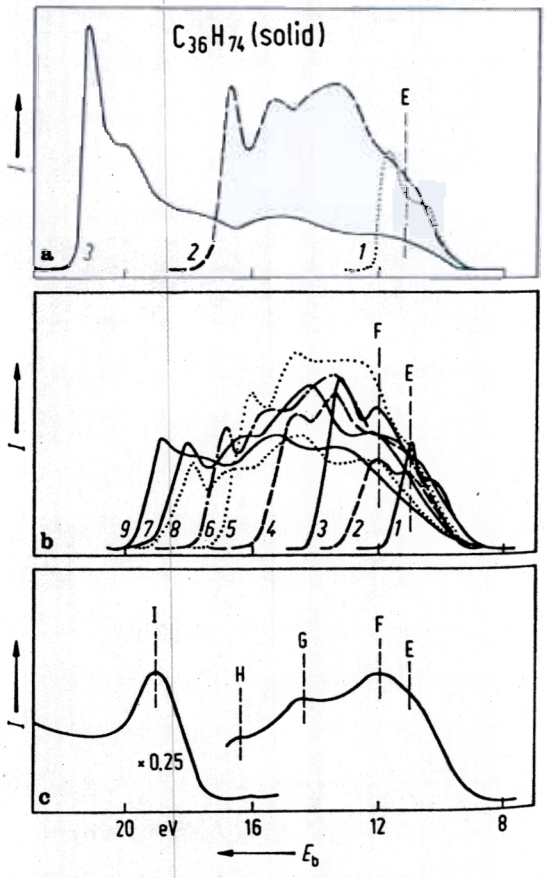

Fig. 178. $C_{36}H_{74}$. Comparison of the results of Fig. 177 with the XPS results of Fig. 171 [77P2, 77S3].

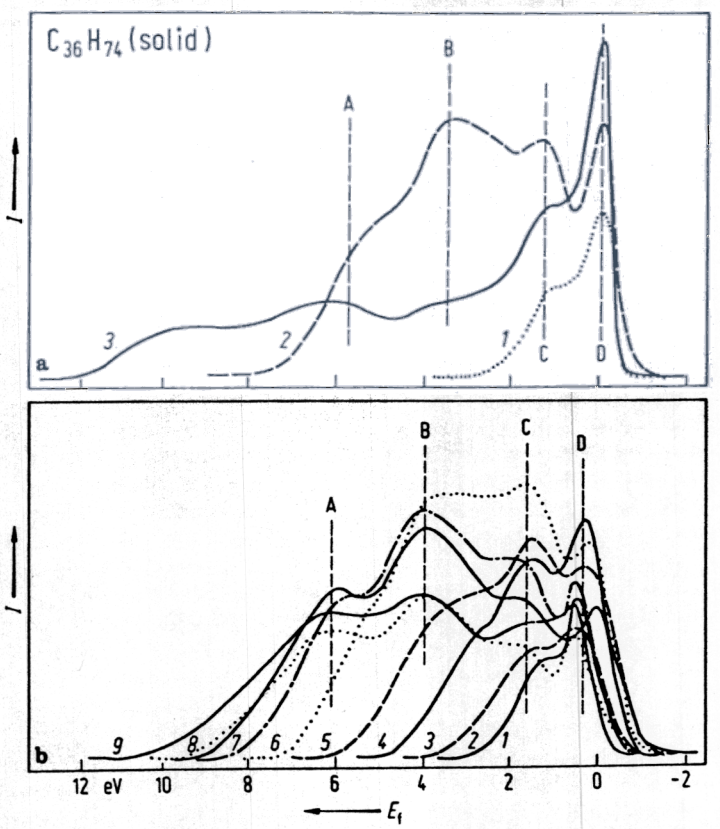

Fig. 177. $C_{36}H_{74}$. The photoelectron spectra of hexatriacontane evaporated film. A-D show the features from the conduction bands. (a) Series of measurements from the C_{36} alkane using the following photon energies: *1*: 11.7 eV, *2*: 16.8 eV, *3*: 21.22 eV. (b) Series of measurements for the same compound using the following photon energies: *1*: 11.4 eV, *2*: 12.5 eV, *3*: 13.4 eV, *4*: 14.9 eV, *5*: 16.3 eV, *6*: 17.3 eV, *7*: 18.1 eV, *8*: 18.5 eV, *9*: 19.3 eV. The spectra are normalized by the incident photon intensity [77S3]. E_f w.r. to E_{vac} of collector.

2.3.24 References for 2.3

49S Structure Reports **12** (1949) 405.
50S Structure Reports **13** (1950) 555.
58B Bak, B., Hansen-Nygaard, L., Rastrup-Andersen, J.: J. Mol. Spectrosc. **2** (1958) 361.
58C Cox, E.G.: Rev. Mod. Phys. **30** (1958) 159.
59S Structure Reports **23** (1959) 519.
60S1 Structure Reports **24** (1960) 517.
60S2 Structure Reports **24** (1960) 542.
61L Lipscomb, W.M., Wang, F.E., May, W.R., Lippert, E.: J. Acta Crystallogr. **14** (1961) 1100.
61S Structure Reports **26** (1961) 754.
63S Siemous, W.J. Bierstedt, P.E., Kepler, R.G.: J. Chem. Phys. **39** (1963) 3523.
65W Wyckoff, R.W.G.: "Crystal Structures", Vol. 1. New York: Wiley-Interscience, **1965**.
66W Wyckoff, R.W.G.: "Crystal Structures", Vol. 5. New York: Wiley-Interscience, **1966**.
67S Structure Reports **32B** (1967) 40.
68G George, G.A., Morris, G.C.: J. Mol. Spectrosc. **26** (1968) 67.
68P Petke, J.D., Whitten, J.L., Ryan, J.A.: J. Chem. Phys. **48** (1968) 953.
68S1 Structure Reports **33B** (1968) 529.

68S2 Sadovskii, A.P., Bertenev, V.M., Blokhin, S.M.: Theor. Exp. Chem. **4** (1968) 342.
70B Brundle, C.R., Robin, M.B., Basch, H.: J. Chem. Phys. **53** (1970) 2196.
70E1 Edqvist, O., Lindholm, E., Selin, L.E., Åsbrink, L.: Phys. Scr.**1** (1970) 25.
70E2 Edqvist, O., Lindholm, E., Selin, L.E., Sjögren, H., Åsbrink, L.: Ark. Fys. **40** (1970) 439.
70O Otto, A., Lynch, M.J.: Aust. J. Phys. **23** (1970) 609.
70P Potts, A.W., Lempka, H.-J., Streets D.G., Price, W.C.: Philos. Trans. R. Soc. London, A **268** (1970) 59.
70S Structure Reports **35** B (1970) 95.
70T Turner, D.W., Baker, C., Baker, A.D., Brundle C.R.: "Molecular Photoelectron Spectroscopy". New York: Wiley-Interscience, **1970**.
71B Billingsley, J., Callear, A.B.: Trans. Faraday Soc. **67** (1971) 589.
71C Cornford, A.B., Frost, D.C., McDowell, C.A., Ragle, J.L., Stenhouse, I.A.: J. Chem. Phys. **54** (1971) 2651.
71E Edqvist, O., Åsbrink, L., Lindholm, E.: Z. Naturforsch. **26**a (1971) 1407.
71H1 Hubin-Franskin, M.J., Collin, J.E.: Bull. Soc. R. Sci. Liege **40** (1971) 361.
71H2 Haensel, R., Koch, E.E., Kosuch, N., Nielsen, U., Skibowski, M.: Chem. Phys, Lett. **9** (1971) 548.
71K Koch, E.E., Kunstreich, S., Otto, A.: Opt. Commun. **2** (1971) 365.
71L1 Landolt-Börnstein, NS, Vol. III/6: Structure Data of Elements and Intermetallic Phases. Berlin, Heidelberg, New York: Springer, **1971**.
71L2 Landolt-Börnstein, NS, Vol. III/5: Structure Data of Organic Crystals. Berlin, Heidelberg, New York: Springer, **1971**.
71M Meyer, W.: Int. J. Quantum Chem. **5** (1971) 341.
71P Potts, A.W., Price, W.C.: Trans. Faraday Soc. **67** (1971) 1242.
71R Rabalais, J.W., McDonald, J., Scherr, V., McGlynn, S.P.: Chem. Rev. **71** (1971) 73.
71S Siegbahn, K., Nordling, C., Johansson, G., Hedman, J., Heden, P.F., Hamrin, K., Gelius, U., Bergmark, T., Werme, L.O., Manne, R., Baer, Y.: "ESCA-Applied to free Molecules". Amsterdam, London: North Holland Publ. Comp., **1971**.
71W Wyckoff, R.W.G.: "Crystal Structures", 2nd Ed., Vol. 6, Part. 2. New York: Wiley-Interscience, **1971**.
72A Allan, C.J., Gelius, U., Allison, D.A., Johansson, G., Siegbahn, H., Siegbahn, K.: J. Electron, Spectrosc. Relat. Phenom. **1** (1972) 131.
72B1 Blechschmidt, D., Haensel, R., Koch, E.E., Nielsen, U., Sagawa, T.: Chem. Phys, Lett. **14** (1972) 33.
72B2 Boschi, R., Murrell, J.N., Schmidt, W.: Discuss, Farady Soc. **54** (1972) 116.
72C1 Cederbaum, L.S.: Thesis, University of Munich, **1972**.
72C2 Clark, P.A., Brogli, F., Heilbronner, E.: Helv. Chim. Acta **55** (1972) 1415.
72Df Donahue, J., Krieger, R.F.: "The Structures of the Elements", New York: Wiley-Interscience, **1972**.
72D2 Dehmer, J.L.: J. Chem. Phys. **56** (1972) 4496.
72H Huebner, R.H., Mielczarek, S.R., Kuyatt, C.E.: Chem. Phys. Lett. **16** (1972) 464.
72K1 Koch, E.E., Skibowski, M.: Chem. Phys. Lett. **14** (1972) 37.
72K2 Koch, E.E., Otto, A., Radler, K.: Chem. Phys. Lett. **16** (1972) 131.
72L LaVilla, R.E.: J. Chem. Phys. **57** (1972) 899.
72S1 Siegbahn, K., Nordling, C., Fahlman, A., Nordberg, R., Hamrin, K., Hedman, J., Johansson, G., Bergmark, T., Karlsson, S.-E., Lindgren, I., Lindberg, B.: "ESCA-atomic, molecular and solid state structure studied by means of electron spectroscopy. Uppsala: Almquist and Wiksells, **1972**.
72S2 Structure Reports **38** B (1972) 52.
72Z Zagrubskii, A.A., Vilesov, F.I.: Sov. Phys Solid State (Engl. Transl.) **13** (1972) 1927.
73A Almlöf, J., Roos, B., Wahlgren U., Johansen, H.: J. Electron Spectrosc. Relat. Phenom. **2** (1973) 51.
73B Boschi, R., Schmidt, W.: Inorg. Nucl. Chem. Lett. **9** (1973) 643.
73H1 Hall, R.I., Chutjian, A., Trajmar, S.: J. Phys. B**6** (1973) L264.
73H2 Hirooka, T., Tanaka, K., Fujihira, M., Inokuchi, H., Harada, Y., Kuchitsu, K.: Chem. Phys. Lett. **18** (1973) 930.
73L1 Landolt-Börnstein, NS, Vol. III/5a: Structure Data of Organic Crystals (1971) and Vol. III/7a: Crystal Structure Data of Inorganic Compounds. Berlin, Heidelberg, New York: Springer, **1973**.
73L2 LaVilla, R.E.: J. Chem. Phys. **58** (1973) 3841.
73S Seki, K., Inokuchi, H., Harada, Y.: Chem. Phys. Lett. **20** (1973) 197.

73W Winter, N.W., Bender, C.F., Goddard III, W.A.: Chem. Phys. Lett. **20** (1973) 489.
74Å1 Åsbrink, L., Fridh, C., Lindholm, E., Codling, K.: Phys. Scr. **10** (1974) 183.
74Å2 Åsbrink, L., Fridh, C.: Phys. Scr. **9** (1974) 338.
74B Boschi, R., Clar, E., Schmidt, W.: J. Chem. Phys. **60** (1974) 4406.
74D Debies, T.P., Rabalais, J.W.: J. Electron. Spectrosc. Relat. Phenom. **3** (1974) 315.
74G1 Gelius, U., Basilier, E., Svensson, S., Bergmark, T., Siegbahn, K.: J. Electron. Spectrosc. Relat. Phenom. **2** (1974) 405.
74G2 Gelius, U.: J. Electron. Spectrosc. Relat. Phenom. **5** (1974) 985.
74P1 Potts, A.W., Williams, T.A.: J. Electron. Spectrosc. Relat. Phenom. **3** (1974) 3.
74P2 Potts, A.W., Streets, D.G.: J. Chem. Soc. Faraday Trans. II **70** (1974) 875.
74W Wight, G.R., Brion, C.E.: J. Electron. Spectrosc. Relat. Phenom. **3** (1974) 313.
75Å Ågren, H., Svensson, S., Wahlgren, U.I.: Chem. Phys. Lett. **35** (1975) 336.
75B1 Banna, M.S., Shirley, D.A.: Chem. Phys. Lett. **33** (1975) 441.
75B2 Berndtsson, Basilier, E., Gelius, U., Hedman, J., Klasson, M., Nilsson, R., Nordling, C., Svensson, S.: Phys. Scr. **12** (1975) 235.
75E Emerald, R., Drews, R., Zallen, R.: unpublished.
75G Gardner, J.L., Samson, J.A.R.: J. Chem. Phys. **62** (1975) 1447.
75H1 Himpsel, F.-J., Schwentner, N., Koch, E.E.: Phys. Status Solidi (b) **71** (1975) 615.
75H2 Hino, S., Seki, K., Inokuchi, H.: Chem. Phys. Lett. **36** (1975) 335.
75L Landolt-Börnstein, NS, Vol. III/7b1: Crystal Structure Data of Inorganic Compounds. Berlin, Heidelberg, New York: Springer, **1975**.
75N von Niessen, W., Cederbaum, L.S., Diercksen, G.H.F., Hohlneicher, G.: Chem. Phys. **11** (1975) 399.
75S Salaneck, W.R., Lipari, N.O., Paton, A., Zallen, R., Liang, K.S.: Phys. Rev. B**12** (1975) 1493.
75U Ueno, N., Hayasi, Y., Kiyono, S.: Chem. Phys. Lett. **35** (1975) 31.
75Y Yee, D.S.C., Stewart, W.B., McDowell, C.A., Brion, C.E.: J. Electron. Spectrosc. Relat. Phenom. **7** (1975) 377.
76B Banna, M.S., Shirley, D.A.: J. Electron. Spectrosc. Relat. Phenom. **8** (1976) 255.
76C Clark, D.T., Peeling, J., Colling, L.: Biochim. Biophys. Acta **453** (1976) 533
76H Hamnett, A., Holl, W., Brion, C.E.: J. Electron. Spectrosc. Relat. Phenom. **8** (1976) 367.
76K Karlson, L., Mattson, L., Jadruy, R., Bergmark, T., Siegbahn, K.: Phys. Scr. **14** (1976) 230.
76L Landolt-Börnstein, NS, Vol. II/7: Structure Data of Free Polyatomic Molecules. Berlin, Heidelberg, New York: Springer, **1976**.
76N von Niessen, W., Cederbaum, L.S., Kraemer, W.P.: J. Chem. Phys. **65** (1976) 1378.
76P Pireaux, J.J., Svensson, S., Basilier, E., Malmquist, P.-A., Gelius, U., Caudano, R., Siegbahn, K.: Phys. Rev. A**14** (1976) 2133.
76S Svensson, S., Ågren, H., Wahlgren, U.I.: Chem. Phys. Lett. **38** (1976) 1.
76W Wight, G.R., van der Wiel, N.J., Brion, C.E.: J. Phys. B**9** (1976) 675.
77C Cermak, V., Yencha, A.J.: J. Electron. Spectrosc. Relat. Phenom. **11** (1977) 67.
77E England, W.B., Ermler, W.C., Wahl, A.C.: J. Chem. Phys. **66** (1977) 2336.
77G Gonska, H., Freund, H.-J., Hohlneicher, G.: J. Electron. Spectrosc. Relat. Phenom. **12** (1977) 435.
77M Martensson, N., Malmquist, P.A., Svensson, S., Basilier, E., Pireaux, J.J., Gelius, U., Siegbahn, K.: Nouv. J. Chim. **1** (1977) 191.
77N Nürnberger, R.: Diplomarbeit, University of Hamburg, **1977**.
77P1 Plummer, E.W., Gustafsson, T., Gudat, W., Eastman, D.E.: Phys, Rev. A**15** (1977) 2339.
77P2 Pireaux, J.J., Caudano, R.: Phys. Rev. B**15** (1977) 2242.
77P3 Pireaux, J.J., Caudano, R., Svensson, S., Basilier, E., Malmquist, P.A., Gelius, U., Siegbahn, K.: J. Phys. **38** (1977) 1221.
77P4 Pireaux, J.J., Caudano, R., Svensson, S., Basilier, E., Malmquist, P.A., Gelius, U., Siegbahn, K.: J. Phys. **38** (1977) 1213.
77P5 Preston, H.J.T., Kaufman, J.J.: Chem. Phys. Lett. **50** (1977) 157.
77R Riga, J., Pireaux, J.J., Caudano, R., Verbist, J.J.: Phys. Scr. **16** (1977) 346.
77S1 Schirmer, J., Cederbaum, L.S., Domcke, W., von Niessen, W.: Chem. Phys. **26** (1977) 149.
77S2 Salaneck, W.R., Duke, C.B., Paton, A., Griffiths, C., Keezer, R.C.: Phys. Rev. B**15** (1977) 1100.
77S3 Seki, K., Hashimoto, S., Sato, N., Harada, Y., Ishie, K., Inokuchi, H., Kanbe, J.: J. Chem. Phys. **66** (1977) 3644.
78Å1 Åsbrink, L., Fridh, C., Lindholm, E.: Z. Naturforsch. **33a** (1978) 172.
78Å2 Ågren, H., Nordgren, J., Selander, L., Nordling, C., Siegbahn, K.: Phys. Scr. **18** (1978) 499.

78B1 Brown, F.C., Bachrach, R.Z., Bianconi, A.: Chem. Phys. Lett. **54** (1978) 425.
78B2 Brion, C.E., Tan, K.H.: Chem. Phys. **34** (1978) 141.
78C1 Cederbaum, L.S., Schirmer, J., Domcke, W., von Niessen, W.: Int. J. Quantum Chem. **14** (1978) 593.
78C2 Cederbaum L.S., Domcke, W., Schirmer, J., von Niessen, W., Diercksen, G.H.F., Kraemer, W.P.: J. Chem. Phys. **69** (1978) 1591.
78D1 Duke, C.B.: Surf. Sci. **70** (1978) 674.
78D2 Duke, C.B., Salaneck, W.R., Fabish, T.J., Ritsko, J.J., Thomas, H.R., Paton, A.: Phys. Rev. B**18** (1978) 5717.
78G1 Gustafsson, T.: Phys. Rev. A**18** (1978) 1481.
78G2 Gustafsson, T., Plummer, E.W., Eastman, D.E., Gudat, W.: Phys. Rev, A**17** (1978) 175.
78H Hitchcock, A.P., Brion, C.E.: J. Electron. Spectrosc. Relat. Phenom. **14** (1978) 417.
78K Köppel, H., Cederbaum, L.S., Domcke, W., von Niessen, W.: Mol. Phys. **35** (1978) 1283.
78L1 Lunell, S., Svensson, S., Malmquist, P.-A., Gelius, U., Basilier, E., Siegbahn, K.: Chem. Phys. Lett. **54** (1978) 420.
78L2 Landolt-Börnstein, NS, Vol. III/7c1: Crystal Structure Data of Inorganic Compounds. Berlin, Heidelberg, New York: Springer, **1978**.
78N Norton, P.R. Tapping, R.L., Broida, H.P., Gadzuk, J.W., Wachawski, B.J.: Chem. Phys. Lett. **53** (1978) 465.
78S Salaneck, W.R.: Phys. Rev. Lett. **40** (1978) 60.
79B1 Brion, C.E., Tan, K.-H.: J. Electron. Spectrosc. Relat. Phenom. **15** (1979) 241.
79B2 Berkowitz, J.: "Photoabsorption, Photoionization and Photoelectron Spectroscopy". New York: Academic Press **1979**.
79C Campbell, M.J., Liesegang, J., Riley, J.P., Leckey, R.C.G., Jenkin, J.G., Poole, R.T.: J. Electron. Spectrosc. Relat. Phenom. **15** (1979) 83.
79D Domcke, W., Cederbaum, L.S., Schirmer, J., von Niessen, W., Brion, C.E., Tan, K.H.: Chem. Phys. **40** (1979) 171.
79E England, W.B., Ermler, W.C.: J. Chem. Phys. **70** (1979) 1711.
79G Grobman, W.D., Koch, E.E.; in: "Photoemission in Solids II", Ley, L., Cardona, M., (eds.). Berlin, Heidelberg, New York: Springer **1979**, p. 261.
79L1 Langhoff, P.W., Gerwer, A., Asaro, C., McCoy, B.V.: Int. J. Quantum Chem. S**13** (1979) 645.
79L2 Landolt-Börnstein, NS, Vol. III/7c3: Crystal Structure Data of Inorganic Compounds. Berlin, Heidelberg, New York: Springer, **1979**.
79M Munakata, T., Kuchitsu, K., Harada, Y.: Chem. Phys. Lett. **64** (1979) 409.
79N1 von Niessen, W., Kraemer, W.P., Diercksen, G.H.F.: Chem. Phys. Lett. **63** (1979) 65.
79N2 von Niessen, W., Kraemer, W.P., Diercksen, G.H.F.: Chem. Phys. **41** (1979) 113.
79S Schmeisser, D., Jacobi, K.: Chem. Phys. Lett. **62** (1979) 51.
79T Tronc, M., King., G.C., Read, F.H.: J. Phys. B**12** (1979) 425.
79V Van Nes, G.J.H., Van Bolhuis, F.: Acta Crystallogr. **35b** (1979) 2580.
80Å Ågren, H., Siegbahn, H.: Chem. Phys. Lett. **69** (1980) 424.
80B1 Bieri, G., Åsbrink, L.: J. Electron. Spectrosc. Relat. Phenom. **20** (1980) 149.
80B2 Brown, R.S., Tse, A., Vederas, J.C.: J. Amer. Chem. Soc. **102** (1980) 1174.
80C Case, D.A., Cook, M., Karplus, M.: J. Chem. Phys. **73** (1980) 3294.
80D Duke, C.B., Schein, L.B.: Phys. Today, **1980**, Febr. Iss.
80G1 Gerwer, A., Asaro, C., McCoy, B.V., Langhoff, P.W.: J. Chem. Phys. **72** (1980) 713.
80G2 Gustafsson, T.: Chem. Phys. Lett. **75** (1980) 505.
80H1 Hitchcock, A.P., Brion, C.E.: J. Electron. Spectrosc. Relat. Phenom. **18** (1980) 1.
80H2 Haller, E., Cederbaum, L.S., Domcke, W., Köppel, H.: Chem. Phys, Lett. **72** (1980) 427.
80K Krummacher, S., Schmidt, V., Wuilleumier, F.: J. Phys. B**13** (1980) 3993.
80M Müller, J., Poulain, E., Goscinski, O., Karlsson, L.: J. Chem. Phys. **72** (1980) 2587.
80S1 Salaneck, W.R., Duke, C.B., Eberhardt, W., Plummer, E.W., Freund, H.-J.: Phys. Rev. Lett. **45** (1980) 280.
80S2 Silinsh, E.A.: "Organic Molecular Crystals, Their Electronic States", Berlin: Springer **1980**.
81D Duke, C.B., Paton, A., in: "Conductive polymers", Seymour, R.B. (ed.), New York: Plenum Press **1981**, p. 155.
81E Eesley, G.L., Burkstrand, J.U.: Phys. Rev. B**24** (1981) 582.
81H Honjou, N., Sasajima, T., Sasaki, F.: Chem. Phys. **57** (1981) 475.

81K1 Kimura, K., Katamuata, S., Achiba, Y., Yamazaki, T., Iwata, S.: "Handbook on HeI photoelectron spectra of fundamental organic molecules" Tokyo: Jpn Sci. Soc. Press, **1981**.

81K2 Kubota, H., Hirooka, T., Fukuyama, T., Kondow, T., Kuchitsu, K., Yencha, A.J.: J. Electron. Spectrosc. Relat. Phenom. **23** (1981) 417.

81L1 Langhoff, P.W., Langhoff, S.R., Resigno, T.N., Schirmer, J., Cederbaum, L.S., Domcke, W., von Niessen, W.: Chem. Phys. **58** (1981) 71.

81L2 Langhoff, P.W., McKoy, B.V., Unwin, R., Bradshaw, A.: Chem. Phys. Lett. **83** (1981) 270.

81M Mootz, D., Wussow, H.-G.: J. Chem. Phys. **75** (1981) 1517.

81R Riga, J., Pireaux, J.-J., Boutique, J.-P., Caudano, R., Verbist, J.J., Gobillon, Y.: Synth. Met. **4** (1981) 99.

81S Salaneck, W.R., Bigelow, R.W., Freund, H.-J., Plummer, E.W.: Phys. Rev. B**24** (1981) 2403.

81S2 Sato, N., Seki, K., Inokuchi, H.: J. Chem. Soc. Faraday Trans. II, **77** (1981) 1621.

81Y Yencha, A.J., Kubota, H., Fukuyama, T., Kondow, T., Kuchitsu, K.: J. Electron. Spectrosc. Relat. Phenom. **23** (1981) 431.

82A Årneberg, R., Ågren, H., Malmquist, P.-A., Svensson, S.: Chem. Phys, Lett. **92** (1982) 125.

82B1 Bredas, J.J., Chance, R.R., Silbey, R., Nicolas, G., Durand, Ph.: J. Chem. Phys. **77** (1982) 371.

82B2 Bigelow, R.W., Salaneck, W.R.: Chem. Phys. Lett. **89** (1982) 430.

82B3 Bigelow, R.W., Freund, H.-J.: J. Chem. Phys. **77** (1982) 5552.

82C1 Campbell, M.J., Liesegang, J., Riley, J.D., Jenkin, J.G.: J. Phys. C**15** (1982) 2549.

82C2 Calis, G.H.M., Swolfs, A.E.M., Trooster, J.M.: Chem. Phys. **64** (1982) 259.

82D Dehmer, J.L., Parr, A.C., Wallace, S., Dill, D.: Phys. Rev. A**26** (1982) 3283.

82H1 Hino, S., Veszpremi, T., Ohno, K., Inokuchi, H., Seki, K.: Chem. Phys. **71** (1982) 135.

82H2 Hayaishi, T., Iwata, S., Sasanuma, M., Ishiguro, E., Morioka, Y., Iida, Y., Nakamura, M.: J. Phys. B**15** (1982) 79.

82K Karl, N., Sato, N., Seki, K., Inokuchi, H.: J. Chem. Phys. **77** (1982) 4870.

82L1 Lau, H.-J., Fock, J.-H., Koch, E.E.: Chem. Phys. Lett. **89** (1982) 281.

82L2 Lau, H.-J.: Diplomarbeit, University of Hamburg **1982**.

82M1 Machado, L.E., Leal, E.P., Csanak, G., McKoy, B.V., Langhoff, P.W.: J. Electron. Spectrosc. Relat. Phenom. **27** (1982) 223.

82M2 Müller, J., Arneberg, R., Ågren, H., Manne, R., Malmquist, P.-A., Svensson, S., Gelius, U.: J. Chem. Phys. **77** (1982) 4895.

82N Nakatsuji, H., Yonezawa, T.: Chem. Phys. Lett. **87** (1982) 426.

82O O'Sullivan, G.: J. Phys. B**15** (1982) 2385.

82R1 Reineck, I., Maripen, R., Veenhuizen, H., Karlsson, L., Siegbahn, K., Powar, M.S., Wu Nian Zu, Ji Ming Rong, Al-Shamma, S.H.: J. Electron Spectrosc. Relat. Phenom. **27** (1982) 15.

82R2 Raynerd, G., Tatlock, G.J., Venables, J.A.: Acta Crystallogr. **38**b (1982) 1896.

82S1 Seki, K., Inokuchi, H.: Chem. Phys. Lett. **89** (1982) 268.

82S2 Southworth, S., Truesdale, C.M., Kobrin, P.H., Lindle, D.W., Brewer, W.D., Shirley, P.A.: J. Chem. Phys. **76** (1982) 143.

82V Veszpremi, T.: Chem. Phys. Lett. **88** (1982) 325.

83C Chong, D.P.: Can. J. Chem. **61** (1983) 1.

83E Eberhardt, W., Freund, H.-J.: J. Chem. Phys. **78** (1983) 700.

83F1 Fock, J.-H.: Thesis, University of Hamburg **1983**.

83F2 Ford, W.K., Duke, C.B., Paton, A.: J. Chem. Phys. **78** (1983) 4734.

83K1 Krummacher, S., Schmidt, V., Wuilleumier, F., Bizeau, J.M., Ederer, D.: J. Phys. B**16** (1983) 1733.

83K2 Keller, P.R., Taylor, J.W., Carlson, T.A., Grimm, F.A.: Chem. Phys. **79** (1983) 269.

83K3 Koch, E.E.: "Organic Molecular Aggregates". Reinicker, R., Haken, H., Wolf, H.C. (eds.). Berlin: Springer **1983**, p. 35.

83L Landolt-Börnstein, NS, Vol. III/17e: Semiconductors. Berlin, Heidelberg, New York: Springer, **1983**.

83N Nakatsuji, H.: Chem. Phys. **75** (1983) 425.

83S1 Schirmer, J., Walter, O.: Chem. Phys. **78** (1983) 201.

83S2 Schmeisser, D., Himpsel, F., Hollinger, J., Reihl, B., Jacobi, K.: Phys. Rev. B**27** (1983) 3279.

83T Tonner, B.P., Kao, C.M., Plummer, E.W., Caves, T.C., Messmer, R.P., Salaneck, W.R.: Phys. Rev. Lett. **51** (1983) 1378.

84A Abe, H., Onaka, R.: J. Phys. Soc. Jpn. **53** (1984) 1176.

84B1 Biester, H.-W.: Diplomarbeit, University of Hamburg **1984**.

84B2 Boutique, J.P., Riga, J., Verbist, J.J., Delhalle, J., Fripiat, J.G.: J. Electron. Spectrosc. Relat. Phenom. **33** (1984) 243.

84F1 Fock, J.-H., Lau, H.-J., Koch, E.E.: Chem. Phys. **83** (1984) 377.

84F2 Fock, J.-H., Koch, E.E.: Chem. Phys. Lett. **105** (1984) 38.

84F3 Fock, J.-H., Schmidt-May, J., Koch, E.E.: J. Electron. Spectrosc. Relat. Phenom. **34** (1984) 225.

84L Lynch, D., Lee, M.-T., Lucchese, R.R., McKoy, V.: J. Chem. Phys. **80** (1984) 1907.

84M Murgai, V., Hulbert, S.C., Johnson, P.D., Strongin, Myron., Eberhardt, W.: Chem. Phys. Lett. **111** (1984) 157.

84R1 Riga, J., Boutique, J.P., Verbist, I.J., Delhalle, J., Fripiat, J.G.: J. Electron. Spectrosc. Relat. Phenom. **33** (1984) 263.

84R2 Rogers, jr., J.W., Houston, J.E., Rye, R.R.: Surf. Sci. **141** (1984) L345.

84S1 Salaneck, W.R.: private communication.

84S2 Seki, K., Karlsson, K.O., Engelhardt, R., Koch, E.E., Schmidt, W.: Chem. Phys. **91** (1984) 459.

85F Fock, J.H., Koch, E.E.: Chem. Phys. **96** (1985) 125.

85H Harada, Y.: Surf. Sci. **158** (1985) 455.

85K1 N. Karl in: Landolt-Börnstein, NS, Vol. III/17i: Semiconductors. Berlin, Heidelberg, New York: Springer, **1985**.

85K2 Kuchta, B.: Chem. Phys. **95** (1985) 391.

85L Landolt-Börnstein, NS, Vol. III/10: Structure Data of Organic Crystals. Berlin, Heidelberg, New York: Springer, **1985**.

85R Rosenberg, R.A., Love, P.J., La Roe, P.R., Rehn, V., Parks, C.C.: Phys. Rev. B**31** (1985) 2634.

85S Salaneck, W.R.: CRC Crit. Rev. Solid State Mater. Sci. **12** (1985) 167.

86C Cederbaum, L.S., Domcke, W., Schirmer, J., von Niessen, W.: Adv. Chem. Phys. **65** (1986) 115.

86F Freund, H.-J., Kossmann, H., Schmidt, V.: Chem. Phys. Lett. **123** (1986) 463.

86S Seki, K., Ueno, N., Karlsson, U.O., Engelhardt, R., Koch, E.E.: Chem. Phys. **105** (1986) 247.

87I Inokuchi, H., Seki, K., Sato, N.: Phys. Scr. T**17** (1987) 93.

87K Koch, E.E.: Phys. Scr. T**17** (1987) 120.

87F1 Freund, H.-J., Bigelow, R.W.: Phys. Scr. T**17** (1987) 50.

87F2 Freund, H.-J., Kossmann, H., Schmidt, V.: Chem. Phys. Lett. **137** (1987) 425.

87L Landolt-Börnstein, NS, Vol. II/15: Structure Data of Free Polyatomic Molecules. Berlin, Heidelberg, New York: Springer, **1987**.

87Y Yamamoto, H., Seki, K., Mori, T., Inokuchi, H.: J. Chem. Phys. **86** (1987) 1775.

88L Landolt-Börnstein, NS, Vol. III/14a: Crystal Structure Data of Inorganic Compounds. Berlin, Heidelberg, New York: Springer, **1988**.